Analysis of Inflammatory Phenotype in Human Endothelial Cell Senescence

Thesis submitted for the degree of Doctor of Philosophy

By

Sadaf Nouman, Pharm D, MRes

Department of Cardiovascular Sciences

University of Leicester

2019

Abstract

Analysis of Inflammatory Phenotype in Human Endothelial Cell Senescence

Sadaf Nouman, Department of Cardiovascular Sciences, University of Leicester

Ageing is the major risk factor for the development of cardiovascular diseases. Endothelial cells play a major role in the normal physiology of vessel wall. Endothelial dysfunction contributes to the development of cardiovascular diseases. In particular, the presence of senescent endothelial cells in the atherosclerotic plaque. Association of senescent endothelial cells in the development of endothelial dysfunction is not clear. This thesis was aimed to investigate the phenotype of senescent (SIPS and REPS) HUVECs and perhaps develop their markers

In vitro models of senescent endothelial cell were developed i.e. SIPS and REPS. Genes identified from previous transcriptomics data analysis, for the first time, notably included *CST1*, *LRRC17* and *CRTAC1* as differentially expressed in senescent HUVEC. Their expression was validated by quantitative PCR but the gene product of *CST1*, cystatin SN, was not identified in Western blotting. Subsequent bioinformatics re-analysis of differentially expressed genes described molecular pathways, molecular functions and diseases that were affected in senescent HUVECs.

Senescent cells are presented with senescent associated secretory phenotype (SASP). Perhaps the pro-inflammatory factors in SASP contribute to the endothelial dysfunction. Characterisation of the secretome from senescent endothelial cells using mass spectrometry did not identify pro-inflammatory factors. Moreover, SASP from senescent HUVECs did not potentiate the binding of monocytic cells to endothelial monolayers. However, functional assays confirmed increased adhesion of monocytes to senescent HUVECs in both static and flow-based cell models *in vitro*. Further investigation of candidate genes involved in the adhesion of monocytes to endothelial cells in these scenarios, identified E-selectin and CD44 as potential mediators.
Taken together, these new data suggest that senescent endothelial cells might represent a pro-inflammatory phenotype via expressing adhesion molecules that could recruit inflammatory cells to sites of vascular damage or endothelial dysfunction.

Acknowledgemenets

First of all, glory to Allah. I am very grateful to Him for giving me everything. Thank you for giving me such a blessed life.

I am extremly thankful to my supervisor, Dr Karl Herbert. Choosing him as my PhD supervisor was amongst the best decisions of my life. All my work could not have been completed without his support. I am very grateful for his tremendous help throughout my PhD. He has always been very approachable. I am sure, during last few years I must have induced some senescence in him.

Thanks to all Team Herbert, our Thursday meetings were always something to look forward to, especially the food.

I am also very thankful to my second supervisor, Dr Salvador Macip. His valuable advice and guidance for my research was always useful. He always suggested right direction for my research.

I am very thankful to all the people in the department, everyone was very helpful. There are few who I would like to mention by their name. Jodie K Sandhu for performing Mass Spectrometry experiments, Pauline Quinn for helping me preparing samples for Mass Spectrometry, Thong Cao Huy for helping with Mass spectrometry data analysis. Pete Jones, Veryan Codd, Matthew Denniff, and Laurence for helping primers design for qPCR, Marcin Wozniak for adhesion assay and his tremendous help with data analysis and bioinformatics using IPA, Sarah Andrews for adhesion assay. Hash, Martha and Julie for dealing with day to day problems in tissue culture. A special thank you to all of those who bought cakes and treats to the department, which kept all of us going.

I am very grateful to all my family members, brothers and sisters (Shehla, Naheed, Shehzadi, Nazli, Sajjad, Younas and Arif). Who were always there for me and always boosted my confidence throughout the journey of my PhD. I have few amazing friends, they are the best people, who made my last four years memorable. A huge thank you to all of you. I want to say thank you to Nawshin Dastagir, who is not only my soul mate but also my favourite sister. All those late nights I spent writing my PhD thesis on your desk was of coarse an important part in this journey and your loud giggle added a lot.

My husband Dr Asim nouman you came in my life after I passed my PhD *viva* but you played best part in motivating me for my final thesis submission. I feel I can achieve anything if you are by my side.

Last but not least, my loving parents; Ammi and papa, you both are great. I am very lucky to have got you, thank you for all your support and love.

Table of contents

Table of Figures

Table of tables

List of abbreviations

ADAMST1	A disintegrin and metalloproteinase with thrombospondin-like motifs
APS	Ammonium persulphate
ATM	ataxia talengectcia mutated
B2M	β 2 microglobulin
BPS	Phosphate buffer sulphate
CHX	cyclohexamide
CCL2	C-C motif chemokine ligand 2
CM	conditioned media
CPDs	Cumulative population doublings
CRTAC1	Cartilage like protein 1
CST1	Cystatin SN
CVD	Cardiovascular diseases
DCR2	Decoy receptor 2
DDR	DNA damage response
DKK1	Dickkopf-1
DTT	Dithiothreitol
ECs	Endothelial cells
EDTA	Ethylenediaminetetracetic acid

EF-1α	Elongation factor 1 alpha
FBS	Fetal bovine serum
FOXO	Forkhead box 03
H2O2	Hydrogen peroxide
HDFs	Human dermal fibroblasts
HUVECs	Human umbilical vein endothelial cells
IAA	Iodoacetic acid
ICAM-1	Intracellular adhesion molecule-1
IGFBP3	Insulin growth like factor binding protein-3
IGFBP5	Insulin like growth factor binding protein-5
IL-6	Interleukin 6
IL-8	Interleukin-8
IPA	Ingenuity pathway analysis
LRRC17	Leucine rich repeat containing 17
LTB	Lymphotoxin beta gene
MEF	Mouse embryonic fibroblasts
miRNA	MicroRNA
MPs	Microparticles
NF-κB	Nuclear factor kappa B

NOS	Nitric oxide synthase
PI3K	Phosphoinositide-3-kinase
PMA	Phorbol 12 myristate 13-acetate
PSMB4	Proteome subunit beta 4 (human)
PTHLH	Parathyroid hormone related peptide
REPS	Replicative senescence
RT-qPCR	Reverse transcriptase quantitative polymerase chain reaction
SA β-gal	Senescence associated beta-galactosidase
SAHF	Senescence associated heterochromatin Foci
SASP	Senescence associated secretory phenotype μ
SDS	Sodium dodecyl sulphate
SILAC	Stable isotope labelling by amino acid in culture
SIPS	Stressed induced premature senescence
SMc	Smooth muscle cells
SMS	Senescence messaging secretome
SPARC	Secreted protein acidic and rich in cysteine
TNF-α	Tissue necrosis factor α
TXNIP	Thioredoxin-interacting protein
VCAM-1	Vascular cell adhesion molecule

VCP	Valosin containing protein

Chapter 1

1 Introduction

1.1 Endothelium

Blood vessel walls are generally composed of three layers: endothelium (intimal layer), smooth muscle cells (medial layer) and supportive connective tissue (adventitial layer). Endothelium is the inner layer of the blood vessel wall and is composed of a monolayer of endothelial cells (EC) (fig 1-1). In an adult human, the endothelium covers approximately 1,000 square meters, lining all the blood vessels and heart chambers and plays a major role in thrombotic and anti-thrombotic activities (Sagripanti, Carpi 2000).

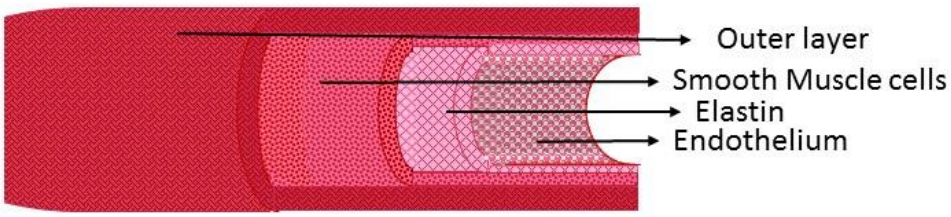

Figure 1-1: Archetype structure of an artery.

Artery is composed of 3 layers. The most inner layer is endothelium, also called tunica intima, composed of endothelial cells. Next layer is composed of elastin, followed by smooth muscle cells. This is called tunica media. The 3rd layer is outer layer, composed of collagen fibres, called tunica adventitia.

1.1.1 Physiological Functions

Initially endothelium was considered to be a cellophane-like membrane with a single important function of nutrient exchange. However, extensive research particularly using the electron microscope, has defined the multiple vital roles of endothelium (Cines, Pollak et al. 1998). The following sections provide an overview to better explain endothelial function.

1.1.1.1 Regulation of vascular tone

The endothelium is not merely a barrier for the exchange of nutrients between the circulating blood and tissues, but it also produces important mediators that regulate vascular homeostasis. Vasodilators such as nitric oxide (NO) and prostacyclin (PGI_2) and the vasoconstrictor, platelet-activating factor, are released by EC in order to regulate blood pressure and blood flow (Cines, Pollak et al. 1998). Endothelial derived relaxing factor is a free radical gas, NO, which is released by endothelium (Furchgott 1999) and is synthesized from L-arginine producing L-citrulline by the enzyme NO synthase (NOS) (Stamler, Singel et al. 1992). Acetylcholine, angiotensin, bradykinin, histamine, adenine nucleotides, shear stress and other mediators induce the release of NO from EC (Denninger, Marletta 1999) (Topper, Cai et al. 1996). NO causes vascular relaxation by diffusing to the smooth muscle cells where it causes the increased formation of cyclic GMP by stimulating guanylate cyclase (Marletta 2001).

Endothelium derived hyperpolarising factors (EDHFs) are several factors released by endothelium that cause hyperpolarisation and relaxation of smooth muscles cells (Feletou, Vanhoutte 2006). EDHF activity is not affected by NOS inhibitors (Brandes, Behra et al. 1997). EDHFs act upon potassium channels (K^+) of smooth muscles cells, allowing K^+ efflux. This results into membrane hyperpolarisation causing relaxation (Ozkor, Quyyumi 2011).

Endothelin is a vasoconstrictor derived from proendothelin in the presence of metalloproteinases. Mediators like thrombin, angiotensin, cytokines and physical factors like hypoxia and shear stress stimulate the release of endothelin (Rubanyi, Botelho 1991).

1.1.1.2 Prothrombotic and anti-thrombotic role of endothelial cells

Expression of tissue factor by endothelium causes fibrin generation (Stern, Nawroth et al. 1985), which suggests that endothelium expresses the binding sites for coagulation factors and thrombin (Brinkman, Mertens et al. 1994). Endothelium expresses binding sites for both thrombin and anti-thrombin. Disease free endothelial cells present an anti-thrombotic surface by expressing a proteoglycan, heparan sulphate (Marcum, Rosenberg 1985). Anti-thrombin III is normally bound to heparin sulphate thus presenting an anti-thrombotic environment (Sagripanti, Carpi 2000, Marcum, McKenney et al. 1984).

Thrombin also stimulates endothelial cells to release chemokines that cause the recruitment of immune cell to bind to endothelial surface (Subramaniam, Frenette et al. 1996). Upregulation of the expression of adhesion molecules, that is VCAM-1, ICAM-1 and E-selectin (Carlos, Harlan 1990) also occurs in response to pathologic stimuli.

However, to maintain homeostasis the anti-thrombotic surface of endothelial cells become pro-thrombotic in response to certain pathological conditions, for example, expression of tissue factor, release of P-selectin and plasminogen activator inhibitor-1 (PAI-1) (Sagripanti, Carpi 2000). In response to local tissue (endothelium) injury endothelium releases tissue factor. Tissue factor activates certain coagulation factors. Activated factor X in turn activates prothrombin to thrombin. Thrombin is a protease that activates Protease activated receptors (PARs) (van Hinsbergh 2012, Osterud, Bajaj et al. 1995). They are G-protein coupled receptors (GPCRs) consisting of seven transmembrane alpha helical moieties and interconnecting loops spanning these transmembrane moieties. There are four members of PAR family receptors PAR1, PAR2, PAR3 and PAR4 (Adams, Ramachandran et al. 2011). Protease activated receptors (PARs) are expressed on EC and are activated by thrombin (Ishihara, Connolly et al. 1997). Thrombin is expressed by endothelial cells in response to vascular injury (Coughlin 2000).

1.1.1.3 Role of endothelial cells in inflammation

Inflammation is a protective response against any harmful stimuli/state for example; microbial infection, tissue injury and any toxic condition. It is an immune response by the cells with an

aim to remove the detrimental effect and to correct the harm caused (Ahmed 2011). Inflammation is an adaptive response which is strongly connected to haemostasis (Medzhitov 2010).

1.1.1.3.1 Features of inflammation

The classical description of inflammation involves the changes observed visually. Inflammation is classically characterised by 5 features of redness, swelling, pain, heat and loss of function. Thus, the sensation of heat is caused by the increased movement of blood through dilated vessels into the environmentally cooled extremities, also resulting on the increased redness. The swelling (oedema) is the result of increased passage of fluid from dilated and permeable blood vessels into the surrounding tissues, infiltration of cells into the damaged area, and in prolonged inflammatory responses deposition of connective tissue. Pain is due to the direct effects of mediators, either from initial damage or that resulting from the inflammatory response itself, and the stretching of sensory nerves due to oedema. The loss of function refers to either simple loss of mobility in a joint, due to the oedema and pain, or to the replacement of functional cells with scar tissue. (Punchard, Whelan et al. 2004).

1.1.1.3.2 Molecular mechanism of inflammation

Host cells express certain transmembrane molecules called Pattern recognition receptors (PRRs) that recognise and sense the presence of any microbial or any other cellular damage (Akira, Uematsu et al. 2006). The recognition of pathogen and internal damage is due to their expression of pathogen associated molecular patterns (PAMPs) or internal injury derived molecules, danger associated molecular patterns (DAMPs). PRRs includes Toll-like receptors (TLRs) and NOD like receptors (Ahmed 2011). The interaction between these molecules results in the activation of transcription factor NF-κ-B and production of pro-inflammatory cytokines for example TNF, IL-1 and IL-6 (Honda, Takaoka et al. 2006), (Medzhitov 2010). Inflammation is an innate immune response in immune cells for example macrophages and neutrophils however, non-immune cells also including endothelial cells, epithelial cells and fibroblasts can also initiate inflammatory reaction (Akira, Uematsu et al. 2006). Mammalian NF-κB family is composed of 5 proteins namely: p50, p52, c-Rel, RelA and RelB (Ghosh, May et al. 1998). In unstimulated cells NF-κB protein is maintained in the cytoplasm by ankyrin repeat-containing

IκB proteins. Upon phosphorylation of IκB, NF-κB is released and translocates to the nucleus. In the nucleus it stimulates the release of inflammatory cytokines (Vallabhapurapu, Karin 2009). Other transcription factors that play roles in the stimulation of inflammatory genes include activator protein-1 (AP-1) (Greenberg, Ziff 1984), cyclic-AMP (cAMP) response element binding protein (CREB), a cAMP-induced factor (Montminy, Bilezikjian 1987) and serum responses factor (SRF) (Treisman 1986).

1.1.1.3.3 Inflammation in endothelial cells

The fact that endothelial cells are in close contact with immune T cells makes it important for immune system to monitor their interaction. Extensive research has been conducted to explore the inflammatory and innate response of endothelial cells while its adaptive immune responses still remain unexplored (Young 2012). Endothelium plays important roles in the inflammatory reaction by expressing different mediators that regulate inflammatory responses (Nathan 2002). Endothelium releases growth factors and cytokines for the recruitment of leukocytes to the site of endothelium injury or infection (Muller 2002). Cytokines induce a proinflammatory phenotype of endothelial cells. In turn, endothelial cells secret PAF in response to tumour necrosis factor α (TNF-α) and interleukin-1α (IL-1) and this recruits neutrophils and platelets (Bussolino et al., 1990). Further to this, leukocytes recruitment occurs due to upregulation of pro-inflammatory genes like cytokines (IL-1, TNF-a), chemokines (IL-8, MCP-1) and adhesion molecules (ICAM-1, VCAM-1, E-selectin) (Collins et al., 1995).

Inflammation is one of the protective responses/mechanism in response to, for example physical trauma and infection. However, it needs to be reversed as uncontrolled inflammation may lead to certain pathological conditions (Michiels 2003). Avirutnan et al showed the release of cytokines from human umbilical vein endothelial cells (HUVECs) in response to dengue viral infection. Their research also showed nuclear translocation of NF-kB, which in turns mediates the release of pro-inflammatory cytokines (Avirutnan, Malasit et al. 1998). In another example, the murine endothelial cell line, b.End5, (mouse endothelial cell line), mediated the release of IL-6 and Toll like receptor 2 (TLR2) in response to a bacterial toxin, obtained from *Staphylococcus epidermidis* (Robertson, Lang et al. 2010). PARs may also be a pro-inflammatory mechanism of endothelial cells. PAR1 mRNA has been found in endothelial and smooth muscle cells of atherosclerotic arteries (Nelken, Soifer et al. 1992). TNFα, IL1-α and

lipopolysaccharide (LPS) are inflammatory mediators which cause an increase in PAR2 at both mRNA and protein level in human endothelial cells (Rollins, Yoshimura et al. 1990).

1.1.2 Heterogeneity of endothelial cells

EC possess different phenotypes at different parts of the vascular tree and even between arterial and venous vessels. Cells from different parts in the same individual will respond differently to the same stimulus and may secrete different mediators (Galley, Webster 2004). For example, the blood brain barrier in the brain and retina is formed due to EC tight junctions which allows no transport of molecules to these tissues. While for efficient absorption of intestinal villi, secretion of endocrine glands and filtering of molecules in kidney, the EC are connected by discontinuous junctions (Dejana 1996). In the mouse, pulmonary post-capillary ECs and some splenic venules secrete Lu-ECAM-1 (lung-specific EC adhesion molecule) while endothelial venules in Peyer's patches of the small intestine express mucosal addressing cell adhesion molecule-1 (Bargatze, Jutila et al. 1995).

1.1.3 Endothelial dysfunction

Endothelial dysfunction refers to all the changes in endothelial function that cause the progression and manifestation/pathogenesis of vessels for example, atherosclerosis (Levine, Keaney et al. 1995). Abnormality related to individual normal functions of vascular endothelium such as anti-inflammatory response, angiogenesis, anti-coagulant and fibrinolytic defense and permeability manifest endothelial dysfunction (Goligorsky 2000), (Goligorsky 2005). Definition of endothelial dysfunction cannot simply include all possible interruption in normal functions, as endothelium serves different functions involving different organ systems, hence any change in endothelial functions might have its effect on these systems at the same time or at different times. Endothelial dysfunction can be manifested by either functional changes or any increase/decrease in its chemical secretions, for example an increase in its permeability (Aird 2005). Endothelial dysfunction is a valuable tool for studying mechanisms relating to cardiovascular disease pathogenesis and therapeutic strategies designed towards their treatment (Vita, Keaney 2002).

Endothelium has several vital physiologic roles as outlined above and so endothelial cell dysfunction is considered a pivotal mechanism for development of CVD (Landmesser, Drexler 2005). Endothelial cell dysfunction is considered as the main cause for the development of cardiovascular diseases and cardiovascular-related complications of kidney disease (Goligorsky 2005). Endothelial vasodilator dysfunction is a recognized tool for assessing endothelial dysfunction and Schachinger et al found that arterial endothelial vasodilator dysfunction is an independent diagnostic tool in the study of progression of atherosclerotic cardiovascular diseases (Schachinger, Britten et al. 2000)

Endothelial phenotype is majorly altered during atherosclerosis (Widlansky, Gokce et al. 2003). Atherosclerosis is a multifactorial cardiovascular disease with multiple aggravating factors including endothelial injury. These factors affect endothelium in a way that the endothelial response is dysfunctional. Of particular importance is the decreased NO production during atherosclerosis which is due to suppression of eNOS activity (Cines, Pollak et al. 1998). Naruse et al investigated this in a rabbit model of atherosclerosis, where the disease process was promoted/exacerbated by long term inhibition of NO production. In vessels from the rabbits given L-NAME (an inhibitor of NOS) impaired relaxation responses to acetylcholine were noted consistent with a defect in NO production. Therefore, endothelial can be a critical target to manipulate in atherosclerosis disease prevention (Naruse, Shimizu et al. 1994).

1.1.4 Importance of vascular ageing in the cardiovascular system

Healthspan is the period of life that an individual is disease free. The deleterious effects of ageing can start at different chronological ages for different individuals (Ovadya, Krizhanovsky 2014). Ageing of an organism starts due to the collective decrease in body functions over a period of a life time (Cutler, Mattson 2006, Ovadya, Krizhanovsky 2014). Research is focusing on the newer factors responsible for ageing in organisms. Cellular senescence is one of the important factors controlling health span of organisms (Ovadya, Krizhanovsky 2014). Senescent cells accumulate with age in humans and animals (Jeyapalan, Ferreira et al. 2007a, Krishnamurthy, Ramsey et al. 2006). The adult human heart is composed of one quarter of endothelial cells (Bergmann, Zdunek et al. 2015), therefore if senescence could occur in endothelial cells it could have major impact on heart functions potentially leading to CVD.

Senescence is a potent barrier against tumorigenesis, however it also contributes its protective role in the non-cancerous pathologies. For example, senescence helps to reduce liver fibrosis induced by treatment with CCl4 in a mouse model (Krizhanovsky, Yon et al. 2008). In addition, these senescent hepatic cells that were developed to limit fibrosis, were depleted after fibrosis was cleared (Krizhanovsky, Yon et al. 2008). Ionizing radiations induce senescence in cardiac endothelial cells *in vivo* with increased expression of senescence markers p21 and p16 (Azimzadeh, Sievert et al. 2015). This might be protective as the presence of senescent endothelial cells inhibits angiogenesis.

Increased production of reactive oxygen species (ROS) is observed with human ageing (Sergiev, Dontsova et al. 2015), which can be responsible for the spread of oxidative damage to its neighboring cells (Wang, Boerma et al. 2016). In endothelial cells ROS are responsible for induction of senescence and overexpression of certain microRNAs that are involved in cellular senescence and apoptosis (Magenta, Cencioni et al. 2011). Senescent endothelial cells secrete a number of proinflammatory cytokines including IL6 and IL8 which can promote a proinflammatory microenvironment (Khan, Awad et al. 2017). Therefore, senescent endothelial cell accumulation in human heart could contribute, in part, to cardiovascular pathologies. This is supported by research conducted by Minamino et al who found SA-beta-gal positive cells in the atherosclerotic plaque from patients with atherosclerosis but not in the internal mammary artery which is not a prime site for atherogenesis. These SA β-gal positive cells were also positive for factor-VIII during immunohistochemical analysis, demonstrating them to be vascular endothelial cells (Minamino et al 2002).

In experimental models, aged endothelial cells are associated with increased monocytic adhesion due to increased expression of certain adhesion molecules e.g. ICAM-1 and CD44 (Miyuki et al, 2011 and Mun et al, 2010). Monocytic adhesion to the endothelium is an early step during atherosclerosis, facilitating the infiltration of monocytes into the vessel wall and thereby initiating atherosclerosis (Dona Lowe Kenneth Raj 2014). Figure 1-2 shows the possible role of senescent endothelial cell in atherosclerosis.

Vascular endothelial cell senescence has been associated with age-related diseases. Human ageing syndromes such as Hutchinson-Gilford progeria are associated with accelerated atherosclerosis (villa-Bellosta et al 2013).

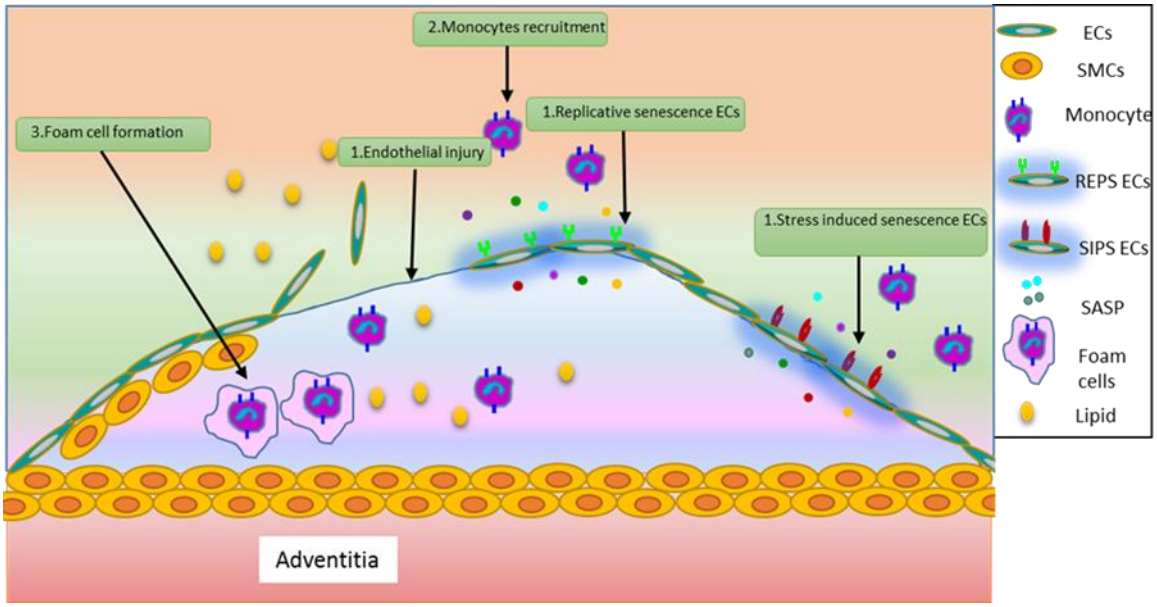

Figure 1-2: Schematic of atherogenesis and formation of atherosclerotic plaque. Adapted from (Wang & Bennett, 2012).

1) Replicative (REPS) and stress induced senescent (SIPS) endothelial cells (ECs) accumulate in the vessel wall due to age or either in response to stress respectively. These senescent ECs release SASP and expresses adhesion molecules (E-selectin, CD44) on the cell surface promoting inflammation. 2) Adhesion molecules recruit monocytes and with endothelial injury they infiltrate into the vessel wall. Lipids also infiltrate into the vessel wall. 3) Macrophages engulf LDL results in foam cells formation, inflammation and atherosclerosis plaque formation.

1.1.5 Endothelial ageing

Apart from the gross morphological changes that are associated with ageing in blood vessels such as increased vascular stiffness and enlargement of the lumina, it is known that ageing also affects the endothelial layer within the blood vessels (Yildiz 2007). As endothelial cells age, a number of changes occur including changes in the structure of the cells e.g. alterations in the cytoskeleton and an increase in the number of cells with polyploid nuclei (Najjar, Scuteri et al. 2005). The production of certain growth factors and vasodilatory factors is also known to alter in ageing cells. These changes can either individually or collectively lead to vascular endothelial dysfunction. This in turn can play a vital role in the cause and progression of cardiovascular diseases (Brandes, Fleming et al. 2005). (fig 1-3).

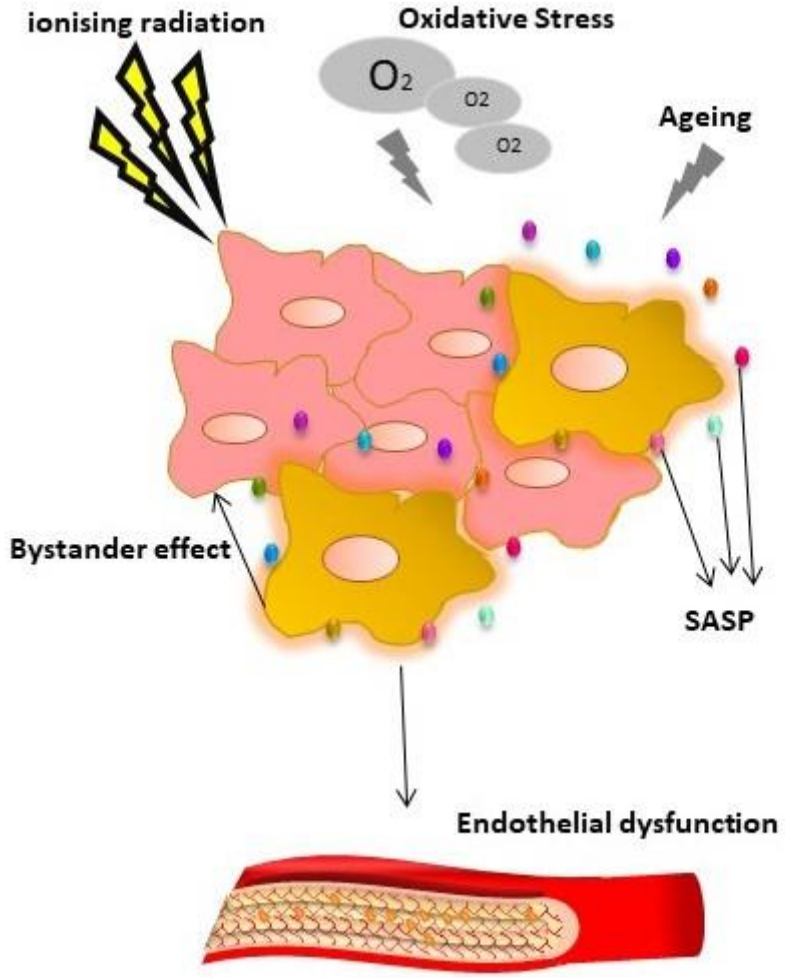

Figure 1-3: Multiple factors triggering senescence in endothelial cells and its proposed effects (SASP and bystander) causing endothelial dysfunction..

Multiple stresses including radiation, oxidative stress or ageing can induce cell senescence in endothelial cells. Senescent EC can be pro-inflammatory with enlarged morphology compared to normal EC. They can recruit immune cells locally or can induce DNA damage in a paracrine manner as a bystander effect through the release of multiple factors (SASP). This results into accumulation of senescent endothelial cells in vasculature causing endothelial dysfunction, contributing to multiple cardiovascular diseases. Red object represent Longitudinal section of vessel and amber colour represents accumulation of senescent ECs.

1.1.5.1 Types of senescence

There are two main types of senescence

1.1.5.1.1 Replicative senescence

Hayflick and Moorhead found the inability of fibroblasts to divide further after serial passaging in culture and termed it as "Replicative senescence" or REPS (Hayflick 1961). Replicative senescence (REP) is determined by inability of *in vitro* primary mammalian cells in culture to divide despite growth stimuli (Becker 2013) and presenting modified cell morphology, functions and gene expression. It is suggested that endothelial cell senescence *in vivo* is associated with a number of age related disorders such as hypertension, diabetes, heart failure and atherosclerosis (Cines, Pollak et al. 1998). The notion is further supported by the fact that senescent cells presenting a senescence associated phenotype caused by telomere shortening have been found in atherosclerotic lesions and they might contribute to atherogenesis (Minamino et al 2002). Replicative senescence is the result of a genetic program. Oxidative damage is one mechanism for triggering REPS (Chen, Q. M. 2000).

1.1.5.1.1.1 Telomeres

In most eukaryotes the distal ends of chromosomes are capped/protected by repeated sequence of guanine rich nucleotides called telomeres. The function of these telomeres is chromosomal stability and its complete replication. Chromosomes with no telomeres result in chromosomal erosion and instability as telomeres prevent the enzymatic effect of exonucleases on chromosomal ends (Blackburn 2001). During cell cycle replication DNA polymerase requires a primer to initiate the uni-directional copying of DNA from 5'-3'. Some of the portion of DNA at 5' lags behind and not copied (Geserick, Blasco 2006) and so DNA polymerase lacks the ability to completely replicate the 5' end of chromosomes during each cell division (Gilson, Geli 2007). This phenomenon was termed the 'end replication problem' by Alexey M. Olovnikov (Olovnikov 1971). DNA double strand breaks arise every day in every cell as a result of reactive oxygen species attack on DNA bases (McKinnon, Caldecott 2007). DNA double strand breaks stimulate DNA damage response and if unrepaired cause the cells to undergo senescence or apoptosis (Blasco, M.A 2005). Telomeres help cells differentiate double strand breaks from natural chromosomal ends (Blackburn 2001), preventing initiation of the cellular DNA damage response besides protection of chromosomes from degradation (Blasco. M.A 2005). In humans, the end of the telomere is composed of repeated sequence of TTAGG; in human somatic cells this consists of ~4kb of this repeated sequence while a higher value of 9kb in human sperm cells.

Telomerase is a ribonucleic protein that is involved in telomere synthesis (Yu et al 1980) by coding for telomere repeats. Telomere length shortens during each cell division (called telomere attrition) due to lack of telomerase in most human cells (Counter et al 1992). The evidence is supported by the work of Calvin *et al* who confirmed the loss of mean telomere length by 2kb in different strains of fibroblasts with each population doubling (Harley, Futcher et al. 1990). The loss of telomeres during each cell cycle functions as a mitotic clock which allows the cell to count the number of cell divisions (Harley 1991) and eventually leads to senescence after significant loss of telomere (Vaziri, Schachter et al. 1993). Kim et al conducted a survey in which they measured the telomerase activity in 100 immortal cell lines and 22 normal somatic cell cultures. Out of 100 immortal cell lines 94 were positive for telomerase activity while none of the normal somatic cell lines were positive for telomerase (Kim, Piatyszek et al. 1994). Blasco et al found a decrease in telomere length accordingly with each cell division in germ cell lines of a mouse model lacking telomerase RNA (Blasco, Lee et al. 1997).

Recently Hewitt et al have investigated the role of genotoxic and oxidative stress causing DDR and its effect on telomeres in cellular senescence. They confirmed that exogenous oxidative damage agents induced telomere associated foci (TAF). Further, to confirm the role of telomere damage in the ageing process, they investigated the age-related telomere damage in the mouse cells expressing telomerase. They found age related TAF irrespective of telomerase presence (Hewitt, Jurk et al. 2012). The possible explanation for senescence, independent of telomere length is that, telomeres inhibit the non-homologous end joining (NHEJ). NHEJ is the important DNA repair mechanism in response to DNA damage. Damage in telomeres is sensed as DNA damage by the cell, but there is no default repair system.

1.1.5.1.2 Stress induced premature senescence

A distinct but related type of cellular senescence is known as stress induced premature senescence (SIPS or ‘Premature Senescence’) (Landmesser, Drexler 2005), which is induced by certain noxious stimuli such as UV light, ionizing radiations and oxidative stress (Jee, Kim et al. 2009), (Yentrapalli, Azimzadeh et al. 2013), (Chen, Q., Ames 1994).Oxygen concentration inside our body is lower than environmental oxygen (21%). By exposing cells to higher concentrations of oxygen than biological oxygen causes the formation of free radicals by biochemical reactions (Chen, Q., Fischer et al. 1995). Human dermal fibroblasts (HDFs)

show increased population doublings (PDs) (by ~20PDs) when they are cultured in an environment having lower oxygen concentration, for example, <3% oxygen (Balin, Goodman et al. 1976). Hydrogen peroxide (H_2O_2) and tertiary-Butyl hydroperoxide (t-BHP) are peroxides that have been use as oxidative stress agents in the study of oxidative stress injury (Schnellmann 1988), (Farber 1994). According to Chen et al the protocol for inducing stress induced premature senescence is the exposure of early passage HDFs to sub lethal concentration of H_2O_2 for short periods of time followed by exposure to normal culture conditions. The resulting cells lose replicative ability even when stimulated with growth factors and serum. H_2O_2 treated early passage HDFs share the same phenotypic features as REP counterparts (Chen, Q., Ames 1994).

We used tertiary butyl hydrogen peroxide (t-BHP) as a stress inducer for induction of stress induced senescence of endothelial cells. Exposure of cells to either t-BHP or H_2O_2 results into the oxidation of enzyme glutathione, and NADPH, lipid peroxidation and altered calcium homeostasis (Schnellmann 1988), (Farber 1994). This suggest that the mechanism of cell injury by both the agents is the same. While a higher concentration of H_2O_2 is required compared to t-BHP to cause the same level of damage in renal cortical slices and human colon carcinoma cells. Whereas, in certain cultured cells both function at the comparable concentration (Kim, Ko et al. 1998). This might suggest a more powerful anti-oxidant mechanism in those tissues against H_2O_2. H_2O_2 is a pale-blue liquid, freely soluble in water. In high concentrations it is toxic in many cell types *in vitro*. H_2O_2 is also very toxic *in vivo* and certain enzymes for example, catalases and peroxidases are required to eliminate it from the body. The cytotoxic potential of H_2O_2 comes from the formation of hydroxyl radical ($OH^{\bullet}$) catalysed by metal ions.

$Fe^{2+} + H_2O_2 = \text{intermediate complexes (ferryl??)} \rightarrow$

$Fe^{3+} + OH^{\bullet} + OH^{-}$

in vivo H_2O_2 is generated by dismutation of superoxide radical ($O_2^{\bullet-}$) by enzymes superoxide dismutase (Halliwell 2006). H_2O_2 is also an intracellular signalling agent and participates in physiological processes (Spencer, Jenner et al. 1996). For example, during inflammatory process phagocytes generate H_2O_2 which in turn modulates the expression of adhesion molecules, cell proliferation and apoptosis (Wang, X., Martindale et al. 1998), (Hampton, Orrenius 1997), (Clement, Ponton et al. 1998).

1.1.5.2 Features of senescence

Senescent human dermal fibroblasts stay alive and metabolically active for a long time in culture, but they will differ from non-senescent HDF in morphological, physiological and biochemical features (Toussaint, Medrano et al. 2000).

1.1.5.2.1 SA-βgal activity

Senescent cells express an enzyme detectable at pH6 known as senescence-associated beta galactosidase. It has been detected in the cultured senescent fibroblasts and aged human keratinocytes at pH6. This activity is not expressed by pre-senescent, terminally differentiated and quiescent cells (Dimri, Lee et al. 1995). SA-β-gal is used as a universal biomarker for detection of senescence but its origin and function in cellular senescence is not very clear. It has not been confirmed yet whether it is an independent enzyme detected in senescent cells at pH6, or whether it is the typical lysosomal β-galactosidase with an increased expression and activity at pH6 in senescent cells. Kurz et al detected the origin of SA-β-gal and found that its activity in senescent cells is due to increase in lysosomal β-galactosidase (Kurz, Decary et al. 2000). REPS and SIPS senescent endothelial cells express increased expression of SA-β-gal (Khan, Awad et al. 2017, Yentrapalli, Azimzadeh et al. 2015).

1.1.5.2.2 Cell morphology

An increase in size and flattened cell morphology are features of senescent cells (Minamino, Miyauchi et al. 2002). Some cell types form senescence associated hemochromatin foci (SAHF). This SAHF is the result of decondensation of centromeric satellite heterochromatin (Swanson, Manning et al. 2013).

Cultured cells reach REPS after some time and then progress to late (deep) senescence. Another process related to late senescent cells is the infiltration of chromatin into the cytoplasm forming cytoplasmic chromatin fragments (CCF) (Ivanov, Pawlikowski et al. 2013).

1.1.5.2.3 SASP

SASP factors from senescent cells are procarcinogenic and favor the malignant transformation of the cells surrounding the senescent cells (Coppe, Desprez et al. 2010). The dual behavior of the senescent cells is better explained by the antagonistic pleiotropy of ageing. According to this theory, a process or mechanism having beneficial effect initially but later in lifespan it has a detrimental effect. All dividing cells are at risk of developing cancer. Organisms have evolved the process of senescence as a protective measure. But the role of senescence in causing ageing is rather the side effect (Campisi, d'Adda di Fagagna 2007). In other example as age progresses, senescence decreases the regenerative ability of the organism causing defects in repair. This put a stop to the cell division (Yun 2015). Release of SASP factors by senescent cells can promote senescence in neighboring normal cells via a bystander effect. For example, Jurk et al (2014) co-cultured radiation-induced senescent mouse embryonic fibroblasts (MEFs) with a reporter cell expressing 53BP1. DDR was observed in bystander cells, confirming the autocrine and paracrine effect of SASP (Jurk, Wilson et al. 2014). Evidence that senescence is beneficial in early life comes from the work of Yun et al, limb amputation in salamander resulted in cell senescence and SASP production. Removal of senescent cells at the time of regeneration of amputated limbs slowed down the regeneration process. After the full development of limb was achieved these SASP producing cells were cleared by the immune system. When extrinsic senescent cells were implanted in the newt developing limb these cells persisted for initial phase and contributed in the limb development. While cleared when limb was fully developed (Yun, Davaapil et al. 2015). A number of studies have characterized SASP but the gene and protein changes are maintained by individual cell types. SASP comprises of few families of factors that act upon the neighboring cells surface receptor and mediate certain pathological conditions including cancer (Coppe, Desprez et al. 2010).

A number of studies have shown that SASP is comprised of several different proteins, including interleukins (IL-1, IL-6 and IL-8), insulin like growth factor binding protein (IGBFP-5) and tumour necrosis factor (TNF-α). There is also evidence that PAI-1 is found to be a marker for oncogene induced senescence. PAI-1 mRNA is also found in radiation induced senescent HUVECs (Xu, Tchkonia et al. 2015a). Whilst experiments showed that PAI-1 is a p53 downstream target and involved in the senescence induction process. The possible prevention of the detrimental effects of SASP can be obtained by selective removal of senescent cells and

effectively switching off SASP. Nevertheless, there is not much evidence that supports the involvement of SASP in the ageing process. Previous research has suggested that inhibition of certain SASP components can contribute to the healthy ageing process (explained later in the possible intervention in senescent endothelial section).

Very few studies have been conducted in order to explore the composition of SASP in endothelial cells. An *in vitro* study conducted by Hampel et al in REPs HUVECs confirmed upregulation of IL-8, IGFBP-3, IGFBP-5 and VEGI proteins (Hampel, Fortschegger et al. 2006a). JAK2 is a JAK family protein, associated with cytokines and growth factor regulation (Richard, Stephens 2011). Ming et al found JAK upregulation in radiation induced senescent HUVECs. Similarly, a JAK inhibitor was able to inhibit SASP components secretion such as; IL6, IL8, MCP1 and PAI-1 in irradiated senescent HUVECs (Xu, Tchkonia et al. 2015b).

In certain cell types, SASP formation requires the DDR. $P16^{INK4a}$ is a common senescence marker Consistent with this Coppe et al showed that ectopic $P16^{INK4a}$ expressing human fibroblasts cells failed to induce DDR. They also confirmed that ectopic $p16^{INK4a}$ expression had no effect on the secretory profile of Ras and X-ray induced senescent W1-38 cells. Thereafter they found that $p16^{INK4a}$ deficient replicative senescent fibroblasts expressed a similar pattern of SASP components in an anti-body array experiment in X-ray induced and replicative fibroblasts (Coppe, Rodier et al. 2011). This confirms that SASP requires the DDR irrespective of the senescence stimulus. Tumours microenvironments also consist of SASP, changing the behavior of tumour cells. As senescent cells accumulate with age, therefore tumours occurring at later age would have a different microenvironment than at it occurring younger age. Brouwers et al have shown that breast cancer in older subjects showed upregulation of genes that are related to migration and invasion compared to younger subject with breast cancer. SASP related genes were also upregulated in older subjects (Brouwers, Fumagalli et al. 2017).

Research for the investigation of endothelial cell SASP is still in its infancy. More research is required in this context for understanding of the potential role of senescence in endothelial cells in disease progression.

1.1.6 Cellular senescence, its mechanism and role in ageing

Ataxia telangiectasia mutated (ATM) is a serine/threonine protein kinase and is a member of phosphoinositide-3-kinase (P13K) related protein kinase (PIKK) family. ATM helps in repair of DNA double strand breaks (DSBs) (Lavin 2008). In cells, ATM is activated (phosphorylated) by DNA DSBs where it interacts with cell cycle check point (CHK), localises at the damaged sites and increases the duration of cell cycle so that DNA repair can be facilitated (Berkovich, Monnat et al. 2007) (fig 1-4). Apart from CHK2, ATM also phosphorylates p53 and other proteins (Pellegrini, Celeste et al. 2006). Following senescence in HUVECS, ATM phosphorylates Akt. Akt in turn is responsible for activation of cyclin dependent kinase inhibitor p21 through senescence inducer p53 *in vitro* (Zhan, Suzuki et al. 2010). p21 decides the cell fate and is the major driver of senescence. SIPS is suggested to play a protective role against the uncontrolled/unchecked cell proliferation which could otherwise lead to cancer development (Gonzalez, Ghadaouia et al. 2016). The presence of senescent cells in premalignant tumours but not in malignant cells is evidence for the protective role of senescence in cancer. The role of senescence as an important tumour suppressive mechanism has been discussed (Michaloglou, Vredeveld et al. 2005a).

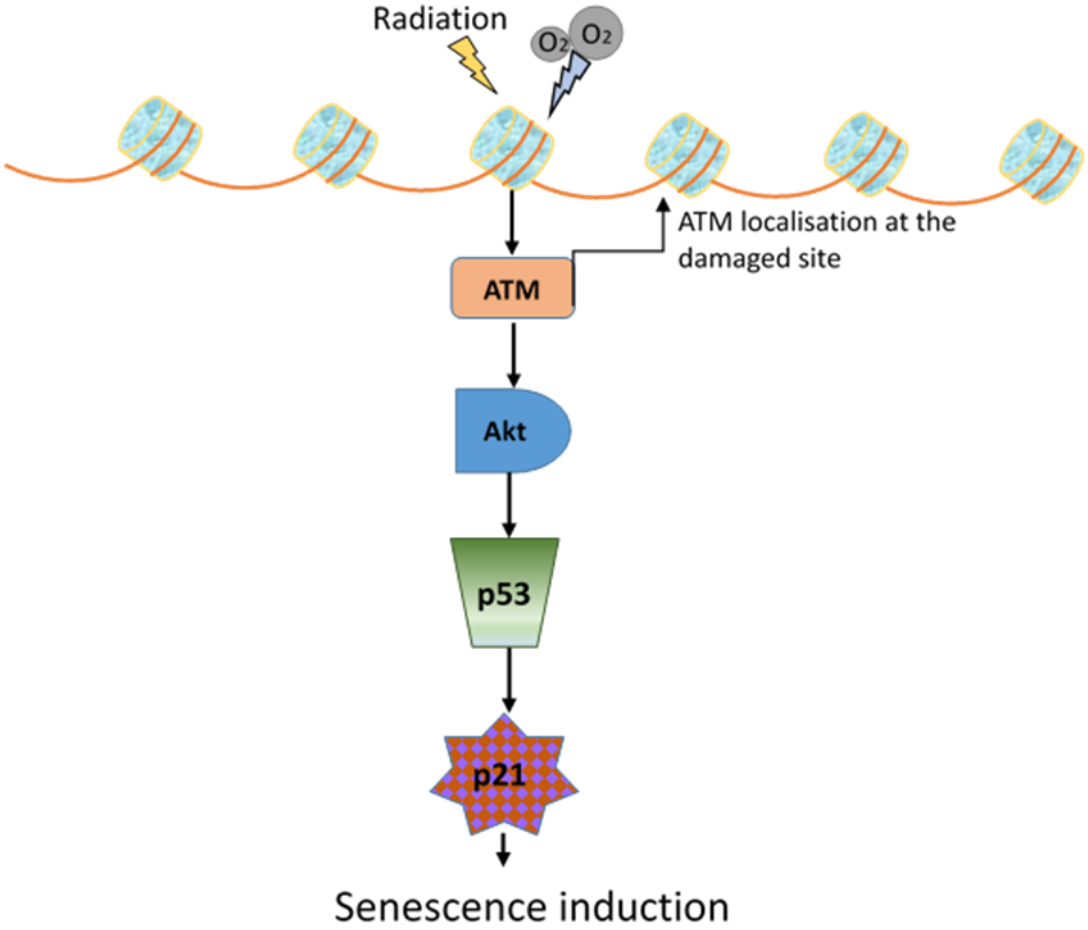

Figure 1-4: Mechanism of senescence induction.

In response to radiation or oxidative stress, DNA DDR is activated. DNA DSBs activate repair protein ATM, which in turn activates Akt while for complete repair ATM is also localised at the site of damage. Senescence is induced when Akt activates the cell cycle dependent kinase inhibitor p21 through p53. p21 is the senescence inducer.

1.1.7 Cellular senescence as a pathophysiological phenomenon

Senescence presents a certain phenotype of flattened morphology, cells staining for the senescence-associated β-galactosidase activity (SAβ-gal) (Dimiri et al 1995) and release of a group of proteins and peptides called senescence-associated secretory phenotype (SASP) or senescent messaging secretome (SMS) (Coppe et al 2008), (Kuilman et al 2008). SASP has some beneficial effects but it also may play a pathophysiological role. SASP reinforces

malignant and premalignant epithelial cell proliferation both in culture and *in vivo* (Krtolica, Parrinello et al. 2001a), (Liu, Hornsby 2007a). Senescent cells have a bystander effect, inducing senescence in neighbouring cells. When senescent mouse adult fibroblasts (MAFs) were co-cultured with non-senescent MAFs, DNA damage was observed in non-senescent MAFs (Jurk et al 2014). In addition to tumour progression and bystander effects, senescent cells are believed to be promoting age-related pathologies because senescent cells accumulates with age in animals including humans, zebrafish and rodents (Dimri, Lee et al. 1995), (Jeyapalan, Ferreira et al. 2007b), (Krishnamurthy, Torrice et al. 2004). Recently Baker et al have shown that selective removal of senescent cells delays the onset of age-related diseases and clearance of senescent cells in elderly mice delays the progression of already established diseases (Baker et al 2011).

FOXO4 belongs to a family of FOXO, a family of transcription factors. FOXO factors are key players in the induction cell death, cell proliferation, and antioxidant stress (Calnan, Brunet 2008), (Burgering 2008). FOXOs were initially classified as downstream signaling components of insulin through phosphoinositide-3kinase (PI-3K) and protein kinase B (PKB/AKT) but later research found their role in tumor suppression and apoptosis (Paik, Kollipara et al. 2007), (Medema, Kops et al. 2000). FOXO favors the cell to undergo senescence by putting a bar to apoptosis. Recently Baar et al used a specific target called FOXO-DRI, against FOXO4 which only blocks the P53-FOXO4 complex and does not affect the functions of these individual (p53 and FOXO4) proteins. They confirmed the selective removal of SASP producing senescent cell. This prevent the loss of renal functions in an ageing mice model (Baar, Brandt et al. 2017).

1.1.8 Evidence of Endothelial cell senescence

Endothelium has a very low cell renewal capacity. There is an increased rate of endothelial replication at the site of arterial bifurcation and branching points (Wright 1968). These are atherosclerotic prone areas in humans most probably because of the haemodynamic forces causing stress and injury to the endothelium (Glagov, Zarins et al. 1988). To overcome this stress, in order to maintain its integrity, endothelium increases cell replication (Langille, Reidy et al. 1986). It is therefore possible that areas of the human vasculature with chronically increased endothelial turnover will have a higher population of replicative senescent cells. Human vasculature is also prone to a number of other stresses i.e. reactive oxygen species,

oxidative lipoproteins and oxidative metabolites released from activated macrophages (Harrison, Griendling et al. 2003) and it is likely that all of these factors together add to the process of senescence *in vivo* (Erusalimsky, Kurz 2005). Endothelial cells from atherosclerotic lesions within aortic, carotid and coronary arteries share morphological feature with REPS endothelial cells in culture (Repin, Dolgov et al. 1984). Aviv et al pointed out that vascular endothelial cells from human aorta exhibit the features of aneuploidy and short telomere length in old individuals as compared to young individuals (Aviv, Khan et al. 2001). Furthermore, a role for endothelial senescence *in vivo* is supported by the work of Minamino *et al* who found enlarged and flattened SA-β-gal positive cells in the atherosclerotic plaque as compared to endothelial cells from non-diseased areas (fig 1-5) (Minamino, Miyauchi et al. 2002). The presence of senescent EC at the site of an atherosclerotic plaque suggests a potential role in the development of stroke, infarct and atherosclerosis (Hampel B 2006).

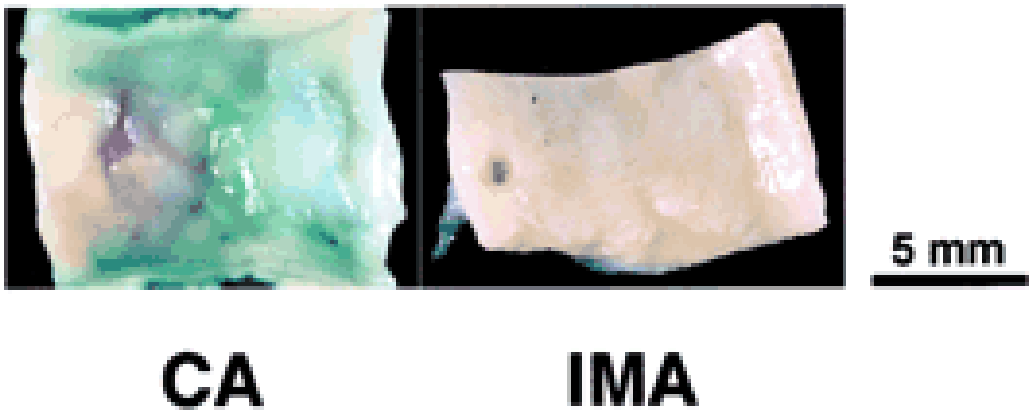

Figure 1-5 SA β gal positive staining in the human coronary artery.

Human coronary artery (left) but not internal mammary artery (right) showed SA β-gal positive stain. (Minamino, Miyauchi et al. 2002a).

1.1.9 Are senescent endothelial cells pro- or anti-inflammatory?

Chronic, low grade inflammation, related to several pathologies, accelerates ageing in mice (Franckhauser, Elias et al. 2008), (Youm, Grant et al. 2013). Age is a major risk factor in many diseases, for example CVD, type II diabetes, arthritis, liver disease and metabolic syndrome (Green, Galluzzi et al. 2011), these pathologies are associated with chronic low-grade inflammation. Based on the above facts senescent cells are considered as major contributors of inflammaging. Inflammaging is a phenomenon of low grade chronic inflammation leading to age related impaired body functions (Franceschi, Campisi 2014).

In agreement, there is an accumulating evidence that NFkB is increased in the endothelial cells of healthy aged men (Donato et al 2002), due to decreased expression of IκBα (Donato et al 2008). IκBα is an inhibitory protein that sequester NFkB in an inactive form in the cytoplasm.

Mitochondria play an important role in senescence induction (Birch, Passos 2017). Studies have shown that mitochondria induce senescence by generation of reactive oxygen species (ROS) that results in a DDR. (Passos, Nelson et al. 2010), (Passos, Saretzki et al. 2007). Similarly, the role of mitochondria in the inflammatory response of senescent endothelial cells is also possibly due to production of ROS as mitochondria-targeted antioxidant treatment attenuated the TNF-α-induced adhesion protein expression in endothelial cells (Zinovkin 2014).

Whether there is a pro-inflammatory or anti-inflammatory role of secreted factors (SASP) from senescent endothelial cells is under some debate. The evidence for an anti-inflammatory role of senescent endothelial cells comes from the work of Coleman et al who have found a novel senescence gene 'SENEX' that appeared to be present only in endothelial cells that was induced into senescence by extrinsic stressors (Coleman, Hahn et al. 2010). When SENEX was over-expressed in endothelial cells, an anti-inflammatory phenotype was noted (Coleman, Hahn et al. 2010). When studied at the single cell level, 50% of the stressed senescent endothelial cell population displayed an anti-inflammatory phenotype (Coleman, Chang et al. 2013, Coleman, Hahn et al. 2010).

Conversely, Azimzadeh et al found increased expression of adhesion molecules including ICAM-1 and VCAM-1 in radiation induced senescent cardiac endothelial cells. Furthermore, functional and biological pathway analysis following proteomics analysis of radiation-treated endothelial cells showed the "inflammatory response" to be most altered (Azimzadeh, Sievert et al. 2015).

The anti-inflammatory properties of SIPS endothelial cells was dependent on the formation of caveolae (and resultant inhibition of NFkB signalling) as blocking this protein with siRNA blocked the anti-inflammatory and increased the proinflammatory phenotype of SIPS endothelial cells. Similarly, upon over-expression of SENEX, endothelial cells isolated from aorta of CAV-$1^{-/-}$ mice failed to develop an anti-inflammatory population (Powter et al, 2015).

The more established view (see fig 1-3) is that cell senescence leads to a pro-inflammatory phenotype via intrinsic changes to the senescent cell itself or due to paracrine effects of secreted factors (SASP) in line with the secretome of a number of different cell types (Coppe, Patil et al. 2008a, Eman, Regan-Klapisz et al. 2006a, Coppe, Desprez et al. 2010, Prattichizzo, Giuliani et al. 2016a) SASP as a mediator in ageing and age-related CVD has been proposed with IL-8 a major up-regulated component of SASP in senescent EC.

Composition of SASP depends on the stimulus that triggers senescence. The most common secreted factors are growth factors, proteases, cytokines and chemokines. Inflammatory proteins such as MMP-1, MMP-3, monocyte chemotactic protein (MCP), IL-1, IL-6 and IL-8 are the most commonly reported secreted of these factors (Kumar, Millis et al. 1992), (Wang, S., Moerman et al. 1996).

Blockade of TNF-α by adalimumab reduced IL6 secretion and increased eNOS in HUVEC cultures implying a pro-inflammatory mechanism of SASP production (Francesco et al 2015).

On balance, there is more evidence to suggest that endothelial cell SASP is pro-inflammatory and that components of this phenotype might be appropriate targets for novel treatments aimed at ameliorating the effect of vascular ageing.

1.1.10 Role of adhesion molecules in leukocytes-endothelium interaction: effect of senescence in endothelial cells

1.1.10.1 ICAM-1 and VCAM-1

ICAM-1 is an immunoglobulin (Ig) like transmembrane protein with molecular weight ranging from 80 -114kDa. It is a cell adhesion molecule expressed by many cell types including endothelial cells and leukocytes (Lawson, Wolf 2009). The ICAM-1 gene consists of 7 exons and six introns (van de Stolpe, van der Saag 1996). ICAM has a very important role in both innate and adaptive immune responses.

VCAM-1 is another member of the Ig superfamily of proteins. Together with other adhesion molecules it has a very important role in the regulation of inflammation. The importance of VCAM-1 has also been reported in cardiovascular diseases (Cook-Mills, Marchese et al. 2011). VCAM-1 is involved in the development of atherosclerosis, as the first adhesion molecules that is expressed before atherosclerotic plaque formation in hypercholesterolemic rabbits and mice (Iiyama, Hajra et al. 1999) , and expression correlates with monocytic adhesion in atherosclerotic carotid artery (Huo, Hafezi-Moghadam et al. 2000).

Trans-endothelial migration during inflammation is an important process which is comprised of four steps (fig 1-6). The first step involves the rolling of leukocytes on endothelium. This step involves selectins i-e E-selectin present on the endothelium and L-selectin present on leukocytes. Respective ligands for both selectins are present on both cell types. Interaction between leukocytes and endothelial cells slows down the rolling of leukocytes, therefore exposing them to chemokines including IL-8. Step 2 involves the firm attachment of leukocytes to endothelium. Integrins are expressed on leukocytes surfaces which require activation and conformational changes by chemokines. This results into stronger adhesion of leukocytes to endothelium. Step three is the spreading and slow migration of leukocytes through the endothelium. ICAM-1 is important for step 3 of trans-endothelial migration (Greenwood, Wang et al. 1995). Although research has also identified the important role of ICAM-1 in the initial step 1 of trans-endothelial migration (Reiss, Engelhardt 1999). Also VCAM-1 is responsible

for the migration step in the trans-endothelial migration, as blocking VCAM-1 inhibits the migration of leukocytes in VCAM-1 expressing endothelial cells (Abdala-Valencia, Berdnikovs et al. 2011). ICAM gene has been reported to be upregulated in the replicative senescent endothelial cells (Yanaka, Honma et al. 2011a). Similarly, recently ICAM-1 and VCAM-1 showed increased expression and monocytic adhesion has been reported in arginase-induced senescent endothelial cells (Zhu, Yu et al. 2017). ICAM-1 and VCAM-1 association with inflammation and senescence suggest its role in age related atherosclerosis.

1.1.10.2 E-selectin

E-selectin (CD62E) is a 115kDa cell surface glycoprotein member of the selectin family, expressed on endothelial cell surfaces. Interleukins (IL-1) induces E-selectin in endothelial cells and studies implicates its role in the early binding of neutrophils (Pober, Cotran 1990). E-selectin gene is regulated by transcription factor nuclear factor (NF)-κB in response to its exposure to TNF-α. Since it is exclusively expressed by endothelial cells, therefore its expression is tightly regulated in a cell specific manner (Rahman, Kefer et al. 1998a). E-selectin is required for the stabilisation and arrest of rolling leukocytes *in vivo* (Kunkel, Dunne et al. 2000a). Khan et al showed that Chronic TNF-α treatment induces senescence and upregulation of E-selectin in HUVECs (Khan, Awad et al. 2017).

1.1.10.3 CD44

CD44 is a receptor for hyaluronic acid and found on the surface of cells including endothelial cells. It is a protein with a molecular mass of 85 – 90kDa. Its transcripts include splice variants and produce different proteins isoforms. It is involved in different important functions like endothelial cell proliferation, inflammation and cancer promotion (Murphy, Lennon et al. 2005a). *in vivo* endothelial cells do not express CD44 but expression is observed once they are cultured *in vitro*. CD44 expression also increases in the vasculature of humans presenting with solid tumour (Griffioen, Damen et al. 1996). Increased expression of CD44 has been shown in the squamous cell carcinoma (Bruno, Fabbi et al. 2000).

Senescent endothelial cells mediate increased monocytic adhesion due to upregulation of CD44 on endothelial cell surface (Mun, Boo 2010). CD44 has also been reported to be upregulated in

irradiation induced senescent endothelial cells (Lowe, Raj 2014a). This demonstrate the potential pro-atherosclerotic effect of senescent endothelial cells through activation of CD44.

Senescence biomarkers identification in human tumour (Michaloglou, Vredeveld et al. 2005b) and the fact that senescent are present in premalignant cells in a mouse model of adenoma and adenocarcinoma shows a link between senescence and tumour (Collado, Gil et al. 2005a). Therefore, a tumour biomarker could also possibly be a senescence biomarker.

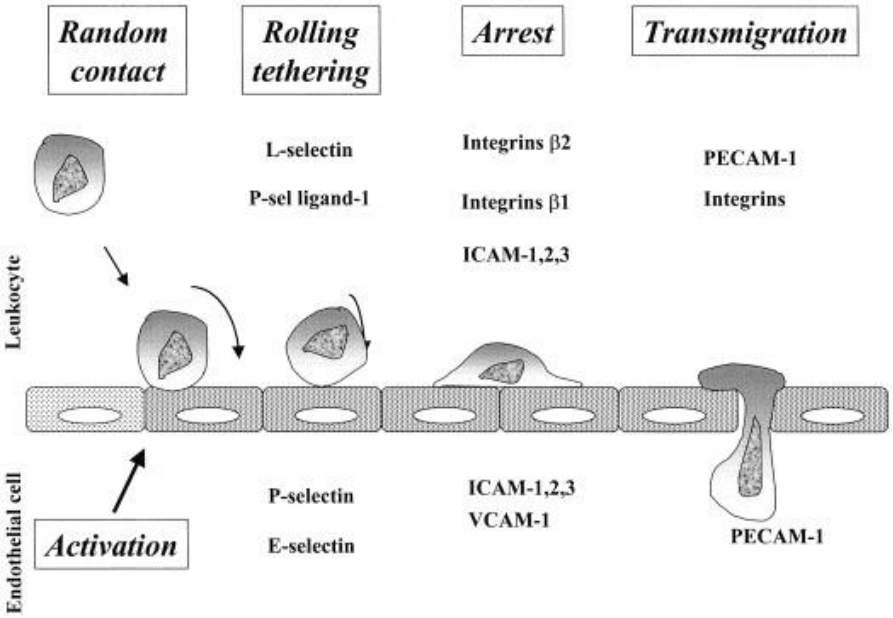

Figure 1-6 Schematic representation of trans-endothelial migration during inflammation.

During the initiation of inflammation leukocytes are recruited at the site of inflammation. E-selectin expressed on the endothelial cells causes the slowing down and attachment of leukocytes, this is followed by firm attachment of leukocytes to the endothelial cells by ICAM-1 and VCAM-1. The final step is the migration of leukocytes through the endothelium. (Blankenberg, Barbaux et al. 2003).

Table 1-1. *In vitro* and *in vivo* senescence markers expressed by different cells under different senescence stimuli

Factor/protein	Expression	Cell type	Stimulus of senescence induction	Reference
P53	↑	MEFs	Glucose deprivation	(Tahara, Sato et al. 1995, Jones, Plas et al. 2005)
P21	↑	BJ, WS1, HUVECs, HDMECs	Ionizing radiations, doxorubicin, H_2O_2, TNF-α	(Zhan, Suzuki et al. 2010, Khan, Awad et al. 2017, Cui, Kong et al. 2013)
SA-β-gal	↑	Human Naevi, mice, diff cells	REPS	(Michaloglou, Vredeveld et al. 2005c)
P16	↑	Mouse lung adenoma, Mice, HUVECs, HDMECs	Oncogene ras, pRB inactivation, TNF-α	(Khan, Awad et al. 2017, Chen, Z., Trotman et al. 2005, Lazzerini Denchi, Attwooll et al. 2005)

P15	↑	Mouse lung adenoma,	Oncogene ras	(Chen, Z., Trotman et al. 2005)
ARF	↑	Mice,	pRB inactivation	(Lazzerini Denchi, Attwooll et al. 2005)
SAHF	↑	IMR90	Reps, ras, p16 activation	(Narita, Nunez et al. 2003)
DEC1/DEC2	↑	Mouse lung adenoma,	Oncogene ras	(Chen, Z., Trotman et al. 2005)
EBP50	↑	EJP21	P21 over expression	(Althubiti, Lezina et al. 2014a)
STX4	↑	EJP21	P21 over expression	(Althubiti, Lezina et al. 2014a)
DEP1	↑	EJP16	P16 over expression	(Althubiti, Lezina et al. 2014a)

NTAL	↑	EJP16	P16 over expression	(Althubiti, Lezina et al. 2014a)
ARMCX3	↑	EJP16	P16 over expression	(Althubiti, Lezina et al. 2014a)
B2M	↑	EJP21, EJP16	P16/p21 over expression	(Althubiti, Lezina et al. 2014a)
DCR2	↑	H358, H1299	P53 overexpression	(Collado, Serrano 2010)
NOTCH3	↑	BJ, WS1, HMECs,	Reps, H2O2, DOX, ionizing radiations	(Cui, Kong et al. 2013)
EBP50	↑	EJP21, EJP16	P21/p16 over expression	(Althubiti, Lezina et al. 2014a)
VAMP3	↑	EJP21, EJP16	P21/p16 over expression	(Althubiti, Lezina et al. 2014a)

Ki-67	↓	HUVECs	TNF-α	(Khan, Awad et al. 2017)

1.1.11 Towards novel biomarkers of endothelial cell senescence

Identification of senescence biomarkers is very important for the demonstration of the exact mechanism and role of senescence in CVD. It will also help to identify possible therapeutic targets for management of certain pathologies associated with ageing. Certain analytical techniques have been applied in this context, for example, transcriptomics, proteomics and epigenomics. The classical biomarkers for senescence are SA beta gal (Dimiri et al 1995), Notch3 (Althubiti, Lezina et al. 2014b), DNA damage foci (von Zglinicki et al., 2005), p21 (Althubiti, Lezina et al. 2014b) and p16 (Braig, Lee et al. 2005) (Table 1).

Despite advancements in proteomics and the importance of endothelial cells in the cardiovascular system, there have been only a few studies on the proteome of senescent endothelial cells (Richardson, Lai et al. 2010, Bal, Kamhieh-Milz et al. 2013). One study showed many proteins with altered expression compared to non-senescent endothelial cells. Table 2 shows SASP components for senescent endothelial cells. These proteins could be identified further as biomarkers for detection of endothelial cell senescence.

Recent research has shown that a number of miRNAs are involved in the regulation of senescence (Feng Jiao Liu et al 2012). miR217 is involved in endothelial senescence (Menghini et al 2009). Similarly, miRNA 34a is related to senescence through regulation of an ageing related protein, SIRT1, in endothelial cells (Ito et al 2010). Mir126-3p is an age-related miR whose circulating levels are found up regulated in healthy aged individuals. In parallel, senescent HUVECs also showed increased expression of Mir126-3p (Fabiola Olivieri et al 2014).

Magenta et al showed that Mir-200 family miRs including, Mir-200c, Mir-200a, Mir-200b and Mir-141 and Mir-429 were upregulated in endothelial cells made senescent by oxidative stress.

1.1.12 Possible intervention in endothelial cell senescence

Senescent cells have been reported to accumulate in various tissues (Campisi 2005) with age, with the suggestion that such cells are responsible for the phenotype of age-related diseases (Rodier, Campisi 2011). Identifying and then selectively killing of senescent cells might be a better strategy to combat age related diseases. Development of a senolytic agent is required that will target senescent cells, and therefore help in rejuvenation. These agents are viewed as a new class of anti-ageing drugs. Research in this context is at a preliminary stage. The two important pathways that are involved in triggering senescence are p53/p21 and $P16^{INK4}$a/pRb (Chen, J., Huang et al. 2006), (Campisi, d'Adda di Fagagna 2007a). Either or both these pathways is expressed by most senescent cells. A genetically modified progeroid mouse model showed fewer senescent cells, when treated with an apoptosis inducer drug AB20187 that selectively kills $p16^{INK4a}$-expressing cells. Clearance of $p16^{INK4a}$ positive cells at young or aged model showed delayed onset of age-related pathologies, which strongly influenced life span. In another study use of the tumour necrosis factor (TNF-α) blocking agent adalimumab was able to attenuate the SASP component, IL-6, and improved endothelial function by increasing eNOS expression in replicative senescent HUVECs (Prattichizzo, Giuliani et al. 2016b).

Senescent cells can bypass apoptosis by relying on pro-survival pathway. Senescent cell survival is dependent on cell survival family proteins, Bcl-2 and BCL-xL activity. Considering this principle, Zhu et al screened several apoptotic agents and confirmed that quercetin, a Bcl-2 family inhibitor was able to kill senescent HUVECs. This agent was able to improve cardiovascular and endothelial function in a progeroid mouse model. Similarly, siRNA against one of the pro-survival proteins, Bcl-2, was able to kill senescent HUVECs.

Consistent with this, Navitoclax, an inhibitor of Bcl-2, was able to decrease viability in senescent HUVECs but not human primary preadipocytes (Zhu, Tchkonia et al. 2016). ABT263 is another Bcl-2 and BCL-xL inhibitor confirmed by Chang et al to be more specific and have a broader spectrum of activity. Short hairpin RNAs (shRNAs) against both of these proteins simultaneously reduced senescent cells

Table 1-2. SASP Components secreted by endothelial cells in response to different stimuli.

Factor	Secretory profile	Cell type	Stimulation	Reference
IL-6	↑	HUVECs	TNF-α, REPS	(Khan, Awad et al. 2017, Prattichizzo, Giuliani et al. 2016a)
IL-8	↑	HUVECs	TNF-α	(Khan, Awad et al. 2017)
IGFBP-5 (mRNA)	↑	HUVECs	TNF-α	(Khan, Awad et al. 2017)
PAI-1	↑	HUVECs	REPS	(Comi, Chiaramonte et al. 1995)

PGI_2	↓	Rat aortic ECs,	REPS	(Nakajima, Hashimoto et al. 1997)
TNF-α	↑	HUVECs	REPs	(Prattichizzo, Giuliani et al. 2016a)
MCP-1	↑	HUVECs	Irradiation	(Xu, Tchkonia et al. 2015)
CHK2	↓	HUVECs	REPS	(Hampel, Fortschegger et al. 2006b)
VEGI	↑	HUVECs	REPS	(Hampel, Fortschegger et al. 2006b)

IGFBP-3	↑	HUVECs	REPS	(Hampel, Fortschegger et al. 2006b)

viability. They showed that in cell culture ABT263 selectively eradicated senescent cells by inducing apoptosis. ABT263 is broad-spectrum as killing senescent cells by ABT263 was cell and species independent. In addition to this oral administration of ABT263 has the ability to selectively kill senescent muscle stem cells (MuSCs) and bone marrow hematopoietic stem cells (HMCs) in aged and irradiated and normally aged mice (Chang, Wang et al. 2016).

These finding shows that senescent cell accumulation is involved in organismal ageing and elimination of senescent endothelial cells is possible in tissue culture. However, targeting pro-survival proteins can be deleterious for the cells. A new class of BH-3 mimetics compounds that induce apoptosis by targeting anti-apoptosis proteins (Oltersdorf, Elmore et al. 2005) was shown to induce mitochondrial outer membrane permeabilization (MOMP). MOMP is responsible for DNA damage and caspase dependent genomic instability (Ichim, Lopez et al. 2015).

Another study conducted by Shafaat et al found that chronic exposure to TNF-α was able to induce senescence and SASP components i-e ICAM1, E-selectin, IL-6 and IL-8 in HUVECs. These phenotypes were permanent, as they did not find much change in the expression of these phenotypes even after 2 weeks of TNF-α withdrawal. In addition to this they were able to successfully reverse growth arrest and the release of SASP from TNF-α-induced senescent HUVECs using N-acetylcysteine and plumericin, glutathione precursor and NF-kB inhibitor respectively. Their study suggests that TNF-α induced senescence in HUVEC was due to oxidant generation acting through NF-kB (Khan, Awad et al. 2017).

Keizer has introduced a new idea to rejuvenate cells (Cahu, Bustany et al. 2012). As aged cells are associated with chronic SASP secretion, this would result into permanent change of neighbouring cells. Senescent cell together with neighbouring reprogrammed cell leads to tissue dysfunction. Therefore, selective removal of senescent cells and replacement with new cells would be required for tissue rejuvenation (de Keizer 2017). Foxos and p53 interaction is related to expression of cell cycle arrest gene $p21^{Cip1}$ (de Keizer, Packer et al. 2010). Similarly, FOXOs have a blocking effect of on cell differentiation (Nakae, Kitamura et al. 2003). There is evidence of physical interaction of p53 and FOXO physical interaction (Wang, F., Marshall et al. 2008). Thus a cell-penetrating peptide (CPP) targeting FOXO-p53 interaction can be used for senescent cell removal and rejuvenation with minimum off site toxicity. CPPs are surface

exposed protein-protein binding motifs (de Keizer 2017). CPP designed for FOXO4 and p53 complex disruption was able to reduce IL-6 expression and reverse the ageing phenotype in aged mice model (Baar, Brandt et al. 2017).

1.1.13 Endothelial cells as model for *in-vitro* studies

Endothelium is a very important organ with autocrine and paracrine functions. Atherosclerosis arises as a result of injury of endothelium. Clinical interventions causing alteration in endothelial dysfunction holds the potential to stabilize cardiovascular risks. Vascular endothelium acts as a critical target for the prevention of cardiovascular diseases. Thus, the study of human endothelium is very important in cardiovascular research in order to identify the role and mechanism of endothelial dysfunction. The limited availability of human vascular endothelial tissue means that endothelial cells in cell culture are often used; these cells were cultured for the first time nearly forty years ago. The use of this experimental model allows the researcher to identify and understand vascular endothelial physiology and study its pharmacological roles under different physical and chemical conditions (Onat, Brillon et al. 2011). To understand the mechanism of blood vessel walls related diseases it is important to obtain endothelial cells for *In Vitro* study. Jaffe et al successfully isolated endothelial cells from neonatal umbilical cord. These cells expressed the biomarkers of endothelial cells and were able to grow in the cell culture for significant periods of time (Jaffe, Nachman et al. 1973). HUVECs are used as an *in-vitro* model system by researchers in different experiments. However, they display short lifespan and represent different characteristics from batch to batch. EAhy.926 is a permanent human cell line derived from fusion of HUVECs and permanent human tumorigenic lung epithelial cell line A549. The doubling time of this cell line is shorter and has reached more than 100 population doublings (Carterson, Honer zu Bentrup et al. 2005).

1.2 Hypothesis:

There is Paucity of senescence endothelial cells secretome research and its (senescence endothelial cells) connection to cardiovascular diseases. We are testing whether two types of senescent endothelial cells (SIPS and REPS HUVECs) express proinflammatory factors through its secretome by using a secretaguage using mass spectrometry. Together with this

analysis of previous transcriptomics data will identify biomarkers and the molecular pathways, functions and diseases that can get affected in senescent endothelial cells *in Vitro*.

1.3 Aims and objectives:

In humans, aging is the major independent risk factor for development of diseases, particularly, cardiovascular diseases. Apart from ageing certain other factor for example oxidative stress can also induce similar phenotypes.

Endothelial dysfunction during the ageing process is hypothesised to play a role in the development of CVD, perhaps by promoting inflammation.

1) In order to study mechanism of endothelial cells senescence causing endothelial dysfunction, *in vitro* cells models will be generated. The aim is to reproducibly induce both replication and stress-induce senescence in human endothelial cells (HUVECS).

2) Following this the thesis aims to describe pathways of senescence induction in endothelial cells by transcriptomics analysis. In order to investigate similarities and difference in replicative versus SIPS, analysis of the secretome will be performed using shotgun proteomics by LC-MS/MS. Both transcriptomics and proteomics will be used to investigate whether a pro or anti-inflammatory secretome is produced by senescent endothelial cells.

3) The final aim of this thesis is to investigate whether induction of senescence in endothelial cells causes a pro-inflammatory phenotype particularly with respect to adhesion of leucocytes to endothelial cells.

Chapter 2

2 Materials and methods

2.1 Cell culture

2.1.1 Materials

EA.hy926 a permanent human cell line that has been derived from fusion of human umbilical vein endothelial cells (HUVECs) and the human lung carcinoma cell line A549 was purchased from the European Collection of Cell Culture (ECACC). HUVECs were purchased from Life Technologies. Human dermal fibroblasts (HDF) were purchased from TCS Cellworks.

The composition of growth media for HUVECs, EA.hy926 and HDF is shown in Table 2-1.

Cells Growth media	volume
Human dermal Fibroblasts (HDFs) & EA.hy926	
Dulbecco's Modified Eagle Media (Life Technologies)	450 ml
Foetal bovine serum (heat inactivated)(Fisher Scientific)	50 ml
Media 200 (Life Technologies)	490 ml
Low serum growth supplement (LSGS) Life Technologies)	10 ml

Table 2-1 Composition of 'complete growth media' for HDF, EA.hy926 and HUVECs

.

Components	Percentage (v/v)
HDF & EA.hy926	
Dimethyl sulfoxide (Sigma-Aldrich)	10%
Foetal bovine serum (Sigma-Aldrich)	10%
Dulbecco's Modified Eagle's Media (Life Technologies)	80%
HUVECs	
Dimethyl sulfoxide (Sigma-Aldrich)	10%
Foetal bovine serum (Sigma-Aldrich)	50%
Media 200 (Life technologies)	40%

Table 2-2 Composition of freezing mixtures required for freezing cells

For culturing HUVECs all plastic ware were coated with 1% gelatine type B solution (obtained from Sigma Aldrich®) diluted in DBPS.

2.1.2 Methods

Cell culture manipulations were carried out in a Class II biosafety cabinet.

2.1.2.1 Coating of flasks and plates with gelatine

All plastic flasks and plates used for culturing HUVECs were coated with gelatine. Freshly made 1% gelatine (type B) solution was added to either T-75 flasks (3 ml), T-25 (2 ml) or 6-well plates (1 ml). After incubation for 10min at 37°C the excess gelatine solution was taken off by pipette. These plastic flasks and plates were then used for HUVECs culturing.

2.1.2.2 Reviving frozen cells

12 ml of growth media for respective cells was added to T-75 m^3 flasks prior to thawing the frozen cells. In the case of HUVECs the flasks were coated with 1% gelatine solution. Cells from liquid nitrogen storage were placed in a 50 ml centrifuge tube in order to safeguard against explosion. Cryovials were warmed in a water bath at 37°C. Care was taken not to thaw the cells completely approximately 0.5 x 10^6 cells were immediately transferred to T-75m^3 flasks though pipette. Depending on the number of cell cryopreserved the respective number of flasks was obtained.

2.1.2.3 Sub-culturing/passaging cells

Cells were passaged when they reached 80-90% confluency. The required concentration of trypsin/EDTA solution was made in DPBS from a 10X stock solution (0.1%). The growth media in the flasks was taken out by pipette and discarded in a waste bottle. 3-4 ml of DPBS were added to each flask in order to briefly wash adherent cells. Flasks were gently rotated and then the DPBS was removed to waste. 4 ml of required trypsin/EDTA solution was added to the flask. These flasks were placed in the incubator at 37°C for 5 minutes with the exception of HUVECs where the flasks were left at room temperature with strict observation. After 5 minutes the flasks were observed under a microscope with continuous gentle tapping. When 95% of cells were taken off from the flasks surface then 9 ml of growth media were added to neutralize the trypsin. All of the cell suspension was transferred into a centrifuge tube by pipette. These tubes were centrifuged at 183xg for 5 minutes at 20°C. The supernatant was discarded and the cell pellet was re-suspended in 1 ml of fresh media. The cell count was determined using a haemocytometer (see section 2.1.2.5). 10 ml of fresh growth media were added to new T-75 flask or 2 ml in 6-well plate (depending on the requirement of experiment) and the appropriate number of cells were added. If freezing of cells was required then cells were frozen down according to the protocol explained below (section 2.1.2.6).

2.1.2.4 Changing growth media

Old growth media was aspirated from the adherent cells and discarded into the waste bottle. The adherent cells were then washed with 3-4 ml of warm DPBS. The flasks were gently rotated and the DPBS was aspirated and discarded. The cells were provided with 10-12 ml of fresh warm growth media. The flasks were placed back into the incubator at 37°C and 5% CO_2.

2.1.2.5 Cell count using a haemocytometer

In order to know the number of cells grown in flasks and plates or the number of cells required for performing an experiment, cells were counted after trypsinizing and reseeding. The haemocytometer and coverslip were cleaned and dried with 70% (v/v) ethanol and the cover slip was affixed on the haemocytometer. 10 µl of trypan blue was added to an Eppendorf tube and to this 10 µl of cell suspension was added. This was gently mixed by pipetting. 10 µl of this mixture was taken and evenly spread under the coverslip by placing the pipette tip on the side of coverslip. The haemocytometer was placed under the microscope and cells were counted at opposite 16 squares at a magnification of 100X. The average number of cells was multiplied by 10^4 to get number of cells in 1 ml. As the area of 1 mm^2 of haemocytometer accommodate 0.1 µl of fluid. If the number of viable cells were required that was also determined in this way by counting the blue staining (dead) cells.

2.1.2.6 Liquid nitrogen storage

For long term storage, cells were cryopreserved in liquid nitrogen. When cells grown became confluent they were passaged as described in section 2.1.2.3. Once the cells have been counted, they were again centrifuged to get the cell pallet and supernatant was discarded. Depending on the cell type, to the appropriate number of cells freezing mixture was added. 1 ml cells were transferred to cryovial. These were placed in a cooling box and stored at -80°C for 24 hr before being transferred to liquid nitrogen.

2.1.2.7 Induction of stress induced premature senescence (SIPS)

To induce senescence in adherent cells, the cells in flask or plates at an early passage (70-80% confluency) were treated with tertiary butyl hydrogen peroxide (t-BHP) at different concentration (25 µM, 50 µM and 100 µM) for 1 hr once daily for three consecutive days. 200 mM t-BHP solution was made in DPBS. 1.25 µl, 2.5 µl and 5 µl of this solution was added to the flasks containing 10 ml of growth media in order to get 25 µM, 50 µM and 100 µM concentration respectively. Flasks were transferred to an incubator and kept for 1 hr. After 1 hr flasks were taken out and the media containing t-BHP was removed and cells were washed. Cells were fed with 10 ml of fresh growth media. This process was repeated for 3 days.

2.1.2.8 Replicative senescence (REPS)

For all the experiments in this thesis HUVECs at passage 6-8 were used as control (young). Replicative senescent endothelial cells (REPS) were established by passaging HUVECs up to 25 population doublings. While HDFs at passage 4-5 were used as control (young) and passage 13 as REPS.

2.1.2.9 Adding conditioned media

10 ml of fresh growth media were added to senescent human dermal fibroblasts (section 2.1.2.4). After 48 hr the media was aspirated and added to 15 ml tubes and centrifuged for 5 minutes at 1000 g to remove dead cells and debris. HUVECs, HDF and EA.hy926 already grown in T-75 flasks at 70% confluency were taken. The old media was aspirated and cells were washed with DPBS. 5 ml of fresh growth media were added to each flask and 5 ml of conditioned media. For control flasks 10 ml of fresh media were added without adding conditioned media. Cells were kept in an incubator for 24 hr, after which total RNA was extracted.

2.1.3 Senescent associated beta galactosidase (SA β-gal) staining

2.1.3.1 Materials

The reagents used for senescence associated beta galactosidase staining (in order to detect senescence), include senescent associated histochemical (SA β-gal) staining kit which was obtained from Sigma-Aldrich and parafilm was purchased from GMBH & co, Germany. Ultrapure water was used for all reagents dilutions.

Components	Chemicals	Volume required for 10ml of staining mixture
10 X fixation buffer	Solution containing 20% formaldehyde, 2% glutaraldehyde, 70.4 mM Na_2HPO_4, 14.7 mM KH_2PO_4, 1.37 M NaCl, and 26.8 mM KCl	
10-X-staining solution		1 ml
X-gal solution		0.25 ml
Reagent B		125 µl
Reagent C		125 µl
Ultrapure water		8.5 ml
DPBS		For washing out cells

Table 2-3 Components of staining mixture for SA β-gal staining of cells

2.1.3.2 SA β-gal Method

After induction of SIPS (section 2.1.2.6) HUVECs were trypsinized and reseeded into gelatin-coated 6-well plates at a density of $4x10^4$ cells per well. Cells were allowed to adhere for 24 hr in an incubator**.** After 24 hours the growth media was aspirated from cells and discarded. Cells were washed twice with DPBS and the required volume of fixation buffer was added to cells

with incubation for 6-7 min during which staining mixture was made (table 2-4). Staining mixture was filtered through a 0.2 µm pore size filter. By the end of 7min cells were washed three times with DPBS. 1 ml of staining mixture was added per well and plates were sealed with parafilm in order to avoid drying out. Cells were placed for 2-24 hr in a CO_2-free incubator in order to prevent a change in the pH (SA β-gal activity is maximum at pH6).

The stained blue cells were visualized using a Nikon trinocular inverted phase contrast light microscope at X100 magnification. Blue stained cells were counted from five different fields of view in each well (counting a total of 400-500 cells) and the percentage of stained to unstained cells was calculated.

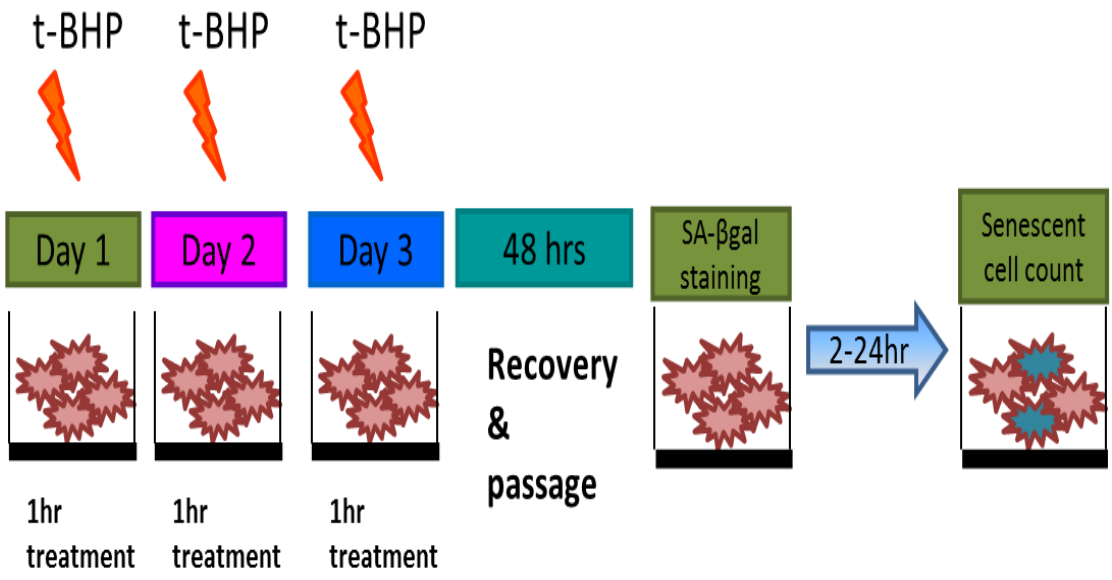

Figure 2-1 SIPS induction in HUVECs and SA-βgal staining.

The above figure shows the t-BHP treatment of HUVECs for 1 hr for 3 consecutive days and then a recovery period of 48 hr followed by SA-βgal staining. The cells were observed and counted for blue staining after 24 hr of incubation with staining reagent

2.2 Amplex red assay

Amplex red assay was carried out to find out the peroxidase activity in old and new growth media. This is a sensitive one step assay to determine the H_2O_2 concentration in the solution. The assay contains the red reagent, Ampliflu™ also called Amplex Red that reacts with H_2O_2 in the presence of horseredish peroxidase and forms a fluorescent product called resorufin. The assay was modified so that we can measure the peroxidases activity.

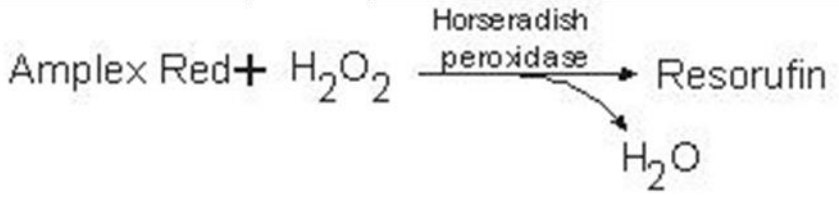

Figure 2-2: Amplex red assay reaction.

Amplex red undergoes a single step reaction. A compound amplex red (ampliflu) which reacts with H2O2 in the presence of peroxidase and generates a fluorescent product called resorufin, while water is also generated.

The assay requires three reagents Ampliflu™, H_2O_2 and peroxidase. We assume there is certain peroxidase level present in our media which will complete the reaction. The fluorescence read out will determine the concentration of peroxidases in the media. If the concentration of H_2O_2 is constant any changes in the fluorescence will be the result of peroxidases in the samples. We also performed this assay to measure the H_2O_2. In this case we added the horseradish peroxidase in the reaction mixture.

2.2.1 Materials

Components	supplier
Ampliflu red	Sigma Aldrich
Dimethyl sulphoxide	Sigma Aldrich
Hydrogen peroxide	Sigma Aldrich
Phosphate buffer saline solution	GIBCO
Horse reddish peroxidase	Sigma Aldrich

Table 2-4 Reagents used in the Amplex red assay

2.2.2 Method (peroxidase measurement)

In order to make the standard curve standard solution for H_2O_2 dilutions were made according to table 2-6.

Reaction mixture for positive control	
Reagent	**Volume**
Ampliflu red (10 mM Ampliflu™ Red stock solution was made by adding 1.943 ml of DMSO to 5 mg Ampliflu™ Red)	50 µl
Peroxidase type II from horse radish (0.00001 g dissolved in 2 ml of PBS)	50 µl
PBS	9.9 ml
Reaction mixture for the samples	
Ampliflu red	50 µl
PBS	9.95 ml

Table 2-5 Reagents and their volumes required to make the reaction mixtures for the samples and positive control in the peroxidase assay.

Conditioned or 'old' media was collected from EA.hy926 cells fed with growth media (phenol free) 24 hr before carrying out the experiment. It was centrifuged at 183 g for 5 minutes in order to pellet any dead cells. 4.5 ml of the supernatant was taken in a 15 ml centrifuge tube. The same volume of fresh (or 'new') EA.hy926 media was also taken, and both media samples were then placed in the 37°C incubator. According to the table 2-7 horse reddish peroxidase solution was made in DPBS. According to table 2-7 2 reaction mixtures were formed. They were warmed in the incubator. Now 0.5 ml of 1 mM H_2O_2 was added to both samples of media to achieve a final concentration of 100 µM. Standards (100 µl) (table 2-6) were loaded into a 96 well plate, then 100 µl from two samples of media in triplicate were also loaded. The sample reaction mixture was added to the corresponding media wells and reaction mixture for positive control added to 2 or 3 separate wells. The plate was covered with aluminium foil and incubated at 37°C for 10 minutes. Fluorescence (560 nm excitation and 590 nm emission) readings were taken in Novostar plate reader every 10 minutes for 70 minutes. In between each reading the plate was transferred to the incubator.

2.2.3 Method (H_2O_2 measurement)

4.5 ml 24 hrs old conditioned media was collected from EA.hy926 cells and centrifuged. An identified volume of fresh EA.hy.926 media was also taken and to both of medias 0.5 ml of 1 mM H_2O_2 solution in PBS was added. Starting from time zero a 100 µl sample from each media was taken and added to wells in a 96 well plate in triplicates. The plate was placed in ice, so that to stop the reaction. Just before the collection of last sample at time point 60 minutes, reaction mixture was made (table 2-7), and kept in the water bath at 37°C. A H_2O_2 standard was also made as shown in table 2-6. When the last sample was collected, 20 µl of the reaction mixture was added to all the wells including the H_2O_2 standard. The fluorescence was read on a Novostar plate reader. Readings were taken at 0, 5 and 10 minutes. Between readings the plate was incubated at 37°C.

2.3 Measurement of gene expression using RT-PCR

2.3.1 Materials

The reagents and other materials used for RNA extraction include: RNeasy mini plus kit purchased from Qiagen®, RNase Zap was obtained from Sigma-Aldrich, DNase 1 kit (RNase free DNase set) was purchased from Qiagen®, 100% ethanol was purchased from Sigma-Aldrich, collection tubes were obtained from Starlabs. To homogenise cells a homogeniser was used. To prepare cDNA a high capacity cDNA reverse transcription kit was obtained from Applied Biosystems. For cleaning the homogeniser, laboratory standard ultrapure water was used.

2.3.2 Total RNA extraction

2.3.2.1 Methods

HDF, EA.hy926 and HUVECs were grown in T-75 flasks. After inducing SIPS or incubation in conditioned media, cells were trypsinised, transferred to cryovials and washed with DPBS and placed on ice. Cells were centrifuged at 67xg for 5min and the supernatant was aspirated and depending on cell number, 350-600 µl RLT buffer were added. Each sample was homogenised with a homogeniser for 30-60 seconds. In between each sample the homogeniser was cleaned with ultrapure water, RNase Zap, again with ultrapure water and dried with 100% ethanol. The same volume (RLT buffer) of 70% ethanol was added and mixed by pipetting up and down. 700 µl of the homogenate was taken and transferred to RNeasy mini spin columns, and centrifuged for 2 min at 67xg. Collection tubes were changed and the remaining sample was added to spin column, vortexed for 2 minutes at 67xg. The spin columns were transferred to new collection tubes before the samples were centrifuged for 2 minutes at 67xg.

To carry out DNA digestion the flow through was discarded and to each sample 350 µl of RW1 buffer was added, mixed 4-5 times, rolled and centrifuged for 2min at 1000 rpm. The flow-through was discarded and 10 l of DNase stock solution was added to 70 µl of RDD buffer per

sample and added directly to the spin column membrane and left at room temperature for 30-40 min. 350 µl of RW1 buffer was added and centrifuged for 2 minutes at 67xg and the flow through was discarded.

500 µl of RPE containing 100% ethanol was added to the spin column, incubated at room temperature for 5 min and centrifuged for 2 min at 67xg. The flow-through was discarded and the step was repeated. The collecting tubes were changed for new tubes and samples were centrifuged for 5 min at 67xg in order to fully eliminate the buffer. At this point the mini spin columns were replaced with 1.5 ml sterile Eppendorf tubes. To elute RNA, 30 µl of RNase-free water were added and centrifuged at 1000 g for 2 min. The eluate was passed through the mini spin column membrane again to elute the remaining RNA and centrifuged for 4 min. The mini spin column was discarded and the RNA obtained was stored in 10 µl aliquots stored at -80°C until required. The quality of RNA obtained was later analysed by UV absorbance using a NanoDrop™ 8000 spectrophotometer

2.3.2.2 cDNA preparation

Total RNA obtained was converted to cDNA to be used in RT-PCR. All the kit components were thawed on the ice. Considering the number of samples 2X master mix was made referring to the following table (2-8) and placed on ice.

Component	Volume/Sample (µl)
10X RT buffer	2.0
25X dNTPs Mix (100 mM)	0.8
10X Random Primers	2.0
MultiScribe Reverse Transcriptase	1.0
Nuclease Free Water	4.2
Total per Reaction	10

Table 2-6 High Capacity cDNA Reverse Transcription Kit components to make 2X Master Mix.

The volume of RNA containing 2 µg of RNA was calculated. In the case of the calculated volume being less than 10 µl, RNA was diluted with RNase free water to make up the volume up to 10 µl. 10 µl of Master Mix were added to 10 µl of RNA in Eppendorf tubes and placed on ice. Samples were mixed by pipetting. Samples were then loaded into the thermal cycler. The following table (2-9) shows the conditions optimised for preparing cDNA.

	Step1	Step 2	Step3
Temperature (° C)	25	37	85
Time (minutes)	10	120	5

Table 2-7 Temperature programme for the thermal cycler required for cDNA synthesis.

The cDNA formed was stored at -20C until required.

2.3.2.3 Quantitation of RNA

To determine the yield of RNA extracted and purity in terms of RNA to protein ratio and RNA to any contaminant ratio, Nano drop was performed.

2.3.2.3.1 Nano drop Analysis

Nano drop software was selected to initialize and nucleic acid mode was selected. The spectrophotometer was initialised by adding 1.5 µl of ultrapure water onto the lower optic surface and covering with the upper optic surface. 'Initialise' was selected and optical surfaces

were wiped clean with wipes. ‘RNA – 40’ was selected for measurements. A blank measurement was carried out before the actual sample by loading 1.5 µl of RNase free water onto the lower optical surfaces, the upper optical surfaces were lowered and ‘blank’ was selected, after which the optical surfaces were again wiped clean with wipes. The actual sample was loaded in the same volume (1.5 µl) and the respective cells were activated and labelled. “Measure” was selected that gave the peaks with values representing the quality and quantity of RNA extracted.

The Nanodrop calculated the concentration of RNA in the units of ng/µl. The yield of RNA was mostly dependent on the number of cells extracted. The purity of RNA was determined by displaying the ratio of OD260/280 and OD260/230 where 260 nm was the peak nucleic acid absorbance and 280 nm peak protein absorbance. 230 nm was the peak absorbance of peptides, aromatic compounds, phenols, carbohydrates absorbance. 260/280 values in range of 1.8-2.1 were classified as acceptable indicating low contamination of RNA with protein and for 260/230 the values in range of 1.8-2.2 were acceptable indicating low contamination of RNA with compounds that absorb at 230 nm. The window of these values was considered as standard and anything out of this range was discarded and RNA extraction performed again.

2.3.3 RT-PCR

2.3.3.1 Materials

Taqman probes and RNase free water were purchased from Life Technologies®. TaqMan Fast Advanced Master Mix was purchased from Applied Biosystems®.

Item	Manufacturer	Catalogue number
TaqMan Fast Advanced Master Mix	Applied Biosystem®	4444557
QuantiFast® SYBR® Green PCR Kit	Qiagen	ID: 204054

Table 2-8 Master Mix used for qPCR.

Probe	Manufacturer	Catalogue number
CST1	Life technologies	Hs00606961_m1
LRRC17	Life technologies	Hs00957873_m1
CRTAC1	Life Technologies	Hs00907892_m1
GAPDH	Life Technologies	Hs02786624_g1
PSMB4	Life Technologies	Hs00160598_m1
ACTB	Life Technologies	Hs01060665_g1
VCP	Life Technologies	Hs00997642_m1
36B4	Life Technologies	Oc03396140_g1

Table 2-9 TaqMan® probes used for gene analysis in RT-PCR.

CST1 (cystatin SN), LRRC17 (leucine rich repeat containing 17), CRTAC1 (cartilage acidic protein 1), GAPDH (glutaraldehyde phosphate dehydrogenase), PSMB4 (proteasome beta subunit type-4), ACTB (beta-actin), VCP (valosin containing protein) and 36B4 (ribosomal protein lateral stalk subunit P0).

2.3.3.2 Methods

2.3.3.2.1 Principle of qPCR

qPCR is a relative quantitative technique which is used to analyse the changes in the level of gene expression of a given sample (treated) compared to a reference sample (untreated). It means that the amount of DNA generated is measured during each PCR cycle. Two parameters within the exponential phase of PCR are monitored: threshold - when the fluorescence level reaches above the background and **C_T;** which is the PCR cycle of the sample when the threshold is attained.

2.3.3.2.2 Protocol

For gene expression analysis RT-PCR was performed. After making cDNA from RNA, RT-PCR was performed by starting with thawing all the Taqman primers and TaqMan Fast Advanced Master Mix components on ice**.** cDNA formed was diluted to a concentration 20 ng/µl. A standard curve was constructed to check the efficiency of the probes. cDNA was thawed and 10µl from all the samples were mixed together to obtain pooled cDNA. According to the calculation below (table 2-10) the master mix was made. Housekeeping gene GAPDH was used as a control.

Reagent	concentration	Volume for 1 sample (µl)
Taqman fast master mix	1x	2.5
Taqman Assay 20X	1x	0.5
Nuclease free water		1
cDNA	20ng	1

Table 2-10 The volumes of components of TaqMan Fast Advanced Master Mix for PCR

Master mixes were prepared for each probe. Each master mix with probe was vortexed to mix well and placed on ice. For all concentrations of standard curve 4 µl was added to respective wells in the 384 well plate except 40 ng input, When 3 µl was added. This was followed by 1 µl and 2 µl of sample respectively, making the final volume 5 µl. plate was sealed with plastic film and briefly centrifuged to ensure thorough mixing.

A standard curve protocol on AB Viia 7 machine was selected. The setting on machine for this protocol was 50°C for 2 min followed by 95°C for 10 min one time, while the cycle temperature fluctuated between 95°C for 16 sec followed by 62°C for 1 min (stage 2 in fig 2-3).

Probe efficiency was calculated as follows:

Efficiency calculation = $(10^{(-1/slope)} - 1) \times 100$

2.3.3.2.3 Comparative cT

For genes of interest expression analysis, on AB Viia 7 machine, comparative cT protocol was selected. A384 well plate was labelled and 4 µl of the master mix with primers were added to the corresponding well. This was followed by 1µl of sample. The plate was sealed and centrifuged at 3000 g for a few seconds in order to bring all the solution to the bottom of the wells.

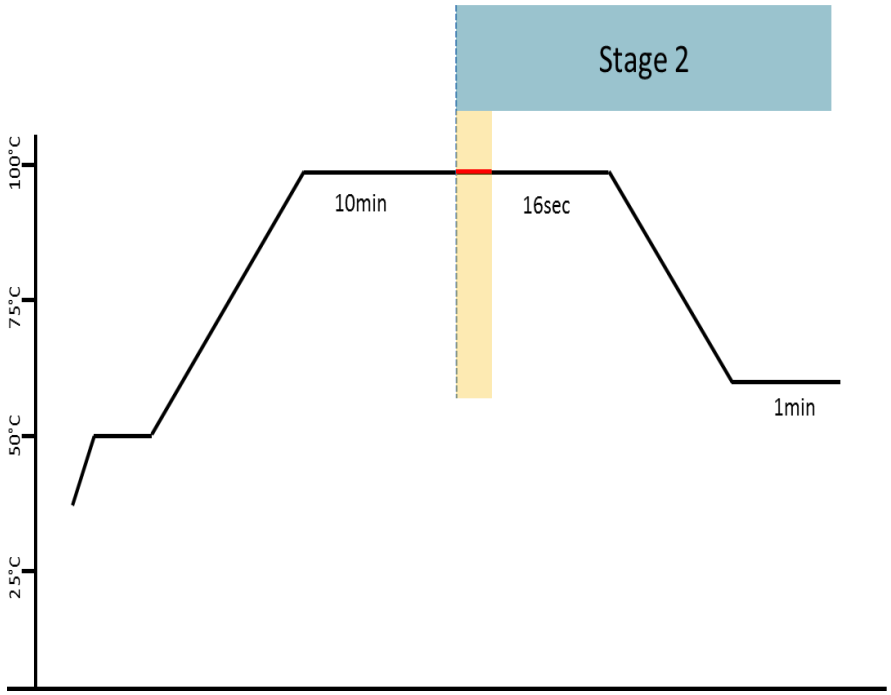

Figure 2-3 Applied Biosystem VII set up for RT-qPCR run.

In order to start the reaction, the plate is heated up to 105°C then the temperature changed between 60°C and 95°C during each cycle.

Applied Biosystem Vii was used for performing RT-PCR. The 384 well plate was loaded with sample was placed in the thermal cycler. The reaction threshold and number of reaction (40) was set up automatically.

qPCR

For expression analysis of cDNA of certain genes we performed qPCR.

2.3.3.2.4 Primer design

For all Housekeeper genes primers apart from VCP, PSMB4 and 36B4 were designed based on the sequences published on GenBank or Ensemble using NCBI primer designing tool (https://www.ncbi.nlm.nih.gov/tools/primer-blast/). Primers for the other housekeeper genes and adhesion genes were kindly provided by Dr. Veryan Codd in the department. While for

CD44, the primer sequence was published by Gyeong and Yong, 2010. The list of all the primer sequences is given in the table 2-15 and 2-16.

Gene Name	Forward primer sequence	Reverse primer sequence
ICAM-1	AACCCCACAGTCACCTATGG	TTCTGAGACCTCTGGCTTCG
VCAM-1	AAGCGGAGACAGGAGACAC	TGGCAGGTATTATTAAGGAGGATG
E-selectin	CCAGAGCCTTCAGTGTACCT	GAGTGGTGCATTCAACCTGG
CD44	GGACCAATTACCATAACTATTG	GCA AAC TGC AAG AATCAA

Table 2-11 List of primer sequences for adhesion molecule gene expression used in qPCR.

Gene name	Forward primer sequence	Reverse primer sequence
GAPDH	GCACCCCTGGCCAAGGTCAT	CAGCGCCAGTAGAGGCAGGG
ACTB	ATATCGCCGCGCTCGTCGTC	ACCATCACGCCCTGGTGCCT
β-tubulin	TGGCGGAGCGTCGGTTGTAG	GCACGTACTTGCCGCCGGT
B2M	TGCCTGCCGTGTGAACCATGT	TGCGGCATCTTCAAACCTCCATGA
TBP	GGGTTCAGTGAGGTCGGGCAG	AGTCATGGCACCCTGGGTCA
PSMB4	GCTGATGGAGAGAGCTTCCT	GAACGGGCATCTCGGTAGTA
36B4	TCGACAATGGCAGCATCTAC	GCCTTGACCTTTTCAGCAAG
VCP	CTTCCGGTGGGCCTTGAG	GGAATTTGTCTGGGTGCTCC

Table 2-12 List of primer sequences for housekeeper genes used in qPCR.

2.3.3.2.5 Protocol

Reaction mixture was prepared according to the table 2-12. The primers sequences are explained in section 2.3.3.2.4.

Table: Reaction set up

Reaction volume 384 well pcr plate		
Component	**volume**	**Final concentration**
Reaction mix 2x QuantiFast SYBR Green PCR Master Mix	5 µl	1x
Primar A*	1 µl	1 µM
Primar B*	1 µl	1 µM
Rnase-free water	1 µl	-
Template (cDNA)	2 µl	20 ng
Total reaction volume	10 µl	

Table 2-13: Composition and volume of components required for SYBR green PCR.

Master mix was prepared by adding all the components for all gene targets except cDNA input. 8 µl of the Master mix were added to each corresponding well in a 384 well plate. This was followed by the addition of 2 µl of cDNA. Plate was sealed and centrifuged briefly.

The reaction was performed by placing the plate in the AB Vii 7 machine. Comparative cT, fast mode method was selected and the reaction threshold and temperature was adjusted according to the manufacturer's protocol as follows:

Step	**Time**	**Temperature**
PCR initial heat activation	5 min	95°C
2-step cycling denaturation	10 sec	95°C
Annealing/extension	30 sc	60°C
Number of cycles	40	

Table 2-14: Temperature set up for using QuantiFast® SYBR® green master mix in thermal cycler

A standard curve was also constructed for all the primers used for gene expression.

2.3.4 Gel PCR

Product	Manufacturer	Catalogue number
GelRed	Biotium	41003
Blue loading buffer	Bioline	BIO-37045
TAE solution		

Table 2-15 Product information used for gel PCR

In order to see the primer size for SYBR green based PCR, primers were validated in gel pcr. For this purpose PCR products were electrophoresed on a 1% agrose gel. A 1% agarose solution was made in 1x triacetate EDTA (TAE) solution. The gel cast was sealed from both top and bottom by using paper tape. Agarose solution was heated in a microwave at high power. A protective glove was used to handle the solution. After careful mixing when all the agarose was dissolved, 1 µl of red gel dye was added, it was poured into the gel cast and a comb was inserted. This was left to set. In parallel, 4 µl of PCR product were taken out in a tube and mixed with 2 µl of blue loading dye. When the gel was set, comb was taken out and the all the samples were loaded, started with a gene ruler (ladder). After loading the sample the gel was electrophoresed at 110 V for 2.5 hrs. When the gel was electrophoresed the bands were visualised using the Gene-Genius Imaging system from Syngene. The Gene Snap software was used to produce the gel image for the study.

2.4 Western blots

2.4.1 Materials

2.4.1.1 Protein extraction

Lysis buffer (RIPA buffer); NaCl, Triton-X-100 and sodium deoxycolate were purchased from Sigma Aldrich. Protease/phosphatase inhibitor cocktail was purchased from Roche-Applied Sciences.

Protein assay; Detergent compatible (DC) Bradford protein assay kit was obtained from Bio-Rad.

RIPA Buffer	
Tris base (50 mM)	0.606 g
NaCl (150 mM)	0.876 g
sodium deoxycholate (0.5%)	0.5
SDS (0.1%)	0.1 g
Triton-X-100	1 ml
dH2O	Make up to 100 ml

Table 2-16: Composition of lysis buffer.

Gels; Sodium dodecyl sulphate (SDS), tetramethylmethylenediamine (TEMED) and Ammonium persulphate were purchased from Sigma Aldrich. Tris base and glycine were purchased from Fisher Scientific. Acrylamide was purchased from Bio-Rad.

Blocking solution; Dried skimmed milk power (Marvel) was purchased from local a supermarket. TBS and Tween-20 was purchased from Sigma Aldrich.Loading buffer; Dithiothreitol(DTT), bromophenol blue and glycine were purchased from Sigma Aldrich

ECL reagent; P-coumaric acid and luminol were purchased from sigma.

Molecular weight marker (Protein) and all apparatus used was purchased from Bio-Rad.

12% 2X Resolving gel	
Tris-HCl pH 8.8	7.5 ml
30% Acrylamide-Bis solution	8 ml
SDS (10% w/v)	200 µl
APS (10% w/v)	100 µl
TEMED	10 µl
Water	4.2 ml

Table 2-17: Composition of resolving gel

4% 2X Staking gel	
Tris-HCL (pH 6.8)	1.25 ml
30% Acrylamide-Bis solution	1.33 ml
SDS (10% w/v)	100 µl
APS (10% w/v)	50 µl
TEMED	10 µl
Water	7.35 ml

Table 2-18: Composition of stacking gel.

1X Tris buffer saline (TBS) 1000 ml	
Tris base	2.44 g
NaCl	8.0 g
Adjust pH with conc HCl	7.6
1XTBS-T (1000 ml)	
0.1% Tween-20	1 ml

Table 2-19 Composition of Tris base saline – Tween (TBS-T) solution.

ECL Reagent	
P-coumaric acid	5 µl of solution
Luminol	2.2 µl of solution
Hydrogen peroxide solution	0.3 µl
TBS-T pH 8.5	10 ml

Table 2-20: Composition of ECL reagent.

1X Gel electrolysis buffer	
Tris-base	3.3 g
Glycine	14.4 g
Sodium dodecyl sulphate	0.5 g
dH2O	Make up to 1000 ml

Table 2-21: Composition of gel electrolysis buffer.

1X Transfer buffer	
Tris-base	2.42 g
glycine	11.25 g
Methanol	150 ml
dH2O	Make up to 1000 ml

Table 2-22: Composition of transfer buffer

2X Loading buffer	
DTT 1M	200 mM
Bromophenol blue	1 ml
Tris-HCl (1M) (pH 6.8)	1.25 ml
glycerol	2 ml
Ultra-pure water	11.35 ml

Table 2-23: Composition of loading buffer.

Stripping buffer		
Glycine	200 mM	15g
SDS	0.1%	5 ml (20% solution)
Tween-20	1%	10 ml
Ultra pure water		Make up to 1000 ml
Adjust the pH to 2.2 with conc HCl		

Table 2-24: Composition of stripping buffer

Primary antibodies list				
Anti-body	Host animal	Company	Catalogue number	Titration
Cystatin SN	Goat	R&Dsystems®	AF1285	1:2000
CD44	Rabbit	Abcam	AB51037	1:500
Puromycin	Mouse	MerckMillipore	MABE343	1:12,000
P21	Mouse	Santa Curz® Biotechnology	sc-6246	1:500
P53	Mouse	Santa Curz® Biotechnology	(DO-1)sc-126	1:500
B-actin	Mouse	Sigma-Aldrich®	A5441	1:10,000

Table 2-25: List of primary antibodies used

Secondary anti-bodies list				
Anti-body	Host animal	Company	Catalogue	Titration
Rabbit anti-mouse	Rabbit	Abcam	Ab6728	1:2000
Mouse anti-rabbit	Mouse	Santa Curz® Biotechnology	Sc-2030	1:2000
Rabbit anti-goat	Rabbit	Jackson ImmunoResearch	305-035-003	1:2000

Table 2-26: List of secondary antibodies used

Product	Manufacturer	Catalogue number
Puromycin	Sigma-Aldrich®	P8833
Cycloheximide	Sigma-Aldrich®	C7698
DL-dithiothreitol (DTT)	Sigma-Aldrich®	D0632-1G
Protease phosphatase cocktail inhibitor	Thermoscientific	1861283
Phorbol 12-myristate 13-acetate (PMA)	Sigma-Aldrich®	P8139

Table 2-27: List of compounds used

P53 overexpressing cell lysate used as positive control was a gift from my supervisor Dr Salvador Macip. pH for all the solutions were adjusted with concentrated HCl.

2.4.1.1.1 Lysis Buffer (RIPA)

Tris and NaCl was weighed out and added to 75 ml of dH_20, corrected to pH 7.4. Then the remaining ingredients were added, adjusting the volume to 100 ml and frozen in aliquots (-20°C). Protease/phosphatase inhibitor cocktail was added before use (1:100).

2.4.1.1.2 Cell lysis

Cells were trypsinised using appropriate concentrations of trypsin. Then the cells were centrifuged to a pellet. Cell pellet was washed with PBS and transferred to a 1.5 ml Eppendorf on ice. 70 µl of lysis buffer (RIPA buffer) (table 2-16) were added to the cell pellet. The centrifuge was set to cool at 4°C. Cells were sonicated for 30 sec each sample (sonicator probe was cleaned with 70% IMS in between each sample). Cell lysate was left on ice for 30 min. followed by centrifugation for 10 min at 4°C and supernatant was transferred to sterile chilled

Eppendorf tubes. Samples were stored at -20°C until further use. Protein content was measured using the detergent compatible (DC) Bradford assay.

2.4.1.2 DC Protein assay

Bovine serum albumin (16 mg) was dissolved in 1 ml of dH2O to make 16 mg/ml solution. This solution was further dissolved into 20 µl of lysis buffer (RIPA) (table 2-16) in order to make serial dilutions. 8 serial dilutions between 16 g to 0.0 mg/ml were made.

Each standard was mixed well. 5 µl of sample and standard were pipetted into each well in a 96 well plate in triplicates. Then reagent A' was prepared by adding 10 µl of reagent S for each 1 ml of reagent A. An aliquot (25 µl) of reagent A' was added to the corresponding wells. Following this, 200 µl of reagent B was added to each well. The plate was incubated for 15-30 minutes at 37°C. The absorbance was measured at a wavelength of 620 nm using a plate reader.

Absorption was plotted against protein concentration to generate a standard curve. Protein concentrations from cell lysates were determined using this standard curve.

2.4.2 Western Blots

The 1.5 mm spacer plates and short plates were cleaned and dried using 70% ethanol and assembled in the casting frame. The plates and casting frame setup was secured into the casting stand. In-order to check the plates for any leakage dH_2O was pipetted in between the plates. In case of any leakage the set up was reassembled, otherwise dH_2O was replaced with 7 ml of 12% resolving gel. For an even surface 1 ml of propanol was added on to the top of gel. The gel was let set at room temperature for 40 minutes. After the gel was set the propanol was taken off and 4 ml of 4% staking gel were added and a 10 well comb inserted in between the plates and the gel allowed to polymerise at room temperature for 40 minutes. Once the gel was set the comb was removed. The cast was removed from the casting stand and transferred into an electrophoresis tank.

2.4.2.1.1 Sample preparation

DTT (200 mM) was added to the 2X sample buffer or loading buffer (table 2-23). Volume of each sample containing 30-40 µg of protein was taken in a 1.5 ml Eppendorf tube. The same volume of sample buffer containing DTT was added to each sample. Total volume of each sample was 40 µl. All the samples were placed in a heating block at 95°C for 5 minutes to denature. After denaturation all the tubes were centrifuged at a high speed of 16,873 for 15 sec to remove all the bubbles from the samples.

2.4.2.1.2 Electrophoresis

1 litre of electrophoresis buffer was added to the tank containing the gel. The wells formed by the comb were loaded with samples (40 µl). In the first well protein ladder was added. The next wells were loaded with positive control followed by the samples. In order to avoid uneven electrophoresis empty wells were loaded with the same volume of sample buffer. Once all the samples were loaded, the tank lid was fitted on to the electrodes and a voltage of 100 V was applied. After 15 minutes, the voltage was increased to 120V. Electrophoresis was performed for approximately 2 hrs or when all the samples had run just about to the bottom of the gel, the voltage was stopped.

2.4.2.1.3 Transfer of proteins

The next step was the transfer of protein from the gel on an Immune-Blot® membrane. While the gel was running transfer buffer was prepared (table 2-22). 2 pieces of filter paper per gel equal in size to the gel (7x9 cm) and fibre pads were soaked in cold transfer buffer. In a separate tub an Immune-Blot® membrane again same size (7x9 cm) was made wet: 20 seconds in methanol, then for 2 minutes UP water and finally for 5 minutes in cold transfer buffer.

To hold the membrane a tweezer was used to avoid touching the membrane. For transfer of protein to the membrane a gel holder cassette was opened and on the black side of the cassette 1 fibre pad was placed. On the top of filter paper fibre pad was placed. The rest was placed in

the following order, gel PVDF membrane filter paper and fibre pad. Any bubbles trapped between the gel and membrane were taken out by using a roller. The gel cassette was closed and locked.

The cassette was placed in the electrophoresis tank and the tank filled with approximately 1.2 L of transfer buffer. An ice pad was placed in the tank to keep the solution cold and a magnetic stirrer for uniform temperature of the solution. This was followed by attaching the lid and power cables of the mini trans- blot transfer cell and electrophoresis performed at 63V for 1 hour.

2.4.2.1.4 Blocking the membrane

Following the electrophoresis, membrane were removed and washed in TBS-T solution. Membrane were blocked with 5% milk solution in TBS-T for 1 hr at room temperature. Membranes were briefly rinsed with TBS-T solution.

Primary antibody solution was made in 5% milk diluted in 5 ml TBS-T solution. Depending on the manufacture's protocol, recommended amount of primary antibody was added to the solution. For experiments where antibody was reused, for example β-actin primary antibody was made in 1% BSA solution. Primary antibody solution was transferred to a 50 ml centrifuge tube. Membranes were incubated in primary anti-body solution overnight at 4°C on a mechanical roller. Following a brief rinse in TBS-T solution membranes were washed with TBS-T for 15 minutes followed by a further two washes for 10 min.

During washing the membranes was placed on a mechanical shaker.

Secondary anti-body solution was made depending on the manufacturer protocol, in 5% milk solution. Membranes were incubated in secondary antibody for 1 hr at room temperature on a mechanical roller.

After 1 hr, the membranes were washed for primary antibody.

This was followed by incubation of membrane for 2-5 minutes in ECL reagent (table 2-20)

2.4.2.1.5 Detection

Excess ECL reagent solution was removed by gentle shaking and the membrane was placed on a clean plastic sheet. The Membrane was sandwiched between two clear sheets and entrapped air bubbles were taken out. Bands were identified using GE healthcare life sciences ImageQuant^{TM} LAS 4000.

2.4.2.2 Re-probing membrane for House keeper protein

For equal loading determination of protein in Western blots for all samples, each experiment where whole cell lysate was used, a house keeper protein was used. Typically β-actin was used. Membrane was washed two times with stripping buffer (see table 2-24) followed by 2 x 10 min washes in PBS and 2 x 10 in washes in PBS-T.

This was followed by 1 hr blocking of membrane with blocking solution at room temperature on a mechanical shaker. After this membrane was incubated with β-actin antibody at a concentration of 1 in 10,000 in 5 ml of 1% BSA solution. The time of incubation was 30 minutes at room temperature in a 50 ml centrifuge tube on a mechanical roller. The membrane was processed as described in section (2.4.2.1.4).

2.4.2.2.1 Quantification

Bands on the membrane were quantified using ImageQuant^{TM} LAS 4000 software. Each band was selected and intensity of the band was obtained. Intensity of the housekeeper protein (β-actin) was also determined. Quantification was performed by taking the ratio of protein of interest intensity to the housekeeper band intensity.

Relative amount of protein of interest = band intensity (protein of interest) / band intensity (housekeeper)

2.4.3 Method to concentrate cell supernatants

Two protocols were used to concentrate the cell supernatant.

Cell supernatant concentration using TCA: Cell supernatant (4.5 ml) from a T-75 flask containing HUVECs was collected in a 15 ml centrifuge tubes. 4.5 ml of ice cold TCA (100 %) was added to the cell supernatant. So that the final concentration of the solution was 50 %.

Cell supernatant using Amicon filters: Cell supernatant was collected and placed on ice. A centrifuge was set up at 4°C and cooled 20 minutes prior to the protein concentration process. 5 ml of the supernatant was added to the Amicon filter tubes with a 5 kDa cut off and centrifuged for 20 minutes at 18,400 g.

2.4.3.1 Protein synthesis monitoring using puromycin

The method to measure the rate of protein synthesis is through incorporation of radiolabelled isotopes (Fritzsche, Springer 2014). Protein synthesis is quantified through the incorporation of labelled amino acid in the polypeptide chain (Rennie, Smith et al. 1994). Schmidt et al introduced a new non-radioactive method for measuring the rate of protein synthesis using the compound puromycin. Puromycin is an antibiotic produced by the bacterium *Streptomyces alboniger,* that is structurally analogous to aminoacyl transfer RNA (aminoacyl-tRNA). During protein synthesis puromycin is incorporated into the newly synthesised polypeptide chain via the formation of a peptide bond and stops the protein formation by blocking the aminoacyl-tRNA activity of protein elongation. *In vitro* when a small amount of puromycin is used, it is incorporated into neosynthesized proteins and directly reflects the rate of mRNA translation. They called this method of protein synthesis monitoring surface sensing of translation or 'SunSet'. SunSet has the ability to monitor protein synthesis in whole cell lysates using Western blotting. Fluorescence activated cell sorting can be used for multiple live cells, while at the single cell level immunofluorescence can be used (Azzam, Algranati 1973), (Schmidt, Clavarino et al. 2009). Godman and Hornberger also confirmed this finding and extended its use for the detection of protein synthesis changes in whole skeletal muscle under *in vivo*

conditions (Goodman, Hornberger 2013a). van Hoewyk measured protein synthesis in plants using SunSet (Van Hoewyk 2016).

2.4.4 Analysis of protein synthesis using puromycin incorporation

The experiments where puromycin was used, initially range of puromycin was used to identify the right concentration of puromycin. Then puromycin at a concentration of 3 µg/ml was added to the HUVECs growth media. HUVECs grown in T-75 flasks were washed with 5 ml of PBS. After that PBS was replaced with HUVECs growth media containing puromycin and T-75 flasks were placed in the incubator for 1hr. After 1hr the cells were harvested using lysis buffer (table 2-20).

In some of the experiments puromycin was used together with phorbol 12-myristate 13-acetate (PMA). In these experiments puromycin was added to the HUVECs growth media for 1hr in T-75 flasks. After 1 hr HUVECs growth media containing puromycin was replaced with HUVECs fresh growth media but serum free. Then in a separate 50 ml centrifuge tube serum free growth media was added and PMA was added, to make the final concentration of 50 nM. Following this, HUVECs were washed with serum free growth media in order to remove any serum protein. Then after this, serum free media containing PMA, 9 ml volume was added to each flask and incubated for 45 minutes at 37°C/5% CO_2. Media was collected and transferred to 10 ml Amicon® ultra centrifugal tubes filter tubes (5 kDa) for protein concentration.

2.5 Growth curves for HDFs and HUVECs

Two types of growth curves were performed.

2.5.1 Growth curves in T-75 flasks

This assay utilised young HUVECs and fibroblast cells to determine the effect of conditioned media from senescent HDFs.

For a continuous source of SASP/conditioned media production, HDFs were also grown in T-75 flasks in parallel. When cells reached a high passage number and stopped growing, they were defined as senescent HDFs. Senescent was confirmed by growth arrest and flattened cell morphology. They were feed with fresh growth media.

$0.5x10^6$ early passage HUVECs or HDFs were seeded in T-75 flasks, after 24 hrs 5 ml of fresh growth media, specific to each cell type was mixed with the 24 hrs old conditioned growth media from REPS HDFs. This process was repeated every 24 hr.

In control experiments, early passage HUVECs or HDFs were fed with fresh growth media. HUVECs have a different type of growth media to HDFs. Therefore as a control HUVECs were cultured in a 1:1 mixture of HUVECs media:HDFs media. The purpose of this type of control was to have a as positive control, that can identify any effect that HDFs growth media might have on HUVECs in the growth curve.

The combination of growth media used for two types of cells was as follows

After 4 days of the cells growth, HUVECs or HDFs were harvested. The total number of cells grown were counted. Following this, the same number of cells ($0.5x10^6$ cells) were seeded, and the process repeated until 7 population doublings. CPD was calculated and according to the formula below:

CPD = (Log10Y – Log10Z) / Log102

CPD – cumulative Population doubling

Where,

Y – Number of cells harvested, Z – Number of cells seeded

Each growth curve was constructed separately. Rate for each growth curve was calculated as follows:

CPD/total number of passages. An average was taken for all the values giving the rate for each growth cure.

2.5.2 Growth curves in trans-wells

Trans-wells were obtained from Appleton Woods Ltd. For the HUVECs growth curve, $0.4x10^5$ cells of late passage HDFs were grown in trans-well inserts. For a control, early passage HDFs were seeded in trans-well inserts. These inserts were placed in trans-wells, having HUVECs seeded already (see fig 2-4). The growth media was replaced with fresh HUVECs growth media in the trans-wells and with fresh HDFs growth media in the inserts every 48 hrs. Inserts were placed in the 6 well plates during the changing of growth media for HUVECs. These inserts were placed back in the trans-well.

Every 4 days the HUVECs in the trans-wells were harvested and the number of total cells were counted. This was followed by re-seeding of the same number of cells ($0.4x10^5$) from the total cells harvested in the new trans-wells. In-order to maintain the same number of early passage HDFs growing in the inserts. Early passage HDFs (in the inserts) were harvested and re-seeded with $0.4x10^5$ young HDFs. To do this we required early passage HDFs every 4^{th} day or twice a week. Therefore, at the start of this experiment $0.4x10^5$ HDFs were grown in inserts and the remaining cells were grown in a 6 well plate. On the day the early passage HDFs were harvested in the trans-wells, HDFs in the 6 well plates were harvested and used in the inserts. The remaining HDFs were seeded in the 6 well plate. This process was repeated every 4 days. Cumulative population doubling and rate of growth were calculated as explained earlier.

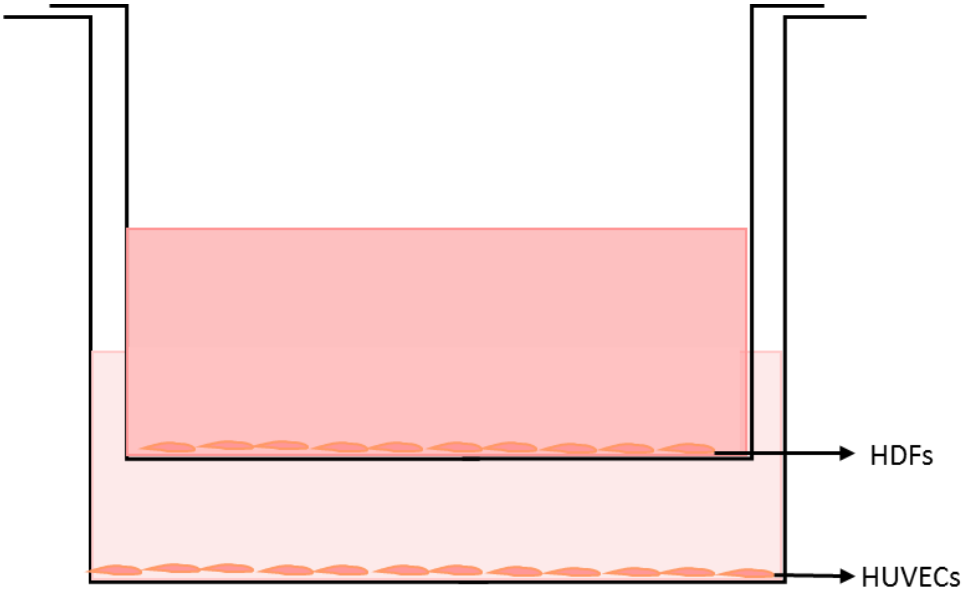

Figure 2-4: Transwells for bioassay.

The figure shows single transwell insert placed in a single well. Transwell insert is a round insert with a membrane bottom and angled sides, slightly smaller in size than six well plate from the sides and bottom. While top is the same size of a well in 6 well plate, with its edges protruding out so that it can sit well and hang from the bottom in a well of six well plate. The two different pink colours represent the two different growth media.

2.6 Proteomics Analysis

Materials

Material	**Grade, Source, Preparation**
3K Filter Units	(Amicon Ultra 0.5 mL centrifugal filters, 3000 MWCO, CAT No. UFC500396)
50 mM AmBic, pH 7.6	0.79 g in 200 mL
100 mM Dithiothreitol (DTT)	15.425 mg in 1.0 mL
200 mM Iodoacetamide (IAA)	35.036 mg in 1.0 mL
Trypsin (1.0 ug/ul)	20 or 25 ug Vial. Thus add appropriate amount to make 1.0 ug/ul.

2.6.1 Protocol

Liquid Chromatography Tandem Mass Spectrometry (LC-MS/MS) was used for the analysis of the secretome from senescent HUVECS. LC-MS/MS is a very powerful technique that combines the physical separation capabilities of liquid chromatography with the mass analysis capabilities of mass spectrometry. Being highly sensitive and selective, vast numbers of proteins can be identified from complex biological fluids.

Young HUVECs were seeded at a density of $5x10^6$ cells in T-75 flasks. After 48 hours when flasks were confluent, cells were treated with t-BHP for 1 hr on 3 consecutive days to generate SIPS with the same protocol as explained in section 2.1.2.6. For control cells only, growth media was replaced with fresh growth media each time.

HUVECs at a low passage were seeded and continuously passaged until reached passage 25, supplied with full growth media. When all the flasks were confluent then they were selected for SASP collection and further analysis.

To collect the secretome, once the cells were ready, the full culture media was removed and discarded. The dishes were washed twice with pre-warmed DPBS followed by another two washes with pre-warmed Serum Free Media (SFM). 50 nM solution of PMA in HUVECs SFM was made. This was followed by addition of 9 ml of SFM containing 50 nM of PMA to each flask. All the flasks were placed in the incubator at 37°C and 5% CO_2. After 45 minutes cell supernatant was collected and transferred to 15 ml centrifuge tubes. Three samples of SFM containing PMA were also obtained as a control to analyse and compare the proteome components in LC-MS/MS analysis that arise from growth media. The supernatant collected was centrifuged at a high speed (3,200 g) for 10 minutes to remove all cell debris.

To begin the sample preparation, all the samples (8 ml each) were transferred to three 4 ml tubes and placed into the SpeedVac™ system overnight to allow them to dry and concentrate into a smaller volume. Amicon Ultra 0.5 ml centrifugal filter was placed into a collection tube which was then cleaned and prepared by loading 500 µl of 50 mM Ammonium Bicarbonate solution (Ambic) onto the filters and then centrifuging the tubes at 18,400 g for 10 min at 4°C.

The filtrate in the collection tube was discarded. This was followed by addition of 400 µl of sample into the Amicon filters and centrifugation at 18,400 g for 10 min at 4°C. The filtrate in the collection tube was discarded. This process was repeated in the same tubes until all the samples were concentrated to 250-300 µl of total volume.

For buffer exchange, 50 mM Ambic solution was loaded in to each tube containing the concentrated samples and centrifugation for 10 minutes repeated and the filtrate was discarded. This process was repeated until a clear liquid of 200-250 µl volume was left behind in each tube.

The filter was then placed upside down into a new collection tube and centrifuged at 18,400 g for 10 minutes at 4°C – the resulting solution was retained. The filter was then turned the right way up in the same collection tube and 100 µl of Ammonium Bicarbonate were added. This was left to incubate at room temperature for 2 minutes and then the filter was turned upside down again and centrifuged at 18,400 g for 10 minutes at 4°C. The resulting solution was again retained and then the protein assay was carried out immediately.

Next step was reduction and alkylation of the samples. 100 mM Dithiothreitol (DTT) was made in 50 mM ammonium bicarbonate, adjusted pH 7.6. This was added to the samples to give a final concentration of 15 mM DTT. The samples were vortexed and incubated at 60°C on a pre-heated heating block for 15 minutes. DTT was used to reduce the disulfide bonds of proteins, whilst the IndoAcetic Amid (IAA) was used to prevent the reformation of disulphide bonds after the protein reduction step with DTT. 200 mM IAA was prepared in 50 mM ammonium bicarbonate, pH 7.6. The solution was wrapped in foil due to IAA being light sensitive. The IAA was added to the sample to give a final concentration of 20 mM and the samples were incubated in the dark at room temperature for 30 minutes. Once the concentration of protein had been determined, trypsin was then added to the samples based on the resulting concentration of protein in the samples. The rule is to use 1 µg of trypsin per 50 µg of protein, however as the protein levels were so low, it was difficult to determine protein content so instead 2 µl of 1 µg/µl trypsin was added to each of the samples as the estimated total protein content would not exceed 100 µg. The samples were then placed in a shaking incubator at 37°C overnight. The reaction was stopped using formic acid – adding 2 µl of 2% formic acid to the digested samples. The samples were vortexed briefly then placed in a shaking incubator at 37°C

for 30 minutes. Following incubation, the samples were centrifuged for 10 minutes at 13,500 g then vortexed briefly and centrifuged at 13,500 g for 10 minutes to prevent sample loss in the subsequent SpeedVac™ step. The samples were then placed in the SpeedVac™ for 1 hr. This was followed by freeze dry step, where all the samples were frozen down in liquid nitrogen and then transferred to freeze dryer for approximately 5 hours to complete dryness where a small powder was formed. The samples were then reconstituted in a 20 µl solution containing 10 µl of 0.1% formic acid and Dried pellets were re-constituted in 10 µl of 0.1% formic acid + 10 µl of 50fMol alcohol dehydrogenase (ADH) as an internal standard enabling absolute quantitation of the proteins post-analysis. A 20 minute centrifuge spin at 13,500 g was carried out and the supernatant was collected and transferred into glass screw neck vials for analysis on the Q Exactive™ Hybrid Quadruple-Orbitrap Mass Spectrometer.

2.6.1.1 Mass Spectrometry on the Q-Exactive:

Samples were digested as described in section 2.6.2. Tryptic peptides were separated on an Ultimate 3000 RSLC nano HPLC system (Dionex/ThermoFisher Scientific, Bremen, Germany). Samples were loaded onto a Cartridge based trap column, using a 300µm x 5mm C18 PepMap (5µm, 100A) and then separated using the Easy-Spray pepMap C18 column (75um x 50cm) with a gradient from 3-10% B in 10mins, 10-50% B in 37mins, 50-90% in 9mins and 90-3% in 26mins, where mobile phase A was 0.1% FA in water and mobile phase B, 80%/20% ACN/Water in 0.1% FA. Flow rate was 0.3 µL/min. The column was operated at a constant temperature of 45 °C.

The nanoHPLC system was coupled to a Q-Exactive mass spectrometer (ThermoScientific, Bremen, Germany). The Q-Exactive was operated in the data-dependent top10 mode; full MS scans were acquired at a resolution of 70,000 at m/z 200 to 2000, with an ACG (ion target value) target of 1e6, maximum fill time of 50ms. MS2 scans were acquired at a resolution of 17,500, with an ACG target of 1e5, maximum fill time of 100ms. The dynamic exclusion was set at 30.0s, to prevent repeat sequencing of peptides.

2.6.1.2 Data analysis:

The raw data files were processed and peptides were assigned to proteins using Proteome Discoverer 1.4. All searches were performed against the UniProt human database, with the precursor mass tolerance set at 10ppm with a maximum of 2 missed cleaveages. Carbamidomethyl of Cysteine was set as a static modifications and oxidation of methionine was set as a dynamic modification. All analysis was filtered using a 1% FDR (false discovery rate).

2.7 Adhesion Assay

2.7.1.1 Preparation of HUVEC's

HDFs and HUVECs at high passage number were grown in T-75 flasks. They were serially passaged until became senescent. HUVECs at passaged 25 were considered as senescent as in the previous experiments, while HDFs were considered senescent once they stopped growing and had a flattened morphology. 48 or 36 hrs before the assay both of these types of senescent cells were fed with their respective full growth media. Young HUVEC's were seeded into 96 well plates at a density of 12,000 cells/well in full media (media 200 containing 1 x low serum growth supplement) and incubated for 24 hours at 37^0C/5% CO_2. The treatment was performed by completely removing growth media from cells and replacing with stimulation media containing TNF-α. During the assay characterisation process, the cells were stimulated with a TNF-α dose response of 3-folds serial dilutions of TNF-α ranging from 10 ng/mL to 0.03 ng/mL. Once the assay was established a dose of 10 ng/mL TNF-α was routinely used for the stimulation. After 24 hr some wells in the 96 well plate were treated with 10 ng/ml of TNF-α (as shown in the figure 2-3) and the cells were incubated for a further 16-24 hours at 37^0C/5% CO_2. Cells not treated with TNF-α were treated with vehicle (fresh media containing (PBS). This was followed by removing TNF-α-containing media completely and replacing with conditioned media from senescent HUVECs and senescent HDFs. Prior to addition of conditioned media, it was centrifuged of 3,200 g, in-order to remove any cell debris. Following

stimulation with conditioned media the cells were incubated at 37°C/5% CO_2 for 12 or 24 hours. The cells were then used in the adhesion assay (see section 2.7.1.1.2.1).

2.7.1.1.1 Adhesion assay using SIPS and REPS HUVECs

Low and high passage HUVECs were grown in T-75 flasks. SIPS was induced in some HUVECs cultured as previously described (section 2.1.3.2). Once the HUVECs become confluent in T-75 all three cell types (young, SIPS and REPS) were seeded at a density of 12,000 cells/ well in a 96 well plate, as shown in figure 2-4. After 24 hrs of seeding cells, 6 columns in 96 well plate were treated with 10 ng/ml TNF-α overnight as shown in the figure 2-5. These cells were then used in the adhesion assay (see section 2.7.1.1.2.1).

2.7.1.1.2 Preparation of THP-1 cells

THP-1 cells were prepared after the HUVECs had been stimulated for 24 hours. THP-1 cells at a density of between 650,000 and 800,000 cells/mL were washed twice in serum free media (RPMI supplemented with L-glutamine). The cells were counted using a haemocytometer and then re-suspended to a density of 1 x 10^6 cells/mL. Calcein-AM was added to the THP-1 cells to a final concentration of 5µM and the cells incubated at 37^0C/5% CO_2 for 30 mins. The calcein-AM loaded cells were then washed twice with serum free media and the cells were re-suspended to a density of 1 x 10^6 cells/mL.

2.7.1.1.2.1 Adhesion Assay

The HUVEC's were washed once with serum free RPMI (RPMI supplemented with L-glutamine). The wash media was completely removed from the HUVEC's and 100 µL of the THP-1 cell suspension was added to the HUVEC's. The cells were incubated at 37^0C/5% CO_2 for 1 hour 30 minutes and then washed with serum free RPMI media (RPMI supplemented with L-glutamine). The number of washes was determined empirically to maximize the signal to background noise by observing the cells under the microscope after each wash. Following optimisation 6 washes using 100 µL serum free RPMI were used routinely. The wash media

was completely removed between each wash. After this 100 µl of serum free RPMI media was added to each well. Images for all the wells were taken at the centre of each well, using the Evos® cell imaging system. Later, all the THP-1 cells adhered to the HUVECs monolayer in the images were counted for each well. The difference between each treatment was expressed as fold change relative to control.

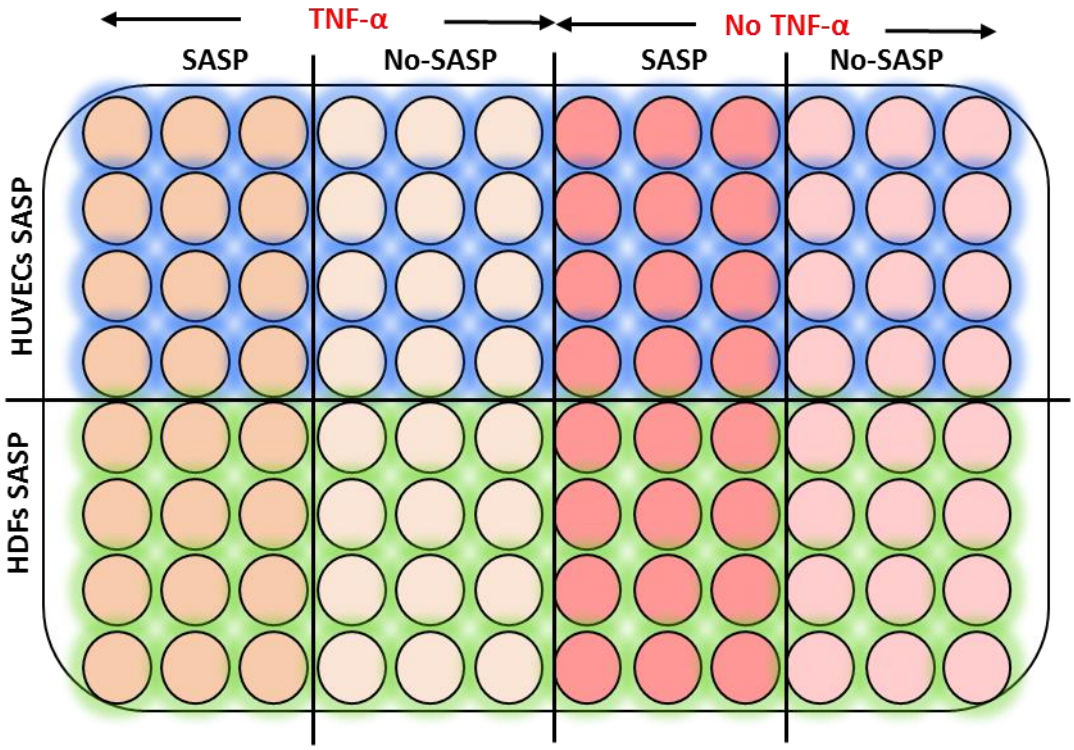

Figure 2-5 Adhesion assay using SASP.

Young HUVECs were grown in a 96 well plate. After 24 hr 6 rows of wells were treated with 10 ng/ml TNF-α overnight, while the rest were fed with fresh media. TNF-α was removed and as shown in the figure SASP (conditioned media) was added to the respective well (as labelled in the image). SASP was both obtained from HUVECs or HDFs and incubated for 12 or 24 hrs. The two different time points, 12 and 24 hrs were performed in separate 96 well plates.

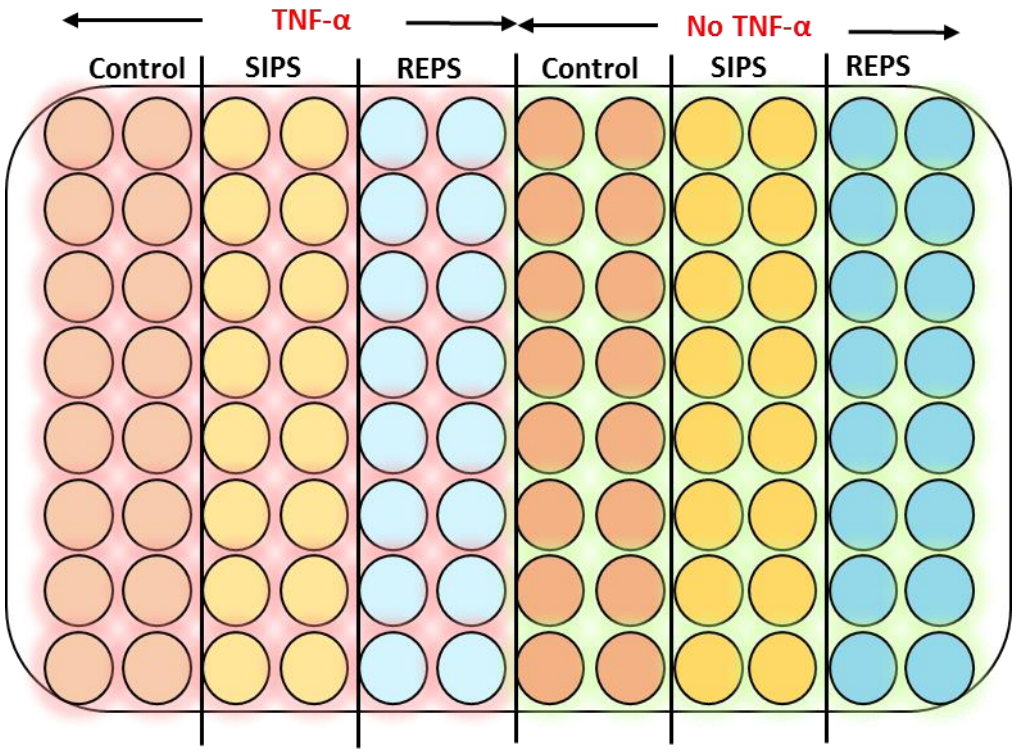

Figure 2-6. Adhesion assay in senescent HUVECs.

Young (control) SIPS and REPS HUVECs were grown in 96 well plate at a density of 12,000 cells/well as shown in the figure. After 24 hrs 6 columns in 96 well plate were treated with 10 ng/ml of TNF-α overnight. Next day the TNF-α containing media was taken off and assay was performed.

2.7.2 Adhesion asssay underflow

2.7.2.1 Preparation of HUVECs

HUVECs were grown in T-75 flasks and SIPS induced (see section 2.1.3.2) REPS and control (Young) HUVECs were grown in parallel. This was followed by seeding these cells in 35mm dishes pre-coated with gelatin (1%). Cells reached confluence in 2 to 3 days. Once cells were confluent they were either treated with or without 10 ng/ml TNF-α overnight.

Preparation of THP-1 cells

THP-1 cells were washed in full RPMI growth media. They were resuspended into 10 ml of RPMI media. The cells were counted using a haemocytometer, and then re-suspended at a

density of 1 x 10^6 cell/ml. 30 ml of THP-1 cells were kept in the flasks for the experiment. Just before the start of running each sample in the experiment, 3 ml of THP-1 cells were taken in a BIJOU and 3 µl of syto 64 at a final concentration of 10 ng/ml was added.

2.7.2.2 Adhesion (flow) Protocol

All the media from HUVECs was taken off and two tubes were connected to the glass disc and the other two ends were in the THP-1 cells, after passing through from a pump. The gasket was fixed on glass disc and placed in the dish containing HUVECs. THP-1 cells in suspension were pumped the HUVECs in the dish and returned to the reservoir with the help of a pump. This setup is placed in a chamber at 37°C on a platform connected to a microscope (Zeiss) and a screen. After the experiment was started THP-1 cells rolling over HUVECs monolayer can be visualised. A field was chosen and observed for 40 minutes. Video was taken every 10 minutes. Later the videos were analysed using a Java based image processing programme, ImageJ Fiji, and the number of THP-1 cells adhered were counted at each time point.

2.8 Illumina Microarray

Illumina microarray is the technology used to explore genome wide gene expression. The technique involves multiple bead based microarrays. The Illumina HumanHT – 12 Expression bead chip used in this project allowed 12 array to be simultaneously processed. Each bead is specific and have hundreds of thousands of copies of 50 base genes specific probes attached to it. There are around 47,000 different genes specific probes with an average of 30 beads per probe. The gene specific probes are used to quantify expression levels. Background intensity is estimated by using control probe.

mRNA obtained from samples were converted to cRNA, using Ambion Illumina Totalprep RNA amplification kit. The cRNA was hybridised to the chip, as instructed by the "Whole Genome Gene Expression Direct Hybridisation Assay Guide". There were several steps involved: the humidifying control buffer was placed in the hybridization chamber and 10 µl of hybridization buffer was added to each sample of cRNA and incubated for 5 mins at 65°C. the following washes were performed on the beadChips; 250 ml E1BC wash solution, wash buffer

at 55°C, E1BC wash, 250 ml ethanol, E1BC wash. The BeadChips were then submerged in a 4 ml of Block E1 buffer and then stained with a block E1 wash containing Streptavidine-Cy3. Finally, the BeadChips were dried by centrifugation.

All the experimental work for transcriptomics gene analysis (Microarray) was performed by a BSc student Miss Arifa Miah.

2.9 Statistical analysis

Data are presented as mean ± S.E.M or SD. Statistical analysis was performed using GraphPad® Prism 7 software (GraphPad Software, Inc., CA, USA). Data were analysed for significance by applying one way ANOVA or an unpaired Student t-test. When data were significant with one way ANOVA, comparison between groups was analysed by applying Tukey's post hoc test. P values less than 0.05 were considered significant. n represents number of experiments.

2.9.1 Microarray analysis

The raw data text files generated on the Bead Scan software were assimilated using Illumina Genome Studio™ in order to produce bead summary data. Data analysis of microarray data was performed using software R and Rstudio R version 3.4.0 (2017-04-21) -- "You Stupid Darkness". A package called limma was used. Functional analysis was carried out using Ingenuity® Pathway Analysis (IPA). IPA is a web-based database used for the analysis and interpretation of proteomics, transcriptomics and metabolomics data. It utilises different algorithms from the available data to generate different pathways, networks and identify the relevent biological processes.

2.9.2 Proteomic data analysis

Proteomics was initially analysed using Thermo Scientific^{TM} ProteinCentre Software for the protein distribution in cellular compartments. It is a software used for proteomics data set analysis, which takes the annotated data and compares it with many different databases and generates the results. Then using IPA an expression intensity analysis was carried out.

Chapter 3

3 Induction of senescence in endothelial cells

3.1 Background

3.1.1 Senescence in endothelial cells

In vitro, mammalian cells have a finite number of cell divisions and eventually enter a state of irreversible growth arrest called 'replicative senescence' (Becker, Haferkamp. 2013) Senescence can also be triggered by certain stressors. This is known as 'stress induced premature senescence' (SIPS) (Chen, J., Goligorsky 2006). A number of stressors have been used to induce SIPS, including TNF-α (Khan, Awad et al. 2017), serum starvation (Keppler, Zhang et al. 2011a), gamma irradiation (Liao, Hsu et al. 2014) and oxidative stress (Toussaint, Medrano et al. 2000).

Friedrich studied the functional morphology of endothelial cells in the atherosclerotic plaque from human carotid and coronary arteries in human hearts removed due to advanced ischemic heart diseases. Large flattened endothelial cells were found at the surface of plaques suggesting, but not proving, the presence of senescent endothelial cells (Burrig 1991). Subsequently, Minamino et al have observed SA-beta gal positive cells within atherosclerotic plaques (Minamino et al 2002). This suggests that senescence of endothelial cells does occur *in vivo* in humans. Progeroid animal models have also shown *in vivo* senescence. BubR1 insufficient mice showed increased expression of two senescence markers, $P16^{INK4A}$ and $p19^{Arf}$ in skeletal muscle and fat tissue (Baker, Perez-Terzic et al. 2008) although endothelial cells were not specifically studied.

3.1.2 Importance of senescence in cardiovascular disease

Cardiovascular diseases (CVD) are the most common diseases in the Western world. Age is the pre-eminent independent risk factor for development of CVD, perhaps because of the chronic exposure to stresses over the lifetime leading to cellular senescence (Pourrajab, Vakili Zarch et al. 2015). Chronologic age and biological age might not progress with the same pace and an organism and an organ age at different rates. For example, this means that an 80 year old person

can be, biologically speaking, as old as a 60 year old person (Chimenti, Kajstura et al. 2003). This tells us that each individual ages at a different rate, depending on their exposure to the stresses but also perhaps due to genetic differences.

In the prevention of CVD, normal endothelial function is very important as initiation of atherosclerosis is attributed mainly to endothelial injury or dysfunction (Chimenti, Kajstura et al. 2003). A literature review on aging and CVD, conducted by Kyriazis and Saridi concluded that, the development of CVD in elderly people is due to senescence of the cardiovascular system. They also added that the senescence of the rest of the organ systems adds to the pathophysiology of CVD (Kyriazis, Saridi. 2010).

3.1.3 SIPS induction in endothelial cells

Oxygen concentration inside the human body is lower than environmental oxygen. Exposing cells to higher concentrations of oxygen than biological oxygen causes the formation of free radicals by biochemical reactions (Chen, Q., Fischer et al. 1995). Human dermal fibroblasts (HDFs) show increased population doublings (PDs) (by ~20PDs) when they are cultured in an environment having a lower oxygen concentration than ambient concentration, for example, <3% oxygen (Balin, Goodman et al. 1976). According to Chen and Ames 1994 the protocol for inducing stress induced premature senescence is the exposure of early passage HDFs to a sub lethal concentration of H_2O_2 for short periods of time followed by exposure to normal culture conditions. The resulting cells lose replicative ability even when stimulated with growth factors and serum. Early passage HDFs treated in this way share the same phenotypic features as Replicative senescent cells (REP) counterparts (Chen, Ames 1994).

There were two main reasons to study induction of SIPS in EA.hy926 and HUVECs. First, as an alternative way to induce senescence. Oxidative stress is one classical way to cause premature senescence. This way we can compare the molecular mechanisms of both types of senescence (REP and SIPS) in endothelial cells. Secondly, as the initial aim of the project was to identify biomarkers for senescent endothelial cells, investigating specific biomarkers for each type of senescence would help identify the type of senescence *in vitro*.

3.1.4 HUVECs as an experimental model

Endothelial cells lining blood vessels, is important in maintaining vascular homeostasis, for example maintaining vascular tone and inflammatory responses. Endothelial cells can secrete several regulatory proteins which help maintain vessel homeostasis. Functional deterioration is the initial step during the setting up of CVD. Therefore, the endothelium is a target for consideration for the treatment of CVD. Considering the above, it is concluded that endothelial dysfunction is a valuable tool for studying mechanisms relating to cardiovascular disease pathogenesis and therapeutic strategies designed towards treatment. Limited availability of primary vascular tissue created the need for a model system that is comparable with vascular endothelial tissue. Nearly 5 decades ago Eric et al successfully derived 'Human umbilical vein endothelial cells' (HUVEC) from human umbilical veins, with characteristics of endothelial cells (Jaffe, Nachman et al. 1973).

3.2 Aims:

The aim of this chapter was to investigate whether SIPS could be induced in EA.hy926 and HUVECs model cell types using tertiary butyl hydrogen peroxide (t-BHP). One part of the aim was also to find the best and most effective way of senescence induction. As differences in the extent of senescence induction were observed between different researchers, different protocols for SIPS induction in endothelial cells were compared.

3.3 Results

3.3.1 Induction of SIPS in EA.hy926 using peroxide

Induction of SIPS has been shown in HDFs (Toussaint, Medrano et al. 2000) and in this group, it has been shown that SIPS could be induced in vascular smooth muscle cells (VSMC) and endothelial cells (HUVECs). Whether EA.hy926 cells were susceptible to induction of SIPS was unknown.

EA.hy926 were treated with t-BHP on three successive days for 1hr each day and growth media replaced; no increase in senescence was observed (fig 3-1a). However, induction of senescence was shown in EA.hy926 by an MSc student in the group supervised by me (fig 3-1b). There was dose dependent increase in senescence which reached about 30% of the total cells.

Following detailed discussion within the group, it was suggested that one difference was the use of fresh media, compared with existing media, at the point of adding t-BHP. Secondly, it was noted that the MSc student added t-BHP directly into the flask, which could possibly result in a transient and local high concentration for a portion of the cells.

This idea was tested here and involved making t-BHP dilutions in media in tubes prior to adding the whole mixture to cells within the flasks. These parameters were investigated using 100μM of t-BHP added to EA.hy926 cells. Cells were again treated for 3 consecutive days either without changing media ('old media') or replacing media ('new media'). t-BHP was either added directly as a stock solution to the flasks ('in') or by making dilutions prior to addition to cells ('out').

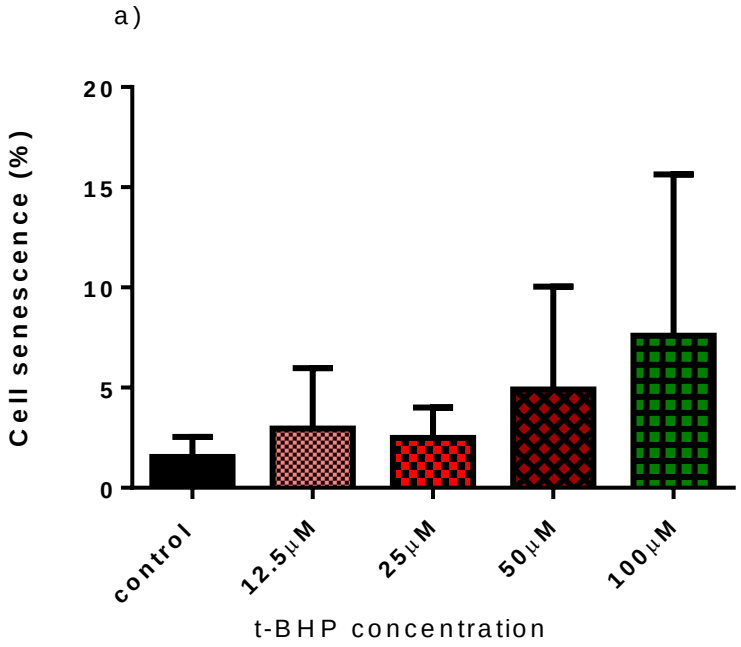

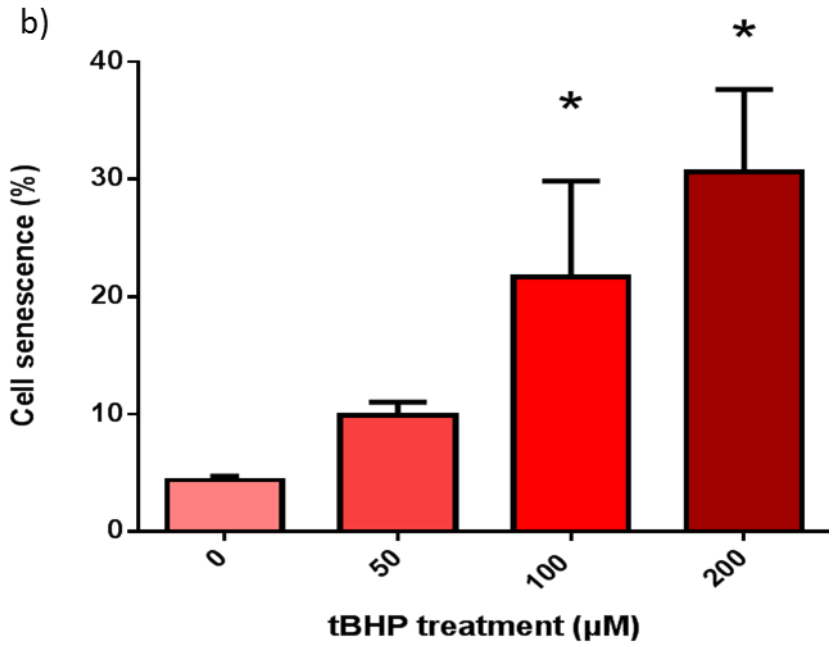

Figure 3-1: Induction of SIPS using two different protocol in EA.hy926 cells.

SIPS was induced in EA.hy926 at different concentration of t-BHP using (a) fresh media (b) old media. n=3. Results represent the mean +SEM. Data analysed with one way ANOVA multiple comparison between groups carried out with Tukey's post hoc test. P*<0.01

Comparative to control cells, senescence was not observed when using new media (Fig 3-2a), but adding t-BHP at 100 µM concentration to old media resulted in a 10% increase in senescence (Fig 3-2b). There was also a slight increase in senescence when t-BHP was added directly to the flasks, rather than pre-mixed before adding to cells, for both old and new media (fig 3-2a).

Based on these data it was hypothesised that there was some peroxidase activity in the new media which might (rapidly) lower the concentration of t-BHP. This was investigated by measurement of peroxidase activity using the Amplex red assay. Oxidation of Amplex red by H_2O_2 in the presence of horseradish peroxidase (HRP) gives rise to a fluorescent product, resorufin. This reaction has been used to measure low concentrations of H_2O_2 in biological samples (Amplex red assay). This assay was modified to measure peroxidase activity. H_2O_2 and Ampliflu^{TM} reagent were added to both old and new media, in the absence of horse radish peroxidase (HRP) and peroxidase activity measured as a change in fluorescence ex/em 560/590 nm over 70 mins (fig 3-2b).

Peroxidase activity was observed both in new and old media (fig 3-4b) but as predicted, peroxidase activity appeared higher in the new media up to at least 50 min. while the time points beyond that made no difference in the peroxidase activity in the two different types of media (old and new) possibly due to substrate depletion.

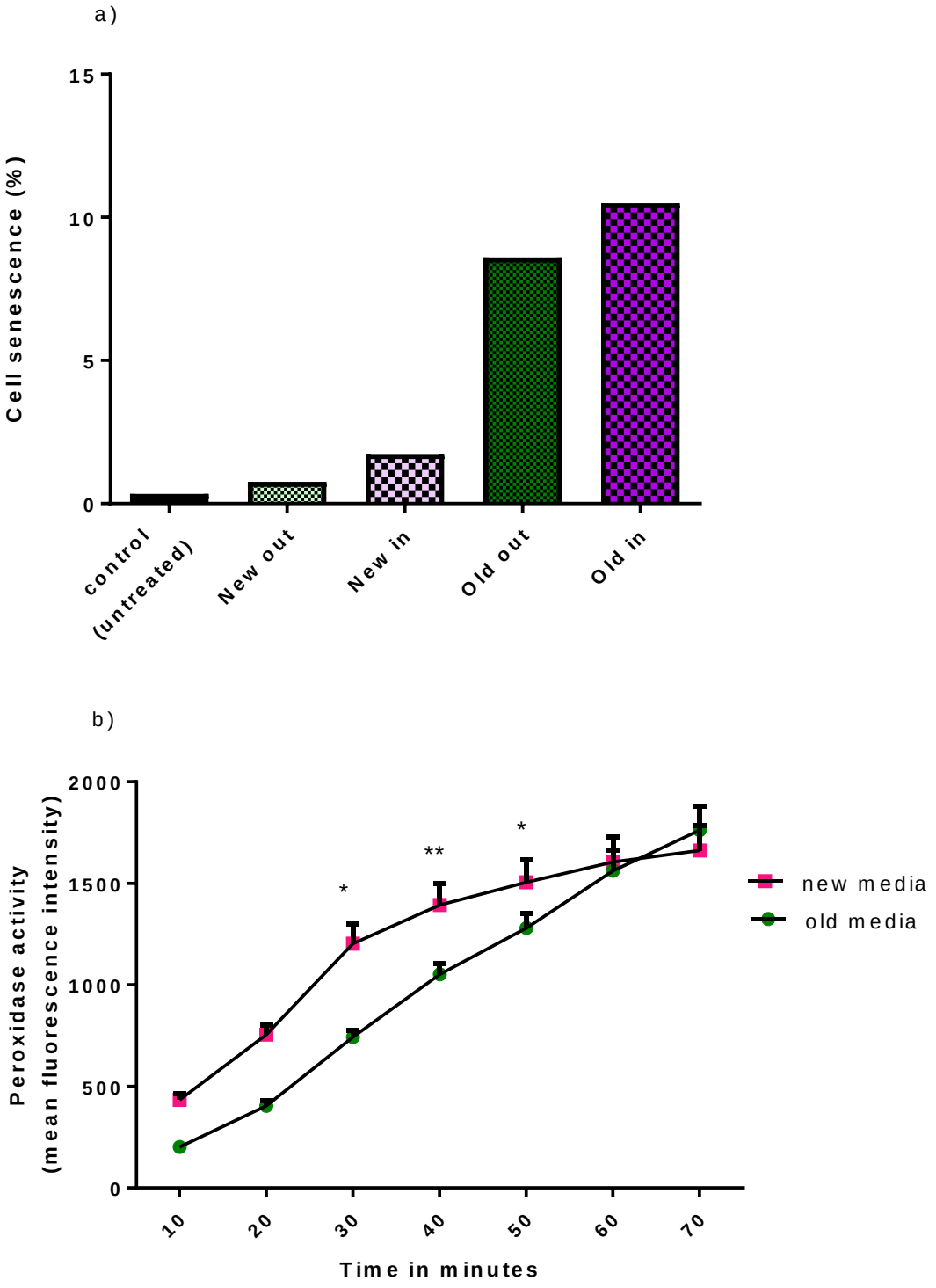

Figure 3-2: Investigation of variation in protocol on SIPS induction in EA.hy926.

(A) EA.hy926 were treated with t-BHP either in fresh growth media (new) or conditioned media (old). t-BHP was added into the flask (in) or added to media prior to addition to cells (out). Values are the mean of two replicates in a single experiment n=1. (B) Measurement of peroxidase activity in fresh and old media using Amplex red assay. Fluorescence values are mean (SEM) of 3 independent experiments. Data analysed with one way ANOVA multiple comparison between groups carried out with Tukey's post hoc test. P*<0.05, P**<0.01.

3.3.1.1 Hydrogen peroxide depletion from new media

Further investigation for looking for loss/metabolism of H_2O_2 from old and new media was carried out using the Amplex red assay. The Amplex red assay does not detect t-BHP, therefore, H_2O_2 was used instead. 24hr old media was collected and new media was taken. To both types of media, H_2O_2 was added. Samples were taken from each type of media and placed on ice (time zero) and this was repeated every 10 minutes. At the end of 60 minutes the mixture of Ampliflu and Amplex red was added to all the samples and change in florescence was measured as described in methods section 2.2.2. Florescence measurement was repeated after 5 and 10 minutes.

As expected, The H_2O_2 concentration at the earliest sampling point (time zero) was similar in the two media types irrespective of when the fluorescence was determined (fig 3-3). With time, the H_2O_2 concentration decreased for both media types but this was more rapid for new media. H_2O_2 concentration remained significantly lower in new media at all time points from at least 30min compared to old media. Half-life was also calculated for all 3 data sets (0, 5, 10 min) and shown in the table 3-1. The half-life of peroxide was reduced when it was added into fresh media (table 3-1).

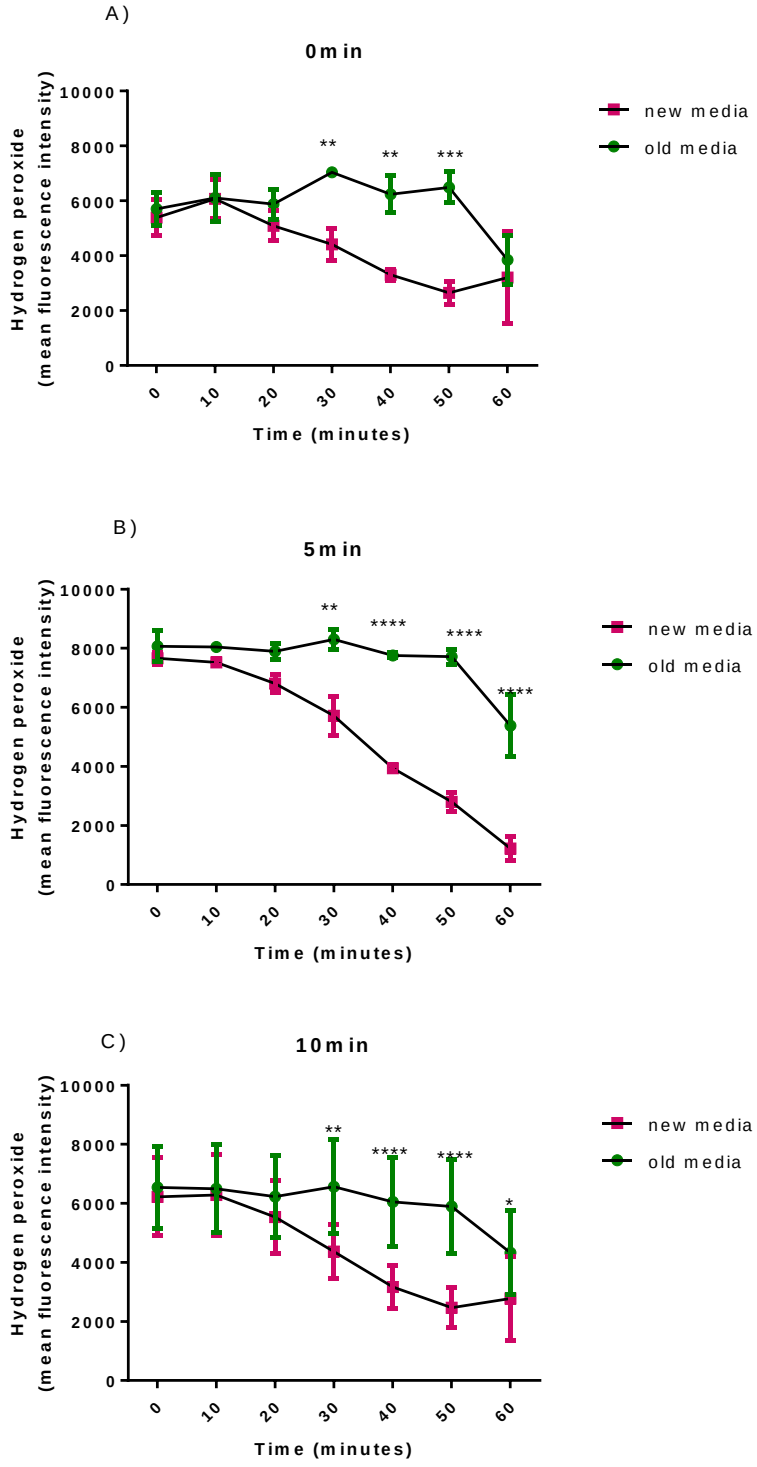

Figure 3-3 New media promotes decrease H_2O_2 concentration in Amplex red assay.

Measurement of H_2O_2 in old and new media for 60min using amplex red assay. Fluorescent reading taken at 0min (a), 5min (b) and 10min (c). Florescent values are mean of 6 independent experiments. Data analysed with one way ANOVA multiple comparison between groups carried out with Tukey's post hoc test. P*<0.01, P**<0.001, P****<0.00001.

Half-life (t ½) calculated for H_2O_2 in min)		
Time	Old media	New media
0 min	105	79
5 min	102	22
10 min	100	51

Table 3-1: Half-life of H_2O_2 in 'new' and 'old' media.

The Half-life was calculated using an online tool. http://www.calculator.net/half-life-calculator.html.

3.3.2 HUVECs treated with H_2O_2 or cultured to passage 25 display characteristics of senescence

Senescent cells express enlarged and flattened morphology (Smith, Lincoln 1984). SIPS HUVECs represented enlarged cell morphology compare to young HUVECs while REPS represented more elongated cell morphology (fig 3-4a-c). REPS HUVECs have been reported to display increased cell-cell junctions (Krouwer, Hekking et al. 2012). We also observed a continuous monolayer in the case of young HUVECs while SIPS and REPS showed gaps between cells in culture.

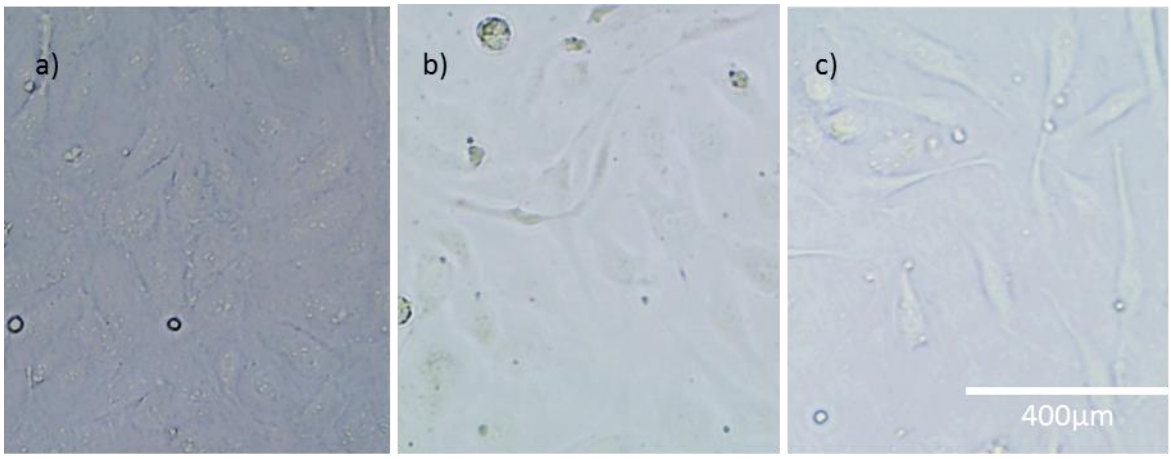

Figure 3-4: Morphology of young HUVEC compared to SIPS and REPS.

Representative photographs showing morphology of HUVECs. HUVECs morphology changes to enlarged and elongated as they become senescent. a) Represents young HUVECs (control) (b) represents SIPS and (c) represents REPS. Images taken using the EVOS® XL light microscope (magnification: x200).

3.3.2.1 Induction of stress-induced premature senescence in human endothelial cells by t-BHP

HUVECs were treated with a sub-lethal concentration of hydrogen peroxide for 1 hr on three consecutive days with return to normal growth media between. Following the final stress on day three, cells were allowed to recover for two days, passaged and re-seeded before staining for SA-beta Gal (fig 3-5) (methods section 2.1.3.2) This protocol was defined as 'stress-induced premature senescence' (SIPS) by Toussaint et al (Toussaint, Medrano et al. 2000). Senescence in SIPS was compared with senescence in cells subject to replicative exhaustion (REPS). In order to confirm the senescence in REPS and SIPS, HUVECs were stained for SA beta gal. An increase in staining was observed both in SIPS and REPS (fig 3-5a-e). t-BHP induced concentration-dependent SIPS in HUVEC which reached statistical significance at 50µM, compared to an untreated control (fig 3-6a). HUVECs were also placed into a state of REPS by serial passaging up until 25 passages. The number of PD for REPS. HUVECs at which they will become senescent was determined by optimising their growth stability in culture. REPS HUVECs showed SA-beta gal staining significantly different than control at passage 25 (fig 3-6b).

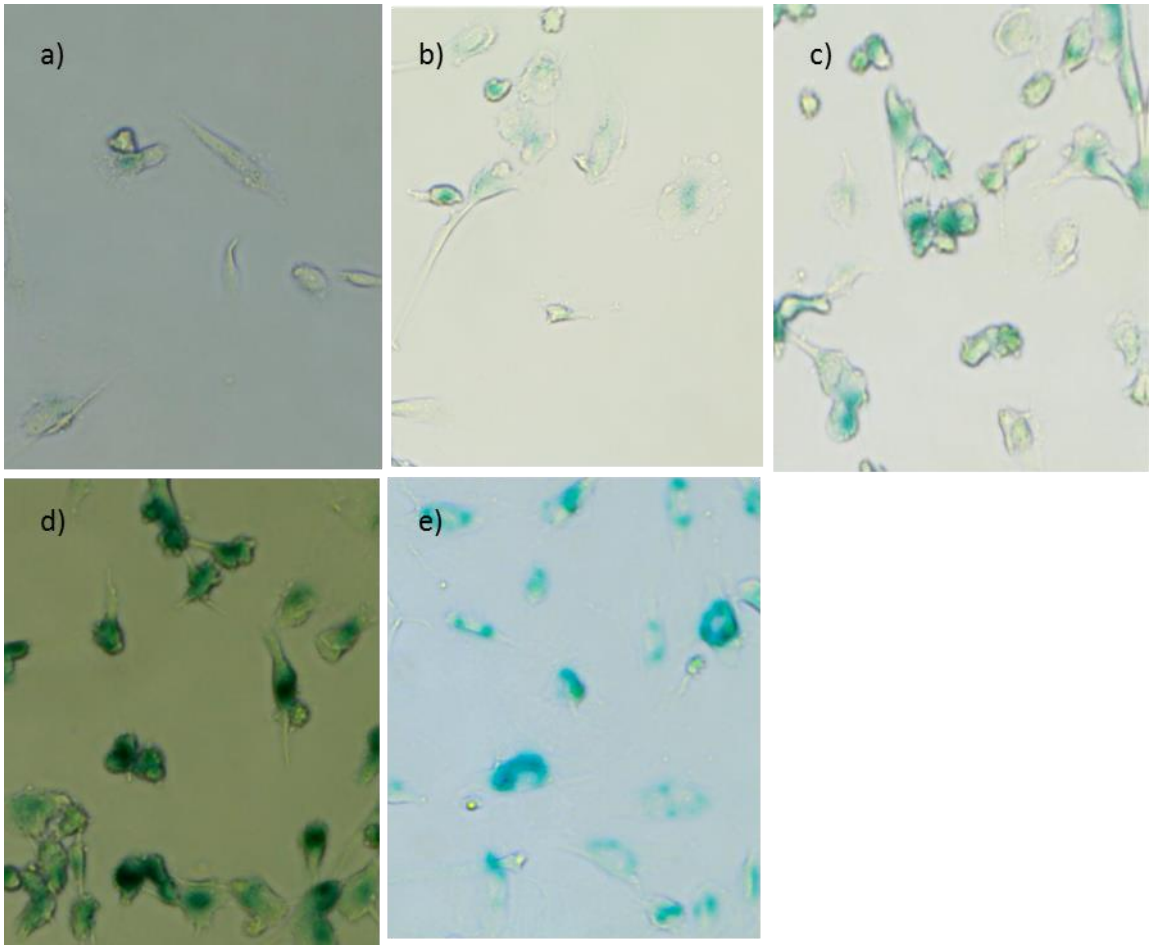

Figure 3-5 : Staining of HUVECs using different concentration of t-BHP.

The images show blue staining of young HUVECs with SA-βgal after treating with t-BHP for 3 days. The SA-βgal staining gradually increases with increase in t-BHP concentration. (a) Represents HUVECs untreated (control) (b) 25 µM concentration of t-BHP (c) 50 µM concentration of t-BHP and (d) 100 µM concentration of t-BHP and (e) REPS. n=4. Images taken using the EVOS® XL light microscope (magnification: x200).

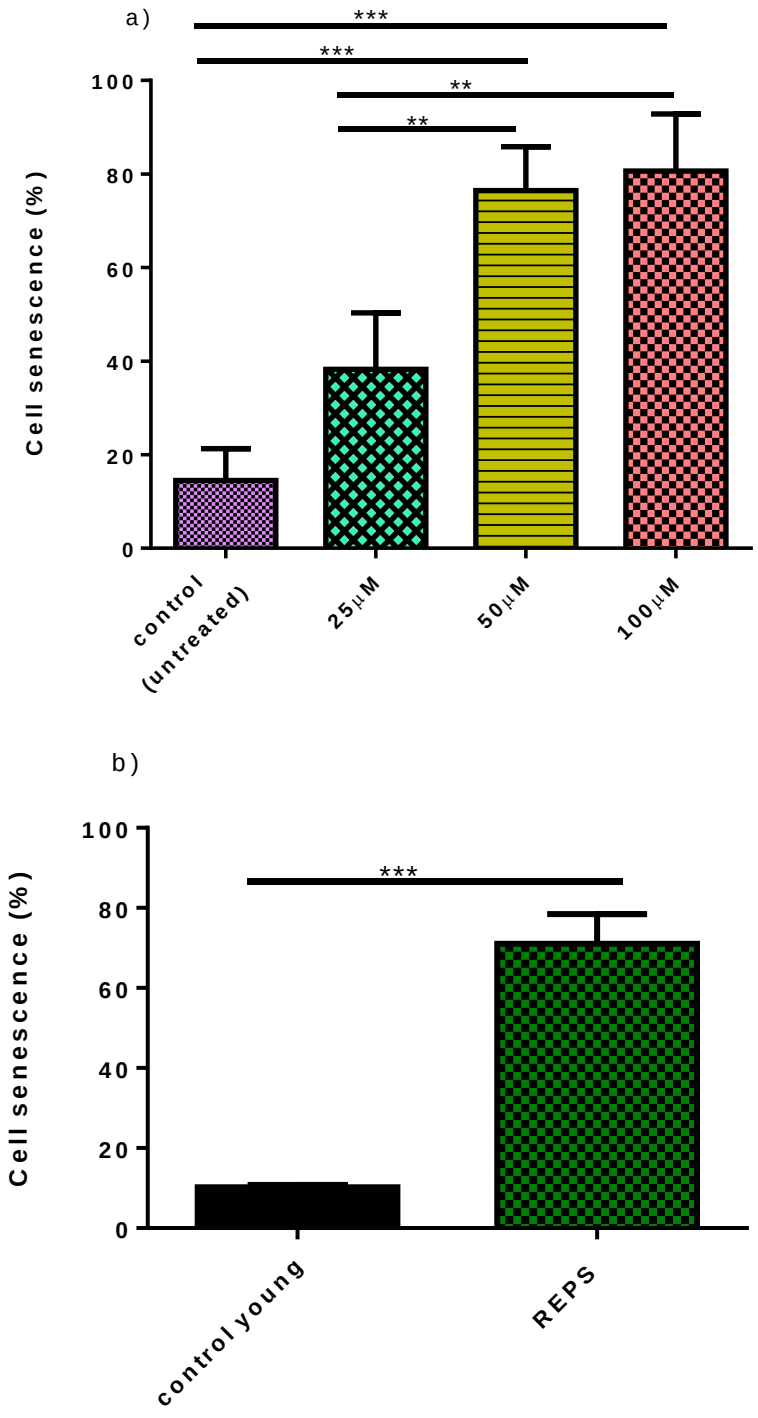

Figure 3-6: t-BHP induced SIPS and REPS in HUVEC.

HUVEC senescence was measured as cells stained blue for SA-βgal after 1 hr treatment with t-BHP for 3 consecutive days (a) or serial passaged REPS (25 passages) (B). The number of blue stained cells was counted after 24hr SA-βgal staining and expressed as a percentage of total cell. The values represent the mean (+SEM) of n=4 independent experiments. Data were analysed for significance with one-way ANOVA, and multiple comparisons were carried out with Tukey's post hoc test. **p<0.01, ***p<0.001.

3.3.3 Effect of 24hr old growth medium on EA.hy926 cell death

In the previous experiments, the use of t-BHP in old growth medium to induce senescence in endothelial cells sharpened the senescence effect, compared to the fresh medium. The Amplex red assay confirmed more peroxidase activity in fresh growth medium compared to old growth medium, metabolising t-BHP. Now to analyse the effect of old growth medium on cell death (fig 3-7A) and cell growth (fig 3-7B) EA.hy926 cells were treated with different concentration of t-BHP, in old and new growth medium. t-BHP was added to fresh growth medium and that was added to EA.hy926 grown in T-75 flasks. To the other set of EA.hy926 cells grown in T-75 flasks, fresh growth medium was added free from t-BHP. After 24 hrs, EA.hy926 treated with t-BHP were harvested and numbers of dead and live cells were counted. While to the second set of EA.hy926 cells, t-BHP was added to the growth medium already used to feed cells 24 hr previously. The same process of cell harvesting and counting was repeated for this set of EA.hy926 cells. In-order to count the number of total dead cells, before harvesting the cells, cell supernatant containing floaters was collected and centrifuged at a high speed. Supernatant was discarded and the floaters concentrated at the bottom was added to the cells harvested. Cell death was analysed as the percentage of total cells. Cell growth was analysed as the number of live cells as a percentage of control cells.

There was no significant effect on cell death in old media at all different concentrations, compared to new media. Also, there was no significant difference observed on the cell growth. There was a slight increase in the growth of EA.hy926 in old media. This difference was probably due to the fact that old growth medium cells were grown for 24hr longer than new growth medium. Most of the H_2O_2 is metabolised after 60 min of its administration (fig 3-3). Therefore its presence in the media longer than 1 h have got no effect on the cells.

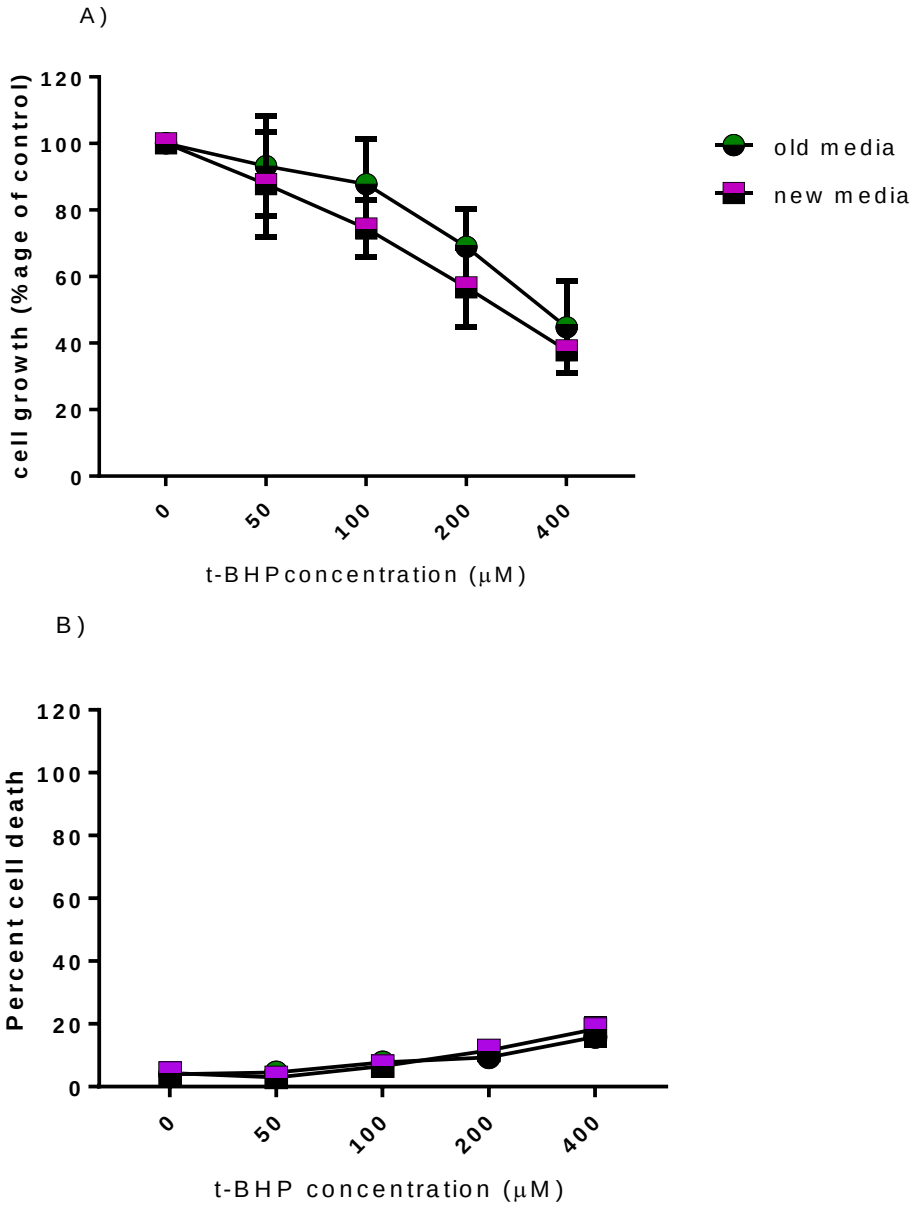

Figure 3-7: 24 hr old growth media has no effect on EA.hy926 cell proliferation and cell death.

EA.hy926 were grown in T-75 flasks, treated with t-BHP in old (green and black circles) or 24 hr fresh (pink and black squares) growth medium for 24 hr. EA.hy926 were harvested and cell growth (fig 1A) and percent of cell death (fig 1B) were analysed. N=3 independent experiments. P*<0.05.

In addition to SA-beta gal, REPS and SIPS also exhibited increased expression of the senescence marker p53 protein (fig 3-8) in Western. SIPS HUVEC showed higher expression of p53 than REPS cells. Analysis of p53 expression did not show significant increase in both SIPS and REPS (fig 3-8).

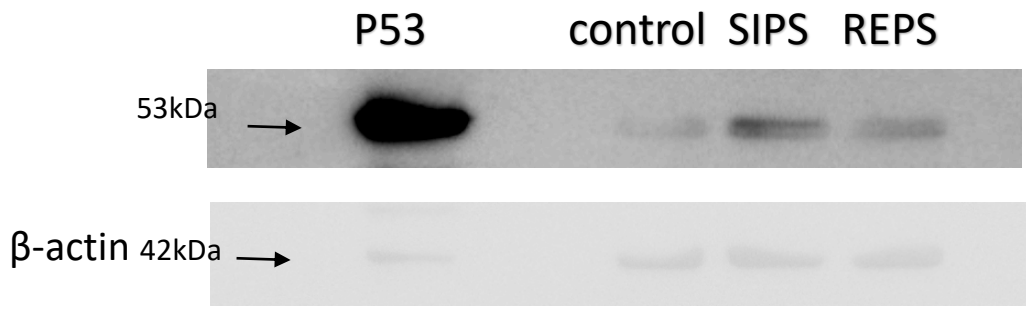

Figure 3-8: p53 expression by SIPS and REPS HUVEC.

30 µg of cell lysate (protein) was loaded for each HUVECs sample. Positive control was cell lysate over expressing p53 far left. Lower blot shows loading control (β-actin). n=5 independent experiments.

3.4 Discussion

Ageing involves gradual molecular changes resulting in loss of homeostasis. This can weaken characteristics at older age and might result into the predisposition of diseases, such as cardiovascular disease, diabetes, cancer and dementia (Lees, Walters et al. 2016). Senescence of endothelial cells, causing irreversible growth arrest might contribute to age-related endothelial dysfunction and vascular pathology (Donato, Morgan et al. 2015).

Cells in culture can be either passaged until they become senescent or stressed with certain stressors to induce SIPS (Chen, Q. M. 2000). Here SA beta gal staining was used to examine the senescence state of REPS and SIPS. In the present experiments both SIPS and REPS HUVECs showed SA beta gal staining. Oxidants are toxins and cells exposed to oxidants show increased expression of genes that are involved in growth arrest for example. p53 (Chen, Q. M. 2000). Previously H_2O_2 has been used to successfully induce SIPS in HUVECs (Coleman, Chang et al. 2013). Similarly to avoid acute toxication, Unterluggauer et al have applied mild concentration of t-BHP in a series of 5 consecutive treatment to induce senescence in HUVECs (Unterluggauer, Hampel et al. 2003). Dumont et al investigated the sublethal long term effect t-BHP of W1-38 human diploid fibroblasts. After treating cells with 30 µM concentration of t-BHP for consecutive 5 days developed followed by a recovery period of 48 hr, developed the typical phenotype of senescence i.e. increase in SA beta gal staining, inability to divide and over expression of p16 (Dumont, Burton et al. 2000).

Because senescence was observed in EA.hy 926 cells only when peroxide was added to conditioned or 'old' media, a further investigation was conducted. The Amplex red/peroxidase assay is a highly sensitive assay that measures small concentrations of H_2O_2 in biological samples. Amplex red is converted by the action of horseradish peroxidase (HRP), in the presence of H_2O_2 to resorufin which is fluorescent (at ex 571 nm and em 585 nm). The assay can measures H_2O_2 concentration as low as 50 nM (Zhou, Diwu et al. 1997). Unfortunately, in this thesis it was found that t-BHP is not a substrate for horseradish peroxidase. Therefore, determinations of peroxidase activity and the half-life of peroxide in media were made using H_2O_2 and not t-BHP. Whilst this is a limitation of the study it does still measure peroxidase activity, however, the data do not directly measure effects on t-BHP. Another limitation of this determination is that resorufin is also a substrate for peroxidases, which convert it to a colorless/nonfluorescing material(s) (Towne, Will et al. 2004) and therefore the product (resorufin) formed during the reaction can react with available peroxidase decreasing the fluorescent read out and masking the peroxidase actual level measurement (Reszka, Wagner et al. 2005). Therefore the assay results are more accurate when peroxidase concentration is more than H_2O_2.

Induction of SIPS in EA.hy926 cells using t-BHP was greater in old media. One possible explanation could be there was less peroxide available in new media. We hypothesised that there is peroxidase activity in new media capable of metabolising peroxide and therefore reducing the concentration in the media. The Amplex red assay was modified such that we did not add horseradish peroxidase, hence the available peroxidase in the media would act as a substrate for Amplex red and would produce a fluorescent end product. This way we able to measure the activity of peroxidase in both new and old media. A higher peroxidase activity showed the potential for increased metabolism of peroxidase and making its concentration lower.

In order to confirm this the amplex red was performed to measure the concentration of peroxide in media over time. Levels of H_2O_2 were measure over a period of 1 hr (this was the time for which cells were treated with H_2O_2 to make them SIPS in culture) and horseradish peroxidase was also added to the reaction mixture. Prior to this H_2O_2 was added to both media types and every 10 minute one sample was analysed. The half-life of H_2O_2 was reduced in new media compared to old media. This confirms that there is less H_2O_2 available in the new media to

cause the oxidative damage in inducing SIPS. Decreased concentration of H_2O_2 concentration was not measured beyond 60 minutes and so it cannot be specified from this experiment the time point where all of the H_2O_2 will be degraded completely.

The possibility that old media might be deprived of nutrients or cells might release factors that could cause increased stressed, was also considered. Cell death was analysed in both old and new media using different concentrations of t-BHP in EA.hy926 cells. EA.hy926 cell death was not affected in old and new media. This suggest that t-BHP addition to the old media had only effect on cells senescence induction in culture.

Krouwer et al evidenced that replicative senescence of endothelial cells (HUVECs) showed a disrupted cell-cell contacts. These disrupted cell-cell contacts are a result of alterations in the distribution of adherens junction proteins and decreased expression of tight junction proteins (Krouwer, Hekking et al. 2012). Similarly, a continuous monolayer of cells was not observed for REPS and SIPS while young HUVECs grow in the form of close compact monolayer.

P53, P21 and p16 have been reportedly expressed by senescent HUVECs (Khan, Awad et al. 2017) confirming senescence in endothelial cells. The data presented in this thesis showed increase p53 protein expression in SIPS or REPS cells.

3.5 Conclusion

Induction of senescence using t-BHP or by serial passaging of HUVEC was achieved. To induce senescence in EA.hy926, which are modified endothelial cells, required either higher concentrations of peroxide or a prolonged half-life in cell culture media. In the old media, it was inferred that due to decreased peroxidase activity there was decreased metabolism of peroxide making it available for longer. Therefore to induce senescence (SIPS) using old media is the suggested option for future studies. In all cases a senescent cell phenotype was observed in REPS and SIPS, for example, SA beta gal staining and enlarged morphology. These protocols will be utilized in the following chapters to investigate molecular changes in senescence using transcriptomic and proteomic analyses.

Chapter 4

4 Comparison of endothelial gene expression profile in replicative and stress induced premature senescence

4.1 Introduction

The transcriptome is the set of all types of RNA including protein coding RNA (mRNA) and non-coding RNA, for example tRNA, long non-coding RNA (lncRNA), micro RNA (miRNA) A transcriptomics data set is the quantitative analysis of all the expressed genes in the samples, carried out through next generation sequencing or microarray platforms. It can be applied to either an organism or specific types of cells or tissues. The results obtained from transcriptomics studies can be used alongside other biologic approaches for example proteomics, to gain deeper understanding of the role of genes and pathways involving genes in biology and disease.

Cellular senescence is associated with changes in gene expression (Marthandan, Baumgart et al. 2016). It is important to identify the genes that are differentially expressed by senescent endothelial cells. This is important for the understanding of mechanism of senescence and changes in biological functions brought about by senescence. This is because the senescence triggered by different stimuli and in different cell types engage different mechanisms. Therefore, identification of a cell specific as well as senescence induction specific biomarker is of interest. In this regard studies have identified several genes and proteins as biomarker for replicative senescence (Shelton, Chang et al. 1999), (Eman, Regan-Klapisz et al. 2006b). Due to their association with different other diseases, however, these molecules cannot be regarded as exclusive hallmarks of senescence (Campisi, d'Adda di Fagagna 2007b).

Researchers have been trying to identify the biomarkers of ageing, but due to the complexity of the ageing process a set biomarkers of ageing has never been identified. A panel of biomarkers of healthy ageing for all the measures of functions has been proposed. These can act as predictive of the individual biological age and researchers can refer to these for assessing the healthy aging of individuals (Lara, Cooper et al. 2015).

4.1.1 Difference in REPS and SIPS

Replicative senescence (REPS) is the cell division arrest observed by Hayflick and Moorehead in HDFs grown in culture (HAYFLICK, MOORHEAD 1961). These terminally growth arrested cells are associated with several phenotypes.

In humans, ageing is the process of frailty and impaired bodily functions collectively leading to diseased state (Lees, Walters et al. 2016). With time, random changes occur in cellular environment, leading to modification in cellular components. Due to the failure of the cell protection machinery and immune system with age (Linton, Dorshkine 2004) to fix or eradicate the cellular component modification, with time progression this will lead to malfunction of cellular machinery. When this damage reaches a certain threshold, where it is beyond repair, the cell will die. Another theory explaining ageing is the 'free radical theory' of ageing. According to this theory reactive oxygen species (ROS) are the important mediators of oxidative damage of cellular components and subsequently cellular ageing. One explanation is that ROS induction in the cells makes the cells undergo senescence, called premature senescence (Dierick, Eliaers et al. 2002). In support of this theory, oxidative damage in DNA, proteins and lipids has been observed in tissues from aged individuals (Chen, Q. M. 2000). There is also an evidence of increased level of free radical generation in senescent cells (Allen, Tresini et al. 1999). Chen et al have confirmed that fibroblasts grown in physiological oxygen level (3%) were able to proliferate more than those which were grown under a higher oxygen tension of 20% (atmospheric oxygen) (Chen, Fischer et al. 1995). Many agents have been identified as inducers of premature senescence and models have been set up *in vitro*. Toussaint et al have defined a method for stress induced premature aging. In this protocol cells are subject to repeated subcytotoxic levels of stressor i.e. t-BHP, hypoxia and H_2O_2 to induce senescence. These cells share the same morphology as REPS (Toussaint, Dumont et al. 2000). The question is now, are these two types of senescence identical with respect to cellular and molecular level changes? Research has been conducted using early passage fibroblasts exposed to subcytotoxic levels of H_2O_2. These cells were unable to divide further and shared similar morphology as REPS cells. Next these cells were compared to REPS fibroblasts for the activity of ornithine decarboxylase or thymidine kinase. Both types of senescent cells expressed the same reduced activity of these enzymes (Chen, Ames 1994).

4.2 Aim and objectives

The aim of this study is to identify and investigate genes and pathways that are related to HUVEC senescence. This current study was aimed at comparing and contrasting gene expression in SIPS versus REPS HUVECs. In addition to looking at similarities and differences in mechanisms between the two types of senescence, it is envisaged that a combination of genes would lead to a more specific and better biomarker in the identification of senescent endothelial cells in culture and possibly in humans.

4.3 Results

4.3.1 Preliminary analysis of differential gene expression in senescent HUVECs using ArrayTrack

Senescence was induced in HUVECs, by replication means (REPS) or by successive treatment of cells with t-BHP as described in methods section 2.1.2.6. Samples of 'young' untreated HUVECs served as a control. Following RNA extraction and reverse transcription, microarray analysis was performed to identify genes differentially expressed in senescence versus control HUVECs. Differentially expressed genes were extracted from ArrayTrack and the top three up- and down-regulated genes for REPS are shown in the table 4.1.

GENE NAME	REPS fold change	SIPS fold change
CST1	109 ↑	-
LRRC17	70 ↑	3 ↑
CRTAC1	3 ↓	2 ↓

Table 4-1: The expression of genes in REPS and SIPS extracted from microarray analysis.

The table shows a list of highly upregulated and down regulated genes expressed by REPS and RIPS HUVECs, obtained from microaaray analysis using a database, ArrayTrack (U.S Food and Drug Administration). The number shows the fold change and the upward arrow shows the upregulated genes. The downward arrow shows the downregulated genes. The dash sign (-) shows no gene expression.

This transcriptomics experimental data were obtained with a previous BSc student (Miss Arifa Miah) from this research group..

4.3.1.1 TaqMan® Probes investigation

The initial steps in carrying out the RT-qPCR involved investigating the efficiency of the TaqMan® gene expression assay probes. The genes of interest CST1, LRRC17 and CRTAC1 and housekeepers genes VCP, β-actin, PSMB4 and GPI qPCR were investigated. mRNA was extracted from young, SIPS and REPS HUVECs and cDNA produced through reverse transcription. The resulting cDNA from all three types of samples was then pooled and a standard curve was constructed for genes of interest and housekeeper genes and qPCR performed (fig 4-1a, b). From standard curve values, efficiencies were calculated for each gene using ThermoFisher© efficiency calculator as (table 4-2). The recommended accepted values for pcr probe efficiencies ranges from 90 to 105%. All the gene efficiencies were within this range. Therefore, these gene of interest were considered for analysis of expression changes in senescent HUVECs compared to young HUVECs. Also, the housekeeper genes were chosen for undertaking comparative quantitative analysis. The standard curve also determined the dynamic range of assay, and as a result 10ng of template input was used in the assay.

a)

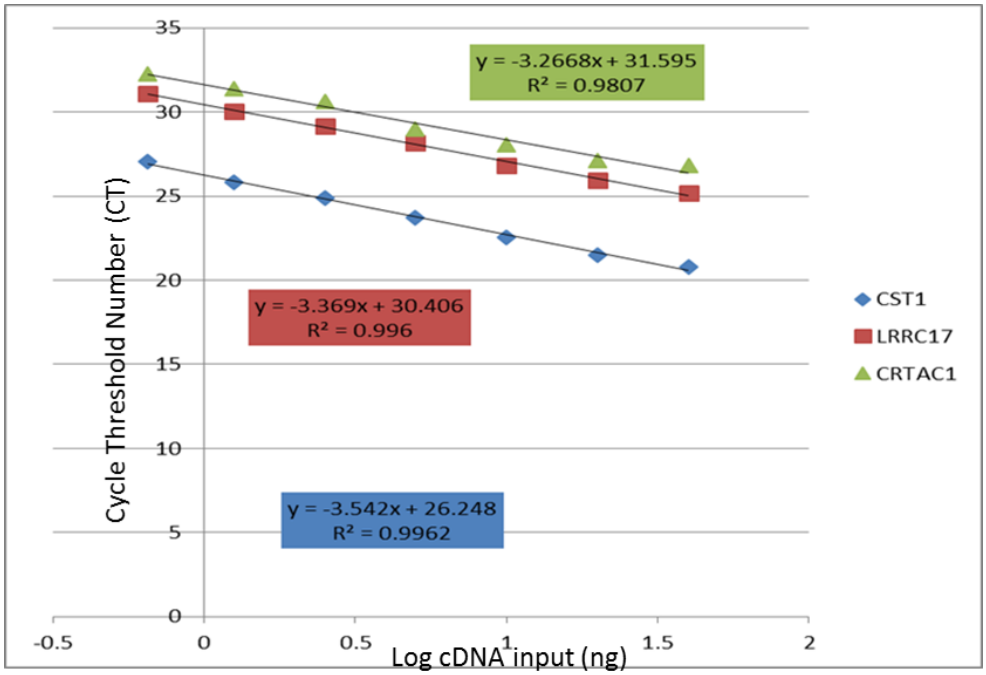

b)

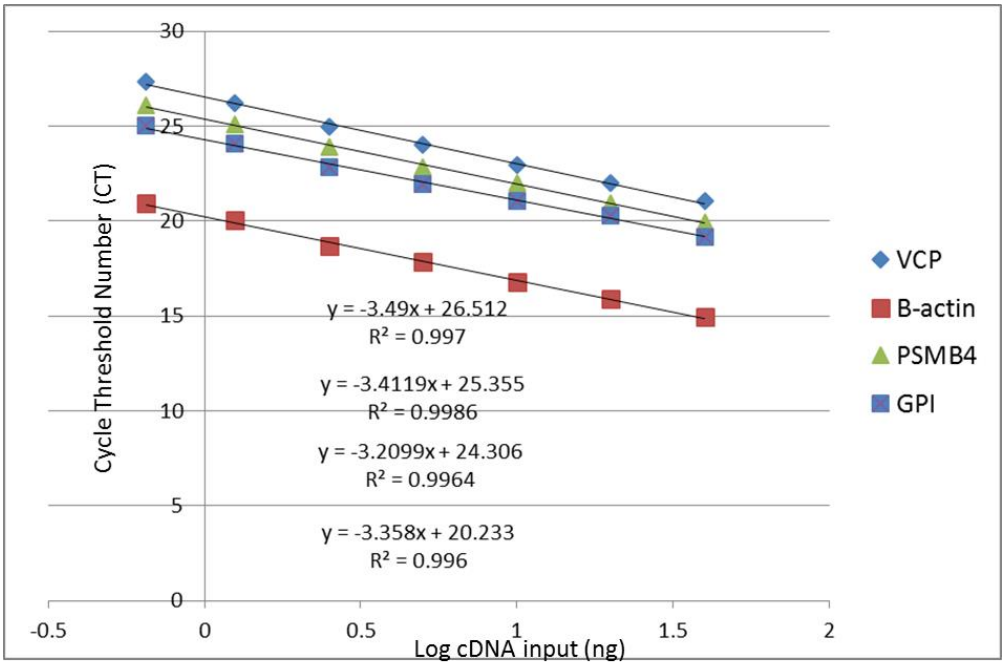

Figure 4-1: Determination of qPCR efficiencies of Taqman® probes.

RNA was extracted from control, untreated young, REPS and SIPS HUVECs. cDNA was reverse transcribed and the cDNA from all the samples pooled. A standard curve was conducted from the pooled cDNA. qPCR was carried out using Taqman® gene expression probes.(a) shows the standard curves for genes of interest while (b) shows for housekeeper genes.

Housekeeping gene	Efficiency (%)
Cst1	91.7
Crtac1	102.0
Lrrc17	98.0
VCP	93.4
B-actin	98.8
PSMB4	96.4
GPI	104.9

Table 4-2: List of qPCR Taqman® probes efficiencies. S

Table hows the efficiency of all the 3 genes of interest and housekeeper genes. Efficiencies are expressed as percentage.

Efficiency was calculated as: $10^{(-1/\text{gradient})-1}$ (ThermoFisher, 2008).

4-2Table (c)

4.3.1.2 Validation of housekeeper genes; VCP, β-actin and PSMB4 expression does not change in senescent HUVECs

Real time PCR is the gold standard for expression analysis of genes. It measures the variation of gene expression between the samples. It is also important to measure true variation in gene expression and eradicate the false variation that comes through the experimental process. Therefore a housekeeper genes are used. It is important to identify a housekeeper gene that is expressed constantly in all the samples under different experimental conditions. Therefore different validation methods are used in order to minimise the error (Vandesompele, Kubista et al. 2009). Glyceraldehyde 3 phosphate dehydrogenase (GAPDH) has been widely used as a housekeeper gene. It has been identified as an appropriate gene in senescent cells, as its expression was not changed in senescent cells (Zainuddin, Chua et al. 2010). However, it has been shown that GAPDH induces the induction of cancer cell senescence via interacting with telomerase (Nicholls, Pinto et al. 2012). This made the choice of using GAPDH as a housekeeper gene, questionable. Therefore, a number of housekeeper genes were selected and

their validation were carried out, before being used in the comparative quantitation analysis. In this regard, four housekeeper genes were selected; VCP, β-actin, PSMB4 and GPI. The respective gene Taqman® gene expression assay probes were obtained from Applied Biosystems and qPCR was carried out. Each sample was repeated in triplicate. All the samples raw CT values were averaged. (fig 4-2) shows the change in the CT values across all nine samples for each housekeeper gene. Among all three housekeeper genes β-actin is highly expressed. All the samples showed the same pattern of housekeeper expression, which mean that if there is slight variation in the expression, it might be due to the construction and impurities in the cDNA. All the three housekeeper genes were selected for further gene quantitation analysis, so that an average of all three values could be taken when comparative CT analysis was conducted. The TaqMan gene expression analysis probe for GPI had good efficiency but its expression was not constant in the senescent HUVECs versus young HUVECs. Subsequently, it was excluded from further consideration in the study.

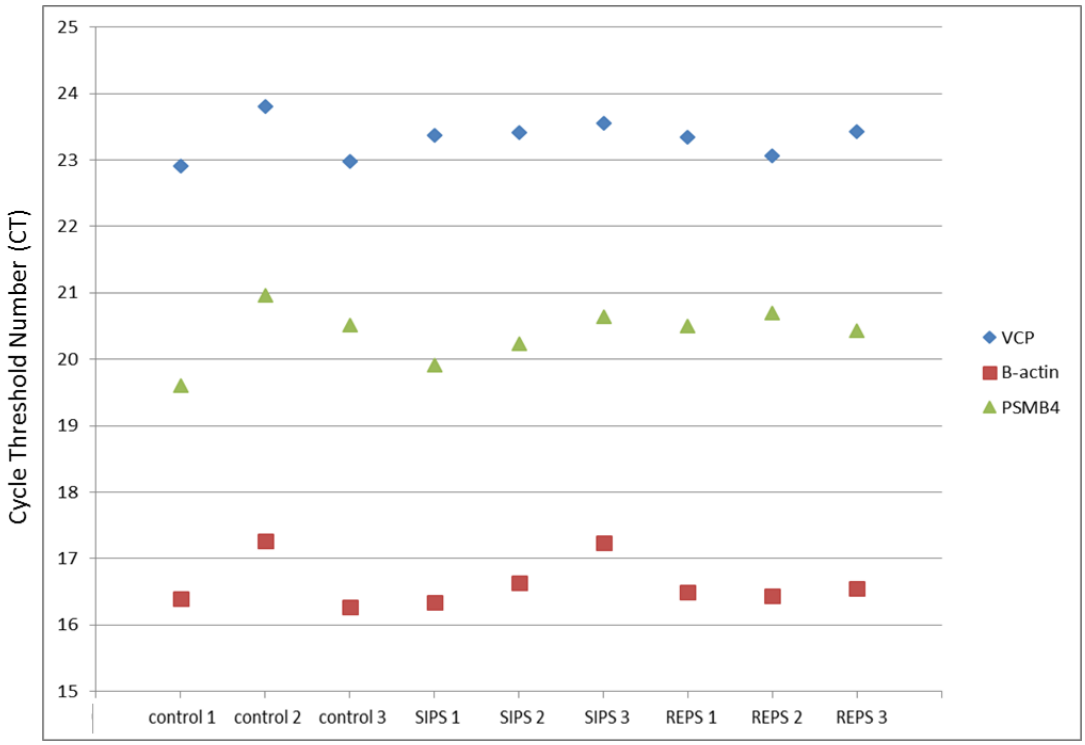

Figure 4-3: Housekeeper gene validation in senescence HUVECs.

mRNA was extracted from young, SIPS and REPS HUVECs. cDNA was reverse transcribed. qPCR was carried out for house keeper genes, using Taqman® gene expression probes. Expression values for all the housekeeper genes were plotted in Microsoft excel. Values represent mean, of 3 replicates, Ct for each sample.

4.3.2 Cystatin SN as a potential biomarker for senescence

Consistent with the transcriptomics data CST1 gene expression by RT-PCR was highly upregulated in REPS HUVECs (fig 4-3A), by approximately 140 folds but there was no increase in SIPS HUVECs. In contrast, levels of LRRC17 and CRTAC1 measured by qPCR were not well correlated with the transcriptomics data. LRRC17 was upregulated both in REPS and SIPS compared to control HUVECs in transcriptomics while with PCR experiments (fig 4-3B) LRRC17 mRNA was not changed in SIPS but increased by 4 folds in REPS.

CRTAC1 was down regulated in both REPS and SIPS in transcriptomics data while in qPCR experiments CRTAC1 mRNA expression was (fig 4-3C) significantly upregulated ($P<0.0001$) by 10 folds in REPS. This highlights the need to validate microarray findings (e.g. by qPCR) but also suggests that these proteins might be novel markers of senescence in endothelial cells and are worthy of further study.

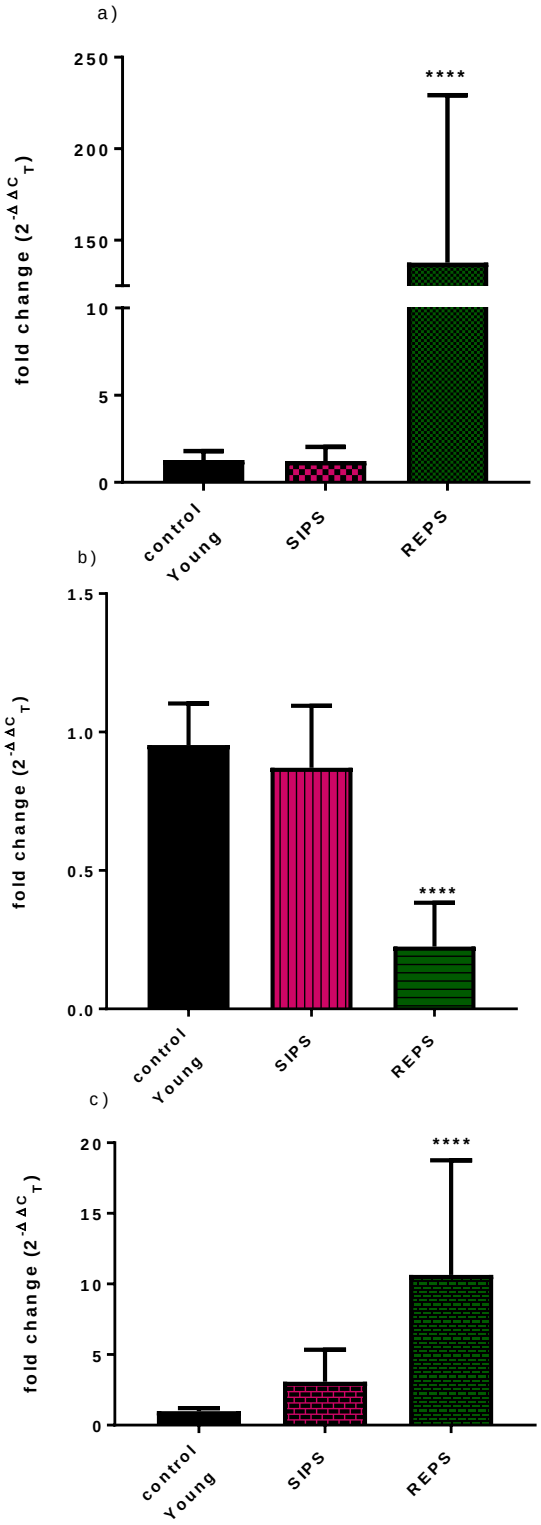

Figure 4-4: Expression of CST1 (a), LRRC17 (b) and CRTAC1 (c) genes in senescent HUVECs.

Total mRNA was extracted from replicative senescence cells (REPS) at passage 25, stress-induced premature senescence (SIPS) and control cells at passage 6 and RT-PCR performed. Each experiment was performed in triplicate and repeated n=5 times. Results were analysed with one-way ANOVA multiple comparison carried out using Dunnets post hoc test ****P<0.0001.

4.3.2.1 Investigation of CST SN expression in senescent HUVECs

CST SN is a secretory protein (Baron, DeCarlo et al. 1999) produced from the cst-1 gene, which is highly expressed by senescent HUVECs at the RNA level according to experimental results of transcriptomics from this group (table 4-1) and PCR data in this thesis (fig 4-3A). Previous studies have demonstrated the expression of this protein in senescent fibroblasts (Keppler, Zhang et al. 2011b) and different cancers tissues (Jiang, Liu et al. 2015), (Choi, Kim et al. 2009). In an attempt to validate the results and look for the expression of this protein in senescent HUVECs, Western Blots were performed. Western blot results using whole cell lysates showed no expression of CST SN (fig 4-4A). As this is a secretory protein we assume this will be secreted by senescent HUVECs and present in the cell's supernatant. The challenge is to deprive cells of serum for 24 hr in order to measure secreted proteins. Serum deprivation of HUVECs results in the death of the majority of cells. A 50% of cell death was observed in HUVECs grown in 0.1% FBS for 24 hr compared to cells grown in 20% FBS (ref). similar results were observed in experiments to collect cell supernatant from HUVECs grown in serum free medium for even 12 hr. To resolve this, the exogenous secretagogue, PMA was used. HUVECs were grown the in serum-free growth media with 50 nM of PMA for 45 minutes.

The use of PMA resulted in very little or no protein expression in Western Blots performed, as there was no staining detected using Ponceau S stain. In a parallel experiment, HUVECs conditioned media (24 hr) containing serum were collected. Proteins were precipitated using trichloroacetic acid (TCA). Precipitated proteins were analysed on a 12% polyacrylamide gel. This again resulted in no detection of CST SN.

Western blots were also performed on cell lysates extracted from REPS and SIPS HUVECs. CST SN was not detected. The antibody used in Westerns has been validated by using cells transient overexpression lysate expressing CST SN protein obtained from Abnova®. This served as a positive control in our experiments (fig 4-4).

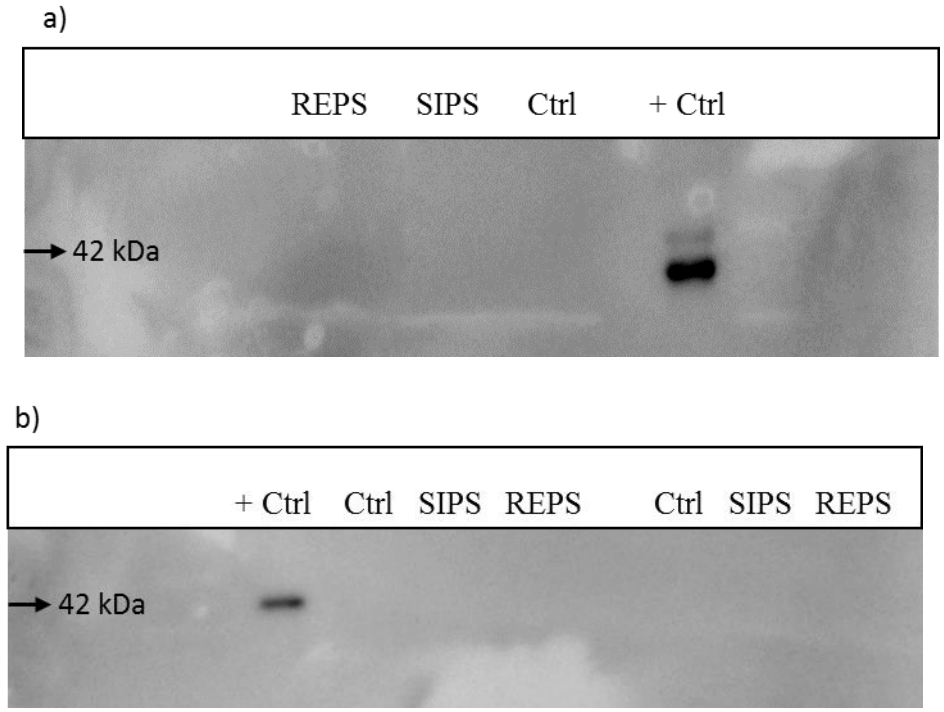

Figure 4-5: CST1 expression in stress induced and replicative senescent HUVECs.

Young HUVECs were stress induced (SIPS), or made replicative senescent (REPS) and were (a) treated with 50 nM PMA and after 45 minutes media was collected and protein concentrated using 20% TCA. In other experiments (b) total protein from cells was extracted using RIPA buffer. Cellular proteins (30µg) were separated using sodium dodecyl sulphate-polyacrylamide gel electrophoresis and analysed by immunoblotting using a polyclonal anti-goat human CST SN antibody. + Ctrl is the CST SN overexpression cell lysate. n=3 independent experiments.

4.3.2.2 Bioinformatics analysis of CST1

To further explore the mechanism for the apparent CST1 mRNA translation inhibition, published data were searched where data was available on senescent HUVECs microRNA (miRNA). The possible explanation for no cystatin SN protein detection, might be the presence of miRNA inhibiting the protein synthesis. Two research groups (Menghilli et al 2009 and Yentrapalli et al 2015) have conducted this type of study. In order to investigate the role of miRNA they profiled the miRNA signature in REPS HUVECs using miRNA array. Menghilli *et al* identified 14 miRNA and Yentrapalli *et al* identified 13 miRNA that were differentially expressed in REPS HUVECs.

Firstly, two data bases, DIANA TOOLS and miRBD were searched for the potential target miRNAs which will block cystatin SN protein translation. http://diana.imis.athena-innovation.gr/DianaTools/index.php and http://www.mirbase.org/. Only ranscripts with a prediction score >80 only were considered to represent an actual mRNA target. The lists of potential miRNAs were compared to the two studies mentioned (Menghini, Casagrande et al. 2009),(Yentrapalli, Azimzadeh et al. 2015) for any identical miRNAs. None of the predicted miRNA's against cystatin SN protein, as generalised by the two miRNAs databases, was matched to the list of miRNA's identified by those two studies (table 4-2 and 4-3).

CST1 predicted Target miRNA	Menghili et al, 2009	Yentrapalli et al, 2015
DIANA TOOLS		
hsa-miR-4685-5p	not identified	not identified
hsa-miR-4722-5p	not identified	not identified
hsa-miR-4651	not identified	not identified
hsa-miR-4483	not identified	not identified
hsa-miR-4756-5p	not identified	not identified

Table 4-3: The list of identified microRNAs against CST1 in DIANA tools.

The table shows the predicted list of miRNAs from online database, DIANA TOOLS which has the ability to block CST1 mRNA translation to CST SN protein. Comparison was made with studies of senescent endothelial cells (Menghini, Casagrande et al. 2009), (Yentrapalli, Azimzadeh et al. 2015).

CST1 predicted Target MiRNA	Menghili et al, 2009	Yentrapalli et al, 2015
miRDB		
hsa-miR-4447	not identified	not identified
hsa-miR-4739	not identified	not identified
hsa-miR-4419a	not identified	not identified
hsa-miR-3173-3p	not identified	not identified
hsa-miR-4483	not identified	not identified
hsa-miR-6756-5p	not identified	not identified
hsa-miR-6766-5p	not identified	not identified
hsa-miR-1321	not identified	not identified
hsa-miR-4756-5p	not identified	not identified
hsa-miR-6876-5p	not identified	not identified
hsa-miR-4476	not identified	not identified
hsa-miR-4722-5p	not identified	not identified
hsa-miR-1233-5p	not identified	not identified

Table 4-4: The list of identified microRNAs against CST1 in miRDB tools.

The table shows the predicted list of miRNAs from online database, miRDB which has the ability to block CST1 mRNA translation into CST SN protein. Comparison was made with studies of senescent endothelial cells (Menghini, Casagrande et al. 2009), (Yentrapalli, Azimzadeh et al. 2015).

4.3.3 Re-analysis of transcriptomics data; Normalisation of data using R

After considering and validating the data already analysed, after an interval of two years, it was decided to re-analyse data with currently available statistics packages and then applying bioinformatics tools to understand the molecular functions and highlight the biological functions, network analysis, disease state and molecular interactions.

Raw data were normalised initially with the control on the microarray chip with the manufacture's software. Next, data were analysed through using statistics software R. A package called Lima was used for microarray data analysis. Initially data were analysed for signal to noise ratio for all samples, because there can be many factors causing noise in the microarray data. After signal to noise normalisation, the data was log transformed. To analyse the probe intensity behaviour between arrays boxplots were drawn. For a meaningful statistical analysis of the data, it is mediatory to ensure that all samples are comparable. Box plot is used to compare the overall distribution of log transformed intensities. It gives the information of the median, the upper quartile, the lower quartile, the range and the individual extreme values. Normalisation of the expression of distribution of log intensities were performed and box plots were plotted. The plot showed that the scale of the boxes were very comparable indicating that the spread of the intensity values on different array is equalised (see appendix III). After the box plot was plotted, its quartile MA plot: A is plotted against M. M is the difference between the intensity of a probe on the array and the median intensity of that probe over all arrays. A is the average of the intensity of a probe on that array and the median intensity of that probe over all arrays. Ideally the cloud of the data points of the MA plot should gather around M=0.

Nearly all of the probes of the data set cloud were gathered around M=0. Results are provided in the supplementary data. Hierarchical cluster analysis was performed for the determination of correlation between the samples of the four groups. A cluster dendrogram was plotted. There was a good correlation between the samples of the same group, apart from two samples from control for SIPS (see appendix III) Ingenuity Pathway Analysis was used to analyse the data. This data base contains up-to-date information on genes and pathways, as it is updated with the latest research information on a regular basis.

4.3.3.1 Highly up and down regulated genes

Nearly 2000 genes were differentially expressed in SIPS and 3200 in REPS compared to control (young) HUVECs in transcriptomics analysis. A good correlation between SIPS and REPS gene expression was observed, as there were 1596 genes with similar expression in two groups (fig 4-5). The list of top 10 highly upregulated (table 4-4) and top 10 down regulated genes have

been listed in the table 4-5 for REPS and SIPS. Some of these genes are discussed later in this chapter (4.4.4.1 and 4.4.4.3). R resolved the gene expression into log fold change, it has been converted to inverse log and the full list shown on the attached CD.

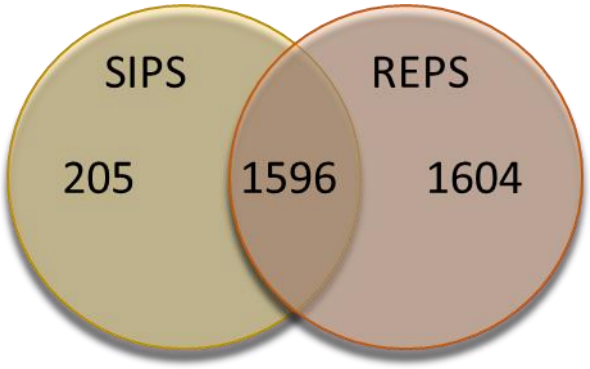

Figure 4-6: Gene expression in microarray experiment.

A total of 1801 genes were expressed in SIPS and 3200 in REPS compared to control (young). Out of these genes 205 genes were uniquely expressed in SIPS and 1604 were expressed in REPS. A total of 1596 genes were found similar in both SIPS and REPS.

Top 10 highly expressed genes			
REPS		SIPS	
Gene name	Fold change	Gene name	Fold change
ADAMTS1	7.9 ↑	TXNIP	19.5 ↑
DKK1	7.5 ↑	IL13RA2	14.4 ↑
DNER	6.3 ↑	ADAMST1	4.7 ↑
SULT1B1	5.1 ↑	DKK1	4.4 ↑
SEMA3C	4.8 ↑	PTHLH	4.0 ↑
IGFBP5	4.5 ↑	PTHLH	3.9 ↑
PTHLH	4.3 ↑	SNAPC1	3.5 ↑
FOXA1	4.3 ↑	NDRG4	3.5 ↑
PTHLH	3.8 ↑	CCNA1	3.5 ↑
CPA4	3.8 ↑	SULT1B1	3.3 ↑

Table 4-5: Top upregulated genes.

List of top 10 upregulated genes in REPS and SIPS (compared to control HUVECs) based on the fold change.

Top 10 down regulated genes			
REPS		SIPS	
Gene name	Fold change	Gene name	Fold change
CPXM2	13.3 ↓	SELE	9.1 ↓
LTB	12.9 ↓	CCL2	8.7 ↓
LITAF	11.8 ↓	LTB	8.6 ↓
SELE	11.6 ↓	NPTX1	7.9 ↓
COX7A1	10.9 ↓	RASD1	7.0 ↓
MGMT	9.3 ↓	CTSK	6.5 ↓
CCL2	9.1 ↓	CYTL1	5.8 ↓
RASD1	7.8 ↓	PRRX2	5.7 ↓
PALM	7.7 ↓	CHRNA1	5.5 ↓
C2CD4B	7.6 ↓	TNFSF10	5.3 ↓

Table 4-6: Top down regulated genes.

List of top 10 down regulated genes in REPS and SIPS (compared to control HUVECs) based on the fold change.

4.3.3.2 Bioinformatics analysis of data using Ingenuity® pathway analysis

After normalisation of the data using statistical software R, the differentially expressed genes between 3 groups, control, REPS, and SIPS were generated. SIPS and REPS were compared to control. This generated two lists of differentially expressed genes.

Next, the IPA database was used to analyse the data and map the differentially expressed genes dataset to the IPA database; highlighting the top canonical pathways, disease and molecular functions, toxicology list and upstream regulators. Based on the gene expression changes, IPA predicts the affected pathways. Disease and function analysis identifies the cellular and biological functions that are affected based on the gene expression and their directional change. A flow chart for the analytical approach is shown in figure 4-6.

Using IPA an expression log fold change was calculated. IPA uses p-value to determine the significance of the number and fold change of proteins in the data set affecting the canonical pathway in the data base indicating the change in molecular expression affecting the pathway is not by chance. But still the information is not enough to predict whether the pathway was upregulated or down regulated. There is another parameter z-score, which is represented as colour coded algorithm. The z-score is an algorithm which utilises the information regarding the number of genes in the dataset regulating the pathway compared to the actual molecules in the pathway and indicates an overall increase in mRNA levels (orange bars) or decrease in mRNA levels (blue bars). The ratio (orange dots connected by a line) indicates the ratio of genes from the dataset that map to the pathway divided by the total number of genes that map to the same pathway. IPA represents the significance of canonical pathways, downstream biological and disease functions and toxicology list with a –log of p value ($-\log_{10}$ (p value)). The significance value (p-value) is calculated by right-tailed Fisher's exact test. A value of ≥ 1.3 of $-\log_{10}$ (p value) equates to a p value of 0.05. UniProt/Swiss-Port Accession IDs and fold change values for differentially expressed proteins were used for data import into IPA.

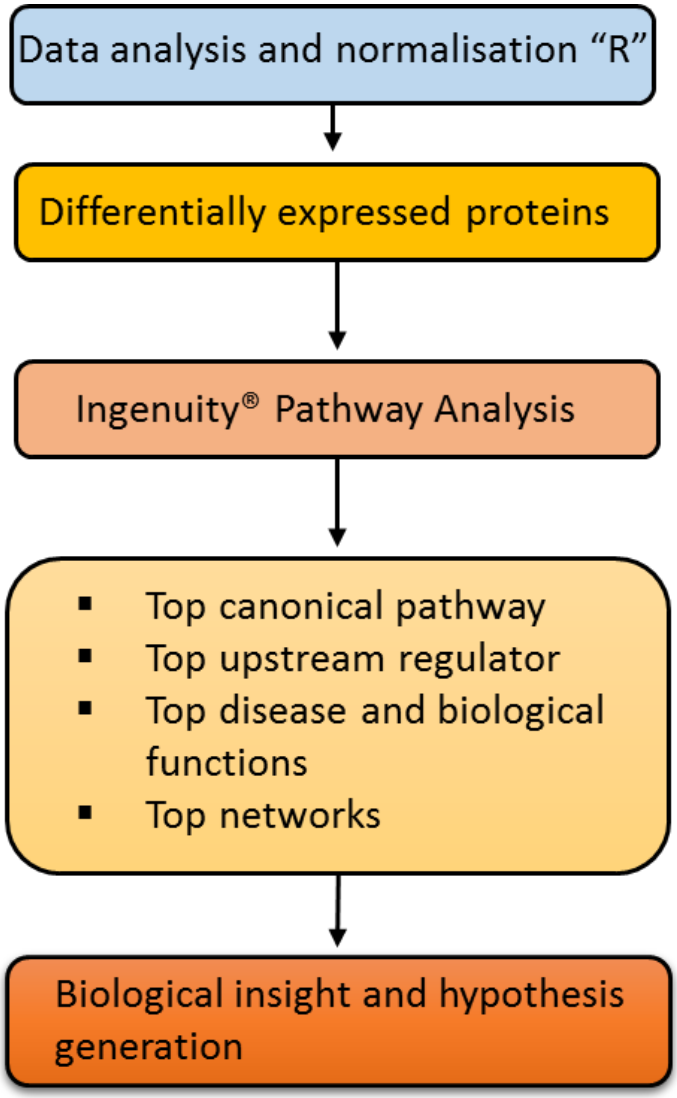

Figure 4-7: Microarray data analysis.

Raw microarray data were normalised and analysis between groups was performed using R. A list of differentially expressed genes was obtained. Next IPA analysis of differentially expressed proteins was performed. The top canonical pathways, upstream regulators, disease and biological functions and networks were determined.

4.3.3.2.1 Top canonical pathways

Analysis of data enabled mapping of the molecules into canonical pathways. 535 pathways for REPS and 497 for SIPS were revealed. The top 5 canonical pathways for REPS and SIPS are displayed in the table 4-6 (Raw data for all the pathways available on CD). The majority of the

pathways z-scores were not calculated and hence their directional change (activated/inhibited) cannot be identified.

REPS	Name	-log$_{10}$ (p-value)	Molecules	Pathway overlap %
	Interferon Signalling	6.76E+00	IRF1,OAS1,IRF9,JAK2,IFITM1,IFNGR2,IFIT3,PIAS1,TAP1,IFNAR1,IFNGR1,IFIT1,STAT1,ISG15,MX1,PSMB8	44
	Role of Macrophages, Fibroblasts and Endothelial Cells in Rheumatoid Arthritis	4.57E+00	CSF2,MRAS,SMO,IL16,ROCK2,NFKBIA,FZD1,FZD6,LRP6,TRAF1,PRKCH,VEGFC,MAPK9,PIK3C3,LTB,IL32,JAK2,IL1B,CTNNB1,TCF4,IKBKB,PIK3C2B,TRAF5,PLCD3,CXCL8,PDGFC,IL1A,CSNK1A1,MAPK14,ATF2,CREB1,CALM1	18
	Activation of IRF by Cytosolic Pattern Recognition Receptors	3.85E+00	TANK,DHX58,NFKB1,IRF9,ATF2,DDX58,IKBKB,PPIB,CD40,IL6,NFKBIA,IFNAR1,IRF7,STAT1,IFIH1,ISG15,MAPK9	27
	Axonal Guidance Signalling	3.2E+00	CDC42,MRAS,SMO,TUBG1,SLIT3,PRKACB,ROCK2,CXCR4,ARHGEF6,FZD1,RAC3,SEMA3C,ERBB2,FZD6,PRKCH,BDNF,VEGFC,PIK3C3,MMP11,MME,NGEF,SEMA6A,PIK3C2B,MYL6B,SEMA3D,RTN4,HHIP,ADAMTS1,PLCD3,PRKAR1A,PDGFC,PLXND1,SLIT2,RAP1B,EFNB3,GNAI1,PAPPA,GNG10,PGF,PDGFB,NTNG1,PIK3R1,EPHB1,RGS3,ADAMTS6,FYN,PIK3CA,PSMD14,MET,ROCK1,EFNA1,VEGFB,TUBA3E,PLCL1,TUBA3C/TUBA3D,PLXNA3,SEMA6B,PPP3CA,UNC5A,ACTR3,EPHA4,PLCG2,SEMA3G,PRKCA,MYL5,PLCG1,MMP10,ABLIM1,EIF4E	15

	Cell Cycle Control of Chromosomal Replication	2.89E+00	CDC7,MCM7,MCM2,ORC6,PRIM2,ORC2,MCM3,ORC5,PCNA,CDC6,ORC3	28
SIPS	Interferon Signalling	3.63E+00	IRF1,IFNGR1,IFITM1,IFNGR2,STAT2,MX1,BAX,TAP1,PSMB8	25
	Antigen Presentation Pathway	3.44E+00	HLA-E,HLA-A,HLA-DMB, CANX, B2M,HLA-B,TAP1,HLA-F,PSMB8	23
	Protein Kinase A Signaling	3.28E+00	FLNB,DUSP10,TDP2,CALM1	10
	Role of IL-17A in Psoriasis	3.15E+00	S100A9,CXCL1,CCL20,CXCL5,CXCL8	38
	Caveolar-mediated Endocytosis Signaling	2.95E+00	FLNB,HLA-A,ITGAV,PRKCA,COPG2,ITGA3,ITGA10,ITGA11,FLNC,B2M,HLA-B,FLOT2	16

Table 4-7: Top 5 canonical pathways based on differentially express genes in REPS and SIPS.

Canonical pathways are presented with significance p value as –log p-value, ≥1.3 is equivalent to a p-value of 0.05. This was considered as statistically significant. Pathway overlap indicates the percentage by which the pathway molecules in the dataset overlap the molecules of the pathway.

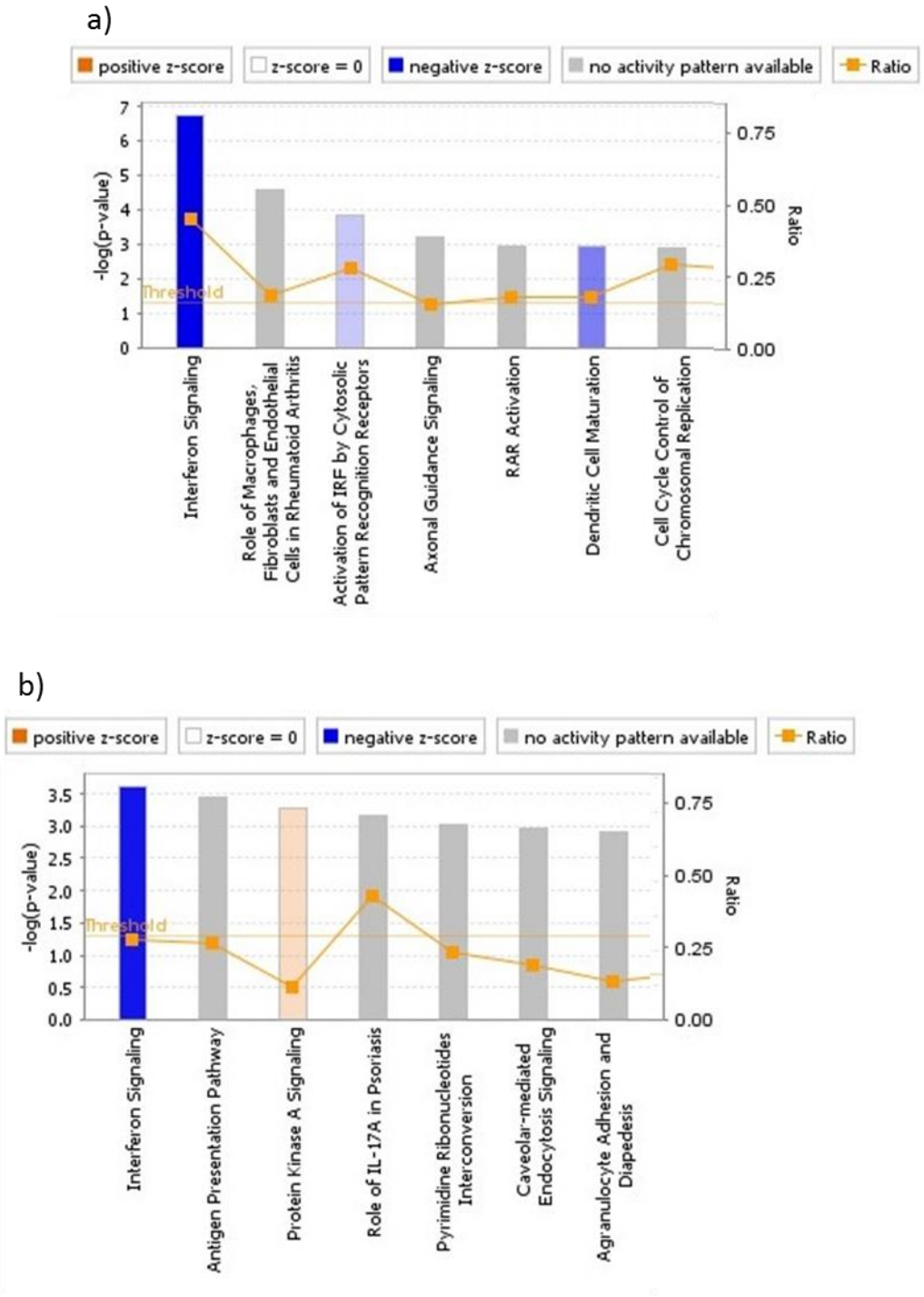

Figure 4-8: Bar chart of the top canonical pathways identified from (a) REPS and (b) SIPS data.

Data are represented as –log (p-value). Canonical pathways are represented as bars, which are colour coded according to the calculated z-score. The o range bar with a positive z-score indicates an overall activation of the respective pathway. The blue bar represent z-score and predicts an overall decrease in the activity. The grey bar indicates that the available information on IPA the data base is unable to predict the activity. The ratio between numbers of proteins in the data set vs the actual number of molecules involved in the data set is shown by orange squares connected by orange lines.

4.3.3.2.2 Top diseases and biological functions

IPA identified the diseases and functions based on the molecules in our dataset. Top 5 of these are shown in table 4-8 for both REPS and SIPS. The identified top main disease and functions, having sub categories. Activation of the sub categories was shown by the Z-score, a z-score of ≥2 was predicting activation while ≤-2 inhibition or decrease of the disease or function. Z-score was unpredictable for most of the diseases and functions. Amongst those mentioned in the table, cancer has been the one which was inhibited in both SIPS and REPS.

4.3.3.2.3 Toxicology lists

The top toxicology list generated by IPA analysis has been shown in the 4-9. The omplete list of toxicology is shown in the supplementary data in attached CD. Significance has been presented with a –log (p-value). Z-score was unpredictable for most of the toxicologies in the analysed data.

REPS	Disease and disorders		Molecular and cellular functions		Physiological system Development and functions	
	Name	p-value	Name	p-value	Name	p-value
	Cancer	2.1E-36	cell movement	1.7E-17	Organismal Survival	6.86E-13
	Infectious Diseases	5.59E-08	cell death	2.12E-14	Cardiovascular System Development and Function	6.75E-11
	chronic inflammatory disorder	1.05E-05	necrosis	2.25E-14	DNA Replication, Recombination, and Repair	1.51E-07
	Hematological Disease, Immunological Disease	3.15E-07	Cell Cycle	7.88E-12	Hematological System Development and Function, Tissue Morphology	5.14E-06
	Cardiovascular Disease	1.13E-06	Cell Morphology	3.2E-12	Tissue Development	2.15E-06

SIPS	Cancer	1.88E-27	cell movement	3.46E-15	Organismal Survival	5.99E-10
	Immunological Disease	2.53E-08	apoptosis	3.96E-14	Cardiovascular System Development and Function,	5.21E-09
	Infectious disease	3.47E-07	Necrosis	8.29E-14	Hematological System Development and Function, Tissue Morphology	5.24E-09
	Connective Tissue Disorders, Inflammatory Disease, Organismal Injury and Abnormalities, Skeletal and Muscular Disorders	2.13E-07	Cell-To-Cell Signalling and Interaction	2.26E-09	Organismal development (morphology)	7.22E-07
	Immunological Disease	1.89E-06			Tissue development	1.91E-06

Table 4-8: Top disease and biological functions.

The main categories diseases and functions have been highlighted in the table for REPS and SIPS. There are sub-categories to each disease and function. P-value is of 0.05 is considered as significant.

Top toxicology list			
REPS		SIPS	
Ingenuity toxicology list	-log(p-value)	Ingenuity toxicology list	log(p-value)
Nongenotoxic Hepatocarcinogenicity Biomarker Panel	4.53	Increases Transmembrane Potential of Mitochondria, Mitochondrial Membrane	3.77
Increases Liver Damage	3.84	Oxidative Stress	2.67
Hypoxia-Inducible Factor Signalling	3.65	Increases Liver Damage	2.63
Oxidative Stress	3.25	Liver Necrosis/Cell Death	2.32
RAR Activation	2.93	Renal Necrosis/Cell Death	2.15
Liver proliferation	2.64	Non genotoxic Hepatocarcinogenecity biomarker panel	2.04
Reversible Glomerulonephritis Biomarker Panel (Rat)	2.31	Liver Proliferation	2.04
p53 Signalling	2.26	Transition of Mitochondria and Mitochondrial Membrane	2.00
Liver Necrosis/Cell Death	2.15	Increases Heart Failure	1.95
Xenobiotic Metabolism Signalling	2.02	Acute Renal Failure Panel (Rat)	1.91

Table 4-9: Top 10 toxicology lists. Toxicology list for both REPS and SIPS data.

Full data set shown in attached CD. Z-values were not predicted for these pathways.

4.3.3.2.4 Top network functions

The top 5 networks are listed in Table 4-9. The complete list can be found in the CD. IPA utilises the known interaction among the target genes and generates the signalling networks. Based on these identified networks, further experiments can be proposed which can identify the novel function of these networks. Significance of the network is presented as score. For REPS and SIPS, most affected networks with higher score were related to molecular transport, damage and repair, developmental disorders, and cell assembly.

REPS		SIPS	
Network functions	**Score**	**Network functions**	**Score**
RNA Post-Transcriptional Modification, Molecular Transport, RNA Trafficking	34	Developmental Disorder, Hereditary Disorder, Ophthalmic Disease	47
Cellular Assembly and Organization, Cell-To-Cell Signaling and Interaction, Reproductive System Development and Function	34	Post-Translational Modification, Protein Folding, Protein Trafficking	42
RNA Damage and Repair, Connective Tissue Development and Function, Tissue Morphology	33	Connective Tissue Disorders, Developmental Disorder, Gastrointestinal Disease	39
Molecular Transport, Protein Trafficking, Cancer	33	Developmental Disorder, Hereditary Disorder, Organismal Injury and Abnormalities	37
Protein Synthesis, Gene Expression, Hereditary Disorder	33	Cellular Compromise, Cell Morphology, Cellular Assembly and Organization	35

Table 4-10: Top 5 network functions.

Top 5 highly scored networks that has been affected in REPS and SIPS. Data are represented as score. A score of ≥3 ($p<0.001$) was considered as significant.

4.4 Discussion

Dumont et al have found similar results of SIPS and REPS fibroblasts sharing the same gene and protein expression features but the expression levels of these genes were higher in REPS than SIPS (Dumont, Burton et al. 2000). Dierick et al have used repeated, sub cytotoxic levels of t-BHP and ethanol to induce SIPS in HDFs. They then performed 2D gel electrophoresis and compared it with REPS HDFs. They analysed 1819 spots. Among these spots they found 50 spots significantly different between REPS and SIPS HDFs (Dierick, Eliaers et al. 2002). This is the first study to describe CST1 expression as a senescent biomarker in REPS *in vitro*. The possible significance of CST1 and other markers of endothelial cell senescence is discussed below.

4.4.1 Cystatin SN

Initial bioinformatics analysis of gene expression data (ArrayTrack) indicated a substantial increase in CST1 in REPS HUVECs. Cystatins are proteins which are inhibitors of cysteine protease family proteins, thus controlling their proteolytic activity. They are also involved in cell proliferation and DNA synthesis (Keppler 2006). Cystatins form families collectively making a cystatin superfamily. The CST1 gene product, cystatin SN, belongs to cystatin family 2 of the super family. Cystatin SN is encoded by the CST1 gene located on chromosome 20 (Ochieng, Chaudhuri 2010). The presence of these inhibitors for cysteine proteinases suggest the protective or controlled breakdown of intracellular or extracellular proteins by cysteine proteinases (Turk, Bode 1991). Cystatin SN is expressed in uterus, gall bladder and submandibular gland (Dickinson, Thiesse et al. 1993). Airborne allergens are mostly proteases. They can induce an inflammatory response. Cystatin SN has been reported to be present in subjects with allergic rhinitis, suggesting the protective role of cystatin SN against protease containing allergens in the nasal mucosa (Imoto, Tokunaga et al. 2013).

Cysteine proteinases are expressed on the surface of metastatic cells. The presence of these proteinases might help the tumour cell during local invasion (Sinha, Gleason et al. 1993).

Cystatin expression may have a role in the tumour microenvironment. An inverse relationship of cystatin level has been observed during different tumour development stages. The levels of cystatins decrease as the tumour progresses towards metastatic stage (Kothapalli, Bailey et al. 2003). Previous researchers have identified cystatin SN as a novel biomarker for gastric (Choi, Kim et al. 2009), colorectal (Yoneda, Iida et al. 2009) and pancreatic cancers (Jiang, Liu et al. 2015).

Recently cystatin SN has been identified as a novel marker of pancreatic cancer (Jiang, Liu et al. 2015). It has also been shown that cystatin SN expression is related to cell proliferation (Jiang, Liu et al. 2015). The evidence also comes from the work of Choi et al, who found increased cell proliferation in cells transfected with CST1 compared to control. They also found upregulated levels of CST1 in human cancer cell lines and tissues from gastric cancer patients, suggesting its role in progression of human gastric cancer (Choi, Kim et al. 2009). Cystatin SN expression can be predictive of the recurrence and metastasis in patients with non-small cell lung cancer (NSCLC). Its increased expression in patients with NSCLC is associated with decreased recurrence and metastasis compared to low expression (Cao, Li et al. 2015).

CST1 has also been reported as a senescence biomarker in replicative and stress-induced senescent fibroblasts (Keppler, Zhang et al. 2011). Most recently extracellular CST1 has been evidenced to be involved in the prevention of senescence and senescent related phenotypes (Oh, Park et al. 2017).

The preliminary analysis of data suggested CST1 was greatly elevated in REPS. However, even though qPCR supported this, no changes were found in protein levels. Indead cystatin SN protein was not detected in HUVEC culture at all. The reason for this is not clear. miRs, identified using bioinformatics analysis of binding sites on CST1 mRNA (putative site for miRNA), that might be inhibitors of CST1 mRNA translation were not identified in the published data on miRNA in senescent HUVECs (table 4-3 and 4-4). One reason for the lack of clarity over CST1 is that there might be differences between the cell samples used. The source of HUVECs used in miRNA identification studies was a single donor. In this thesis, a pooled HUVECs sample was utilised. There might be variation from donor to donor. More confirmatory studies would require identification of potential miRNA for cystatin SN, and then their detection through carrying out qPCR in REPS and SIPS cells.

However, it should be emphasised that subsequent re-analysis of the same gene expression data (using R) did not identify CST1 over expression in REPS HUVEC cells (complete list of genes can be found in the supplemental data on the CD). The reason for this is unclear and does not agree with qPCR data.

4.4.2 Cartilage acidic protein 1

Cartilage acidic protein 1 gene, CRTAC1, encodes an acidic protein. It is expressed in chondrocytes and articular cartilage. Its transcript is also identified in lungs and a smaller size alternative splice variant transcript is expressed by brain (Steck, Braun et al. 2007). The function of CRTAC1 has not been identified fully but its structure, consisting of a N-terminal integrin, a chain-like domain and a C-terminal EGF-like Ca^{2+}-binding motif, suggests its role in cell-cell and cell-matrix adhesion (Cioci, Mitchell et al. 2006). The role of CRTAC1 expression in senescent HUVECs might be related to cell adhesion. Its expression in the brain and nervous system also suggests additional roles (Anjos, Morgado et al. 2017). This protein is of interest due to its expression, but unknown role, in certain diseases like multiple sclerosis (Hammack, Fung et al. 2004).

4.4.3 Leucine rich repeat containing 17

Leucine rich repeat containing 17 (LRRC17) expression levels have been found to be decreased in elderly breast cancer patients compared to younger cancer patients. Elderly cancer patients have more senescent cells in their tumours (Brouwers, Fumagalli et al. 2017). A subtype of breast cancer, triple negative breast cancer (TNBC) is an aggressive type of cancer with high resistance to therapy. A microarray data analysis for identification of a TNBC specific signature showed LRRC17 to be a target gene (M. U. Zaka, Y. Peng et al. 2014). Osteosarcoma is a type of bone tumour. In another study profiling of miRNA and correlating with gene expression in several osteosarcoma cell lines LRRC17 was down regulated (Baumhoer, Zillmer et al. 2012). LRRC17 is related to stem cells senescence (Heo, Kim et al. 2016).

4.4.4 Second iteration of microarray data

When the microarray data was revisited and analysed using statistical software R package a different list of genes was observed for REPS and SIPS. There could be many reasons for this, as the data normalisation method could affect the analysis. Also, the data were normalised and log transformed in the second analysis using R.

Based on the second gene expression analysis, the SELE gene (representing the gene CD62E which encodes protein E-selectin) was down regulated in both REPS and SIPS (table 4-6). However, this was not confirmed by qPCR (chapter 6). This showed that transcriptomics data did not correlate with qPCR results. Microarrays are able to profile the whole genome. qPCR is the tool used to validate the gene expression analysed by microarray. The correlation between microarray and qPCR does not always agree. The use of different microarray platforms and procedure can cause variation in results. Additionally biological and technical variation can influence the results (Bustin 2002), (Chuaqui, Bonner et al. 2002), (Freeman, Walker et al. 1999), (Yang, Dudoit et al. 2002). The other important reason might be because qPCR is very sensitive technique (Morey, Ryan et al. 2006) which is able to pick and amplify a very small signal that has been missed by microarray.

One of the canonical pathways, 'Interferon Signalling', was been inhibited by both REPS and SIPS. Suppression of type 1 interferon signalling bypasses oncogene induced senescence and promotes melanoma development (Katlinskaya, Katlinski et al. 2016). As interferon signalling is predicted to be upregulated in senescence, one would expect that there would also be an increase in interferon signalling by senescent cells. Another pathway, the Protein kinase A signalling pathway (PKA), was upregulated in REPS only.

Studies on SASP components have shown IL-6 and IL-8 elevation by senescent endothelial cells as well as ICAM-1 and E-selectin (Khan, Awad et al. 2017). A common biomarker of senescence is $P16^{INK4a}$ (Krishnamurthy, Torrice et al. 2004). The current study showed down regulation of genes for aforementioned (IL-6, IL-8, ICAM-1 and E-selectin) proteins in REPS and SIPS transcriptomics. There are certain other biomarkers, for example Dec1, DCR2, Ki-67, p15 (Collado, Gil et al. 2005b) and certain other SASP components (reviewed in (Freund, Orjalo et al. 2010), (Coppe, Desprez et al. 2010). Despite being identified as SASP components

in senescent cells biomarker studies, these genes have not been identified in HUVECs transcriptomics. In this thesis, there are other factors that have been reported as senescent biomarkers, identified in the HUVECs transcriptomics, they are discussed below.

4.4.4.1 Top downregulated genes

Atherosclerosis is the result of pathological endothelial damage leading to endothelial dysfunction (Libby, Ridker et al. 2011). A pro-inflammatory state is associated with endothelial dysfunction causing the expression of adhesion molecules i.e. ICAM and P-selectin (Collins, Velji et al. 2000) accompanied by the release of cytokines such as IL6 and C-C Motif Chemokine Ligand 2 (CLL2) (Boring, Gosling et al. 1998). Elevated levels of CLL2 were found in radiation-induced senescence in endothelial cells (Baselet, Belmans et al. 2017). The expression of the CLL2 gene was down regulated in REPS and SIPS transcriptomics analysis in this thesis.

The **CPXM2** gene was uniquely expressed in REPS in this thesis. It was one of the highly down-regulated genes. It has been found to be upregulated in cancer associated fibroblasts (Madar, Brosh et al. 2009). Its high expression has also been reported in the synovial fluid obtained from patients with osteoarthritis (Sekiya, Ojima et al. 2012). Its role in endothelial senescence is unclear and is worthy of further study.

Lymphotoxin beta gene (LTB) (TNF superfamily, member 3) is another gene expressed by SIPS and REPS in transcriptomics. Its role in senescence induction has not been reported but is reported to be decreased in expression upon human ageing (Harries et al 2011).

4.4.4.2 Top upregulated genes

A disintegrin and metalloproteinase with thrombospondin-like motifs (ADAMST1) is an inflammation related gene and its expression is upregulated in the human aorta and coronary artery (Jonsson-Rylander, Nilsson et al. 2005). It has also been reported to be an important

regulator of SPARC mediated ageing (Toba, de Castro Bras et al. 2016). It is found to be more than 7 and 5 folds upregulated in REPS and SIPS transcriptomics.

Dickkopf-1 (DKK1) was also found to be upregulated in both REPS and SIPS. DKK1 is a secreted glycoprotein which is a p53-induced inhibitor of wnt signalling pathway (Wang, J., Shou et al. 2000). Wnt signalling promotes human cancer progression (Polakis 2012). Further to this DKK1 expression was reported to be upregulated following chemotherapy in human primary mesenchymal stem cells (Hare, Evans et al. 2016). Increased senescence after chemotherapy (Gordon, Nelson 2012) suggests a role of DKK1 in senescence induction.

PTHLH was upregulated in REPS and SIPS. Human PTHLH encodes parathyroid hormone related peptide (PTHrH) (Campos, Zhang et al. 1994). Parathyroid related peptide regulates vascular tone and is a naturally occurring angiogenesis inhibitor (Bakre, Zhu et al. 2002) PTHrP can be secreted from cells or localise to the nucleus. These two different states have opposing physiological functions (Boras-Granic, Dann et al. 2014). In a rat carotid angioplasty model secreted PTHrP was able to abolish the neointima formation after angioplasty (Fiaschi-Taesch, Takane et al. 2004). PTHLH is a cytokine which is suggested to be responsible to the extravasation of colon cancer cell to lung by inducing lung microvascular endothelial cell death (Urosevic, Garcia-Albeniz et al. 2014).

Thioredoxin-interacting protein (TXNIP) was a SIPS specific protein in transcriptomics and upregulated more than 19 folds compared to young (control). Inflammasomes are multiprotein complexes that initiate the inflammatory response by activating pro-IL-1β to IL1 through caspase 1 (Martinon, Burns et al. 2002). NLRs including NLRP3 are associated with inflammasome formation and induction of immune-senescence (Davis, Wen et al. 2011), (Youm, Kanneganti et al. 2012). The NLRP3 inflammasomes-induced senescence mechanism was investigated in endothelial cells. It was reported that oxidative stress could promote the binding of (TXNIP) to NLRP3 and activate NLRP3 induced inflammasomes (Yin, Y., Zhou et al. 2017).

4.5 Conclusion

CST1, a biomarker of senescent HUVECs identified in transcriptomics analysis using ArrayTrack could not be identified in protein identification methods. Transcriptomics analysis using different statistical tools/software generated different results. This thesis, therefore, highlights the care required when interpreting transcriptomics data. Nevertheless, some of these findings were replicated using qPCR and are worthy of further consideration.

This study supports further gene expression analysis using protein identification techniques such as proteomics analysis; this is described in the next chapter for senescent HUVECs.

Chapter 5

5 Investigation of the secretome of senescent HUVECs: characterisation of SASP using proteomics.

5.1 Importance of secreted protein as biomarkers

Transcriptomics is the gene expression analysis tool which is used in the study of many biological processes to identify differentially expressed genes as molecular signatures. Using transcriptomics, gene expression changes related to a biological process can be compared globally at the level of mRNA. This can identify the genes that can be used as biomarkers for many diseases. However, gene expression changes do not reflect the direct changes associated in the blood physiology (Vathipadiekal, Wang et al. 2015). Therefore, identification of the blood-based proteins is important, which can be extended to actual measurement of blood proteins as a biomarkers for a clinical condition. A combination of blood proteins as a biomarker panel will serve as the best identifier of any clinical condition. Biomarker panels may be used for diagnosis, monitoring disease progression e.g. in its response to treatment.

5.1.1 Proteomics of secreted proteins

Proteomics is the group of techniques used to determine several hundred proteins simultaneously in a sample. Quantitative proteomics is the technique used to identify proteins that are differentially expressed in different samples (Ha, Soo Cho et al. 2006). Proteomics has been applied to the study of senescent fibroblasts in terms of whole cell proteomics (Boraldi, Bini et al. 2003) and SASP characterisation (Won, Kwon et al. 2012). Endothelial cell proteomics, particularly its SASP, characterisation, is still in its infancy.

SASP characterisation is an important aspect of this PhD project. It will give an insight into the effect of senescent endothelial cells on neighbouring cells and also help identifying novel potential biomarkers for senescence (see Section 5.3.1). Despite the potential role of senescent endothelial cells in the development of atherosclerosis, SASP of senescent endothelial cells has not been profiled. Currently, proteomics for a secretome analysis ideally requires serum free samples, whilst for collecting SASP at least 12 to 24h old conditioned media is required. The challenge is to deprive cells of serum for 24h, which results in the death of many cell types. To

resolve this the exogenous secretagogue phorbol myristate acetate (PMA) was used. Another group has used PMA for this very purpose; that is, exposure of HUVECs to serum free growth media with 50 nM PMA for a short period of 45 minutes (Yin, Bern et al. 2013). PMA is a secretagogue which acts via Protein kinase C (PKC). PMA secretagogue function is not Ca^{2+} dependent (Billiard, Koh et al. 1997).

As explained in Chapter 1 (Introduction) senescence can be introduced following cell stress (e.g. oxidative stress) or classically due to telomere depletion due to exhaustive replication. Therefore, two senescent models in culture were used, SIPS and REPS. Studying the two types will help us find the similarities and differences as well as the level of detrimental effects related to each type.

5.1.2 Beneficial role obtained by removal of senescent cells:

Many studies have focused on supressing the identified markers of senescence and then senescence suppression and reversal of senescence detrimental effects (Strzyz 2016). For example, $p16^{INK4a}$ is a known maker of senescence. Targeted removal of p16 positive cells in a progeroid mice helped delaying the age related phenotype. These mice had preserved muscle function, delayed onset of sarcopenia and cataract formation (Baker, Wijshake et al. 2011a).

Chromatin binding high mobility group protein (HMGB2) a transcription factor is identified as a regulator of SASP genes and may be involved in mediating the detrimental effect of tissue ageing. Down regulation of HMGB2 is associated with inhibition of SASP genes (Aird, Iwasaki et al. 2016). This shows that there could be a possibility to achieve the beneficial effect of cell growth termination in senescence while, blocking the detrimental effect of SASP. Growth differentiation factor 6 (GDF6) belongs to transforming growth factor-β super family. Overexpression of GDF6 was effective in blunting pro-inflammatory SASP factors and similarly lymphopoiesis, muscle repair capacity and neurogeneration in aged mice. These effects were comparatively similar to young mice (Hisamatsu, Naka-Kaneda 2016).

Total body irradiation induces senescence of hematopeoeitic stem cells (HSC) manifested by decrease self-renewal and hematopoietic function. (Shao, Feng et al. 2014). Selective removal

of senescent HSC from irradiated mice caused the reversal of SASP effects and enhanced lymphopoiesis and self-renewal capacity of HSC. It also enhanced the clonogenicity and long term engraftment ability of irradiated HSC analysed after transplanted into primary and secondary recipients (Chang, Wang et al. 2016).

These studies highlight the opportunity, in the future, to investigate removal of senescent cells and their SASP as a means of delaying the onset of a wide variety of age-related pathologies, including CVD. A better understanding of the composition and effects of endothelial SASP is currently required in order to design such interventions.

5.2 Aims

The initial aim of this chapter study is to characterise the SASP from both replicative senescent (REPS) and stress-induced senescent (SIPS) HUVECs by using a proteomic approach and compare these to the secretome of young (early passage) HUVECs. The resulting protein list will be analysed using bioinformatics tools with an aim to determine the biological process and pathways that have been changed and provide information about the biology of ageing endothelial cells and mediators likely to be produced by them. Subsequently, these studies will be used to identify important proteins as biomarkers of senescence *in vitro* and with a view to identifying markers in human plasma, for example CST1, CRTAC17 and LRRC17.

5.3 Results:

5.3.1 Characterising the composition of SAPS using proteomics

The protocol for senescent HUVECs proteomic analysis is shown in the fig 5-1. Proteomics was performed on HUVECs grown in T-75 flasks. HUVECs were either made SIPS or REPS as described in Methods Section 2.1.2.7 and 2.1.2.7. Once the cells in the flasks were confluent they were treated with 50 nM PMA for 45 minutes. After this stimulation, the supernatant (conditioned media) was collected and concentrated with the help of filter columns (see method section 2.6.2). The experiment was conducted on three groups of cells: young HUVECs

(control), stresse induced (treated with 100 µM t-BHP) and REPS. A fourth group, 'media only' was used to identify the components specific to media.

Several hundred proteins were found in the PMA-induced secretome from young, control HUVEC cultures supernatant in agreement with published data (Yin, Bern et al. 2013). The list of proteins generated included certain classical endothelial cells markers, for example, von Willebrand factor, platelet endothelial cell adhesion molecule (PECAM) and ICAM-2. When the results were compared for control HUVECs (fig 5-2), overall, 30% of the proteins reported by Yin et al were observed in control HUVECs in this study. While between 34 and36 % of proteins were specific to each of the two studies (Fig 5-2). Supplementary data available on CDxx shows the list of proteins that were common after comparing the mass spectrometry analysis of the SASP here to the list of protein obtained by Yin et al 2013 using PMA as secretagogue.

The number of proteins identified was lower for media from SIPS and REPS HUVECs (fig 5-3). Only 52 proteins were identified in REPS supernatant. The original assumption was that more proteins will be expressed by REPs HUVECs than SIPS. In previous transcriptomic data more genes were differentially expressed by REPS HUVECs. The possible explanation for this unexpected result might be that the mechanism of action of release of protein/SASP from senescent HUVECs by PMA treatment is compromised.

It is also possible that mRNA does not get translated into corresponding proteins following induction of senescence.

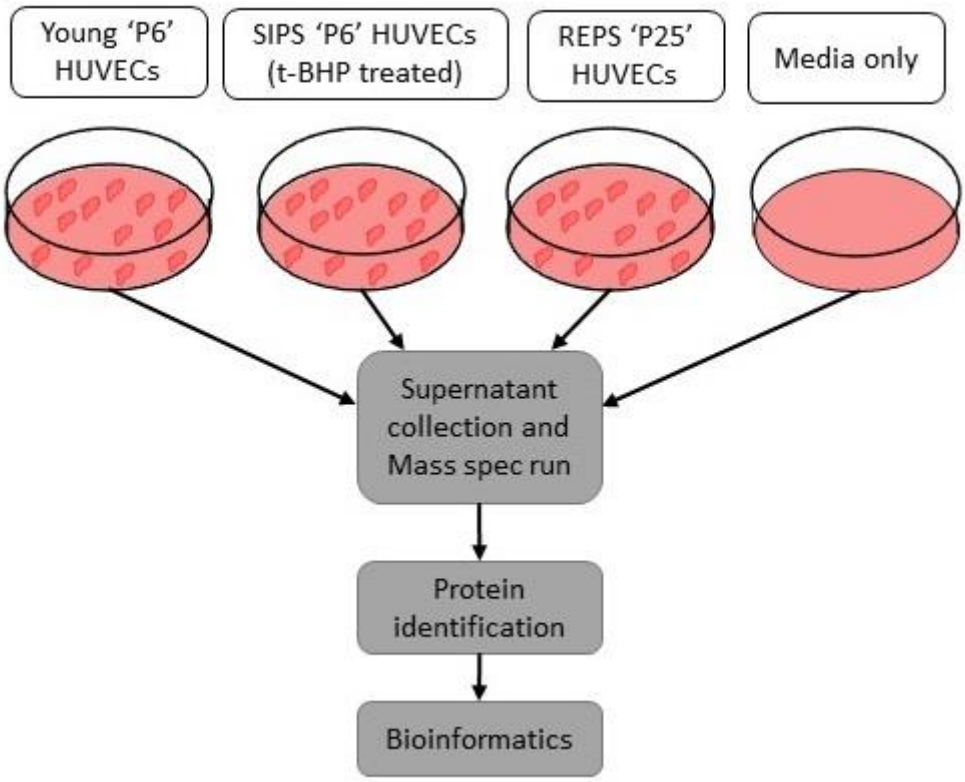

Figure 5-1: Workflow for proteomics analysis.

Four sample groups: young HUVECs, SIPS, REPS and HUVECs growth media only (without cells) PMA-treated were analysed. Serum-free supernatant was collected and analysed by LC-MS/MS. Proteins were identified using a protein library. To further identify the biological functions of these proteins bioinformatics was performed.

The proteomics data showed (fig 5-3 and supplementary data available on CD) some proteins were specific for SIPS (28) but a large number were expressed both by SIPS and control but varied in concentration. 28 proteins specific to SIPS have been shown in table 5-1. Only one protein "Cell Elongation protein" was specific for REPS. 45 proteins could be compared in terms of levels between control, REPS and SIPS.

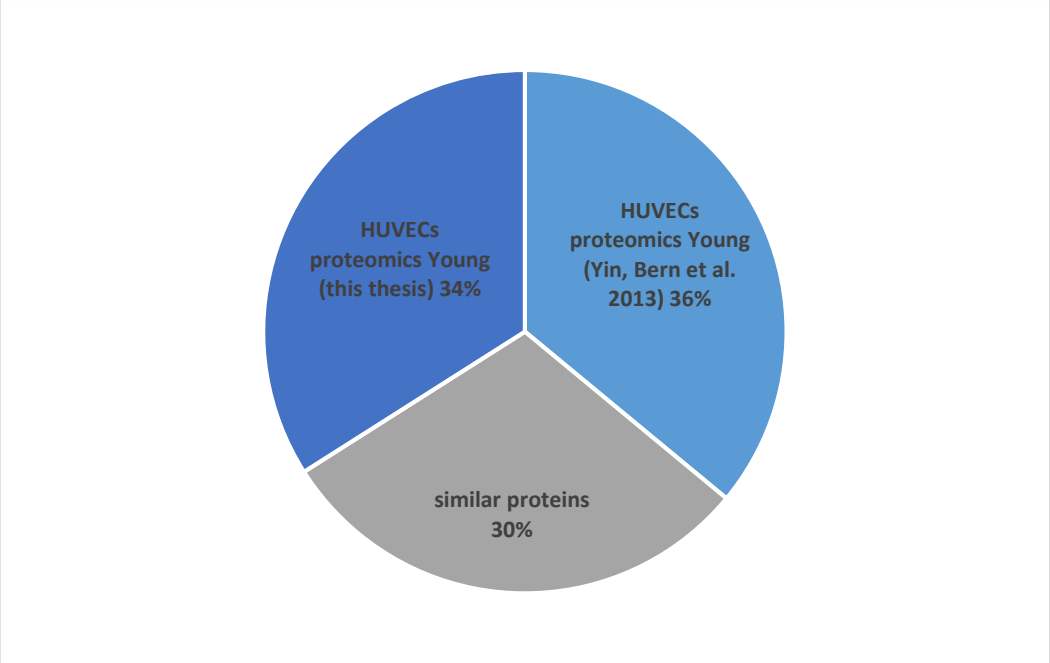

Figure 5-2: Comparison of proteomics data.

Pie chart shows the percentage of proteins found unique in the proteomic data set in this thesis compared with those reported by Yin, Bern et al. 2013, in control HUVECS (untreated) using PMA stimulation. The percentages of similar and unique proteins to each data set is shown.

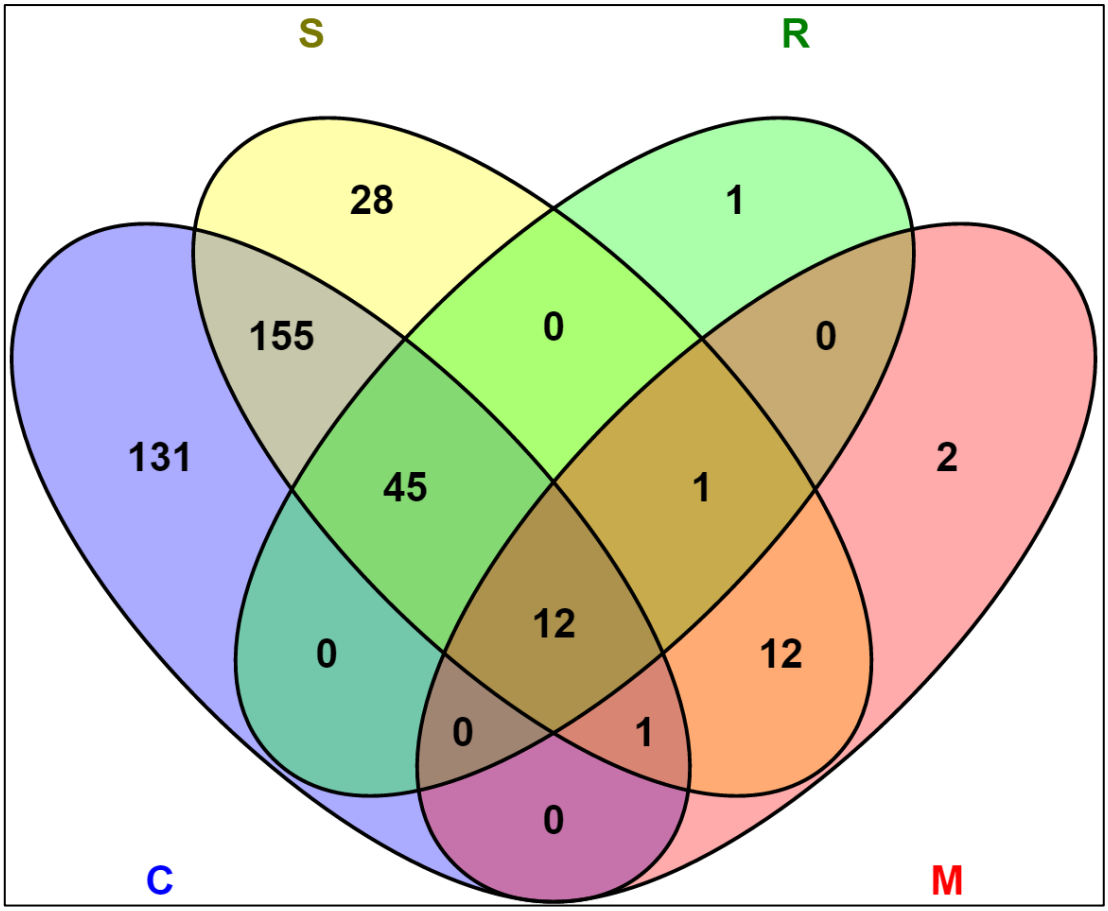

Figure 5-3: Venn diagram showing protein distribution in senescent and control HUVECs.

Venn analysis of young, REPS, SIPS stimulated with PMA and media only proteomes. In total 383 poteins were identified in all four groups. A common 45 proteins were identified in 3 groups except media only. 28 proteins were uniquely identified in SIPS and only 1 protein in REPS. In diagram "S" represent SIPS (yellow), "R" represent REPS (green), "C" represents control (purple) and "M" represent Media only (pink). The overlapping area shows the common proteins within groups.

5.3.1.1 Analysis of SASP profiles

ProteinCentre a Thermo Scientific™ software was used for the analysis of the secreted proteins in response to PMA. Tables and pie chart were generated describing the distribution of proteins depending on cellular components. The highest number of proteins released was from the cell membrane (fig 5-4) while the second most abundant protein group was from the cytoplasm followed by the cytosol. There was a substantial number of proteins released from the nucleus, comprising 32% of the total released proteins (fig 5-4). This confirms that PMA does not only

release the cell membrane proteins, PMA has the ability to release proteins from all components of cells, at least in endothelial cells.

Released proteins were analysed depending on their involvement in biological processes. The highest number of secreted protein were involved in metabolic processes. The second highest number of proteins belonged to 'response to stimulus', followed by 'cell organisation and biogenesis' (see attached CD).

A)

GO Slim Cellular Components	Number of proteins	%
vacuole	32	8.3
spliceosomal complex	4	1.0
ribosome	1	0.2
proteasome	1	0.2
organelle lumen	83	21.7
nucleus	125	32.8
mitochondrion	59	15.4
membrane	204	53.5
Golgi	31	8.1
extracellular	104	27.2
endosome	21	5.5
endoplasmic reticulum	53	13.9
cytosol	144	37.7
cytoskeleton	56	14.6
cytoplasm	198	51.9
chromosome	3	0.7
cell surface	38	9.9
Unannotated	13	3.4

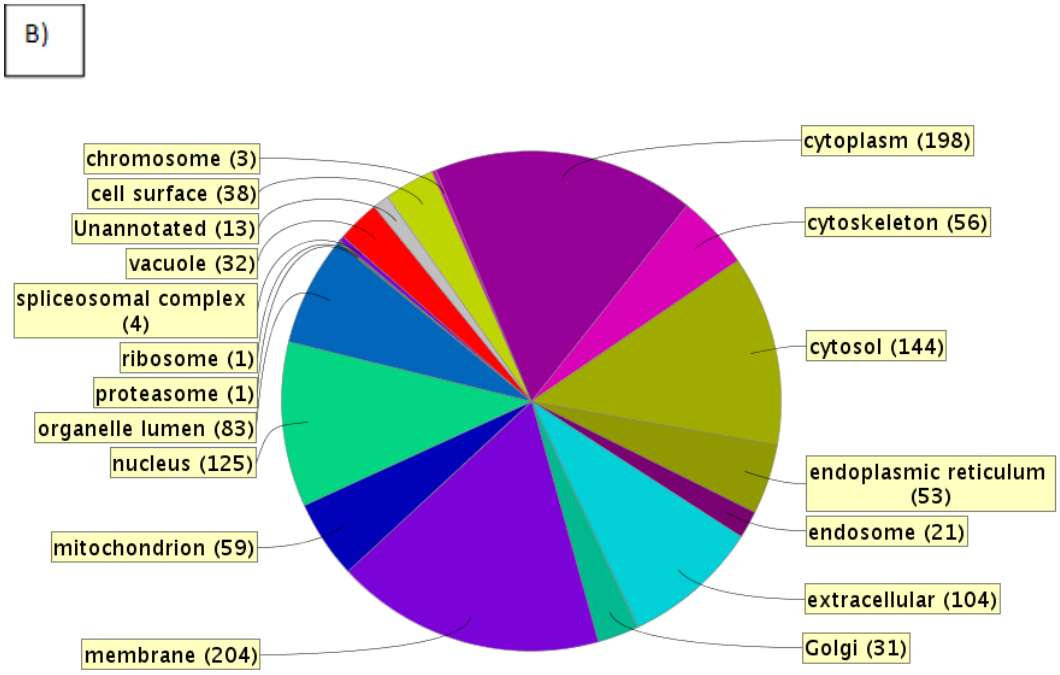

Figure 5-4: Cellular localisation of all secreted proteins (list available in AppendixII).

A) ProteinCentre Thermo ScientificTM software. Table shows the differentially expressed protein number and percentage of secreted proteins. B) The pie chart shows the released protein distribution in the different cellular components, depending on their abundance. The portion of the pie chart represents the abundance of the released proteins related to the cell component obtained from mass spectrometry analysis.

Accession number	protein IDs
P02647	Apolipoprotein A-I
Q9NZT1	Calmodulin-like protein 5
P31944	Caspase-14
Q15517	Corneodesmosin
P01040	Cystatin-A
Q08554	Desmocollin-1
Q02413	Desmoglein-1
P15924	Desmoplakin
Q01469	Fatty acid-binding protein, epidermal
P02671	Fibrinogen alpha chain
Q5D862	Filaggrin-2
P47929	Galectin-7
Q9HC38	Glyoxalase domain-containing protein 4
P42357	Histidine ammonia-lyase
Q86YZ3	Hornerin
P01857	Ig gamma-1 chain C region
P01859	Ig gamma-2 chain C region
P05089-2	Isoform 2 of Arginase-1
P13716-2	Isoform 2 of Delta-aminolevulinic acid dehydratase
P81605-2	Isoform 2 of Dermcidin
Q14240-2	Isoform 2 of Eukaryotic initiation factor 4A-II
P12814-3	Isoform 3 of Alpha-actinin-1
P14923	Junction plakoglobin
P51688	N-sulphoglucosamine sulphohydrolase

P31151	Protein S100-A7
P05109	Protein S100-A8
P06702	Protein S100-A9
Q08188	Protein-glutamine gamma-glutamyltransferase E
Q96P63	Serpin B12
P25311	Zinc-alpha-2-glycoprotein

Table 5-1: List of SASP proteins unique to SIPS.

Proteins identified in proteomics were analysed and uniquely expressed proteins in SIPS were further analysed through IPA. Analysis was based on n=3 independent samples of HUVECs. Expression was made relevant to internal standard, alcohol dehydrogenase.

Once the proteins were identified in the secretome determination using mass spectrometry, IPA was used to identify and highlight the biological functions, network analysis, disease state and molecular interactions comparing senescence secretome to young HUVECs (see section 4.3.3.2 chapter 4). A flow chart (fig 5-5) shows the bioinformatics approach of IPA analysis for the data. Data analysis with IPA is built upon the Ingenuity knowledge base which is a repository of manually gathered information of biological functions and interactions created from all proteins, genes, diseases, cells and tissues. This is coupled with a powerful algorithm to discover the most significant pathways and the novel regulatory network. Using IPA a logfold change analysis was carried out between different groups i.e. control vs REPS, control vs SIPS and SIPS vs REPS. IPA identified canonical pahways, networks and toxicology lists, disease and biological functions of the differential expressed genes.

5.3.2 Proteomics data analysis using IPA

Proteomics generated a list of secreted proteins specific to REPS, SIPS and control (young) HUVECs. When the proteins were compared between the three groups there was only 1 uniquely expressed protein in REPS, while in SIPS there were 28 uniquely expressed proteins. Those uniquely expressed proteins from the HUVECs SIPS secretome were imported into IPA and expression intensity analysis was carried out (See Methods section 2.8.2) for IPA analysis (explained in section 4.3.3.2).

5.3.2.1 Top canonical pathways (SIPS secretome)

Analysis of data enabled mapping of the molecules into top canonical pathways for SIPS table 5-2). A total of 90 pathways were affected. The top 5 pathways with highest –log(p-value) have been listed in the table 4-3. Raw data are shown in the attached CD, which contains a list of all the canonical pathways. For all of the pathways, either z-score cannot be predicted or it was calculated as zero. Therefore, the direction of these pathways has not been identified i-e whether these were upregulated or down regulated. A –log (p-value) ≥1.3 which is equivalent to p-value of 0.05 was considered to be significant.

5.3.2.2 Top disease and biological functions (SIPS secretome)

IPA identified the diseases and functions based on the molecules in the SIPS dataset. The top 5 of these are shown in table 5-4. These are 5 top main disease and functions, having sub categories. Activation of the sub categories was shown by the Z-score, a z-score of ≥2 was predicting activation while ≤-2 inhibition or decrease of the disease or function. Z-score was unpredictable for most of the disease and functions. This means that inhibition or activation of the disease and biological function cannot be predicted.

Top canonical pathways			
Name	-log10 (p-value)	Molecules	Pathway overlap
Role of IL-17A in Psoriasis	6.15	S100A8,S100A9,S100A7	4%
LXR/RXR Activation	3.19	S100A8,APOA1,FGA	2%
Hematopoiesis from Pluripotent Stem Cells	2.7	IGHG2,IGHG1	4%
Autoimmune Thyroid Disease Signalling	2.7	IGHG2,IGHG1	2%
Primary Immunodeficiency Signalling	2.69	IGHG2,IGHG1	4%

Table 5-2: Top 5 canonical pathways for SIPS SASP.

Canonical pathways are presented with significance p value as –log p-value, ≥1.3 is equal to a p-value of 0.05. This was considered as statistically significant.

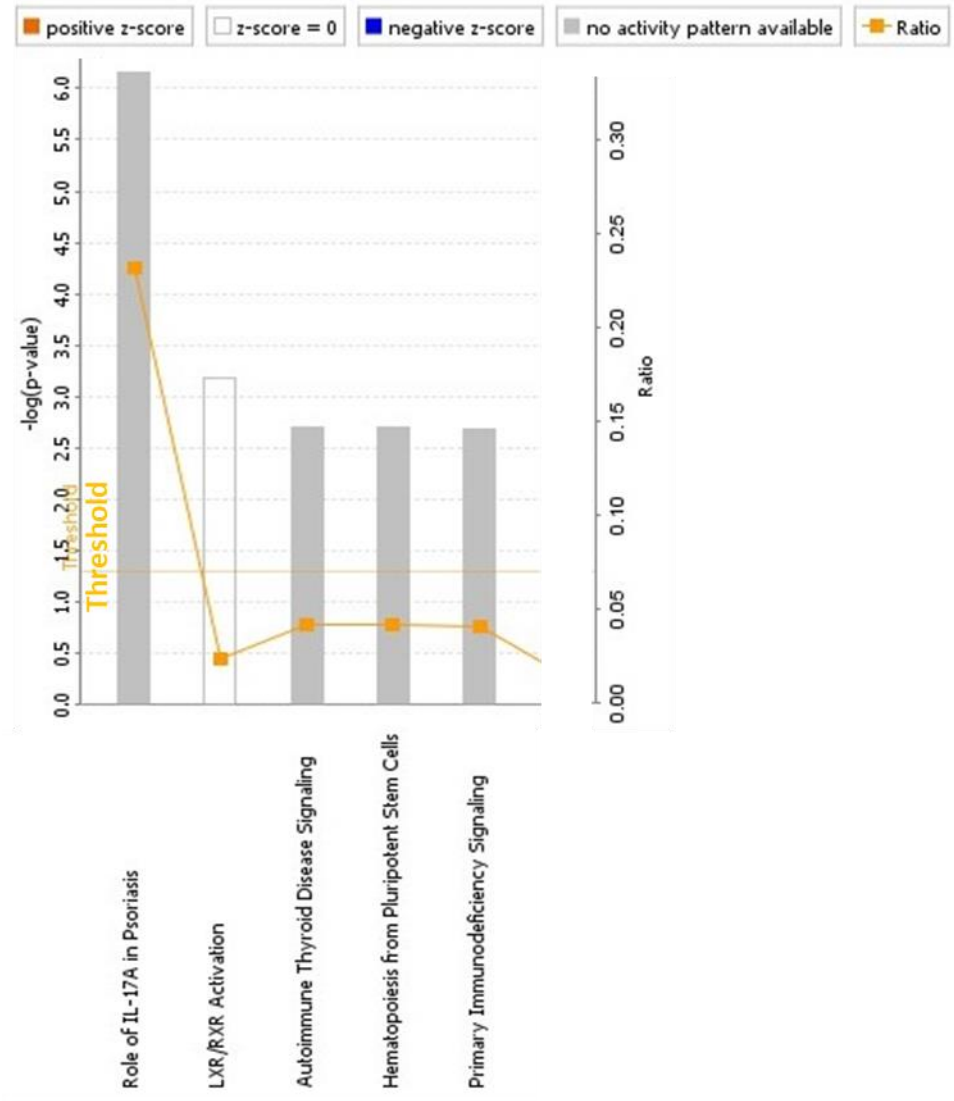

Figure 5-5: Bar chart of the top canonical pathways affected by SIPS.

Data were analysed, representing –log (p-value). Canonical pathways are represented as bars, which are colour coded according to the calculated z-score. An orange bar with a positive z-score indicate an overall activation of the respective pathway. A Blue bar represents the z-score and predicts an overall decrease in the activity. Grey bar indicates that the available information on IPA data base is unable to predict the activity. The white bars represent that the z-score is zero and that this pathway is not affected. Figure shows top 5 canonical pathways. These represent a negative z-score or a z-score with no activity prediction. The ratio between the numbers of proteins in the data set versus the actual number of molecules involved in the pathway is shown by orange squares connected by orange lines

Disease and disorder		Molecular and cellular functions		Physiological system development and functions	
Name	p-value	Name	p-value	Name	p-value
Dermatological diseases and conditions	1.88E-14	Cell-To-Cell Signaling and Interaction, Cellular Assembly and Organization, Cellular Function and Maintenance	2.5E-09	Embryonic Development, Hair and Skin Development and Function, Organ Development, Organismal Development, Tissue Development	1.66E-11
Immunological Disease	1.61E-10	Inflammation	8.99E-08	Hematological System Development and Function, Tissue Development	3.65E-06
Cardiovascular Disease, Cell-To-Cell Signaling and Interaction, Inflammatory Response, Organismal Injury and Abnormalities	5.71E-06	Post-Translational Modification	3.78E-06	Cellular Movement	5.55E-05
Hereditary Disorder, Organismal Injury and Abnormalities, Renal and Urological Disease	1.14E-05	Cellular assembly and organisation	3.98E-05	Cardiovascular System Development and Function, Cellular Development, Cellular Function and Maintenance, Cellular Growth and Proliferation, Organismal Development, Tissue Development	2.07E-04

Metabolic disorders	1.59E-04	Cell death and survival	1.88E-05	Hematological System Development and Function, Immune Cell Trafficking, Inflammatory Response, Tissue Development	2.2E-04

Table 5-3 Top diseases and biological functions affected by SIPS.

The main categories of diseases and functions have been highlighted in the table for uniquely expressed SIPS SASP proteins. There are sub-categories to each disease and function. P-value of <0.05 is considered as significant.

5.3.2.3 Toxicology list (SIPS secretome)

For the SIPS SASP secretome, the top toxicology list generated by IPA analysis is shown in table 5-5. The complete list of toxicology is shown in the CD. Significance has been presented with a –log (p-value). The z-score was unpredictable for most of the toxicologies in the analysed data. The dataset generated only 6 toxicities with a significant p-value.

Top toxicology list	
Ingenuity toxicology list	-log (p-value)
LXR/RXR Activation	3.17
Oxidative stress	2.54
Negative Acute Phase Response Proteins	1.95
Cardiac Fibrosis	1.47
Renal Proximal Tubule Toxicity Biomarker Panel (Rat)	1.43
Positive Acute Phase Response Proteins	1.38

Table 5-4: Top 6 toxicology list.

A toxicity having a –log (p-value) of above 1.3 was considered significant and presented in the above table. The above top 5 toxicities had a –log (p-value) above 1.3 for uniquely expressed SIPS SASP proteins.

5.3.2.4 Top networks (SIPS secretome)

Based on identified SASP components from SIPS HUVECs only two networks have been identified in IPA analysis they have been listed in the table 5-6.

Network functions	Score	Focus molecules
Dermatological Diseases and Conditions, Organismal Injury and Abnormalities, Embryonic Development	57	21
Embryonic Development, Hair and Skin Development and Function, Organ Development	22	10

Table 5-5: Top networks affected by SIPS.

Focus molecules are the number of molecules from SIPS SASP that participate in the respective network.

5.3.3 Comparison of protein synthesis and secretion in senescent versus young HUVECs

As the secretome study contained fewer individual proteins in SIPS and even fewer in REPS HUVECs, we hypothesised that there might be reduced protein synthesis in the REPS and SIPS compared to control. In order to measure the global protein synthesis in senescent HUVECs we performed protein synthesis monitoring using puromycin and Western blotting. Puromycin can be used in several techniques for determination of neoprotein synthesis, for example, in flow cytometry, immunohistochemistry and Western blots (Azzam, Algranati 1973). Initially to optimise the method, a concentration response curve was carried out. EA.hy926 cells were grown in T-75 flasks and then treated with 5 different concentrations of puromycin (fig 5-7). The time of incubation,

that is 1 hr was referenced from the original research article (Schmidt, Clavarino et al. 2009). A range of molecular weight proteins was present for each sample in all puromycin concentrations tested. Each sample presented like a smear. The lowest concentration of 0.3 µg/ml was best for higher molecular weight proteins while the highest concentration of puromycin (10 µg/ml) was optimised for the proteins at low and medium molecular weights. The middle concentration of 3 µg/ml was chosen to analyse the protein synthesis across the entire molecular weight range. Therefore, 3 µg/ml concentration of puromycin incubation of cells for 1 hr was the optimum concentration for protein synthesis measurement. Next REPS and SIPS cells were treated with 3 µg/ml puromycin for 1 hr and cells were trypsinised and lysed using lysis buffer. Protein assay was performed and 30 µg of protein were loaded into a SDS gel and electrophoresed. Anti-puromycin antibody was used for detection of puromycin labelled proteins. An equal amount of protein synthesis was observed in all senescent and young HUVECs (fig 5-8A). Equal loading of protein was confirmed with housekeeper protein β-actin. Western blots were stripped but some of the staining remained. However, a 42 kDa band for β-actin was still observed (fig 5-8B).

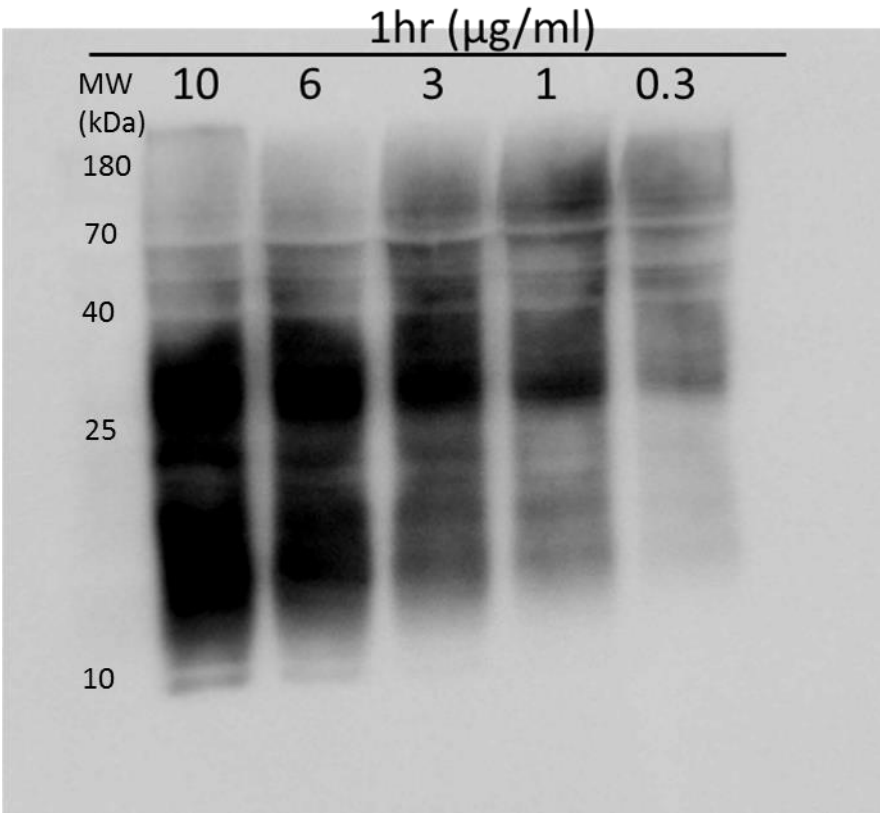

Figure 5-6: Protein synthesis monitoring in EA.hy926 using puromycin-labeled proteins.

EA.hy926 cells were treated with different concentrations of puromycin for 1 hr. Cells were harvested and lysed using lysis buffer. Cell lysate proteins were electrophoresed on a 12% SDS gel and analysed by Western blotting with antibody to puromycin. n=2 independent experiments.

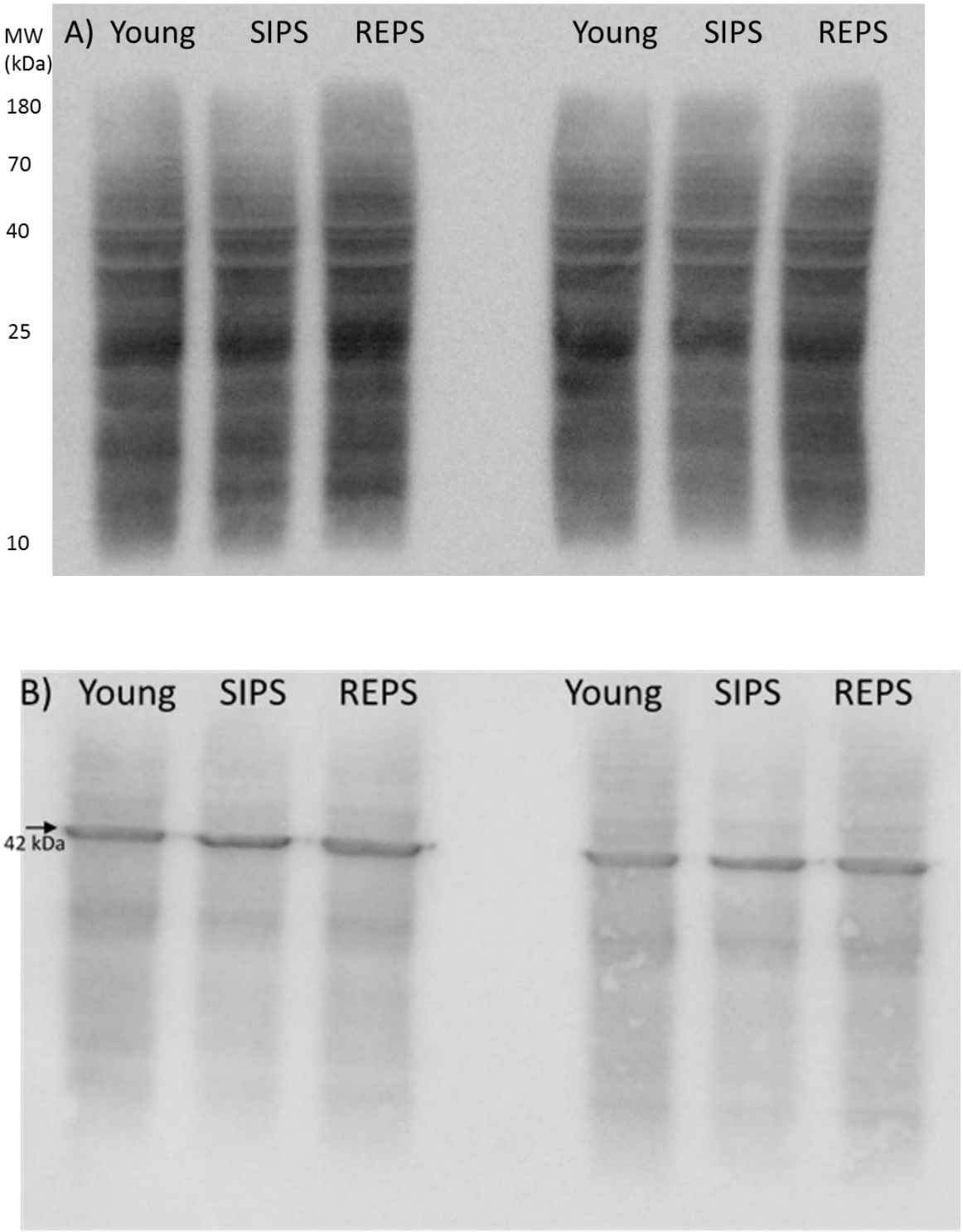

Figure 5-7: Protein synthesis monitoring in senescent HUVECs using puromycin-labelled proteins.

(A) Young, SIPS and REPS HUVECs treated with 3 µg/ml of puromycin for 1 hr. Cells were harvested and lysed. Equal amounts of protein were loaded on a 12% SDS gel. Puromycin incorporation into HUVECs is detected by an anti-puromycin blot visualised through GE Healthcare Life Sciences ImageQuant. (B) Immunoblot for β-actin following partial stripping of the puromycin antibody staining. n=3 independent experiments.

5.3.3.1.1 Secreted protein synthesis using puromycin and PMA

Global protein synthesis measurement showed no difference between the young and senescent HUVECs. Therefore, it was hypothesised that the unexpected results were due to the effects of senescence on PMA-induced secretion of proteins. As a preliminary experiment young HUVECs were treated with puromycin for 1 hr, followed by treatment with PMA in the same concentration and duration used for the conditioned media collection for secretome study. In the same way 9 ml of serum free media (cell supernatant) were collected and concentrated using a spin column. Concentrated supernatant was buffer exchanged with 50 mM ammonium bicarbonate and freeze dried as explained earlier in methods (section 2.4.3.2). EA.hy926 cells cell lysate was loaded as a positive control for the antibody validation. Puromycin was able to measure the secreted proteins induced by the secretagogue, PMA (fig 5-9).

This method was repeated for the media of REPS and SIPS HUVECs treated with puromycin and PMA (fig 5-10) using EA.hy926 cell lysate as a positive control. The three smears for young, SIPS and REPS were very similar in intensity and molecular weight range (fig 5-10). This time to confirm that neither PMA nor puromycin is concentrated and detected in our Western blots, we added puromycin to serum free HUVECs growth medium. To the same medium we later added PMA. All the conditions were kept the same. There was no band detected in the “GM” blot as shown in the fig 5-10.

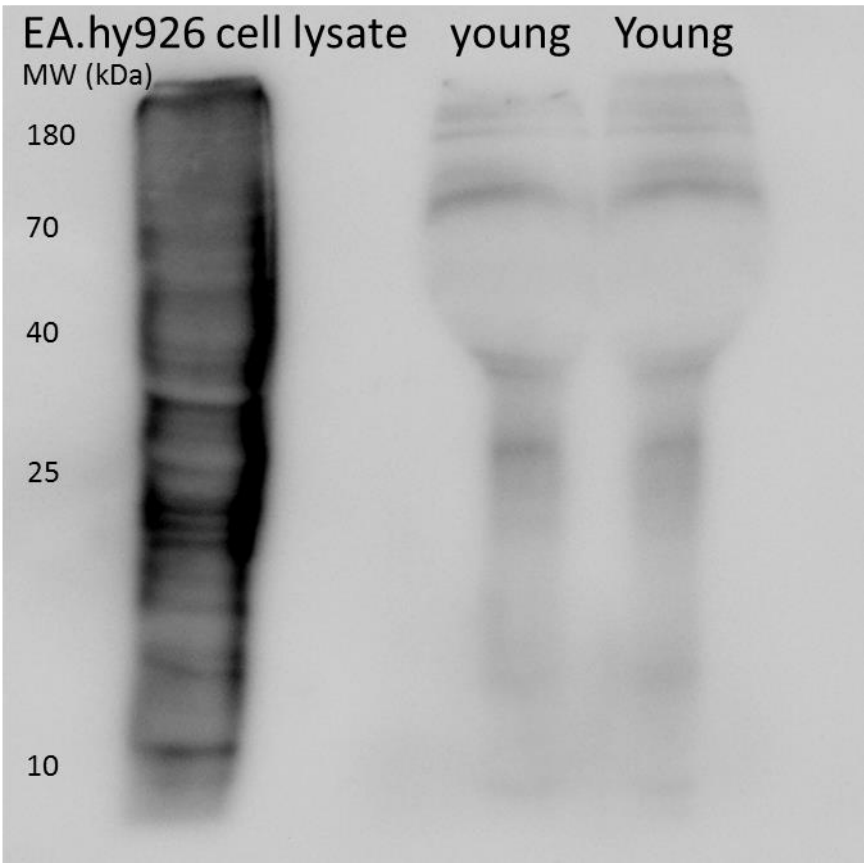

Figure 5-8: Protein synthesis can be measured for secreted proteins induced by PMA.

Young HUVECs were treated with puromycin (3 µg/ml for 1 hr), to label new proteins synthesised, followed by PMA treatment (50 nM for 45 min) to initiate protein secretion. Cell supernatant was collected and analysed by Western blotting using an antibody against puromycin. On the left EA.hy926 cell lysate treated with puromycin used as a positive control. n=3 independent experiments.

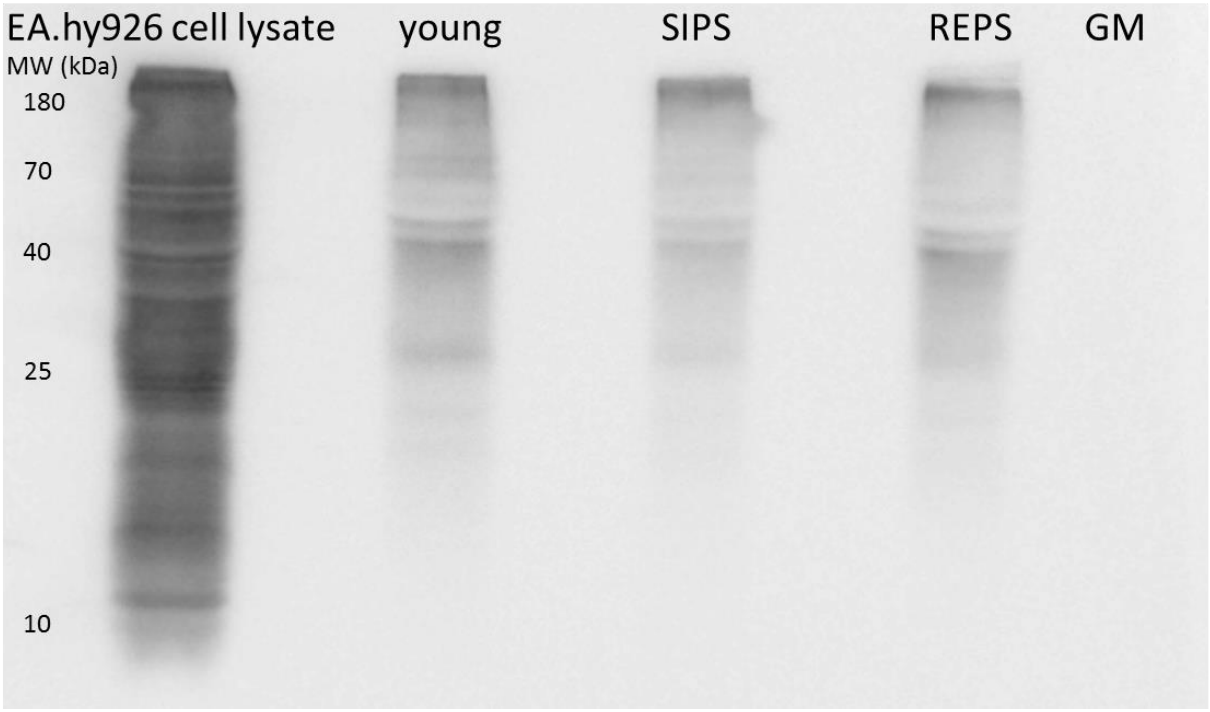

Figure 5-9: PMA-induced secreted protein synthesis in senescent HUVECs.

Young, SIPS and REPS HUVECs were treated with puromycin at a concentration of 3 µg/ml for 1 hr before being treated with PMA (50 nM, 45 min). The supernatant was collected and run on an SDS gel. GM is a control where PMA and puromycin were added in the absence of cells in HUVECs growth medium. On the left EA.hy926 cell lysate treated with puromycin was used as a positive control. n=3 independent experiments.

5.3.3.1.2 Puromycin measures newly synthesised proteins

To confirm that the observed proteins in Western blots were only newly synthesised proteins, cycloheximide (CHX) was used as a translation inhibitor. At high doses it also inhibits transcription processes (Schneider-Poetsch, Ju et al. 2010). The exact mechanism is not known, but it has been used for long time in research to inhibit protein translation (Schneider-Poetsch, Ju et al. 2010).

EA.hy926 were treated with 50 µM of CHX for up to 240 min. This was followed by treatment with puromycin. Cells were harvested and lysed using lysis buffer. Protein synthesis inhibition was detected using Western blotting with an antibody to puromycin (fig 5-11). This experiment was repeated in HUVECs, (fig 5-12) but this time two concentrations of CHX were used, 50 and 100 µM, for two different time points. As for

EA.hy926 cells, protein synthesis inhibition caused decreased protein levels as analysed using puromycin confirming the usefulness of the puromycin method.

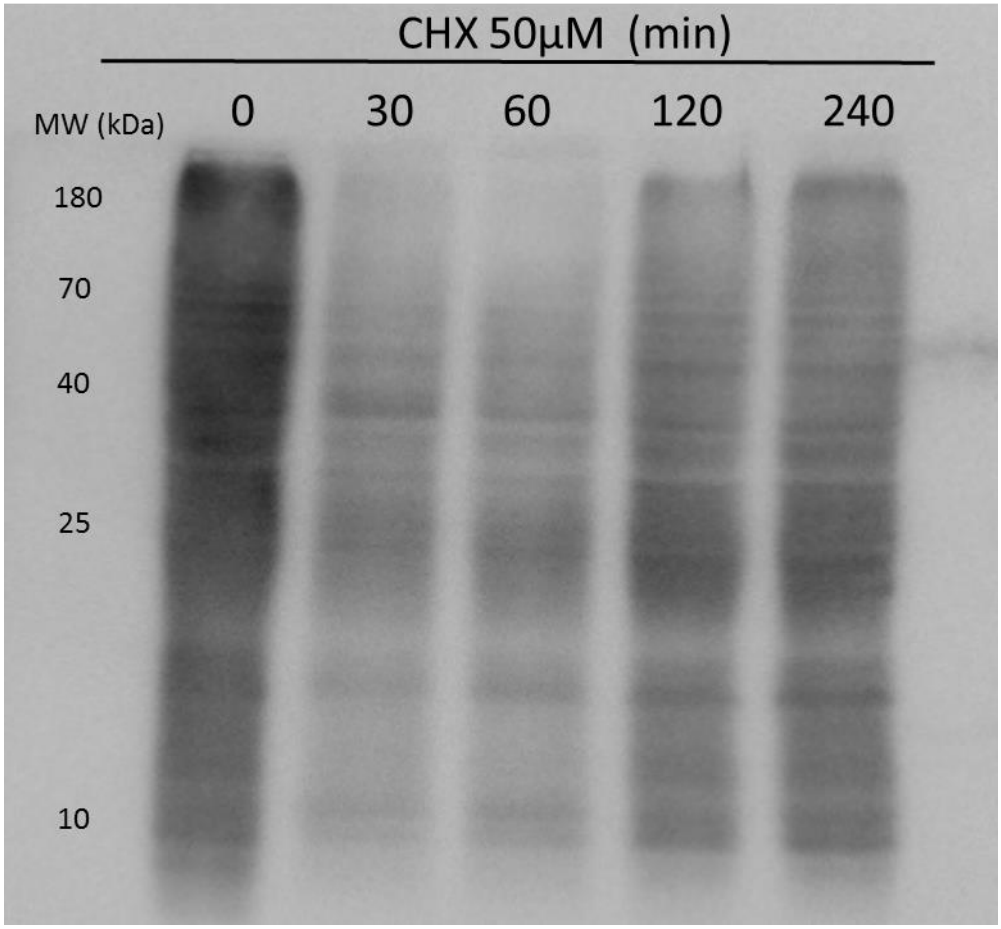

Figure 5-10: Protein synthesis measurement by puromycin is blocked by cycloheximide in EA.hy926.

EA.hy926 cell were treated with cycloheximide at a concentration of 50 µM for up to 240 min. Thereafter, cells were treated with puromycin (3 µg/ml) for 1 hr. An antibody against puromycin was used to detect protein synthesis. n=3 independent experiments.

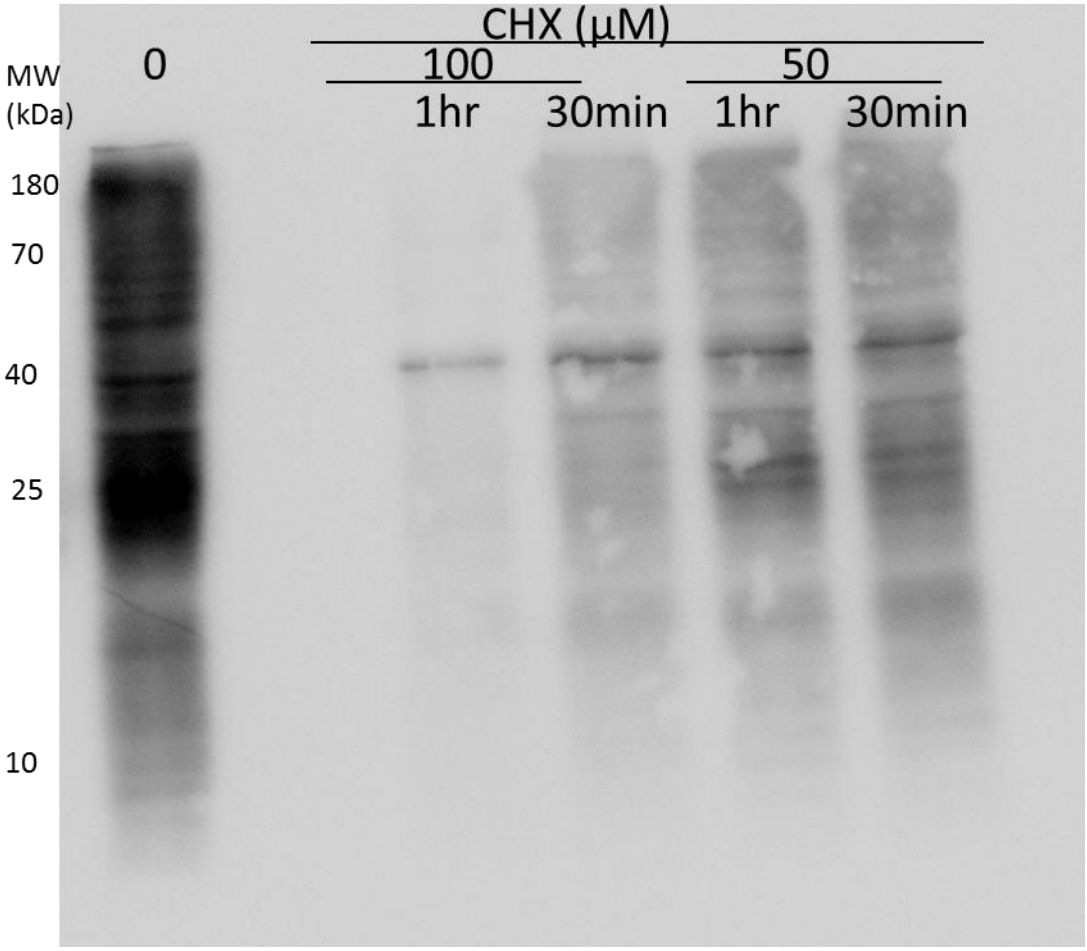

Figure 5-11: Cycloheximide treatment blocked protein synthesis in HUVECs monitored by using puromycin.

Young HUVECs were treated with 100 µM and 50 µM of cycloheximide for either 1hr or 30 minutes (at each concentration), followed by treatment with puromycin in the same concentration and duration as previously used. Protein synthesis was measured using an antibody against puromycin. n=3 independent experiments.

5.4 Discussion

5.4.1 Proteome analysis of secreted proteins

Lara et al proposed a panel of biomarkers of healthy ageing. These biomarkers can be considered for future interventional studies promoting healthy ageing. They classified these functions into five main domains, including physical function as one of the domains. One of the major subdomains of physical function is cardiovascular function (Lara,

Cooper et al. 2015). This highlights the importance of the cardiovascular function and its role in ageing. Understanding cardiovascular ageing mechanisms and developing biomarkers that can identify the ageing process and then the development of intervention based on these findings for the eradication of senescent cells could have a major contribution towards the common aim of healthy ageing.

The ultimate goal of biomarker discovery is to provide tools that enable improvement in clinical practice, in terms of diagnostic and therapeutic purpose. Age is the major risk factor for age related frailties and the development of CVD (Chimenti, Kajstura et al. 2003). Accumulation of senescent endothelial cells causes endothelial dysfunction and subsequently development of cardiovascular diseases (Childs, Baker et al. 2016a), (Silva, Abbas et al. 2017). The presence of senescent endothelial cells in atherosclerotic plaque suggests a role of senescence in CVD (Minamino, Komuro 2002). Therefore, the study of the senescent endothelial cell secretome (SASP) is of interest. A literature search of 3 different databases Scopus, Web of Science and PubMed, resulted into 23 articles related to biomarkers and secretome studies of senescent endothelial cells. Most of the research articles were conducted using whole cells lysates and 2-D gel proteomics to analyse the differentially expressed genes (full list is shown in appendix III). Some of the researchers have analysed senescent HUVECs SASP for individual targeted factors. For example, most common factors are IL-1, IL-8, TNF-α, PAI, IGFBP3, vimentin (Yentrapalli, Azimzadeh et al. 2013, Hampel, Fortschegger et al. 2006a), (Khan, Awad et al. 2017). No research has been conducted on the whole secretome from senescent HUVECs using liquid chromatography tandem mass spectrometry (LC MS/MS). The study described in this thesis is the first that has determined the secretome of REPS and SIPS HUVECs.

Endothelial cells are the inner-most layer of the vessel wall and therefore in direct contact with the circulating blood. Due to their important spatial and physiological functions, endothelial cells should be under strict surveillance. SASP is an important phenotype of senescent cells, hence it is very important to identify the senescent endothelial SASP factors. This will determine the functional abnormalities in endothelium due to the ageing process.

The secretome is defined as the complete compliment of proteins that have been secreted by cells under certain conditions over a particular period of time. The composition of secreted protein is highly dependent on the cell type, which can determine the biological and molecular processes within the cell. Secreted proteins may have an autocrine and paracrine function by changing the cell environment. HUVECs secrete a large number of factors responsible for biological functions. Considering tissue culture conditions for example, use of protein and serum free medium are important before secretome analysis as the abundant serum proteins will mask the important low abundant proteins secreted from cells (Bal, Kamhieh-Milz et al. 2013).

To gain insight into the biology of endothelial senescence, a proteomics study of the endothelial secretome was attempted. In this regard, initially the method to collect SASP from HUVECs was identified and optimised, before selection of PMA. Researchers had previously used 72 and 48 hr growth media as a source of SASP (Ozcan, Alessio et al. 2016). Similarly, in an attempt to collect SASP from HUVECs, cells were fed with serum-free media. After 12 hr, observation of HUVECs was carried out and the majority of cells were dead. This made us find a method for SASP collection, which either allows the use of serum in the growth medium or some other alternative. Several options were considered and discussed, for example the use of an albumin depletion kit. Every option had its own limitations and compatibility issues with mass spectrometry.

For further analysis and characterisation of senescent HUVECs SASP, when use of serum free media for a 12 hr time period was not possible, LC MS/MS was carried out using PMA as a secretagogue. In line with this, PMA has been used for the proteomics analysis of young HUVECS secretome (Yin, X., Bern et al. 2013). When HUVECs reached passage 25 or young HUVECS were made SIPS, the samples were prepared for mass spectrometry analysis. The data obtained only showed one uniquely expressed protein in REPS while 28 in SIPS. Most of the proteins in SIPS and REPS were down regulated compared to control (young). To facilitate the analysis only uniquely expressed proteins in SIPS were further analysed using IPA. The sample of medium only was not exposed to HUVECs. Most of protein from this sample were subtypes of keratin. These keratins were excluded from analysis, as they are commonly found contaminants present on the outer layer of skin, nails and hairs (Hodge, Have et al. 2013). Sample preparation for mass

spectrometry was performed while considering proper protective measures, for example wearing protective gloves and lab coat but still these contaminants were found in the samples.

5.4.1.1 Cellular localisation

As mentioned earlier, the secretome is defined as the group of proteins secreted from cells. It would be expected that most of the proteins should be secretory proteins. However, in this study, many of the proteins were proteins belonging to the intracellular compartment. Bal et al has performed secretome proteomics on young endothelial cells and in response to interleukin stimulation on 16 hr old conditioned media, without induction with a secretagogue. They have also found proteins that are mainly belong to the cellular compartment (Bal, Kamhieh-Milz et al. 2013). This can be explained by exocytosis of caveolae. These caveolae contain a large number of molecules and enzymes. In endothelial cells caveloae are fused with secretory pods and release their cargo in response to inflammation, hypoxia and trauma (Garnacho, Shuvaev et al. 2008), (Metcalf, Nightingale et al. 2008). Typically membrane proteins constitute 30% of the proteome (Chandramouli, Qian 2009). While GO protein centre analysis (section 2.8.2) revealed 53% of protein belonged to membrane in this thesis.

5.4.2 Molecular function of uniquely expressed proteins in REPS and SIPS proteomics

Secretome profiling of REPS SASP revealed a single uniquely expressed protein elongation factor 1-alpha 2 (EF-1α) compared to SIPS and control. EF-1α contributes to multiple cellular process including cell growth, differentiation and transformation (Negrutskii, El'skaya 1998). EF-1α is involved in the protein translation process, particularly the elongation phase by catalysing the efficient delivery of tRNA to the ribosome (Uetsuki, Naito et al. 1989). EF-1α promotes long term viability in response to growth factor withdrawal induced death and protects against ER stress (Talapatra, Wagner et al. 2002). In the current results EF-1α might be the driver of senescence in REPS while putting a halt to cell division and bypassing apoptosis. In the future it would

be worth studying the overexpression of EF-1α in young HUVECs under certain conditions, for example apoptotic stress and cell death.

SPARC (a secreted protein acidic and rich in cysteine) is a calcium binding ECM glycoprotein (Bornstein, Sage 2002). In bovine aortic endothelial cells SPARC inhibits cell growth, it also inhibits endothelial cell adhesion (Motamed, Sage 1998). SPARC is widely studied in cancer research and has been shown to inhibit cell growth and proliferation in multiple cancers including, prostate, lung, breast and pancreas (Nagaraju, Dontula et al. 2014). Previously SPARC has also been reported to be involved in the increased invasiveness of glioma tumours by mediating production of intergins and growth factors (Thomas, Alam et al. 2010). In response to fibroblast growth factor-2, SPARC inhibits endothelial cell chemotaxis (Yan, Sage 1999). In the current study, lower levels of SPARC were expressed in REPS and SIPS compared to control (see attached CD). According to Nagaraju et al SPARC has divergent roles of tumour suppressor and increased invasiveness, which means its function is more cell specific. Similarly in the current study this protein might favour senescence induction but its role of decreased adhesiveness may be more important than senescence induction. Further work would be required to investigate the role of SPARC in endothelial cell senescence.

Caspase 14 was expressed exclusively in the SIPS secretome and is a member of the cysteinyl aspartate–specific proteinases family mainly responsible for inflammation and apoptosis. However, recently their expression has also been reported in certain cancers (Denecker, Ovaere et al. 2008). Hornerin is an S100 family protein which is expressed in psoriatic skin (Wu, Meyer-Hoffert et al. 2009). Induction of apoptosis upregulates hornerin expression in breast cells (Fleming, Ginsburg et al. 2012). Its expression in psoriatic skin is involved in the regeneration of skin and it is only expression in the parts of skin undergoing regeneration. Other proteins of this family including S100A8 and S100A9. These are reported to be upregulated in basal type breast cancers compared to non-basal type breast cancers (McKiernan, McDermott et al. 2011). While overexpression of S100A7 is related to increased breast cancer cell growth and invasiveness *in vitro* (Fleming, Ginsburg et al. 2012), (Takaishi, Makino et al. 2005). These proteins were expressed in SIPS SASP exclusively in the current study.

Serpine 1 is found as a senescent biomarker in radiation induced senescent HUVECs (Yentrapalli, Azimzadeh et al. 2015). Serpine b12, a member of serpine B family has been uniquely expressed in SIPS in the current study but its function in senescence remains unknown.

5.4.3 Possible role of endothelial cell senescence in cardiovascular disease

Senescent endothelial cells were detected in the aorta obtained from elderly individual (Vasile, Tomita et al. 2001). Senescent endothelial cells have also been detected in atherosclerosis plaque in a mouse model of atherosclerosis. Selective removal of all the senescent cells in the same atherosclerotic model showed a decrease in number and size of plaque (Childs, Baker et al. 2016b). In advance atherosclerosis, the release of the SASP component matrix metalloproteases (MMPs) may be, in part, responsible for the degradation of the fibrous cap. This results in rupture of the plaque and subsequently thrombosis. The detrimental effects caused by the release of endothelial cell-derived SASP components highlight the role that senescence may play in the pathogenesis of vascular ageing (Childs, Baker et al. 2016b).

Immune cells recruitment is the initial step in the development of atherosclerosis. This and previous studies have shown that senescent endothelial cells are associated with a pro-inflammatory phenotype. In addition to expression of adhesion molecules, pro-inflammatory mediators including cytokines and chemokines are also released by senescent endothelial cells (Mun, Boo 2010), (Khan, Awad et al. 2017). SASP characterisation showed expression of adhesion molecule CD44 but its expression is lower in REPS and SIPS compared to young HUVECs (see supp data available on CD). Also we did not find expression of pro-inflammatory cytokines and chemokines. As explained earlier endothelial cells are the most inner layer of vessel wall, which is in direct contact with blood and therefore, it is very important that endothelial cells are strictly regulated. This also suggests that there might be a potential feedback signal which prevents the further pro-inflammatory behaviour of senescent endothelial cells.

5.4.4 Protein synthesis by senescent endothelial cells

The reduced number and levels of proteins in the secretome of senescent HUVECs suggested either an intrinsic effect of the ageing programme or interference in the mechanism of secretion due to PMA.

In this thesis, puromycin was used to monitor protein synthesis in senescent HUVECs. The neo-protein synthesis by three groups (control, SIPS and REPS) showed only a very slight shift in the protein concentration in cells and in secreted proteins. While, proteomics analysis showed fewer proteins in REPS and SIPS compared to young HUVECs. A proteomics analysis of senescent HUVECs SASP while depleting high abundance serum protein or using a tag (section 7.7.3) can identify and confirm the SASP in senescent HUVECs. Comparing the results with the proteomics carried out in this thesis can validate and confirm the best method for senescent HUVECs SASP characterisation.

A rise in intracellular Ca^{2+} concentration facilitates the extracellular release of vesicles but the release of the same secretory vesicles can be facilitated through a non- Ca^{2+} dependent manner. This shows that there can be factors other than Ca^{2+} that help exocytosis of vesicles. Yin et al used a compound, PMA. They confirmed it to be a secretagogue which could be used in mass spectrometry, and was specifically applied to HUVECs (Yin, Bern et al. 2013). In this thesis, there was no difference in PMA-induced protein synthesis and secretion between young HUVECs and senescent cells.

When puromycin followed by PMA was added to media only and the sample was prepared in the same way as the other samples (HUVECs supernatant) there was no band detected in our Western blots experiments, confirming that puromycin is only detected when it is incorporated in to the newly synthesised proteins.

Cycloheximide inhibits protein synthesis by blocking the transfer of peptidyl-tRNA from acceptor site to the donor site on ribosomes. Thus it stops the protein translation elongation (McKeehan, Hardesty 1969). Similarly, 100 µM concentration of CHX for 1

hr in EA.hy926 has the ability to inhibit protein synthesis measured by puromycin in Western blots (fig 5-12).

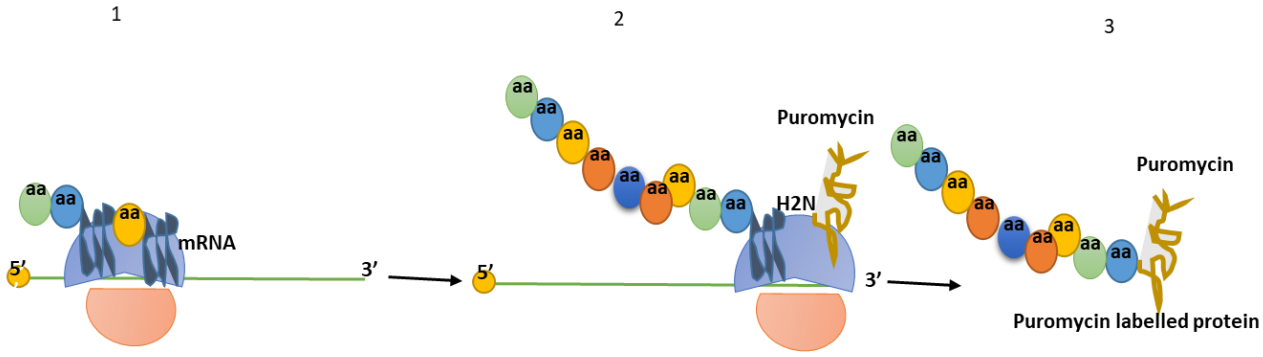

Figure 5-12: Mechanism for puromycin incorporation during protein synthesis.

1) During the protein translation phase, the ribosome subunit starts the uncoding of mRNA, tRNA incorporate amino acids to make a polypeptide chain. 2) During elongation phase, puromycin forms a peptide bond with amino acids. 3) puromycin gets incorporated into the polypeptide chain and terminates the protein elongation phase, and puromycin labelled protein is released. (Adapted from (Goodman, Hornberger 2013b).

Green line is mRNA. Light blue and pink objects are ribosome subunits, multicolour circles are amino acids while, the dark blue objects are tRNA.

5.5 Conclusion

This study reveals a list of HUVECs proteins secreted into media in response to PMA. Bioinformatics analysis reveals canonical pathways and molecular functions which are related to inflammation, the stress response, regeneration and the immune response. REPS did not express unique proteins but the proteins exclusive to SIPS were mostly related to cancer, inflammation and regeneration.

Puromycin was able to measure newly synthesised proteins, and puromucin together with PMA was able to measure secreted protein levels. There was no difference in the secreted

protein synthesis in REPS and SIPS compared to young HUVECs. I therefore, in future work senescent HUVECs SASP should be characterised by employing a high abundance serum protein depletion method using proteomics. and then compare tTe two methods then should be compared.

Chapter 6

6 Characterisation of senescence associated secretory phenotype and pro-inflammatory mechanism associated with senescent endothelial cells

6.1 Introduction

Accumulation of senescent cells in multiple tissues and stem cells during physiological aging (Dimri et al. 1995; Baker et al. 2016) is involved with development of certain age related diseases (Baker, Wijshake et al. 2011b). This accumulation of non-proliferating cells contributes to the loss of functional and regenerative capacity in aged tissues, preventing proliferation of both somatic and stem cells in a cell-intrinsic manner (Janzen et al. 2006; Krishnamurthy et al. 2006; Molofsky et al. 2006; Sharpless and DePinho 2007; Sousa-Victor et al. 2014; Baker et al. 2016; Garcia-Prat et al. 2016). Additionally, senescent cells can contribute to loss of tissue function during ageing through non-cell-autonomous mechanisms. This can result from SASP proteins disrupting homeostasis (Ritschka, Storer et al. 2017). Elimination of senescent cells has been studied in different disease states. Jeon et al confirmed that accumulation of senescent chondrocytes, in part, plays a role in the development of osteoarthritis, a chronic disease associated with pain and physical disability due to degeneration of cartilage. Selective elimination of senescent cells in transgenic mouse models of induced osteoarthritis resulted in reduced pain and development of cartilage (Jeon, Kim et al. 2016). Therefore, it is important to understand the mechanism of senescence and exploit that for the potential therapeutic alternatives *in vivo*.

6.1.1 Association of inflammation and senescence

Research has identified the importance of inflammation in atherosclerosis. The evidence comes from both clinical and basic research (Blankenberg, Barbaux et al. 2003). Endothelium plays an important role in development of atherosclerosis. One of the primary causes of cardiovascular disease development might be due to accumulation of senescent endothelial cells. Endothelial cells might play an important role in control of inflammation and the immune system. Ageing is associated with immune cell dysfunction

causing delayed response of the immune system. This might be associated with functional decline of the immune system to clear senescent cells and eradicate the source of inflammatory reactions. Increased levels of circulating lymphocytes and pro-inflammatory cytokines including, IL-1α, IL-1β, IL-6, IL-17α, interferon gamma (IFNγ) and TNF-α have been observed in a premature ageing mouse model. This data suggest that senescence is associated with systemic inflammation (Revechon, Viceconte et al. 2017). Similarly, patients of a rare human disease of premature ageing, Hutchison Gilford progeria syndrome die at an early age in the majority of the cases due to myocardial infarction. This condition is mainly due to the accumulation of a protein called progerin. Progerin is the mutant form of a mammalian nuclear envelope component lamin A (Trigueros-Motos, Gonzalez et al. 2011). Lamin A has also been found in healthy human arteries, interestingly its level increases with age (Olive, Harten et al. 2010).

6.1.2 Functions of senescent associated secretory phenotype

Senescent cells generally also develop a complex senescence-associated secretory phenotype (SASP), in culture and *in vivo* (Coppe, Patil et al. 2008a), (Bavik, Coleman et al. 2006), (Liu, Hornsby 2007b). SASP can disrupt normal mammary differentiation (Parrinello, Coppe et al. 2005), promote endothelial cell invasion (Coppe, Kauser et al. 2006), and stimulate cancer cell growth and invasion in culture and tumour growth *in vivo* (Ohuchida, Mizumoto et al. 2004, Vakkila, Lotze 2004, de Visser, Eichten et al. 2006) Additionally, some SASP factors can reinforce the senescence arrest by autocrine or paracrine mechanisms (Acosta, O'Loghlen et al. 2008). IL-6 and IL-8 are among the pro-inflammatory SASP factors expressed by senescent HUVECs (Khan, Awad et al. 2017). SASP does not always play a negative role during senescence. It does have some beneficial roles, for example, during limb regeneration in the salamander, the presence of senescence cells and SASP helps in limb regeneration. Also, SASP from senescent cells is responsible for the tissue formation during embryo development (Munoz-Espin et al. 2013; Storer et al. 2013). Senescent cells also play a beneficial role to limit tissue fibrosis during wound healing by recruitment of immune cells (Jun, Lau 2010) Ratischka *et al* found that transient exposure to SASP improves the regenerative capacity of the cells, while prolonged exposure is associate with the stimulation of cell intrinsic senescence mechanism, causing senescence induction and decreased regenerative capacity (Ritschka,

Storer et al. 2017). This confirms that to decide the positive or negative role of senescence and its phenotype depends on the physiological function and system studied. A tight immune surveillance is required, in order to utilise the beneficial aspects of senescence and then eliminate senescent cells to prevent its detrimental effects.

6.1.3 Adhesion molecules and their role in atherosclerosis

Adhesion molecules are cell surface molecules that mediates the adhesion of cell to other cells or to the extracellular matrix. Adhesion molecules are expressed on the majority of cell types. Their presence on cell surface is very important as they participate in a number of cell surface interactions, these interactions can be between cell surface of another cell of the same type or a different type, cell microenvironment or a released cell soluble factors (Blankenberg, Barbaux et al. 2003).

Research in the recent years has focused on the role of inflammation in atherosclerosis (Pant, Deshmukh et al. 2014). Enhanced leukocyte adhesion to vessel wall and localized intravascular coagulation at the site of inflammation or vessel injury are considered to be inflammatory process (Mason, Sharp et al. 1977).

Inflammatory molecules including E-selectin, ICAM-1 and VCAM-1 are abundantly found in atherosclerotic intima, with highest abundance of VCAM-1, then of ICAM-1 and a lower expression of E-selectin. The expression of these molecules is not restricted to the plaque it is also observed in the intima of patients with atherosclerotic coronary artery disease. ICAM-1 and VCAM-1 is present on normal arteries (O'Brien, McDonald et al. 1996). Leeuwenberg *et al* found an increase in the release of E-selectin from HUVECs activated with TNF-α for 4 hrs (Leeuwenberg, Smeets et al. 1992). CD44 is a surface glycoprotein, activated by its ligand, hyaluronic acid. CD44 is responsible for cell-cell and cell-extracellular matrix interaction. In addition to other cells, CD44 is expressed on endothelial cells (Bruno, Fabbi et al. 2000). CD44 is expressed on endothelial cells under normal physiological conditions, while its expression is increased during ECs activation by cytokines (Murphy, Lennon et al. 2005b).

6.1.4 Validation of reference genes using validation software

Expression analysis of genes is carried out through real time PCR. This method measures the variation of gene expression between different cells and treatment conditions. This biological variation in genes can be affected by certain factors called non-biological variation. The method of normalisation is used in order to remove the non-biological variation. Use of more than one reference gene is recommended. One problem that is associated with reference genes is their variation in expression under different experimental conditions. There are available simple programmes to identify the best individual or combination of housekeeping genes i.e. those with least variation in expression under certain experimental condition (Vandesompele, Kubista et al 2009).

6.2 Aims

The previous chapters identified gene expression changes in REPS and SIPS and protein/peptide secretome changes in SIPS, in particular. The aim of this chapter was investigating changes in biological function attributable to senescent human endothelial cells; specifically, whether senescent HUVECs cells can transfer senescence to bystander cells via SASP and whether endothelial cell senescence presents a pro- or anti-inflammatory phenotype through leucocyte adhesion.

6.3 Results

6.3.1 Characterisation of SASP

6.3.1.1 Adhesion of monocytes to early passage HUVECs exposed to TNF-α

A TNF-α concentration response curve was investigated to find out the optimal concentration for HUVECs stimulation. Leukocytes pre-labelled with a fluorescent dye Calcein AM were co-incubated with both early passage (young) and senescent HUVECs (REPS and SIPS) for 1 hr. Calcein AM is a fluorescein derivative (acetoxymethyl ester,

that diffuse through the membrane of viable cell. Cytosolic esterases convert it to a green fluorescent calcein (Bratosin, Mitrofan et al. 2005).

Adhesion of THP-1 cells to stimulated HUVECs increased with TNF alpha concentration and reached a maximum from 10 ng/ml (fig 6-1). At 1 ng/ml approximately 50 % of the maximum THP-1 cell binding was observed, therefore this concentration was chosen as an appropriate concentration for adhesion of monocytes.

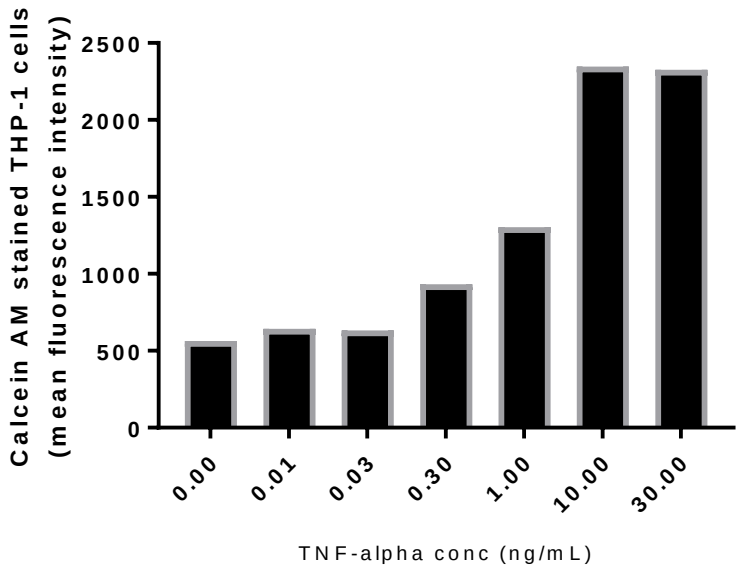

Figure 6-1: Adhesion of THP-1 monocytes to HUVECs in response to TNF-α.

HUVECs were stimulated with TNF- α at concentrations of 0.01 to 30 ng/ml for 6 h. Adhesion of THP-1 cells to HUVECs was measured as described in methods section 1.7.1.2.2. Values are the mean of 8 repeats in one experiments.

6.3.1.2 REPS HDFs present a senescent phenotype

The senescent state of HUVECs was shown in chapter 3 (fig 3-6a, b). Late passage HDFs were used in the experiments in this chapter. They were used as a source of SASP and to use as a positive control for SASP. Literature confirms that SASP is released from senescent HDFs (Krtolica, Parrinello et al. 2001b) and these cells have been used as an established model of SASP production. To confirm that the late passage HDFs were

senescent, their morphology was observed. Cellular senescence in many human cell types shows the characteristics of large, flattened cell morphology and expression of a senescence-associated b-galactosidase (Adams 2007). Senescent cells express an enzyme detectable at pH6 known as senescence-associated beta galactosidase (SA β-gal). It has been detected in the cultured senescent fibroblasts and aged human keratinocytes at pH6. This activity is not expressed by pre-senescent, terminally differentiated and quiescent cell (Dimri, Lee et al. 1995). Late passage HDFs presented a flattened and enlarged morphology (fig 6-2b) compared to young HDFs, which were elongated (fig 6-2a). Late passage HDFs (fig 6-2d) presented a significant increase in the SA β gal staining compared to young HDFs; cell enumeration showed that >90 % REPS HDFs were senescent compared with <10 % for young cells (other Fig fff).

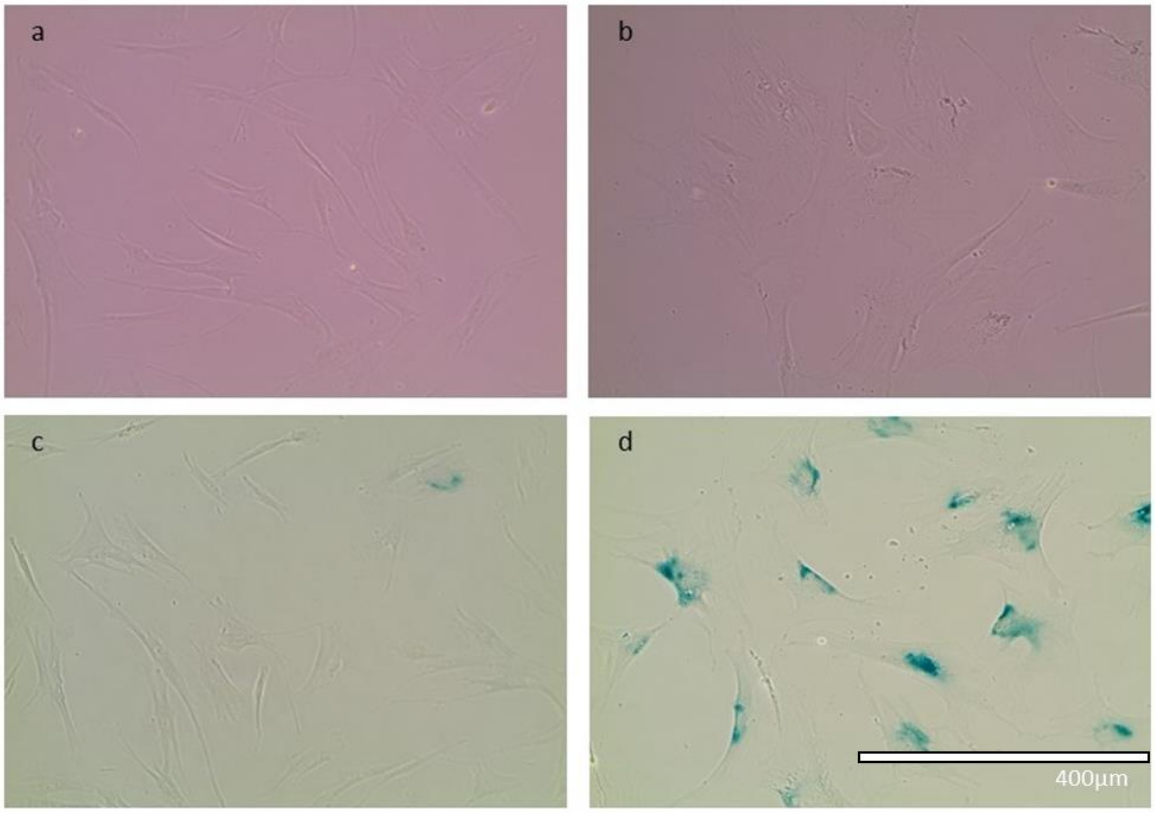

Figure 6-2: Confirmation of senescence in REPS HDFs.

Late passage (b) HDFs (REPS) showed an enlarged and flattened cell morphology compared to (a) young HDFs. The number of blue stained cells (SA-beta gal stain positive) (d) were increased in high passage HDFs compared to (c) young HDFs

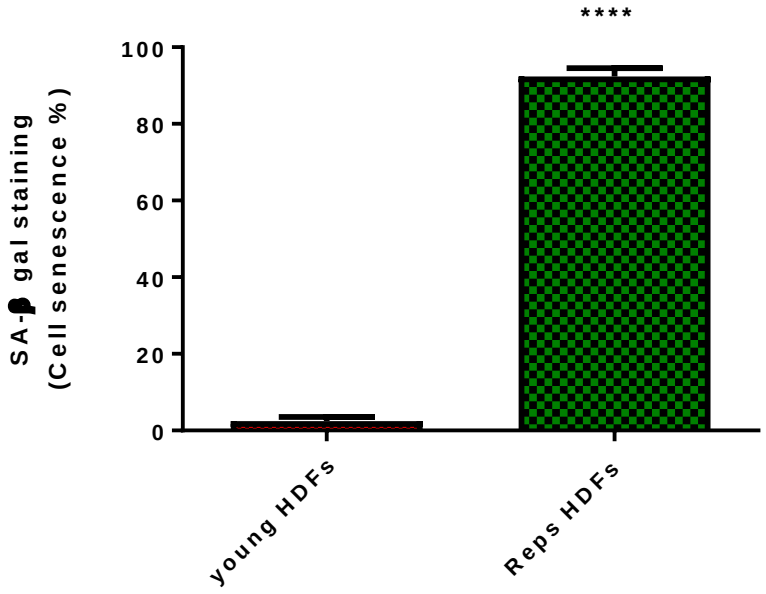

Figure 6-3: Late passage HDFs are senescent (REPS).

Late passage (REPS) HDFs showed significant increase in SA-β gal stain compared to control (young HDFs). Number of blue cells and total cells were counted in 5 different fields and the percentage calculated. Values represent mean (+SEM) of n=3 independent experiments. P****<0.0001.

6.3.1.3 Pro-inflammatory effect of HDFs SASP in an adhesion assay

To evaluate the SASP generation from senescent HUVECs and its pro-inflammatory effect in terms of binding of monocytes to endothelial cells, an adhesion assay was performed. In these experiments TNF-α was used as a positive control. Young HUVECs were grown in 96 well plates and treated for 24 hr with conditioned media (SASP) from replicative senescent HUVECs collected over 12 h (fig 6-4 and B) or 24 h (fig 6-4C and D), or with SASP from senescent HDFs or no conditioned media. These young HUVECs were either treated with (fig 6-4B and D) or without (fig 6-4A and C) TNF-α at a concentration of 10 ng/ml. Overnight. Compared to control (no SASP) HDFs SASP significantly increased the number of adhered THP-1 cells in the absence of TNF-α (see fig 6-4). While SASP from REPS HUVECs did not show increased adhesion of THP-1 cells both in TNF-α treated and untreated HUVECs. An explanation for the no significant effect of HDFs SASP in TNF-α treated HUVECs compared to young HUVECs might be

because, young HUVECs grow in a monolayer, growing more cells/ cm^2 area of tissue culture flask compared to the REPS HUVECs. In such case where there are more cells in control (Young), TNF-α induction might release more interleukins from control HUVECs compared to REPS HUVECs. One other possible reason could be that the concentration of TNF-α used was higher which saturated the maximum pro-inflammatory stimulation and further addition of HDFs SASP did not make much difference to the pro-inflammatory effect on HUVECs.

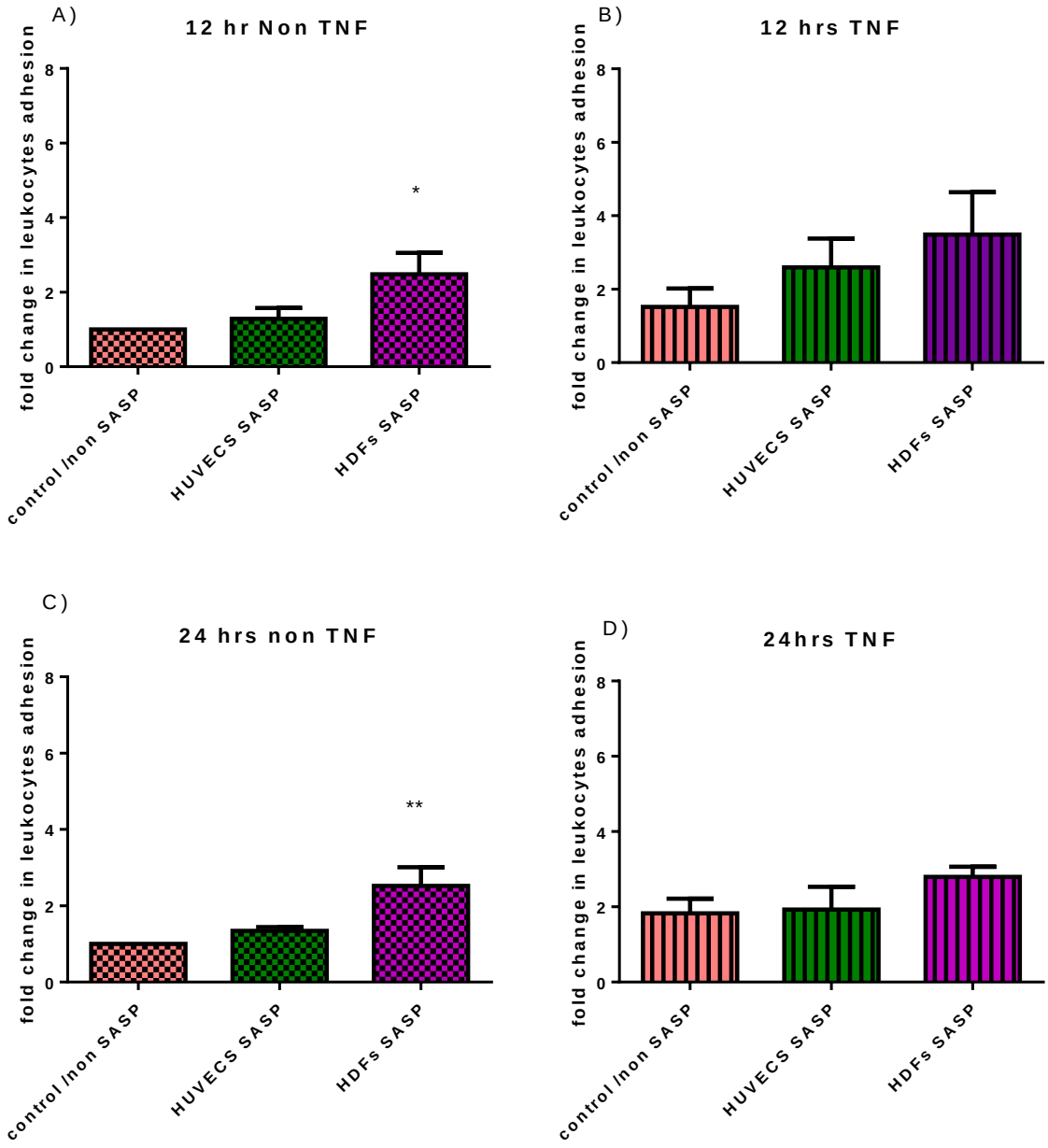

Figure 6-4: Adhesion of THP-1 monocytes to HUVECs in the presence of SASP.

Adhesion assay was performed in young HUVECs grown in 96 well plates, exposed to 12 or 24 hr conditioned media (SASP), obtained from REPS HUVECs and REPS HDFs. HUVECs were pre-treated overnight with or without TNF-α at a concentration of 10 ng/ml. values represent the mean (SEM) of fold change of n=5 independent experiments. P*<0.05, P**<0.01.

6.3.1.4 Effect of conditioned media from senescent HDFs on HUVECs and HDFs growth

Cellular senescence is the process which stops the cell from dividing further in response to stress in an attempt to stop the damage being transferred to the next cell generation. Hence cellular senescence is considered to be a protective mechanism. While senescent cells present a certain phenotype of morphological changes, there are also gene expression changes and often release of a group of proteins collectively called senescent associated secretory phenotype (SASP). Depending on the cell type this SASP can be deleterious to the surrounding microenvironment (Acosta, O'Loghlen et al. 2008). Previous research has shown fibroblasts SASP to be inflammatory in nature and promoting cell division (Hampel, Fortschegger et al. 2006c). In order to investigate this on HUVECs, growth curves were carried out. Young HUVECs or human dermal fibroblasts (HDFs) were treated with HDF condition media (SASP). In-order to prevent nutrient deprivation this SASP was mixed with an equal volume of fresh growth medium. The "age" of conditioned media used was maintained throughout the experiments. HUVECs require a different growth media to HDFs, therefore as a control some HUVECs were cultured with equal amounts of HUVECs fresh growth medium and HDFs fresh growth medium.

In 3 separate experiments, a decrease in growth rate of HDF cultured with SASP (fig 6-5A-C) was observed. For HUVECs cultured with HDF SASP slight alteration in cell culture growth was observed (fig 6-5D). HUVECs growth curve was not repeated therefore, its rate could not be constructed.

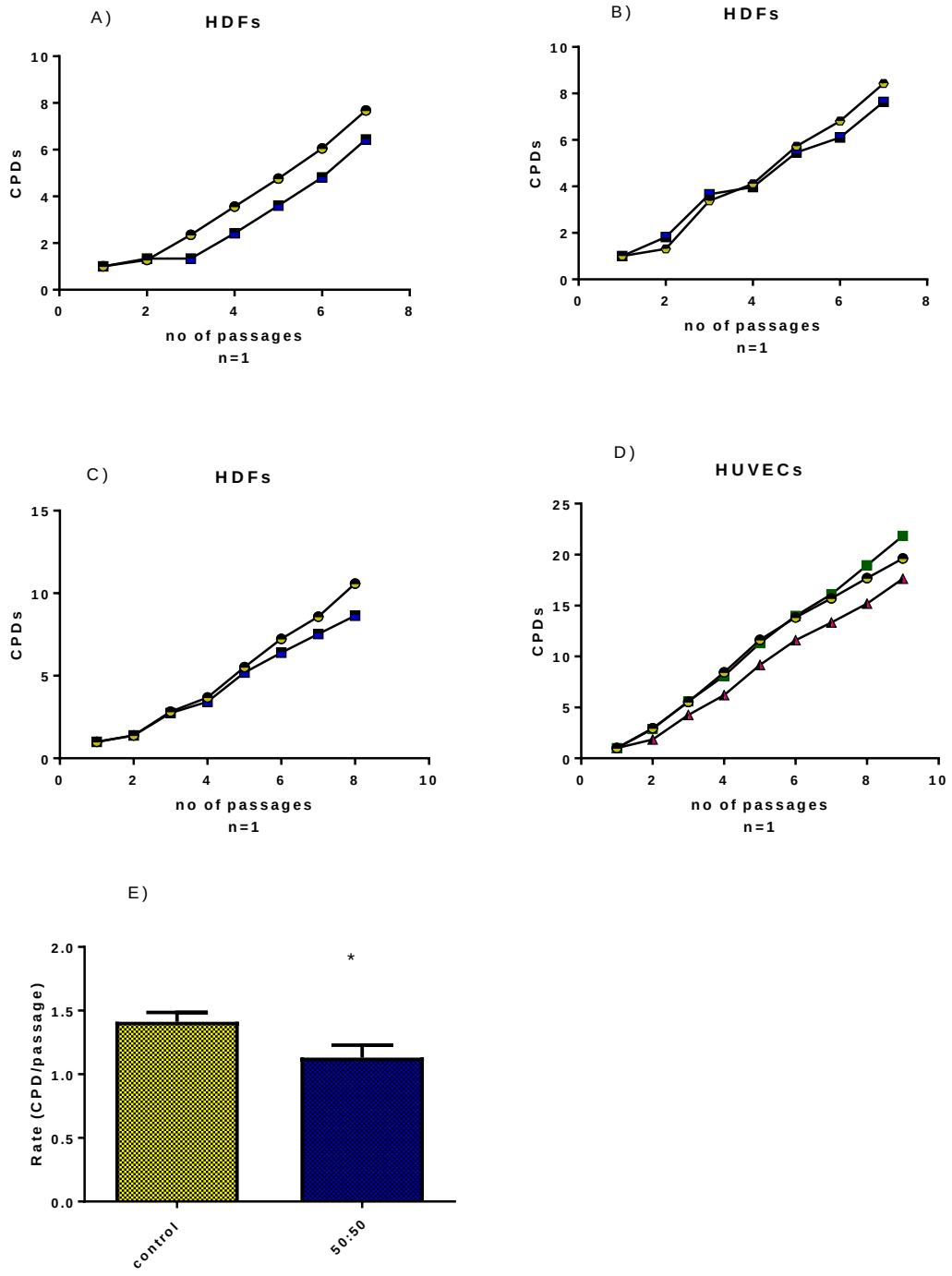

Figure 6-5 SASP has a negative effect on the cell growth of HDFs and HUVECs.

HDFs (A-C) (each line scattered graph representing individual growth curve, n=1) and HUVECs (D) were cultured for up to 8 passages in the presence of conditioned media (squares) from senescent cells. Equal volumes of conditioned and fresh media were applied. For HUVECs, since the basal media types were different, an extra control was necessary; a 50:50 mixture of the two types of fresh media (triangles). The mean rate of growth was calculated (E) for HDFs in control media and exposed to SASP (50:50) (HDFs fresh media:HUVECs fresh media). *$p<0.05$ for n=3 independent experiments. Cumulative population doubling (CPD) and rate was calculated as explained in section 2.5.2.

6.3.1.5 Effect of co-culturing with senescent HDFs on growth of young HDFs and young HUVECs

It was previously shown, in the SASP adhesion assay, that there was a SASP effect of the conditioned media obtained from senescent HDFs (section 6.1.1.3). Therefore, to further analyse the SASP effect on cell growth, the effect of SASP on HDFs and HUVECs growth was investigated. In the growth curves performed previously a conditioned media was obtained from senescent HDFs, mixed with 1:1 to fresh growth medium. One of the pitfalls of this method could be the nutrient deprivation of the conditioned media. Certain factors might be altered or degraded after being present in the growth medium for several hours. Therefore, it was important to grow the two types of cells together and determine the effect of soluble factors (SASP) on young cell growth. In these experiments, senescent HDFs were grown in well inserts and young HUVECs or HDFs were grown in a 6 well plate. For a control experiment the same number of young HDFs were grown in the inserts and young HUVECs were grown in the wells in 6 well plates. Inserts were placed in the 6 well plates. Cell type specific growth media was replaced with fresh growth media every 48 hours. Cells grown in the 6 well plates were serially passaged for 7 (HDFs) or 8 (HUVECs) population doubling. REPS HDFs grown in the inserts were maintained to keep a constant number of cells in the inserts compared to senescent HDFs. These young HDFs (in the control inserts) were passaged and replaced with the same number as REPS HDFs back in the inserts.

Growth suppression was observed in the growth curves of HDFs (fig 6-6A-C) and HUVECs (fig 6-7A-C) exposed to senescent HDFs. Growth curves of both the cells types (fig 5 and fig 6) showed a decrease at most of the CPDs comparatively to the control, particularly at the later passages. The overall growth rate (see section 2.5.1), showed a significant decrease in both HDFs (fig 6-6D) and HUVECs (fig 6-7D). Formulae for calculation of CPDs and rate was explained in the methods section 2.5.1.

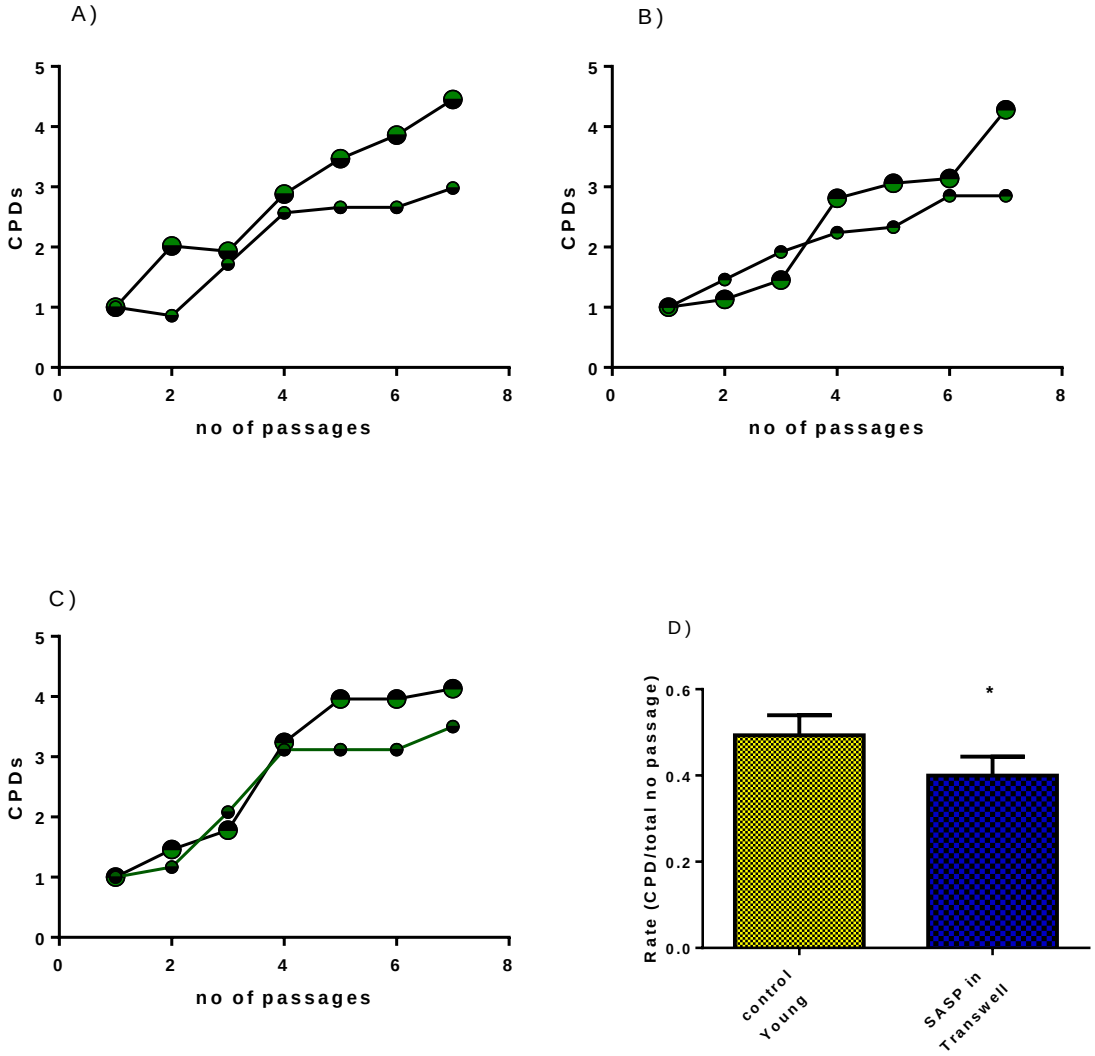

Figure 6-6: SASP released from co-cultured senescent HDFs has a negative effect on the growth of young HDFs.

Young. HDFs were co-cultured with senescent HDFs (smaller circles) in the trans-well inserts for up to 7 passages. For control experiments (larger circles) young HDFs were co-cultured with young HDFs in the same confluency. Young HDFs (A-C) were cultured for up to 8 passages in 6 well plates. The mean rate of growth was calculated (D) for HDFs. Values are mean (+SD) for n=3 independent experiments. *$p<0.05$. Cumulative population doubling (CPD) and mean rate of growth was calculated as explained in section 2.5.2.

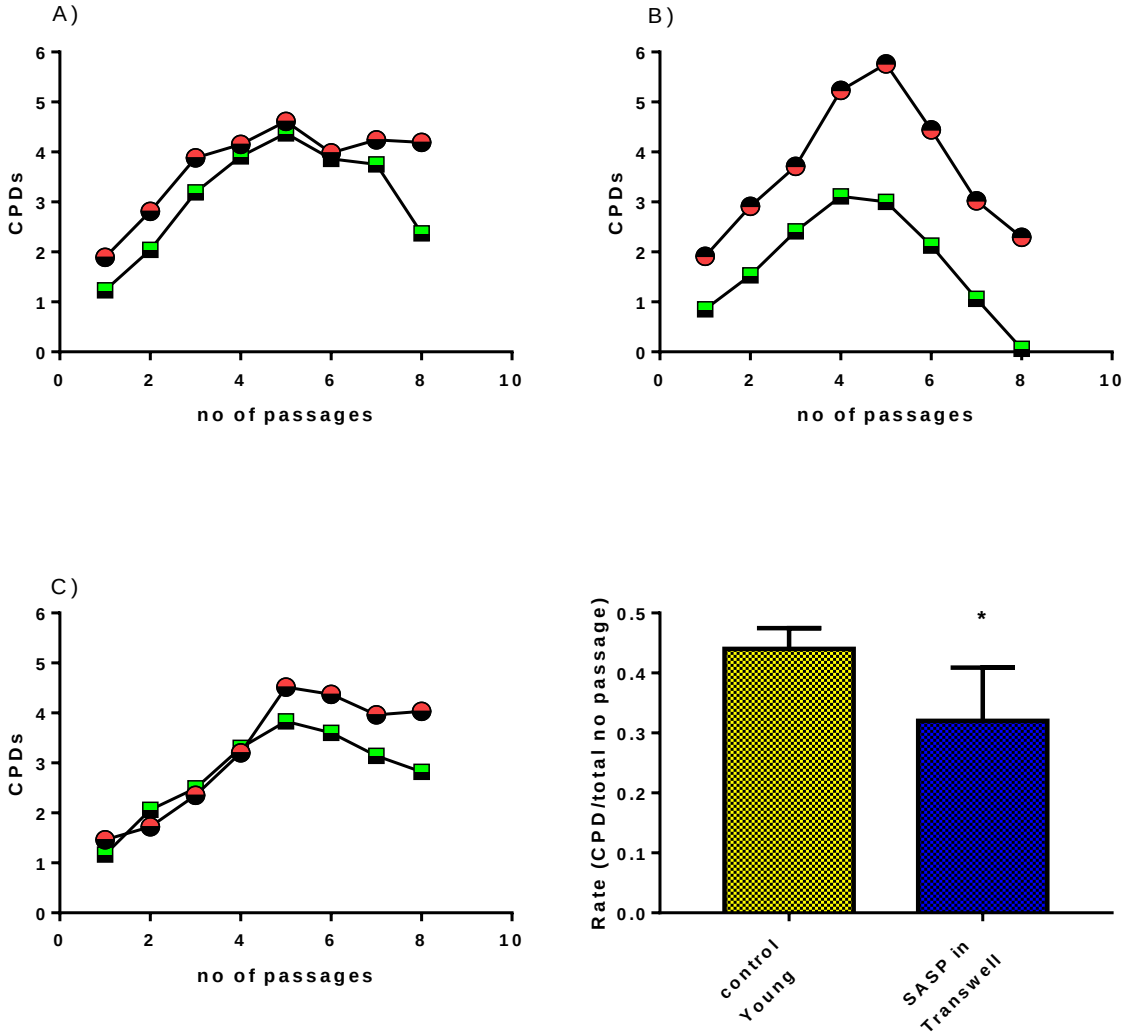

Figure 6-7: SASP released from co-cultured senescent HDFs has a negative effect on the growth of young HUVECs.

Young HUVECs (A-C) were co-cultured with senescent HDFs in the trans-well inserts for up to 8 passages. For control experiments young HDFs were co-cultured with young HUVECs in the same confluency. The mean rate of growth was calculated (D) for HUVECs. Values are mean (+SD) for n=3 independent experiments. *p<0.05

6.3.2 Pro-inflammatory role of senescent endothelial cells and its role in ageing

6.3.2.1 Senescent Endothelial cells promote monocyte adhesion to a static endothelial monolayer

The purpose of these experiments was to examine the inflammatory role of senescent endothelial cells. The idea being that, senescent endothelial cells express high levels of potential adhesion molecules which will provide an inflammatory microenvironment resulting in atherogenesis. An experiment was carried out to compare the adhesion of leucocytes (THP-1) to young and senescent HUVECs (both REPS and SIPS). These HUVECs were TNF-α stimulated or unstimulated. $1x10^6$ of THP-1 cells were added to each well of HUVECs in a 96 well plate. After 1 h, wells were washed 6 times gently in order to remove the non-adhered THP-1 cells. Cells that were firmly attached to the HUVECs monolayer were counted at the centre of each well.

There was an increase in the adhesion of monocytes to senescent HUVECs with or without TNF-α stimulation, compared to control, untreated HUVECs ($P<0.05$) (fig 6-9A, B). THP-1 adhesion was similar to REPS or SIPS. As REPS HUVECs never grow to a complete monolayer, it may be that adhesion in REPS might be higher than to SIPS cells as the former provide less surface area for THP-1 cells to adhere. The fig 6-8 shows that THP-1 cells are not adhered to the plastic bottom of the well, but rather to the HUVECs surface.

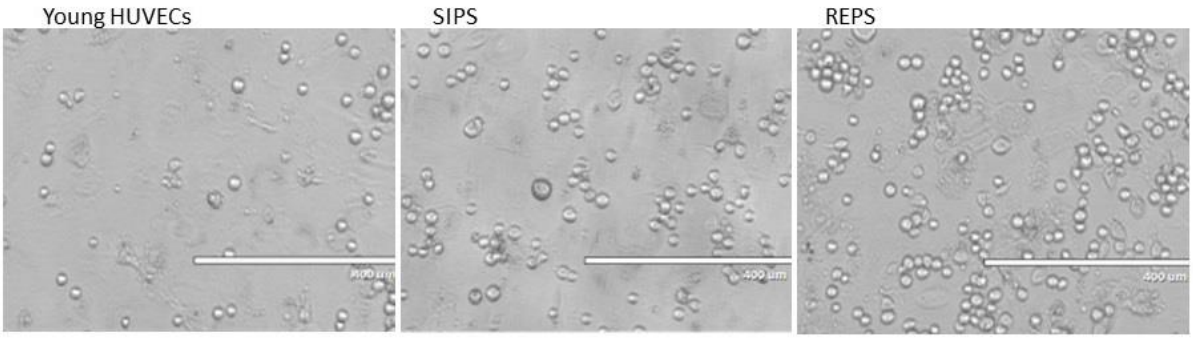

Figure 6-8: Adhesion of monocytes (THP-1) to HUVECs monolayer.

Either untreated (control), SIPS or REPS HUVECs were treated with vehicle or TNFa. Following washing, bound THP-1 cells were quantified by microscopy and cell counting. The bars show the size of 400 µm.

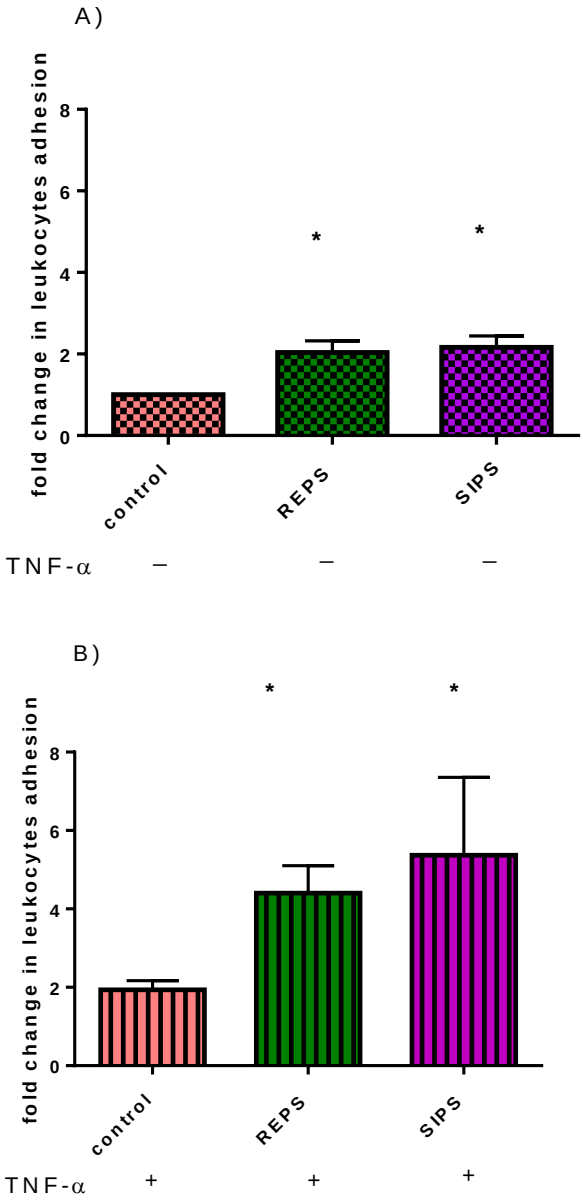

Figure 6-9: Increased adhesion of THP-1 cells to senescent HUVECs.

Adhesion assay was performed using REPS and SIPS HUVECs, in the absence (fig 6-9A) or presence of TNF-α (10 ng/ml for 12 hr) (fig 6-9B) in a 96 well plate. Data were normalised against control (young) and expressed as fold change. Values are mean (+SD) of 4 independent experiments p*<0.05.

6.3.2.2 Increased adherence of monocytes to senescent HUVECs under flow

In order to better mimic the conditions of *in vivo* adhesion, a circulating adhesion assay was performed. Labelled THP-1 cells were allowed to flow over a monolayer of HUVECs in a flow chamber coupled with a camera and Zeiss microscope (see section 2.7.2 for

experimental protocol). The temperature was set at 37°C. In order to minimise the activation of THP-1 cells during the circulation, tubes length were kept to a minimum. HUVECs were observed for 40 minutes. A video of rolling THP-1 cells was recorded every 10 minutes. Adhered THP-1 cells were counted and analysed relative to the control. This assay was performed in the presence or absence of TNF-α at the same concentration and duration of time as for the other experiments (10 ng/ml).

There was a significant increase in adhesion of THP-1 cells observed at every time point in both SIPS and REPS, except at time point "0" of REPS (fig 6-10B). This effect was only observed for TNF-α treated HUVECs. Non-TNF-α treated HUVECs showed no difference in adhesion of circulating THP-1 cells compared to control (young HUVECs) (fig 6-10A).

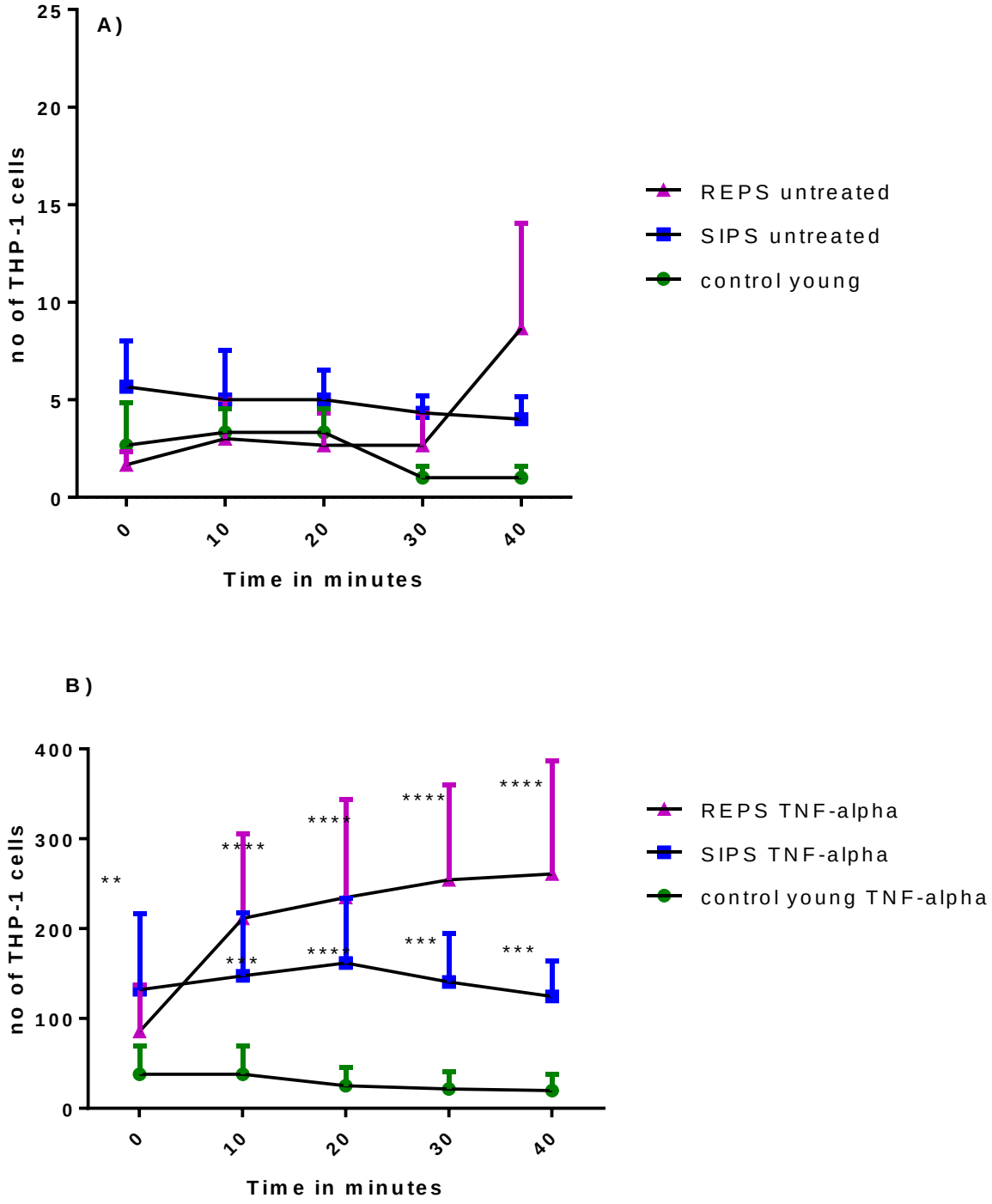

Figure 6-10: Senescent HUVECs promote leukocyte adhesion in a circulating THP-1 adhesion assay.

THP-1 cells were circulated over a HUVEC monolayer at a rate of 4-5 dynes/sec in a flow chamber. Labelled THP-1 cells were circulating over young, SIPS or REPS HUVECs monolayers, treated with (fig 6-10B) or without (fig 6-10A) TNF-α overnight. Videos were taken every 10 minutes and analysed for the number of adhered THP-1 cells. Values are mean (SEM) of n=3 independent experiments. P**<0.01, P***<0.001 and P****<0.0001.

6.3.3 Gene expression changes for adhesion molecules in senescent HUVECs

6.3.3.1 Validation of primers

Results in this chapter showed increased monocyte adhesion to senescent HUVECs. SIPS and REPS SASP characterisation in Chapter 5 and here did not identify pro-inflammatory factors. Therefore, expression of adhesion molecules within senescent cells was suggested. Four candidate adhesion genes were selected based on literature (Yanaka, Honma et al. 2011b, Mun, Boo 2010) and their primers were designed and tested in qPCR. The melting curve suggested that the specificity of all the primers that has been designed was good. Each product demonstrated one specific melting temperature (Fig 6-11). There was no primer dimer formation for any of the primers designed for genes of interest or housekeeper genes.

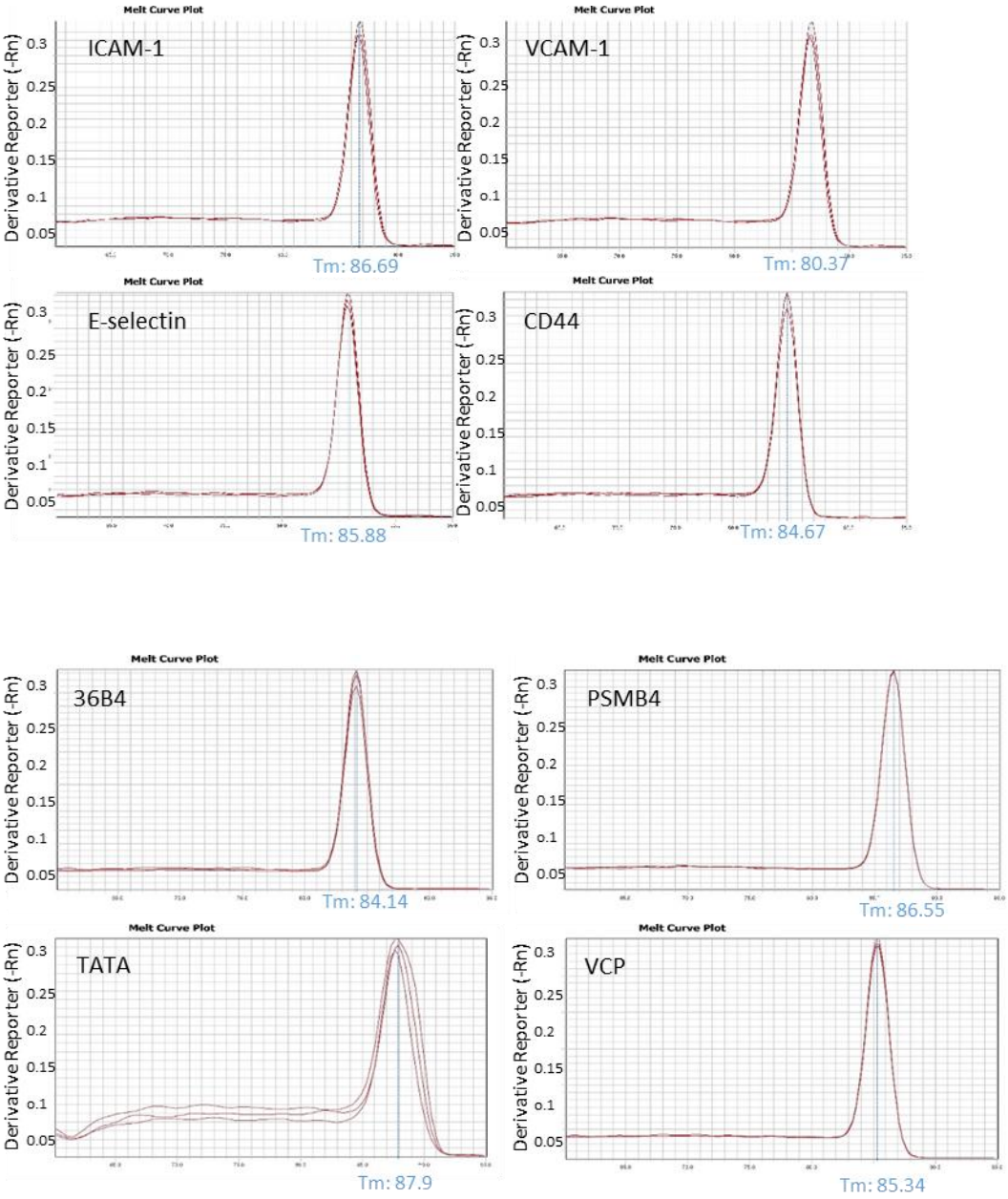

Figure 6-11: Melt curve for the qPCR products.

Melt curves demonstrate that all pcr products have specific melting temperature. Melting temperature (Tm) is shown for each primer used. There is a single peak amplified which shows no non-specific amplification.

6.3.3.1.1 qPCR standard curves

Standard curves for adhesion genes were constructed in-order to find the efficiency and the right input amount of the transcript, for the gene of interest. In this regard, pooled

cDNA from REPS and SIPS HUVECs, treated with and without TNF-α was analysed. Nine concentrations of pooled cDNA were added from 0 to 40 ng/µl.

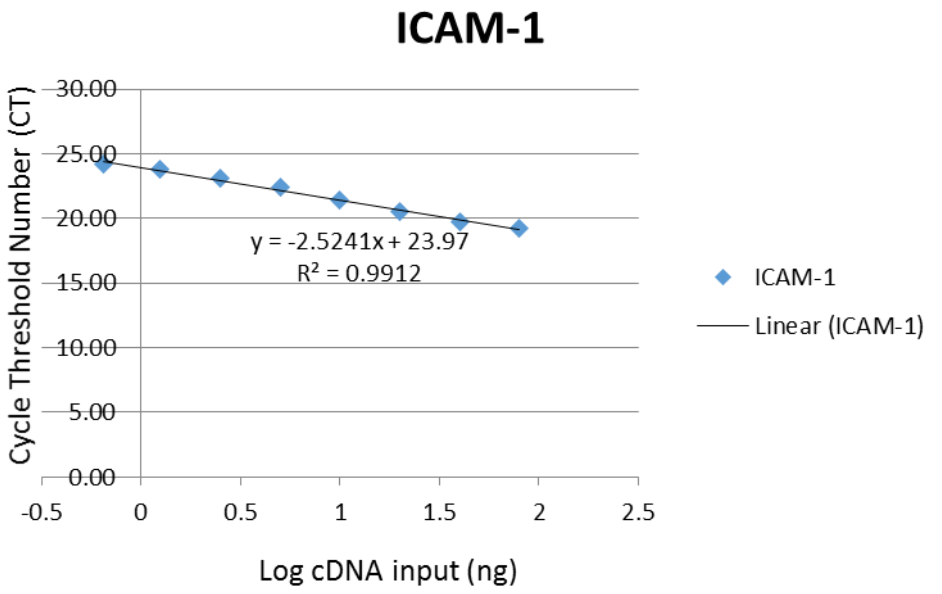

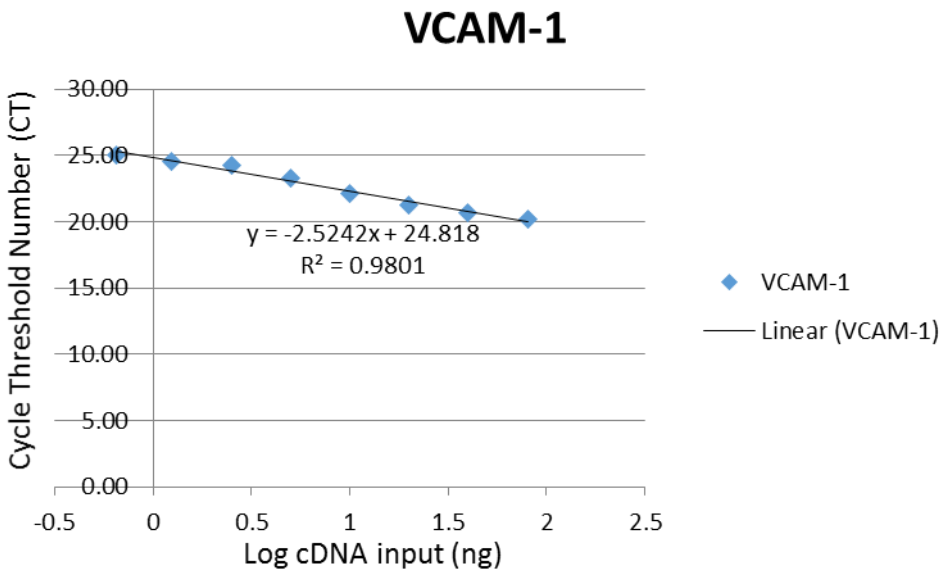

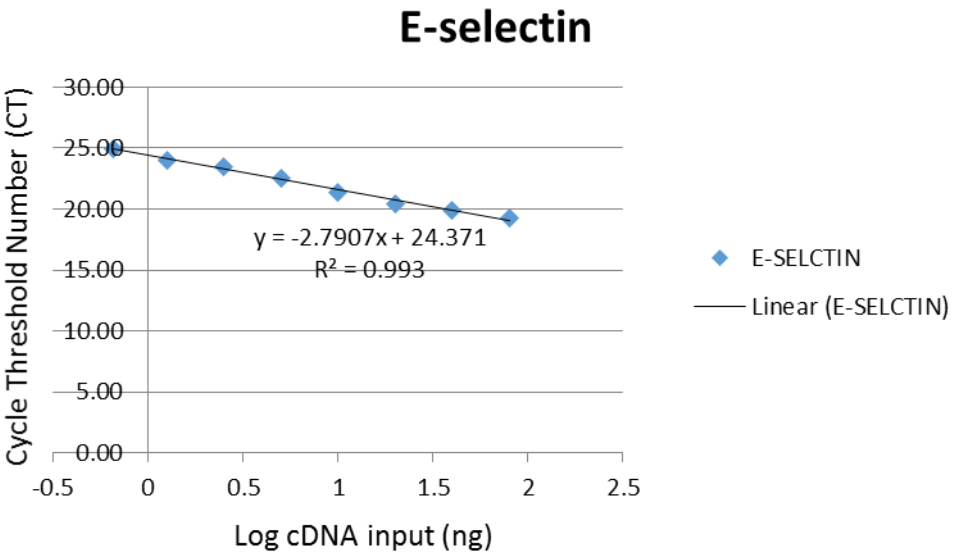

Figure 6-12: Standard curves for adhesion molecule genes.

mRNA was extracted from control (young), SIPS and REPS HUVECs. cDNA was reverse transcribed and the cDNA from all the samples pooled. A standard curve was constructed from the pooled cDNA. The range of template input was 0 to 40 ng. Values represent the mean of 3 replicates in single experiment.

6.3.3.1.2 Housekeeper gene validation

Several genes have been used as housekeeping genes and choosing an appropriate reference gene is important for accurate quantitative RNA expression in real time RT-PCR techniques. Ideally, the expression levels of reference genes should remain constant under different experimental conditions. Previously when mRNA gene expression analysis was performed, in order to select the best housekeeper gene in the experiment, a screen of house keeper genes was performed. Multiple housekeeper genes were analysed in the SIPS, REPS and young HUVECs. The best housekeeper gene was selected based on the raw qPCR data i-e CT values. Later, a literature search suggested the requirement of performing the screen for housekeeper genes, using available online tools (algorithms). Glyceraldehyde 3 phosphate dehydrogenase (GAPDH) has been recommend using as a reference gene for quantitative mRNA analysis in studying the cellular senescence of human diploid fibroblasts (Zainuddin, Chua et al. 2010). GAPDH has also been found to induce cancer cell senescence and shortens telomere length through inhibition of telomerase activity (Nicholls, Pinto et al. 2012). Together with this, according to Dheda *et al* the use of inappropriate reference gene for real-time reverse transcription PCR data

normalization can result in an incorrect conclusion of a biological effect (Dheda, Huggett et al. 2005). Therefore, it was highly desirable that the suitability of GAPDH and other selected genes as housekeeping genes was properly validated for each experiment, that is confirmation that their expression was unaffected by different experimental conditions in REPS, SIPS and young HUVECs. Vandesompele *et al* performed extensive research and included a broader range of algorithms and methods for validation of reference genes on using previously used d ata. They did not find large differences in the gene rankings by applying different tools, apart from minor shifts. They recommended the use of at least one of the methods for reference gene validation (Vandesompele, Kubista et al 2009)

In this thesis, the algorithm NormFinder was used as an add-in macro in the Microsoft Excel spreadsheet for gene ranking. The best housekeeper gene in senescent HUVECs not treated with TNF-α, determined by NormFinder analysis, was GAPDH; whilst the best combination of housekeeper genes was 36B4 and VCP (table 6-1). The best housekeeper gene for TNF-α treated HUVECs using NormFinder was TATA binding protein and the combination of reference genes was PSMB4 and TATA binding protein (table 6-2).

Gene name	Stability value
B2M	0.231
36B4	0.168
B-actin	0.191
PSMB4	0.274
GAPDH	0.141
VCP	0.149
TATA	0.168
B-Tubilin	0.298

Best gene	GAPDH
Stability value	0.141
Best combination of two genes	36B4 and VCP
Stability value for best combination of two genes	0.105

Table 6-1: NormFinder analysis representing the best reference gene and the combination of best reference genes in REPS and SIPS.

HUVECs in the absence of TNF-α. The lowest stability value is used to determine the most suitable gene and represent lowest variation under experimental conditions.

Gene name	Stability value
B2M	0.149
36B4	0.155
B-actin	0.134
PSMB4	0.146
GAPDH	0.175
VCP	0.243
TATA	0.106
B-Tubilin	0.295

Best gene	TATA
Stability value	0.106
Best combination of two genes	PSMB4 and TATA
Stability value for best combination of two genes	0.084

Table 6-2: Norm finder analysis representing the best reference gene and combination of best reference genes in REPS and SIPS.

HUVECs treated with TNF-α (10 ng/ml for 6 h). The lowest stability value is used to determine the most suitable gene and represent lowest variation under experimental conditions.

6.3.3.2 Identification of adhesion genes in senescent HUVECs

In an approach towards identifying the genes that are responsible for increased monocytic adhesion in replicative and stress-induced senescent HUVECs, microarray gene expression data were analysed. Adhesion genes were expressed by SIPS and REPS HUVECs.

In order to determine the pro-inflammatory genes involved in the pro-inflammatory behaviour associated with SIPS and REPS HUVECs 4 pro-inflammatory genes, ICAM-1, VCAM-1, E-selectin and CD44 were analysed using RT-PCR. Adhesion genes expression was observed both in the presence and absence of TNF-α. A time course was performed to select the time point for maximum adhesion gene expression following TNF-α. The maximum gene expression was observed at 12 hr for all 3 adhesion genes (fig 6-13). Next maximum adhesion gene expression was observed by 3 hr for VCAM-1

and E-selectin, but not for ICAM-1. The 6hr time point was chosen for two reasons mainly: firstly, it was more practical to treat cells and then extract mRNA after 6hr for gene expression analysis in PCR. Secondly, the ideal time point for robust ICAM-1 expression was 6 hr. Therefore, the 6 hrs time point was selected.

Analysis of the four adhesion molecule genes in senescent HUVECs was performed using qPCR in the presence (fig 6-14) and absence of TNF-α (fig 6-15). ICAM-1 and VCAM-1 expression was not different from control in senescent HUVECs exposed to TNF-α or not (fig 6-14 A, B and fig 6-15 A, B). Expression of E-selectin was not affected in REPS HUVECs (fig 6-14C and fig 6-15C) but was significantly increased (mean 3 folds, $P<0.05$) in SIPS HUVECs compare to control (young) cells (fig 6-14C). CD44 mRNA gene expression was upregulated two folds in TNF-α untreated (fig 6-14D) and 7 folds in TNF-α treated (fig 6-15D) REPS HUVECs. Both of these changes in CD44 expression reached statistical significance ($P<0.01$).

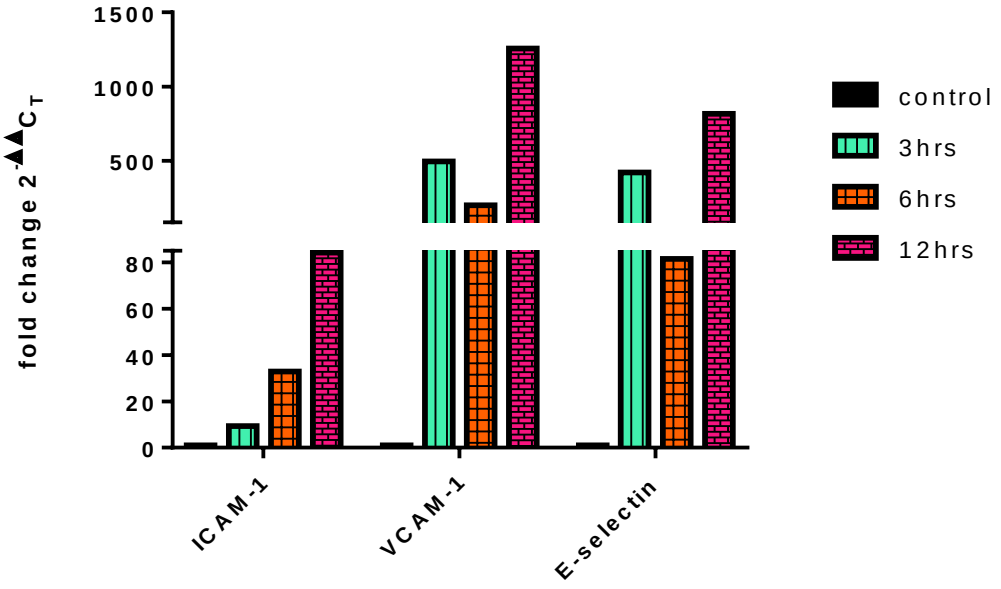

Figure 6-13: Time course for adhesion gene expression in TNF-α treated HUVECs.

Young HUVECs were treated with TNF-α at a concentration of 10 ng/ml, for different time points and mRNA extracted. Graph represents qPCR expression of all three adhesion genes at four different time points as fold change compared to time 0 control.

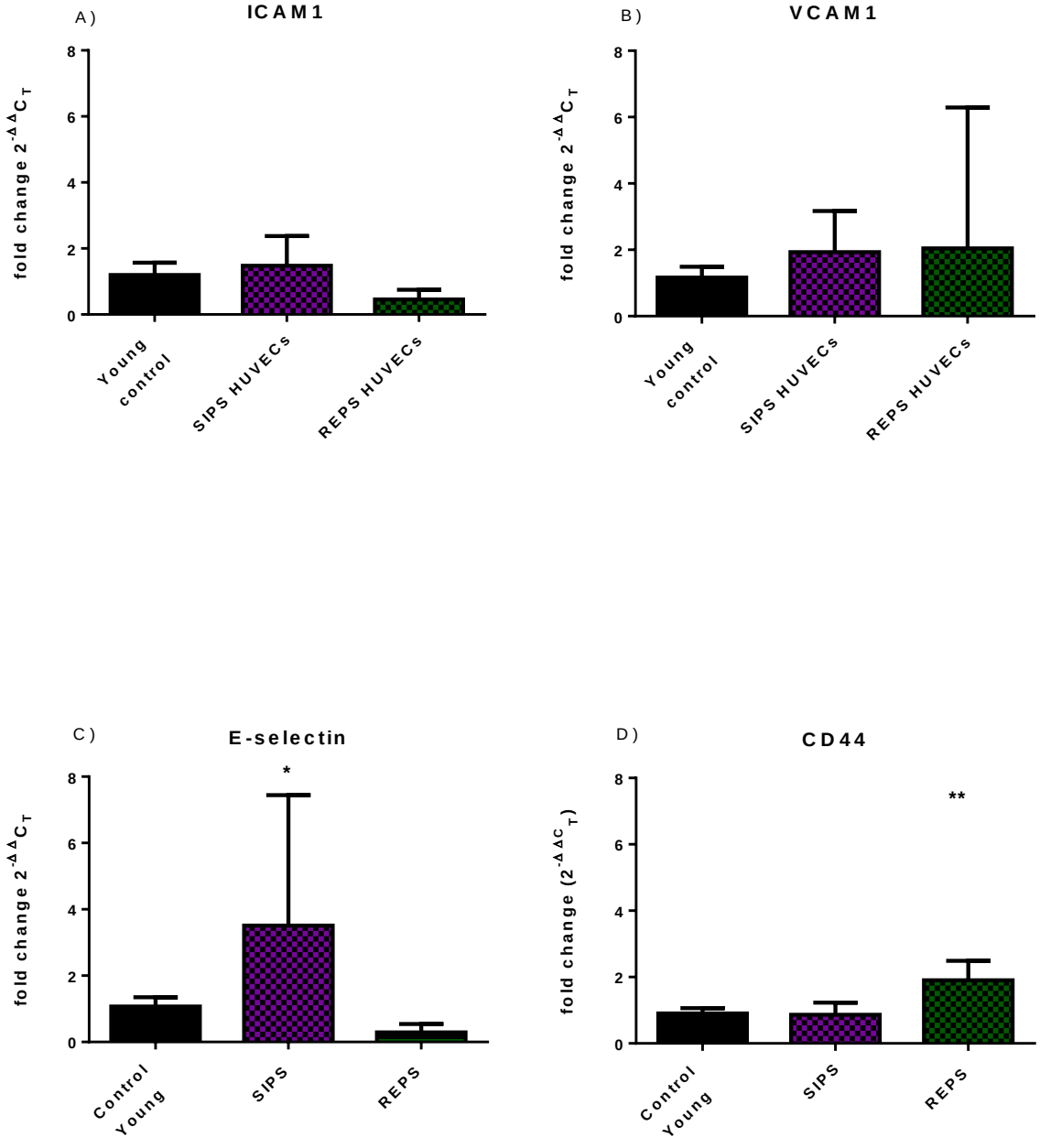

Figure 6-14 Adhesion genes expression in untreated SIPS and REPS HUVECs.

qPCR analysis of adhesion genes, figure showing expression of mRNA (A) ICAM-1, (B) VCAM-1, (C) E-selectin and (D) CD44 in SIPS and REPS HUVECs. Data were normalised against control (young) and expressed as fold change. Values are mean of (SEM) of n=6 independent experiments. P*<0.05 and P**<0.01.

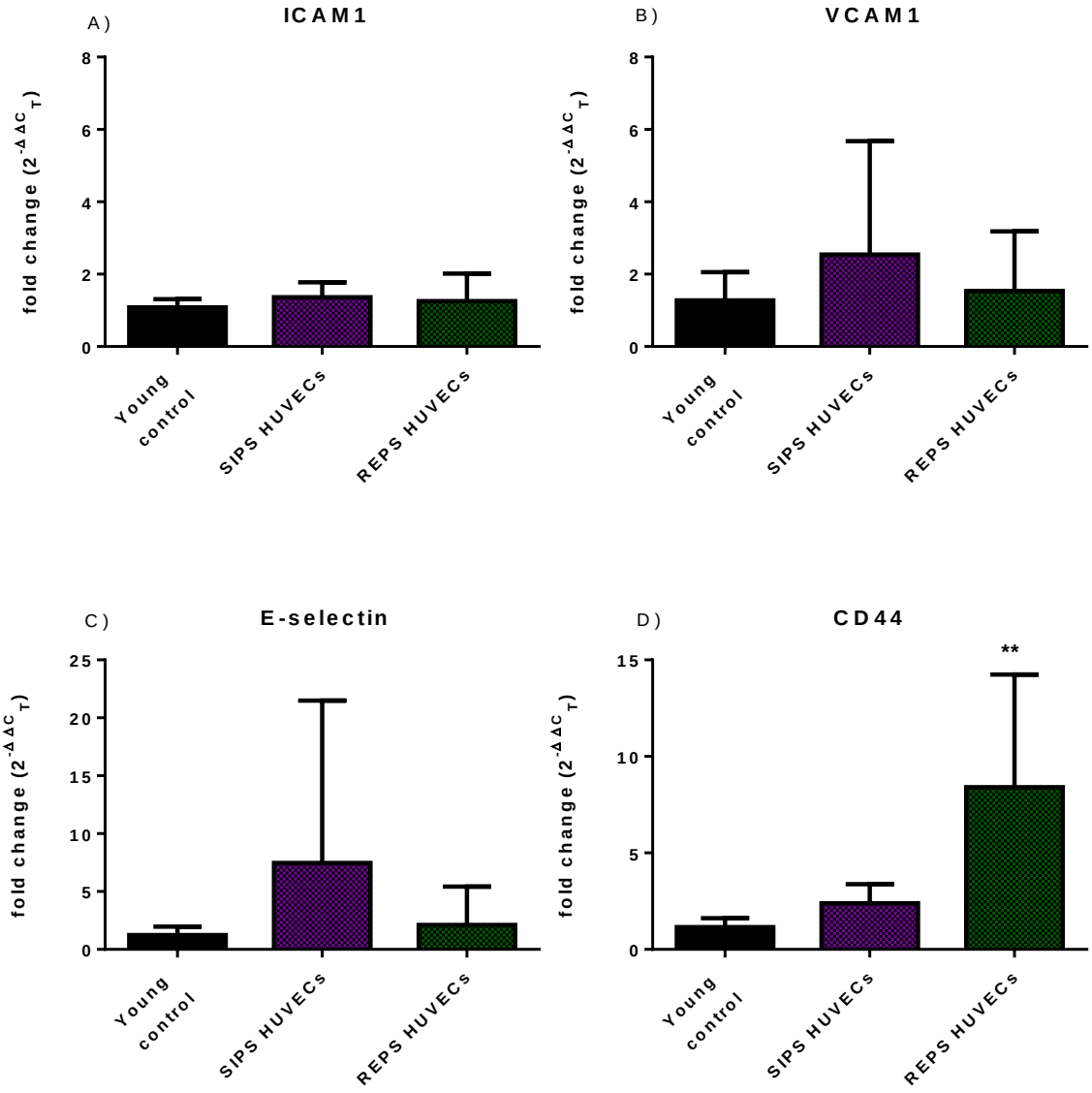

Figure 6-15: Adhesion genes expression in TNF-α treated SIPS and REPS HUVECs.

qPCR analysis of adhesion genes, figure showing mRNA expression of (A) ICAM-1, (B) VCAM-1, (C) E-selectin and (D) CD44 in SIPS and REPS HUVECs treated with TNF-α (10 ng/ml for 6hr). Data were normalised against control (young) and expressed as fold change. Values are mean of (SEM) of n=6 independent experiments. P**<0.01.

6.3.3.3 CD44 is upregulated in replicative senescent HUVECs

CD44 was chosen for further validation for protein expression in senescent HUVECs (REPS and SIPS) in presence and absence of TNF-α. Cell lysates from senescent HUVECs (REPS and SIPS) were obtained through either scraping the monolayer and then suspending in lysis buffer or trypsinizing first and then suspending the cell pellet in

lysis buffer. Samples were analysed by SDS-PAGE (see methods section 2.4.2). Following blotting a rabbit monoclonal antibody against CD44 protein was used.

CD44 expression was significantly increased in REPS HUVECs with or without TNF-α pre-treatment (fig 6-16a).

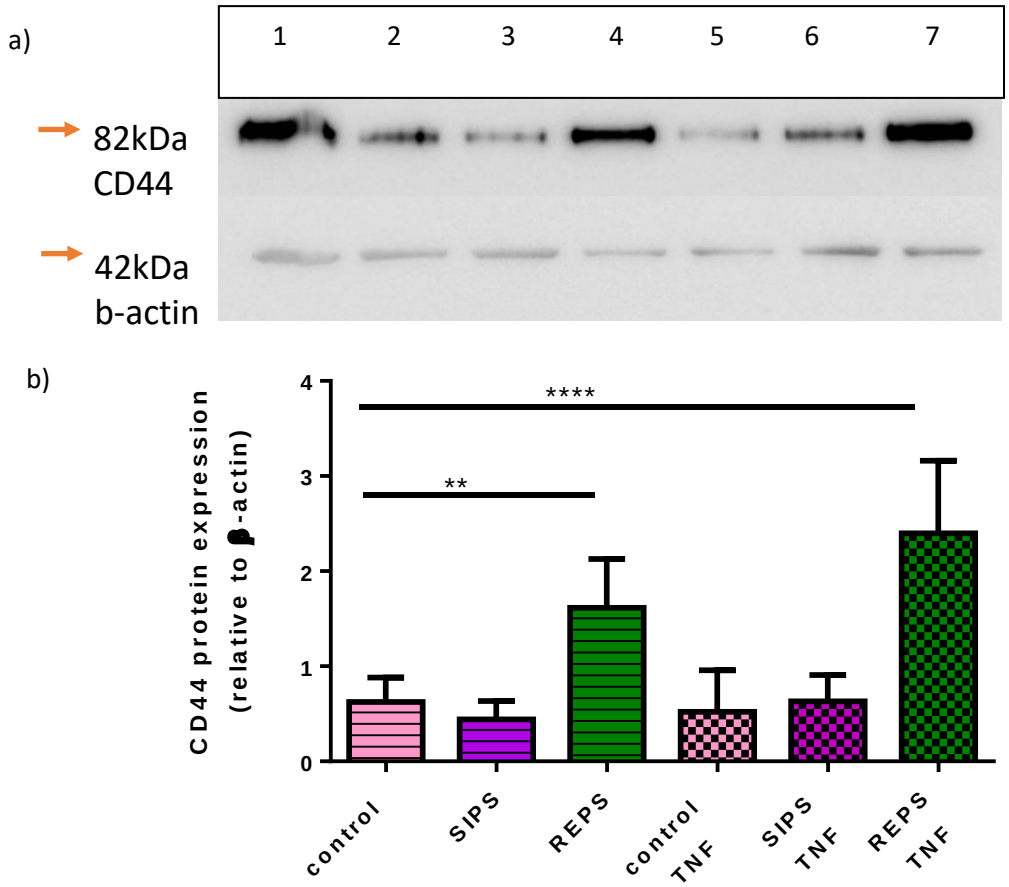

Figure 6-16. Increase in adhesion molecule CD44 is associated with REPS HUVECs.

(a) Image showing expression of CD44 in REPS (lane 4, 7) and SIPS (lane 3, 6) and positive control (far left lane) was HeLa cell lysate. Lane 2 and 5 are control cells. Semi quantitation of CD44 protein was made relative to β-actin (b). Values are mean (+SEM) of n=5 independent experiments. P**<0.01, P****<0.0001

6.4 Discussion

Cellular senescence helps to supress cancer by arresting cell growth in proliferating cells (Beausejour, Krtolica et al. 2003). However senescent cells can also secrete a variety of

proteins collectively called SASP. SASP has a different composition in different types of cells. SASP is formed only in senescent cells that exhibit a persistent DNA damage response (DDR), hence SASP is a result of genotoxic stress (Coppe, Patil et al. 2008b). Therefore, SASP requires DDR proteins, for example, ATM, CHK2 and NBS1. While cell cycle arrest proteins P53 and pRb do not guarantee the formation of SASP (refs). IL-6 and IL-8 are the common factors observed in SASP (Hampel, Fortschegger et al. 2006a). A high dose radiation in human diploid fibroblasts increased IL-6 secretion 5 to 6 folds. ATM depletion using a lentivirus, prevented this increased secretion of IL-6 (Rodier, Coppe et al. 2009). Ectopic expression of $p16^{INK4a}$, a common senescent biomarker induced senescence in W1-38 cells, but it failed to induce secretion of SASP components (Coppe, Rodier et al. 2011). SASP has a different composition and physiological function in different types of cells and senescence stimulus (Coppe, Patil et al. 2008b).

The experiments described here did not confirm that senescent HUVECs released pro-inflammatory factors, because the conditioned media obtained from SIPS and REPS HUVECs failed to increase the adhesion of monocytes in the adhesion assay, while REPS HDFs were able to enhance the adhesion of monocytes.

6.4.1 Adhesion of monocytes to senescent HUVECs

The proteomics data for SASP characterisation in Chapter 5 did not produce a protein signature related to inflammation. Therefore, it was hypothesised that the senescent endothelial cells might share a different physiology than young cells, which make them pro-inflammatory. Irradiation-induced premature senescent human coronary artery endothelial cells (HCAEC) resulted in increased adhesion of monocytes in the adhesion assay (Lowe, Raj 2014b). In this thesis, enhanced adhesion of monocytes to static cultures of senescent HUVECs was found in both the presence and absence of TNF-α. Similarly, others have also found increased monocytic adhesion to REPS HUVECs (Mun, Boo 2010). Both of these studies utilised conventional static cell cultures. An adhesion assay was then performed under flow conditions, more closely mimicking *in vivo*. Senescent HUVECs showed increased adhesion of monocytes but only in the presence of TNF-α. However, this experiment is different to *in vivo* conditions. Limitations of the model

include the absence of other blood components and chemoattractants that might alter the adhesion of monocytes to the endothelial cells compared to i*n vitro*. Continuous superfusion of the cells/tissue may also wash away some chemoattractant. However, monocyte adhesion increased reproducibly and robustly even with continual superfusion. If there were high levels of chemoattractant washout, adhesion would be expected to decrease, or at least remain constant, as chemoattractant levels decreased. In the case of SIPS, after 20 minutes (fig 6-10B), the adhesion of monocytes started to decrease. Kunkil *et al* demonstrate that activation of rolling leucocytes by chemoattractant can be gradual *in vivo*, the gradual activation response may be due to low local chemoattractant concentrations on the vascular endothelium in combination with adhesion molecule-mediated activation (Kunkel, Dunne et al. 2000b). In REPS it can be hypothesised that together with surface expression of adhesion molecules, there might be release of chemoattractant that caused the enhanced adhesion of monocytes with time, although we were unable to measure any cytokines in the proteomics experiments. One suggestion, for future development, would be to enhance SASP by treatment of HUVECs with a very low dose of TNF-α.

6.4.2 Housekeeper gene validation

The sensitivity, resolution and high speed of real time PCR makes it the standard and most widely used method for expression analysis of a limited number of genes. The availability of array based devices has made it possible to analyse a greater number of genes and samples using PCR. One of the limitations of the method could be the non-biological variation caused by a number of factors, for example template input quantity, template quality and enzymatic reactions. It is highly recommended to normalise to remove these variations in order to get the true results. There are certain recommended methods and together with algorithms available that can minimise the non-biological variation (Vandesompele, Kubista et al 2009). The best method of normalisation is the use of an internal reference gene. The use of reference gene is the gold standard, because reference genes are an internal control, expressed by the same cells, and affected in the same way during the experimental stages as the genes of interest. For example, during cell treatments, enzymatic treatment during mRNA extraction, storage, reverse

transcription and even their expression analysis method that is using pcr (Vandesompele, Kubista et al 2009).

Spiegelaere *et al* validated different reference genes in RT-qPCR while comparing different available software packages, including GeNorm, NormFinder and BestKeeper. They used qPCR efficiency corrected relative values versus non-corrected values. They found slight differences in the final ranking of genes, while the efficiency varied within the range of 90-110% but did not have a significant effect on the final ranking of genes.

Further to this, they also found that the ranking of the genes by the original Excel based NormFinder add-in were similar compared to the NormFinder algorithm within the R-based NormqPCR package and within the NormFinder for R script. NormFinder was suggested as the best tool for the selection of reference genes when there are different sample groups to be assessed, because it accounts for intra- and inter-group variation (De Spiegelaere, Dern-Wieloch et al. 2015). NormFinder was applied in this thesis. Reference genes for 3 groups i.e. SIPS, REPS and young HUVECS showed different combination of genes stability under TNF-α treated and untreated conditions. This confirms that different housekeeper genes will be required for different experimental condition even with same cell type (table 6-1, 2).

6.4.3 Candidate genes for mediating adhesion of monocytes to senescent HUVECs

As the experiments here did not provide much evidence of the SASP release from senescent HUVECs, the hypothesis of the presence of surface molecules on senescent HUVECs was tested. From the positive pro-inflammatory effect of senescent HUVECs in the adhesion assay, the presence of some pro-inflammatory adhesion proteins was hypothesised. A number of pro-inflammatory genes were screened using RT-PCR. The present study identified the “senescence- induced cell adhesion genes” whose expression was upregulated in senescent cells compared with younger cells, in the presence and absence of TNF-α. Among these genes, ICAM-1, VCAM-1, E-selectin and CD44, well-known cell adhesion molecules, were chosen for further studies. These adhesion genes were assumed to be the potential candidate genes, responsible for the enhanced monocyte adhesion to senescent endothelial cells, in both adhesion assays (static and circulating).

The normal physiological function of endothelium is the manifestation of vasodilatation, coagulation, secretion of certain mediators, inflammation and immune response in certain cases of microbial invasion (Drexler 1997). Apart from these functions endothelium also functions as a physical barrier between the blood and the subendothelial layers. While in pathophysiological conditions endothelium can be activated, become inflammatory and express adhesion molecules. This will result in recruitment of inflammatory cells and eventually formation of atherosclerotic lesions (Rao, Yang et al. 2007). Similarly, atherosclerosis is the gradual detrimental process in artery vessels, starting with the endothelial cell injury/inflammation, followed by inflammatory cells migration, then lipid infiltration, formation of the plaque with smooth muscle cells growth and finally the rupture of the plaque causing cardiovascular complications (Rodriguez, Mago et al. 2009). There are certain risk factors associated with cardiovascular complications. One of the most important risk factors is ageing (Wang, J. C., Bennett 2012). The mechanism for the effect of ageing on atherosclerosis is not fully understood yet, but identification of endothelial cell senescence in atherosclerotic lesions and elderly people's vessels, confirms the potential role of endothelial cell senescence in cardiovascular complications and ageing (Minamino, Miyauchi et al. 2002b). This is supported by the research conducted by Matsushita *et al*, who found decreased expression of eNOS and increased of monocyte binding to replicative senescent endothelial cells. While an increase in eNOS and NO activity was observed by stable expression of hTERT (Matsushita, Chang et al. 2001). Using a promyelocytic cell line (HL-60), having the ability to adhere in an E-selectin dependent manner to activated endothelial cells, adhesion in response to TNF-α increased by 10 folds to Human intestinal microvascular endothelial cells (HIMEC). This effect was blocked by 40% when an antibody was used against E-selectin (Haraldsen, Kvale et al. 1996).

CD44 undergoes splice variation in 4 different splice variants. Variant 4 is the most common and highly expressed in endothelial cells (Mun, Boo 2010). The results in this thesis are consistent with research conducted by Donna and Kenneth. They found CD44 upregulation in radiation induced human coronary artery endothelial cells (Lowe, Raj 2014a). Therefore, it can be hypothesised that, senescent endothelial cells expresse specific adhesion molecules, depending on the type of senescence stimulus (E-selectin in SIPS and CD44 in REPS *In Vitro*). Which is responsible for the potential pro-

inflammatory microenvironment, whether this plays a role in the initiation of atherosclerosis remains to be seen. An antibody used against VCAM-1 in an atherogenic mice model showed an anti-atherogenic effect (Park, Ryu et al. 2013).

6.4.4 Further identification of known adhesion molecules

Initiation of inflammatory responses in vascular endothelial cells, for example, adhesion of circulating monocytes, is induced by lymphokines and monokines, particularly TNF *in vitro* (Bevilacqua, Pober et al. 1984). According to Bevilacqua et al soluble mediators generated during inflammatory responses can alter the endothelial cells functional surface properties by directly acting on them. This results into increased endothelial-leukocyte adhesion. In this regard, IL-1 treatment of endothelial cells resulted into increased adhesion of human polymorphonuclear leukocytes and monocytes (Bevilacqua, Pober et al. 1985). Increased expression of adhesion molecules in response to IL-1 is concentration and time dependent, reaching a maximum expression at 4-6hr of activation and decline after 48 hrs (Bevilacqua, Pober et al. 1984). VCAM-1 and E-selectin are not expressed by unstimulated human intestinal microvascular endothelial cells (HIMEC). In response to LPS, TNF-α and IL-1β, E-selectin expression increased reaching a maximum at 4-6 hr and was stable for 24 h. The same pattern was observed in HUVECs (Haraldsen, Kvale et al. 1996a). CCL2 (Daly, Rollins 2003), ITGB3, ITGAV (Shimizu, Irani et al. 1995), and ITGB1 (Pilarski, Yacyshyn et al. 1991) are adhesion molecules. Their mRNA was identified in senescent HUVECs. In addition to this C1orf38, CEACAM1, COL4A6, DCBLD2, LPXN are adhesion responsive genes identified only in REPS HUVECs (Mun, Boo 2010). Investigation of these genes in REPS and SIPS can identify adhesion molecules other than previously identified (in this thesis), responsible for increased monocytic adhesion.

6.4.5 Effect of SASP on senescence

In experiments designed to investigate the effect of SASP on the growth of HUVECs, the ideal situation would be to have a control where REPS HUVECs could be grown in culture well inserts, but the behaviour of REPS HUVECs in tissue culture is not the same

as the REPS HDFs. In the experiment REPS cells were required to be grown in the inserts for 5-6 weeks and provide a continuous SASP. Compared to REPS HDFs, REPS HUVECs can only be grown on a plastic or glass surface for a few days, before they start to die and floats off in the media. However, senescent HDFs grow in tissue culture for a longer duration of time i.e. months to years. There was some cell death observed in the REPS HDFs, but replacing the old growth medium washed away those dead HDFs. HUVECs growth curves showed a different pattern than the HDFs. HUVECs tend to grow with an increase CPD but soon reach a plateau and started to decline. For HDFs an increase in CPDs was observed throughout all the passages. The reason behind the decline in growth of HUVECs might not be that they become senescent but rather, possibly be the gap in between the two passages. HUVECs and HDFs were harvested each time on a fixed time twice a week, independent of the confluency of the two cells types. As HDFs are big cells and grow quickly becoming confluent in 3 to 4 days. While HUVECs grow more slowly and require longer (4 to 5 days after harvesting) to become confluent. The reduced cell growth caused HUVECs to show a decline in the growth, which became more apparent in the later passages in the growth curves. In future experiments cells showed not be harvested at a fixed time point (which was practised in the current experiments), rather cells should let get confluent. Once the cells are 80% confluent, then they would be harvested and the process repeated for the same number of PDs as performed in growth curves.

6.5 Conclusion

The findings presented here confirm that senescent HUVECs, whether SIPS or REPS, did not secrete a pro-inflammatory SASP as there was no significant increase (or decrease) in the adhesion of monocytes in the presence of SASP. On the other hand, there was enhanced adhesion of monocytes to HUVECs treated with conditioned media from senescent HDFs in the presence and absence of TNF-α. Moreover, senescent HDFs expressed a SASP that caused a change in the growth rate of co-cultured HDFs and HUVECs.

However, results presented here confirm that SIPS and REPS HUVECs express a pro-inflammatory phenotype probably due to the presence of increased expression of the

adhesion molecules E-selectin and CD44 respectively. Further validation of expression of E-selectin protein is warranted in SIPS HUVECs.

Chapter 7

7 Discussion and future work

7.1 Synopsis of findings

This thesis aimed to characterise senescence in HUVECs induced by replicative and oxidative stress (Chapter 3) in order to develop an understanding of possible biomarkers and to utilise these cells to study pro- or anti-inflammatory properties. Firstly, gene expression analysis of senescent HUVECs was performed using transcriptomics (Chapter 4). Secreted proteins were the primary focus with a view to use for the identification of senescent HUVECs in culture.

Characterisation of protein/peptide components of the secretome (SASP) from REPS and SIPS HUVECs was achieved using proteomics analysis (Chapter 5). There was no evidence that SASP from senescent HUVECS was pro-inflammatory. The hypothesis that the senescent HUVECs might present the pro-inflammatory phenotype by cell surface adhesion molecules expression was tested. Surface expression of CD44 and E-selectin was found to be upregulated by REPS and SIPS respectively (Chapter 5). In line with these findings on adhesion molecule expression, induction of senescence resulted in increased binding of leucocytes either under static culture or flow conditions (Chapter 6).

Future work is required for full understanding of SASP composition and the complexity of phenotype of senescent HUVECs on inflammation.

7.2 Is biologically active SASP induced in senescent HUVECs?

Cellular senescence is the process which stops the cell from dividing in response to stress in an attempt to stop the damage being transferred to next cell generation (Campisi, d'Adda di Fagagna 2007). Hence, cellular senescence is considered to be a protective mechanism. On the other hand, senescent cells also show a certain phenotype of morphological changes, gene expression changes and release of a group of proteins collectively called senescence associated secretory phenotype (SASP) (Krtolica, Campisi 2002). Depending on the cell type this SASP can be deleterious to the surrounding

microenvironment. Previous research has shown SASP from human dermal fibroblasts (HDFs) to be inflammatory in nature and promotes cell division (Coppe, Patil et al. 2008). In order to investigate whether a biologically active SASP is produced by senescent cells, firstly, the effect of conditioned media from senescent cells was investigated with respect to the growth of normal HDF and of autologous early passage HUVECs. Early passage cells (HUVECs and HDFs) were treated with media from senescent HDFs. Cultures. In-order to address nutrient deprivation this media was mixed with equal amount of fresh growth medium. HUVECs required a different growth medium to HDFs and therefore a control of HUVECs with equal amounts of HUVECs fresh growth medium and HDFs fresh growth medium was utilised. A decrease in cell growth was observed with HDF SASP treatment in both HDFs and HUVECs. This confirms two things, first that senescent HDFs produce SASP and second that the SASP produced by HDFs is biologically active having a negative effect on HDFs growth.

In the growth curves cells are maintained in culture for up to 5 weeks. Which require a continuous source of SASP. Conditioned media collection from REPS and SIPS HUVECs in culture was not possible. Senescent HUVECs in culture are not stable for longer, as they start to detach from the plastic ware and die. Therefore, only HDFs SASP was used.

Adhesion assay using SASP from HUVECs did not stimulate adhesion of monocytes, while HDFS SASP was able to show increase adhesion of monocytes in adhesion assay. Also proteomic characterisation of senescent HUVECs SASP did not identify pro-inflammatory factors. Therefore, it could be concluded that this thesis did not identify a biologically active SASP from senescent HUVECs in culture.

7.3 Does endothelial cell senescence represent a pro-inflammatory phenotype?

E-selectin belongs to the selectin family of cell surface glycoproteins (integrins) (Rahman, Kefer et al. 1998b). Each member of the integrin family plays a different role in leukocyte recruitment on endothelial surfaces. The role of E-selectin is to create a weak bond between leukocytes and activated endothelial cells (Blankenberg, Barbaux et al.

2003). Current results showed two different proteins involved in the pro-inflammatory phenotype of two types of senescent HUVECs, CD44 for REPS and E-selectin for SIPS. This is beneficial in the sense that it tells us what type of senescence is associated with HUVECs in tissue culture.

Importantly, binding of leucocytes to REPS or SIPS HUVECs was increased compared to young, control HUVECS (Chapter 6) in a static cell culture model, either in the presence or absence of TNF. However, under flow conditions adhesion of THP-1 cells to senescent HUVECs was observed only in the presence of TNF-α. Chang et al compared the expression of adhesion molecules, ICAM-1, VCAM-1 and E-selectin in young and senescent HUVECs in response to TNF-α. They found low or no increase in these molecules in senescent HUVECs compared to young HUVECs in response to TNF-α. Similar to our results this is probably a consequence of *in vitro* cultivation of cells in comprehensive growth medium. HUVECs treatment with angiogenic factors results in inhibition of adhesion molecules in response to TNF-α (Griffioen, Damen et al. 1996).

One of the ways in which these data on monocyte cell adhesion to senescent HUVECs might be explored further is in relation to ageing and cardiovascular disease. Age is the major risk factor for cardiovascular disease. In addition, inflammation and senescence have been linked at both the clinical and molecular levels (Coleman, Chang et al. 2013). In general, senescent cells have been described as pro-inflammatory based on their SASP (Khan, Awad et al. 2017).

Inflammatory adhesion molecules which are hallmark of atherosclerosis are upregulated in senescent endothelial cells in which senescence has been induced by different stimuli (Kunkel, Dunne et al. 2000), (Zhu, Yu et al. 2017),

7.4 Gene expression in REPS and SIPS

Senescence is the phenomenon of the inability of cells to enter the cell cycle irreversibly, despite possessing metabolic activity. Senescence is characterised by morphological changes. This is accompanied with changes in gene and protein profile (Kuilman,

Michaloglou et al. 2010). Cellular senescence occurs due to telomere erosion. Human senescent endothelial cells exhibit telomere erosion with age (Aviv, Khan et al. 2001). However, senescence depends mainly on two tumour suppressor pathways; p53 and $p16^{INK4a}$ regulators. In the absence of p53, cells continue to proliferate even with shorter telomeres (Shay, Wright et al. 1991). Replicative senescence is suggested to be a tumour suppressing process and many genes that are oncogenes and mutated in cancer are important for cellular senescence induction i.e. p53 (Campisi 1997). IPA analysis for differentially expressed genes in both REPS and SIPS highlighted cancer as the top disease and disorder affected. While TP53 was one of the top upstream regulators in REPS and SIPS. This strongly suggests the senescence mechanism.

In this thesis both REP and SIPS were induced in HUVECs under the appropriate conditions (Chapter 3) and these models used to study changes in gene expression and biological function.

Other researchers have found IL-6 and IL-8 elevation by senescent endothelial cells as well as ICAM-1 and E-selectin (Khan, Awad et al. 2017). A common biomarker of senescence is $P16^{INK4a}$ (Krishnamurthy, Torrice et al. 2004). Another biomarker is TNF-α. The current study showed down regulation of genes for aforementioned proteins in REPS and SIPS analysed by transcriptomics (see supplementary data on CD provided). The decrease in the pro-inflammatory markers by REPS and SIPS HUVECs suggests that cells may be releasing feedback signals to prevent a further pro-inflammatory environment (as cells also express pro-inflammatory molecules CD44 and E-selectin in REPS and SIPS respectively). There are certain other biomarkers for example, Dec1, DCR2, Ki-67, p15 (Collado, Gil et al. 2005b), certain other SASP components reviewed in (Freund, Orjalo et al. 2010), (Coppe, Desprez et al. 2010). Despite being identified as SASP components in senescent cell biomarker studies, these genes were not identified in HUVECs transcriptomics and proteomics. There are other factors and genes that have been reported as related to senescence, such as ADAMST1, DKK1, PTHLH, IGFBP5 and SPARC which were identified in the HUVECs transcriptomics and proteomics analysis. Apart from IGFBP5 these gene products have not previously been associated with senescence of any cell type, particularly endothelial cells. Whether any of these

could be developed as biomarkers of the senescence process in endothelial cells remains to be tested.

Senescent cells are associated with condensation of chromatin material and formation of SAHF and increased epigenetic histone marks i-e H3K9me2/3. This SAHF formation promotes the decreased transcription of proliferation promoting genes. It has also been reported that loci for genes promoting proliferation are sequestered in the SAHF, while permitting transcription of only SASP secreting genes. HMGB2 is a transcription factor which promotes the transcription of SASP producing genes in fibroblasts (Aird, Iwasaki et al. 2016). In senescent HUVECs the SAHF formation might extend and spread to the whole genomic DNA with an exclusion of certain important genes for cell survival. This might result in less protein synthesis in senescent HUVECs compared to young cells. The other possible explanation in this regard could be that, senescence is the result of accumulation of damaged biomolecules beyond repair, which results in activation of the unfolded protein response in the endoplasmic reticulum (Matos, Gouveia et al. 2015). This might shut down protein synthesis in senescent cells. This could be investigated in the future in REPS and SIPS HUVECs compared to young cells. The endoplasmic stress response proteins for example, the three master regulators of unfolded protein response, Inositol Requiring 1 (IRE1), PKR-like ER kinase (PERK), and Activating Transcription Factor 6 (ATF6) could be investigated using Western blots. However, data presented in this thesis did not suggest that protein synthesis was reduced in either REPS or SIPS HUVECs. This was true for total cellular proteins and for proteins secreted into media as a result of PMA stimulation.

7.5 Investigation of CST1 as a biomarker of endothelial cell senescence

7.5.1 CST1

Cathepsins are cysteine proteinases that are expressed on the cell surface of metastatic cells (Turk, Stoka et al. 2012) that are involved in inducing an immune or inflammatory reaction in response to antigen invasion. Cystatins are cysteine proteinases inhibitors. Cystatins works as check and balance proteins for the normal function of cysteine proteinases. The expression of these enzymes might be related to invasion of metastatic

cells. The increased expression of CST1 in many cancers might be a protective mechanism to prevent metastatic cells from invasion into the normal tissues (Keppler 2006). In our experiments, following the primary analysis of transcriptomics data, CST1 was highly upregulated in RT-qPCR, but no protein expression was observed. This means that CST1 mRNA was expressed in REPS HUVECs but it was not translated into proteins. The high expression of CST1 mRNA could be the result of a positive feedback loop for the CST1 gene. As mRNA was not translated into cystatin SN protein perhaps the feedback was ongoing and the CST1 gene was stimulated with accumulation of CST1 mRNA.

miRNAs are small non-coding RNAs that regulate gene repression. They are single stranded and have the ability to anneal to specific target regions in mRNA transcript. miRNA can repress genes either by degrading mRNA or repressing mRNA translation (Browning, Bailey-Serres 2015). Cystatin SN protein was not identified in REPS HUVECs, despite more than 120 folds increases in mRNA levels. Therefore, miRNA with proposed specificity for CST1 could be investigated in REPS HUVECs, using qPCR.

Keppler et al found CST1 protein to be a senescent biomarker in human fibroblasts (IMR90 cell line). They used salivary gland as positive control for CST1 expression in immunochemistry experiments (Keppler, Zhang et al. 2011). Immunocytochemical detection for CST1 was attempted in this thesis but without success. A control; either salivary glands or cells in which CST1 is over expressed should be used for these experiments.

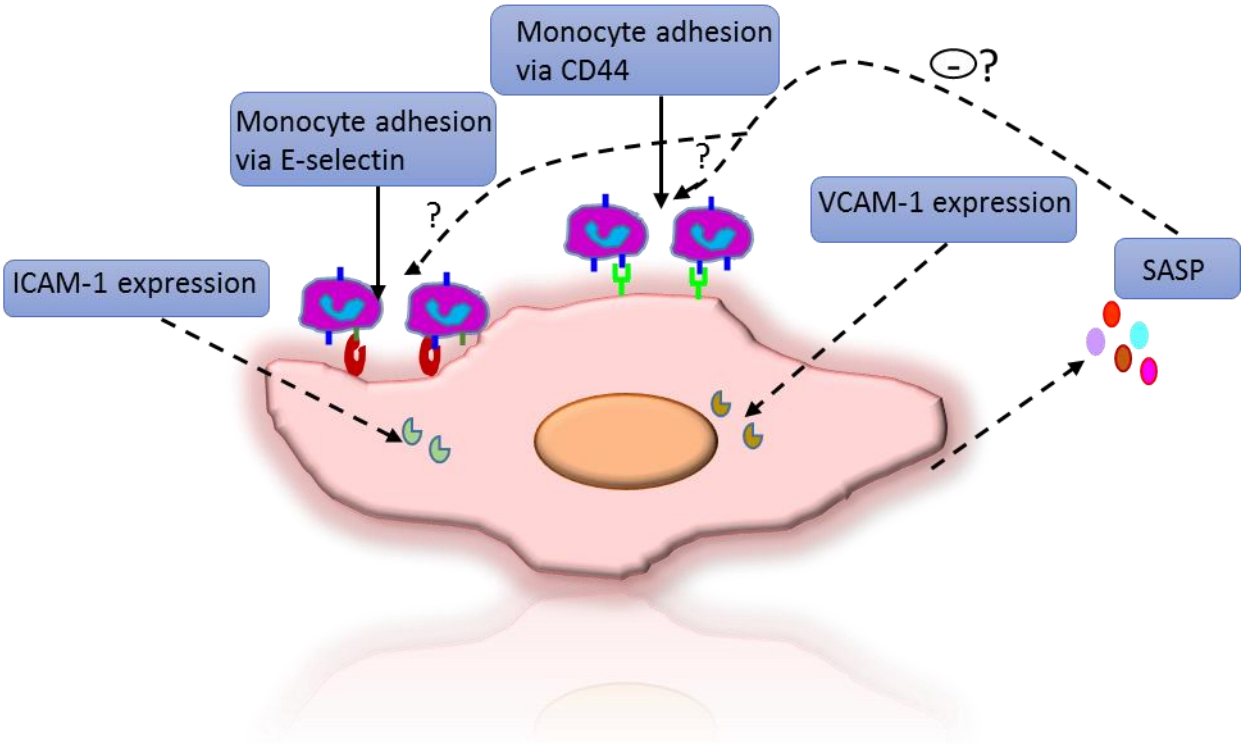

Figure 7-1: Proposed mechanism of monocyte adhesion to senescent endothelial cells.

When endothelial cells become senescent via either REPS or SIPS, they express adhesion molecules, CD44 and E-selectin respectively. There is also expression of ICAM-1 and VCAM-1. Senescent HUVECs represent pro-inflammatory SASP. However, no apparent evidence of pro-inflammatory SASP was observed. Endothelial cells present a pro-inflammatory behaviour and recruit immune cells. But the anti-inflammatory SASP might have a negative effect on immune cell adhesion. Immune cell recruitment is the initial step in the development of atherosclerosis. Solid arrows show the mechanism where the data support the mechanism. Dashed arrows show the proposed mechanism.

7.6 Limitations of experimental approaches

7.6.1 *In vitro* models

In order to understand the vessel wall properties in cardiovascular related diseases, endothelial cells in culture have been used as a relevant model (Onat, Brillon et al. 2011). The model used in the current study is *in vitro* (endothelial cells). This model can be used to identify and develop the mechanism(s) of senescence and its potential biomarkers in

tissue culture studies only. The mechanism of senescence is cell and stimulus specific. *In vivo* study in animal models or patients is required for the understanding of senescence mechanisms in the cardiovascular system for diagnostic and therapeutic purposes. *In vitro* models of senescence are subject to a single stressor. While in *in vivo*, cells experience multiples pressures i.e. mitotoxic, genotoxic and proteotoxic (Siegel, Amon 2012). Therefore an *in vivo* model is best for the understanding of molecular mechanisms associated with organismal ageing.

7.6.2 Knock out p16 in ApoE$^{-/-}$ mice and intravital microscopy

Intravital microscopy is the optical microscopy technique that enables the imaging of sub-cellular processes in animals at resolution that is comparable to cells in culture (Weigert, Sramkova et al. 2010). The INK-ATTAC mouse model, upon drug treatment targets and kills any p16 positive (senescent) cells (Baker, Wijshake et al. 2011). Atherosclerotic prone e.g. (Apo E$^{-/-}$) mice crossed into INK-ATTAC model could be considered for studies aiming to investigate the effect of senescent cell eradication on the development of atherosclerosis. The number and size of atherosclerotic plaques will be determined and compared to the control. Other cardiovascular functions for example, cardiac output could also be measured.

7.6.3 Investigation of proteomics and transcriptomics for better biomarker discovery

Biomarkers can be used for the diagnosis of disease and to measure the severity of a disease as well as the effectiveness of a treatment. Transcriptomics and proteomics have provided a new direction for disease understanding and may become a better option for the diagnostic and therapeutic monitoring of cardiovascular disease management (de Franciscis, Metzinger et al. 2016). Transcriptomics studies are important for the understanding of molecular mechanisms of a disease. Due to the existence of complex post-transcriptional processes such as transcript de/stabilization, translation, posttranslational modifications and protein degradation which determine and modulate the quality and quantity of expressed proteins, transcription is not co-ordinately associated with translation resulting in a limited correlation between mRNA levels and protein abundance (Waters, Pounds et al. 2006). The differences in protein concentrations

are only 20–40% attributable to altered mRNA levels (Tian, Stepaniants et al. 2004). Therefore, the differential expression of mRNA levels does not guarantee the protein translation. For *in vivo* biomarker development proteomics should be focused upon.

7.6.4 Alternative endothelial cell types

HUVECs are widely used as a model for cardiovascular related research. A more relevant cell type, for example, endothelial cells from human coronary artery would have been a better choice. Comparison between HUVECs and coronary artery endothelial cells would have been ideal.

7.7 Future work

7.7.1 SASP collected from senescent cells treated with TNF-α

SASP from senescent endothelial cells may be a phenomenon of inflammation. Therefore, it would be interesting to repeat the adhesion assay with SASP collected from REPS and SIPS pre-treated with TNF-α. Senescent endothelial cells might require a mild inflammatory response in order to initiate the SASP release.

7.7.2 Released microparticle characterisation

Microparticles are small heterogeneous membrane bound structures released from disturbed cells including endothelium. They are a result of membrane blebbing and shedding of membrane fragments into the extracellular space. Microparticles transport a large array of molecules, facilitating cell signalling (Horstman, Jy et al. 2004, Raposo, Stoorvogel 2013, Boulanger 2010). MP release is increase in aged endothelial cells. Furthermore, MPs obtained from young mouse endothelial cells had the ability to induce senescence in mouse aortic endothelial cells (Burger, Kwart et al. 2012). Therefore, the effects of growth retardation observed in the bioassay growth curves might include the effect of MPs generation from endothelial cells, rather than SASP. It is important to study the release of MPs from senescent HUVECs and their effects on young HUVECs in terms of cell phenotype and function.

7.7.3 Pro-inflammatory phenotype validation in REPS and SIPS

CD44 and E-selectin expression was observed in REPS and SIPS HUVECs respectively. Protein expression of E-selectin was not validated, while CD44 was validated in Western blot. Further immunochemistry validation of CD44 in REPS and E-selectin in SIPS HUVECs is required for the confirmation of their pro-adhesion, pro-inflammatory phenotype. It would also be of value to identify cell surface CD44 and E-selectin specifically. To achieve this, binding of fluorescent-labelled anti-CD44 (and E-selectin) antibody to live cells could be employed followed by confocal microscopy and flow cytometry.

7.7.4 Adhesion assay using antibody against CD44 and E-selectin

CD44 increases adhesion of monocytes in irradiated endothelial cells (Lowe, Raj 2014c). Antibodies against CD44 epitopes were able to reduce monocytic adhesion in an adhesion assay (Lowe, Raj 2014). It would be ideal to use an antibody against CD44 and E-selectin protein in the monocyte adhesion assay and confirm that increased monocytic adhesion in REPS and SIPS HUVECs is due, at least in part, to expression of these adhesion proteins.

7.7.5 HUVECs SASP determination using proteomics

Based on puromycin analysis of protein synthesis (chapter 5) and secretion by PMA there was no difference between secretion by senescent cells compared with control (young) cells. Unlike traditional methods of protein identification which can only identify a single protein at a time, proteomics enables the identification and measurement of variety of proteins simultaneously (proteomics serum free Annika Thorsel 2008). Due to intrinsic difficulties, only a few studies have performed the proteomic study. In this regard conditioned media is most the commonly used method for secretome analysis, as this would mimic the secretion phenotype of *in vivo* conditions. Analysing the secretome of cells in culture has the advantage that the secretome of cells can be analysed and compared under different conditions. However, the disadvantage is the low concentration of secreted protein and the masking effect of high abundance serum proteins. Fetal bovine

serum (FBS) is a particular problem. High levels of proteins are a challenge for shotgun proteomics via LC MS/MS (Finoulst, Vink et al. 2011), (Pellitteri-Hahn, Warren et al. 2006), (Nonnis, Maffioli et al. 2016). On the other hand, serum deprivation will cause a decrease in cell growth and increase in cell death (Hasan, Adams et al. 1999). To avoid the contamination and masking with the use of full growth media a specialised growth media with known growth factors could be used for the secretome profiling of senescent endothelial cells.

The profiling of secreted proteins released into conditioned media is very difficult due to the very complex mixture of proteins. A strategy called equalization for protein concentration has been developed, which is based on the generation of hexapeptide ligands on beads. Incubation with hexapeptide resin depletes the high abundant proteins and enriching low abundant proteins. Colzani et al used labelling with denatured valine D8 (D8-Val) for the proteome profiling (using LC MS/MS) of two human breast cancer cell lines grown in 10% FBS. After labelling they used the denaturing method for enrichment of low abundance protein. Once proteins were identified they were differentiated from bovine proteins (Colzani, Waridel et al. 2009).

Identification of secreted factors in conditioned media is of significant importance in biological research. The presence of dynamic range of high abundance protein in the serum remains a bottle neck in the proteomics and biomarker discovery (Seibert, Ebert et al. 2005). The presence of high abundance proteins in growth medium masks the important low abundance protein in SASP proteomic analysis. HUVECs unlike other cell types do not tolerate serum starvation. Upon serum starvation their susceptibility to cell death increases which is a major challenge for their secretome analysis in proteomics (Yin, Bern et al. 2013). Use of antibodies to deplete the high abundance proteins present in the growth media can be a suitable option for secretome profiling and biomarker discovery. Albumin depletion kit/magnetic beads can be used for albumin and IgG depletion.

Stable isotopic labelling with amino acid (SILAC) has emerged as a valuable proteomic technique. It can effectively be applied to compare the differential expression level of different samples proteins. It does not require chemical manipulation (Hodge, Have et al.

2013, Chandramouli, Qian 2009). SILAC requires the growth of cells in two different media. One in normal amino acid growth media and the other in heavy amino acid growth media. The heavy amino acid contains ^{15}N instead of ^{14}N, ^{13}C instead of ^{12}C and ^{2}H instead of H. When new proteins are synthesised the heavy amino acids will be used and therefore the new protein will have a higher mass than the ones that grow in the normal media (Mann 2006). The use of this media for characterisation of SASP from REPS and SIPS will benefit in a way that, HUVECs will be provided full growth medium for the period of SASP collection. The SASP collection time will also be increased to 24 hr, rather than 45 min in response to PMA.

Undertaking the aforementioned techniques for senescent HUVECs SASP analysis will determine and confirm the best method for SASP characterisation.

8 References

ABDALA-VALENCIA, H., BERDNIKOVS, S. and COOK-MILLS, J.M., 2011. Mechanisms for vascular cell adhesion molecule-1 activation of ERK1/2 during leukocyte transendothelial migration. *PloS one,* **6**(10), pp. e26706.

ACOSTA, J.C., O'LOGHLEN, A., BANITO, A., GUIJARRO, M.V., AUGERT, A., RAGUZ, S., FUMAGALLI, M., DA COSTA, M., BROWN, C., POPOV, N., TAKATSU, Y., MELAMED, J., D'ADDA DI FAGAGNA, F., BERNARD, D., HERNANDO, E. and GIL, J., 2008. Chemokine signaling via the CXCR2 receptor reinforces senescence. *Cell,* **133**(6), pp. 1006-1018.

ADAMS, P.D., 2007. Remodeling of chromatin structure in senescent cells and its potential impact on tumor suppression and aging. *Gene,* **397**(1-2), pp. 84-93.

AKIRA, S., UEMATSU, S. and TAKEUCHI, O., 2006. Pathogen recognition and innate immunity. *Cell,* **124**(4), pp. 783-801.

ALLEN, R.G., TRESINI, M., KEOGH, B.P., DOGGETT, D.L. and CRISTOFALO, V.J., 1999. Differences in electron transport potential, antioxidant defenses, and oxidant generation in young and senescent fetal lung fibroblasts (WI-38). *Journal of cellular physiology,* **180**(1), pp. 114-122.

ALTHUBITI, M., LEZINA, L., CARRERA, S., JUKES-JONES, R., GIBLETT, S.M., ANTONOV, A., BARLEV, N., SALDANHA, G.S., PRITCHARD, C.A., CAIN, K. and MACIP, S., 2014a. Characterization of novel markers of senescence and their prognostic potential in cancer. *Cell death & disease,* **5**, pp. e1528.

ALTHUBITI, M., LEZINA, L., CARRERA, S., JUKES-JONES, R., GIBLETT, S.M., ANTONOV, A., BARLEV, N., SALDANHA, G.S., PRITCHARD, C.A., CAIN, K. and MACIP, S., 2014b. Characterization of novel markers of senescence and their prognostic potential in cancer. *Cell death & disease,* **5**, pp. e1528.

AVIRUTNAN, P., MALASIT, P., SELIGER, B., BHAKDI, S. and HUSMANN, M., 1998. Dengue virus infection of human endothelial cells leads to chemokine production, complement activation, and apoptosis. *Journal of immunology (Baltimore, Md.: 1950),* **161**(11), pp. 6338-6346.

AVIV, H., KHAN, M.Y., SKURNICK, J., OKUDA, K., KIMURA, M., GARDNER, J., PRIOLO, L. and AVIV, A., 2001. Age dependent aneuploidy and telomere length of the human vascular endothelium. *Atherosclerosis,* **159**(2), pp. 281-287.

AZIMZADEH, O., SIEVERT, W., SARIOGLU, H., MERL-PHAM, J., YENTRAPALLI, R., BAKSHI, M.V., JANIK, D., UEFFING, M., ATKINSON, M.J., MULTHOFF, G. and TAPIO, S., 2015. Integrative proteomics and targeted transcriptomics analyses in cardiac endothelial cells unravel mechanisms of long-term radiation-induced vascular dysfunction. *Journal of proteome research,* **14**(2), pp. 1203-1219.

AZZAM, M.E. and ALGRANATI, I.D., 1973. Mechanism of puromycin action: fate of ribosomes after release of nascent protein chains from polysomes. *Proceedings of the National Academy of Sciences of the United States of America,* **70**(12), pp. 3866-3869.

BAAR, M.P., BRANDT, R.M., PUTAVET, D.A., KLEIN, J.D., DERKS, K.W., BOURGEOIS, B.R., STRYECK, S., RIJKSEN, Y., VAN WILLIGENBURG, H., FEIJTEL, D.A., VAN DER PLUIJM, I., ESSERS, J., VAN CAPPELLEN, W.A., VAN IJCKEN, W.F., HOUTSMULLER, A.B., POTHOF, J., DE BRUIN, R.W., MADL, T., HOEIJMAKERS, J.H., CAMPISI, J. and DE KEIZER, P.L., 2017. Targeted Apoptosis of Senescent Cells Restores Tissue Homeostasis in Response to Chemotoxicity and Aging. *Cell,* **169**(1), pp. 132-147.e16.

BAKER, D.J., PEREZ-TERZIC, C., JIN, F., PITEL, K.S., NIEDERLANDER, N.J., JEGANATHAN, K., YAMADA, S., REYES, S., ROWE, L., HIDDINGA, H.J., EBERHARDT, N.L., TERZIC, A. and VAN DEURSEN, J.M., 2008. Opposing roles for p16Ink4a and p19Arf in senescence and ageing caused by BubR1 insufficiency. *Nature cell biology,* **10**(7), pp. 825-836.

BAKER, D.J., WIJSHAKE, T., TCHKONIA, T., LEBRASSEUR, N.K., CHILDS, B.G., VAN DE SLUIS, B., KIRKLAND, J.L. and VAN DEURSEN, J.M., 2011a. Clearance of p16Ink4a-positive senescent cells delays ageing-associated disorders. *Nature,* **479**(7372), pp. 232-236.

BAKER, D.J., WIJSHAKE, T., TCHKONIA, T., LEBRASSEUR, N.K., CHILDS, B.G., VAN DE SLUIS, B., KIRKLAND, J.L. and VAN DEURSEN, J.M., 2011b. Clearance of p16Ink4a-positive senescent cells delays ageing-associated disorders. *Nature,* **479**(7372), pp. 232-236.

BAKRE, M.M., ZHU, Y., YIN, H., BURTON, D.W., TERKELTAUB, R., DEFTOS, L.J. and VARNER, J.A., 2002. Parathyroid hormone-related peptide is a naturally occurring, protein kinase A-dependent angiogenesis inhibitor. *Nature medicine,* **8**(9), pp. 995-1003.

BAL, G., KAMHIEH-MILZ, J., STERZER, V., AL-SAMMAN, M., DEBSKI, J., KLEIN, O., KAMHIEH-MILZ, S., BHAKDI, S. and SALAMA, A., 2013. Proteomic profiling of secreted proteins for the hematopoietic support of interleukin-stimulated human umbilical vein endothelial cells. *Cell transplantation,* **22**(7), pp. 1185-1199.

BALIN, A.K., GOODMAN, B.P., RASMUSSEN, H. and CRISTOFALO, V.J., 1976. The effect of oxygen tension on the growth and metabolism of WI-38 cells. *Journal of cellular physiology,* **89**(2), pp. 235-249.

BARGATZE, R.F., JUTILA, M.A. and BUTCHER, E.C., 1995. Distinct roles of L-selectin and integrins alpha 4 beta 7 and LFA-1 in lymphocyte homing to Peyer's patch-HEV in situ: the multistep model confirmed and refined. *Immunity,* **3**(1), pp. 99-108.

BARON, A., DECARLO, A. and FEATHERSTONE, J., 1999. Functional aspects of the human salivary cystatins in the oral environment. *Oral diseases,* **5**(3), pp. 234-240.

BAVIK, C., COLEMAN, I., DEAN, J.P., KNUDSEN, B., PLYMATE, S. and NELSON, P.S., 2006. The gene expression program of prostate fibroblast senescence modulates neoplastic epithelial cell proliferation through paracrine mechanisms. *Cancer research,* **66**(2), pp. 794-802.

BEAUSEJOUR, C.M., KRTOLICA, A., GALIMI, F., NARITA, M., LOWE, S.W., YASWEN, P. and CAMPISI, J., 2003. Reversal of human cellular senescence: roles of the p53 and p16 pathways. *The EMBO journal,* **22**(16), pp. 4212-4222.

BERKOVICH, E., MONNAT, R.J.,Jr and KASTAN, M.B., 2007. Roles of ATM and NBS1 in chromatin structure modulation and DNA double-strand break repair. *Nature cell biology,* **9**(6), pp. 683-690.

BIRCH, J. and PASSOS, J.F., 2017. Targeting the SASP to combat ageing: Mitochondria as possible intracellular allies? *BioEssays : news and reviews in molecular, cellular and developmental biology,* **39**(5), pp. 10.1002/bies.201600235. Epub 2017 Feb 20.

BLANKENBERG, S., BARBAUX, S. and TIRET, L., 2003. Adhesion molecules and atherosclerosis. *Atherosclerosis,* **170**(2), pp. 191-203.

BORALDI, F., BINI, L., LIBERATORI, S., ARMINI, A., PALLINI, V., TIOZZO, R., PASQUALI-RONCHETTI, I. and QUAGLINO, D., 2003. Proteome analysis of dermal fibroblasts cultured in vitro from human healthy subjects of different ages. *Proteomics,* **3**(6), pp. 917-929.

BORAS-GRANIC, K., DANN, P., VANHOUTEN, J., KARAPLIS, A. and WYSOLMERSKI, J., 2014. Deletion of the nuclear localization sequences and C-terminus of PTHrP impairs embryonic mammary development but also inhibits PTHrP production. *PloS one,* **9**(5), pp. e90418.

BORNSTEIN, P. and SAGE, E.H., 2002. Matricellular proteins: extracellular modulators of cell function. *Current opinion in cell biology,* **14**(5), pp. 608-616.

BRAIG, M., LEE, S., LODDENKEMPER, C., RUDOLPH, C., PETERS, A.H., SCHLEGELBERGER, B., STEIN, H., DORKEN, B., JENUWEIN, T. and SCHMITT, C.A., 2005. Oncogene-induced senescence as an initial barrier in lymphoma development. *Nature,* **436**(7051), pp. 660-665.

BRANDES, R.P., BEHRA, A., LEBHERZ, C., BOGER, R.H., BODE-BOGER, S.M., PHIVTHONG-NGAM, L. and MUGGE, A., 1997. N(G)-nitro-L-arginine- and indomethacin-resistant endothelium-dependent relaxation in the rabbit renal artery: effect of hypercholesterolemia. *Atherosclerosis,* **135**(1), pp. 49-55.

BRATOSIN, D., MITROFAN, L., PALII, C., ESTAQUIER, J. and MONTREUIL, J., 2005. Novel fluorescence assay using calcein-AM for the determination of human erythrocyte viability and aging. *Cytometry.Part A : the journal of the International Society for Analytical Cytology,* **66**(1), pp. 78-84.

BRUNO, S., FABBI, M., TISO, M., SANTAMARIA, B., GHIOTTO, F., SAVERINO, D., TENCA, C., ZARCONE, D., FERRINI, S., CICCONE, E. and GROSSI, C.E., 2000. Cell activation via CD44 occurs in advanced stages of squamous cell carcinogenesis. *Carcinogenesis,* **21**(5), pp. 893-900.

BURGERING, B.M., 2008. A brief introduction to FOXOlogy. *Oncogene,* **27**(16), pp. 2258-2262.

BURRIG, K.F., 1991. The endothelium of advanced arteriosclerotic plaques in humans. *Arteriosclerosis and thrombosis : a journal of vascular biology,* **11**(6), pp. 1678-1689.

BUSTIN, S.A., 2002. Quantification of mRNA using real-time reverse transcription PCR (RT-PCR): trends and problems. *Journal of Molecular Endocrinology,* **29**(1), pp. 23-39.

CAHU, J., BUSTANY, S. and SOLA, B., 2012. Senescence-associated secretory phenotype favors the emergence of cancer stem-like cells. *Cell death & disease,* **3**, pp. e446.

CALNAN, D.R. and BRUNET, A., 2008. The FoxO code. *Oncogene,* **27**(16), pp. 2276-2288.

CAMPISI, J., 2005. Senescent cells, tumor suppression, and organismal aging: good citizens, bad neighbors. *Cell,* **120**(4), pp. 513-522.

CAMPISI, J., 1997. Aging and cancer: the double-edged sword of replicative senescence. *Journal of the American Geriatrics Society,* **45**(4), pp. 482-488.

CAMPISI, J. and D'ADDA DI FAGAGNA, F., 2007a. Cellular senescence: when bad things happen to good cells. *Nature reviews.Molecular cell biology,* **8**(9), pp. 729-740.

CAMPISI, J. and D'ADDA DI FAGAGNA, F., 2007b. Cellular senescence: when bad things happen to good cells. *Nature reviews.Molecular cell biology,* **8**(9), pp. 729-740.

CAMPOS, R.V., ZHANG, L. and DRUCKER, D.J., 1994. Differential expression of RNA transcripts encoding unique carboxy-terminal sequences of human parathyroid hormone-related peptide. *Molecular endocrinology (Baltimore, Md.),* **8**(12), pp. 1656-1666.

CARTERSON, A.J., HONER ZU BENTRUP, K., OTT, C.M., CLARKE, M.S., PIERSON, D.L., VANDERBURG, C.R., BUCHANAN, K.L., NICKERSON, C.A. and SCHURR, M.J., 2005. A549 lung epithelial cells grown as three-dimensional aggregates: alternative tissue culture model for Pseudomonas aeruginosa pathogenesis. *Infection and immunity,* **73**(2), pp. 1129-1140.

CHANDRAMOULI, K. and QIAN, P.Y., 2009. Proteomics: Challenges, Techniques and Possibilities to Overcome Biological Sample Complexity. *Human Genomics and Proteomics : HGP,* **2009**, pp. 10.4061/2009/239204.

CHANG, J., WANG, Y., SHAO, L., LABERGE, R.M., DEMARIA, M., CAMPISI, J., JANAKIRAMAN, K., SHARPLESS, N.E., DING, S., FENG, W., LUO, Y., WANG, X., AYKIN-BURNS, N., KRAGER, K., PONNAPPAN, U., HAUER-JENSEN, M., MENG, A. and ZHOU, D., 2016. Clearance of senescent cells by ABT263 rejuvenates aged hematopoietic stem cells in mice. *Nature medicine,* **22**(1), pp. 78-83.

CHEN, J. and GOLIGORSKY, M.S., 2006. Premature senescence of endothelial cells: Methusaleh's dilemma. *American journal of physiology.Heart and circulatory physiology,* **290**(5), pp. H1729-39.

CHEN, J., HUANG, X., HALICKA, D., BRODSKY, S., AVRAM, A., ESKANDER, J., BLOOMGARDEN, N.A., DARZYNKIEWICZ, Z. and GOLIGORSKY, M.S., 2006. Contribution of p16INK4a and p21CIP1 pathways to induction of premature senescence of human endothelial cells: permissive role of p53. *American journal of physiology.Heart and circulatory physiology,* **290**(4), pp. H1575-86.

CHEN, Q. and AMES, B.N., 1994. Senescence-like growth arrest induced by hydrogen peroxide in human diploid fibroblast F65 cells. *Proceedings of the National Academy of Sciences of the United States of America,* **91**(10), pp. 4130-4134.

CHEN, Q., FISCHER, A., REAGAN, J.D., YAN, L.J. and AMES, B.N., 1995. Oxidative DNA damage and senescence of human diploid fibroblast cells. *Proceedings of the National Academy of Sciences of the United States of America,* **92**(10), pp. 4337-4341.

CHEN, Q.M., 2000. Replicative senescence and oxidant-induced premature senescence. Beyond the control of cell cycle checkpoints. *Annals of the New York Academy of Sciences,* **908**, pp. 111-125.

CHEN, Z., TROTMAN, L.C., SHAFFER, D., LIN, H.K., DOTAN, Z.A., NIKI, M., KOUTCHER, J.A., SCHER, H.I., LUDWIG, T., GERALD, W., CORDON-CARDO, C. and PANDOLFI, P.P., 2005. Crucial

role of p53-dependent cellular senescence in suppression of Pten-deficient tumorigenesis. *Nature,* **436**(7051), pp. 725-730.

CHILDS, B.G., BAKER, D.J., WIJSHAKE, T., CONOVER, C.A., CAMPISI, J. and VAN DEURSEN, J.M., 2016a. Senescent intimal foam cells are deleterious at all stages of atherosclerosis. *Science (New York, N.Y.),* **354**(6311), pp. 472-477.

CHILDS, B.G., BAKER, D.J., WIJSHAKE, T., CONOVER, C.A., CAMPISI, J. and VAN DEURSEN, J.M., 2016b. Senescent intimal foam cells are deleterious at all stages of atherosclerosis. *Science (New York, N.Y.),* **354**(6311), pp. 472-477.

CHIMENTI, C., KAJSTURA, J., TORELLA, D., URBANEK, K., HELENIAK, H., COLUSSI, C., DI MEGLIO, F., NADAL-GINARD, B., FRUSTACI, A., LERI, A., MASERI, A. and ANVERSA, P., 2003. Senescence and death of primitive cells and myocytes lead to premature cardiac aging and heart failure. *Circulation research,* **93**(7), pp. 604-613.

CHOI, E.H., KIM, J.T., KIM, J.H., KIM, S.Y., SONG, E.Y., KIM, J.W., KIM, S.Y., YEOM, Y.I., KIM, I.H. and LEE, H.G., 2009. Upregulation of the cysteine protease inhibitor, cystatin SN, contributes to cell proliferation and cathepsin inhibition in gastric cancer. *Clinica chimica acta; international journal of clinical chemistry,* **406**(1-2), pp. 45-51.

CHUAQUI, R.F., BONNER, R.F., BEST, C.J., GILLESPIE, J.W., FLAIG, M.J., HEWITT, S.M., PHILLIPS, J.L., KRIZMAN, D.B., TANGREA, M.A., AHRAM, M., LINEHAN, W.M., KNEZEVIC, V. and EMMERT-BUCK, M.R., 2002. Post-analysis follow-up and validation of microarray experiments. *Nature genetics,* **32 Suppl**, pp. 509-514.

CINES, D.B., POLLAK, E.S., BUCK, C.A., LOSCALZO, J., ZIMMERMAN, G.A., MCEVER, R.P., POBER, J.S., WICK, T.M., KONKLE, B.A., SCHWARTZ, B.S., BARNATHAN, E.S., MCCRAE, K.R., HUG, B.A., SCHMIDT, A.M. and STERN, D.M., 1998. Endothelial cells in physiology and in the pathophysiology of vascular disorders. *Blood,* **91**(10), pp. 3527-3561.

CLEMENT, M.V., PONTON, A. and PERVAIZ, S., 1998. Apoptosis induced by hydrogen peroxide is mediated by decreased superoxide anion concentration and reduction of intracellular milieu. *FEBS letters,* **440**(1-2), pp. 13-18.

COLEMAN, P.R., CHANG, G., HUTAS, G., GRIMSHAW, M., VADAS, M.A. and GAMBLE, J.R., 2013. Age-associated stresses induce an anti-inflammatory senescent phenotype in endothelial cells. *Aging,* **5**(12), pp. 913-924.

COLEMAN, P.R., HAHN, C.N., GRIMSHAW, M., LU, Y., LI, X., BRAUTIGAN, P.J., BECK, K., STOCKER, R., VADAS, M.A. and GAMBLE, J.R., 2010. Stress-induced premature senescence mediated by a novel gene, SENEX, results in an anti-inflammatory phenotype in endothelial cells. *Blood,* **116**(19), pp. 4016-4024.

COLLADO, M., GIL, J., EFEYAN, A., GUERRA, C., SCHUHMACHER, A.J., BARRADAS, M., BENGURIA, A., ZABALLOS, A., FLORES, J.M., BARBACID, M., BEACH, D. and SERRANO, M., 2005a. Tumour biology: senescence in premalignant tumours. *Nature,* **436**(7051), pp. 642.

COLLADO, M., GIL, J., EFEYAN, A., GUERRA, C., SCHUHMACHER, A.J., BARRADAS, M., BENGURIA, A., ZABALLOS, A., FLORES, J.M., BARBACID, M., BEACH, D. and SERRANO, M., 2005b. Tumour biology: senescence in premalignant tumours. *Nature,* **436**(7051), pp. 642.

COLLADO, M. and SERRANO, M., 2010. Senescence in tumours: evidence from mice and humans. *Nature reviews.Cancer,* **10**(1), pp. 51-57.

COMI, P., CHIARAMONTE, R. and MAIER, J.A., 1995. Senescence-dependent regulation of type 1 plasminogen activator inhibitor in human vascular endothelial cells. *Experimental cell research,* **219**(1), pp. 304-308.

COOK-MILLS, J.M., MARCHESE, M.E. and ABDALA-VALENCIA, H., 2011. Vascular cell adhesion molecule-1 expression and signaling during disease: regulation by reactive oxygen species and antioxidants. *Antioxidants & redox signaling,* **15**(6), pp. 1607-1638.

COPPE, J.P., DESPREZ, P.Y., KRTOLICA, A. and CAMPISI, J., 2010. The senescence-associated secretory phenotype: the dark side of tumor suppression. *Annual review of pathology,* **5**, pp. 99-118.

COPPE, J.P., KAUSER, K., CAMPISI, J. and BEAUSEJOUR, C.M., 2006. Secretion of vascular endothelial growth factor by primary human fibroblasts at senescence. *The Journal of biological chemistry,* **281**(40), pp. 29568-29574.

COPPE, J.P., PATIL, C.K., RODIER, F., SUN, Y., MUNOZ, D.P., GOLDSTEIN, J., NELSON, P.S., DESPREZ, P.Y. and CAMPISI, J., 2008a. Senescence-associated secretory phenotypes reveal cell-nonautonomous functions of oncogenic RAS and the p53 tumor suppressor. *PLoS biology,* **6**(12), pp. 2853-2868.

COPPE, J.P., PATIL, C.K., RODIER, F., SUN, Y., MUNOZ, D.P., GOLDSTEIN, J., NELSON, P.S., DESPREZ, P.Y. and CAMPISI, J., 2008b. Senescence-associated secretory phenotypes reveal cell-nonautonomous functions of oncogenic RAS and the p53 tumor suppressor. *PLoS biology,* **6**(12), pp. 2853-2868.

COPPE, J.P., RODIER, F., PATIL, C.K., FREUND, A., DESPREZ, P.Y. and CAMPISI, J., 2011. Tumor suppressor and aging biomarker p16(INK4a) induces cellular senescence without the associated inflammatory secretory phenotype. *The Journal of biological chemistry,* **286**(42), pp. 36396-36403.

COUGHLIN, S.R., 2000. Thrombin signalling and protease-activated receptors. *Nature,* **407**(6801), pp. 258-264.

CUI, H., KONG, Y., XU, M. and ZHANG, H., 2013. Notch3 functions as a tumor suppressor by controlling cellular senescence. *Cancer research,* **73**(11), pp. 3451-3459.

CUTLER, R.G. and MATTSON, M.P., 2006. The adversities of aging. *Ageing research reviews,* **5**(3), pp. 221-238.

DALY, C. and ROLLINS, B.J., 2003. Monocyte chemoattractant protein-1 (CCL2) in inflammatory disease and adaptive immunity: therapeutic opportunities and controversies. *Microcirculation (New York, N.Y.: 1994),* **10**(3-4), pp. 247-257.

DAVIS, B.K., WEN, H. and TING, J.P., 2011. The inflammasome NLRs in immunity, inflammation, and associated diseases. *Annual Review of Immunology,* **29**, pp. 707-735.

DE KEIZER, P.L., 2017. The Fountain of Youth by Targeting Senescent Cells? *Trends in molecular medicine,* **23**(1), pp. 6-17.

DE KEIZER, P.L., PACKER, L.M., SZYPOWSKA, A.A., RIEDL-POLDERMAN, P.E., VAN DEN BROEK, N.J., DE BRUIN, A., DANSEN, T.B., MARAIS, R., BRENKMAN, A.B. and BURGERING, B.M., 2010. Activation of forkhead box O transcription factors by oncogenic BRAF promotes p21cip1-dependent senescence. *Cancer research,* **70**(21), pp. 8526-8536.

DE SPIEGELAERE, W., DERN-WIELOCH, J., WEIGEL, R., SCHUMACHER, V., SCHORLE, H., NETTERSHEIM, D., BERGMANN, M., BREHM, R., KLIESCH, S., VANDEKERCKHOVE, L. and FINK, C., 2015. Reference gene validation for RT-qPCR, a note on different available software packages. *PloS one,* **10**(3), pp. e0122515.

DE VISSER, K.E., EICHTEN, A. and COUSSENS, L.M., 2006. Paradoxical roles of the immune system during cancer development. *Nature reviews.Cancer,* **6**(1), pp. 24-37.

DEJANA, E., 1996. Endothelial adherens junctions: implications in the control of vascular permeability and angiogenesis. *The Journal of clinical investigation,* **98**(9), pp. 1949-1953.

DENECKER, G., OVAERE, P., VANDENABEELE, P. and DECLERCQ, W., 2008. Caspase-14 reveals its secrets. *The Journal of cell biology,* **180**(3), pp. 451-458.

DHEDA, K., HUGGETT, J.F., CHANG, J.S., KIM, L.U., BUSTIN, S.A., JOHNSON, M.A., ROOK, G.A. and ZUMLA, A., 2005. The implications of using an inappropriate reference gene for real-time reverse transcription PCR data normalization. *Analytical Biochemistry,* **344**(1), pp. 141-143.

DIERICK, J.F., ELIAERS, F., REMACLE, J., RAES, M., FEY, S.J., LARSEN, P.M. and TOUSSAINT, O., 2002. Stress-induced premature senescence and replicative senescence are different phenotypes, proteomic evidence. *Biochemical pharmacology,* **64**(5-6), pp. 1011-1017.

DIMRI, G.P., LEE, X., BASILE, G., ACOSTA, M., SCOTT, G., ROSKELLEY, C., MEDRANO, E.E., LINSKENS, M., RUBELJ, I. and PEREIRA-SMITH, O., 1995. A biomarker that identifies senescent human cells in culture and in aging skin in vivo. *Proceedings of the National Academy of Sciences of the United States of America,* **92**(20), pp. 9363-9367.

DONATO, A.J., MORGAN, R.G., WALKER, A.E. and LESNIEWSKI, L.A., 2015. Cellular and molecular biology of aging endothelial cells. *Journal of Molecular and Cellular Cardiology,* **89**(Pt B), pp. 122-135.

DREXLER, H., 1997. Endothelial dysfunction: clinical implications. *Progress in cardiovascular diseases,* **39**(4), pp. 287-324.

DUMONT, P., BURTON, M., CHEN, Q.M., GONOS, E.S., FRIPPIAT, C., MAZARATI, J.B., ELIAERS, F., REMACLE, J. and TOUSSAINT, O., 2000. Induction of replicative senescence biomarkers by sublethal oxidative stresses in normal human fibroblast. *Free radical biology & medicine,* **28**(3), pp. 361-373.

EMAN, M.R., REGAN-KLAPISZ, E., PINKSE, M.W., KOOP, I.M., HAVERKAMP, J., HECK, A.J., VERKLEIJ, A.J. and POST, J.A., 2006a. Protein expression dynamics during replicative senescence of endothelial cells studied by 2-D difference in-gel electrophoresis. *Electrophoresis,* **27**(8), pp. 1669-1682.

EMAN, M.R., REGAN-KLAPISZ, E., PINKSE, M.W., KOOP, I.M., HAVERKAMP, J., HECK, A.J., VERKLEIJ, A.J. and POST, J.A., 2006b. Protein expression dynamics during replicative senescence of endothelial cells studied by 2-D difference in-gel electrophoresis. *Electrophoresis,* **27**(8), pp. 1669-1682.

FARBER, J.L., 1994. Mechanisms of cell injury by activated oxygen species. *Environmental health perspectives,* **102 Suppl 10**, pp. 17-24.

FELETOU, M. and VANHOUTTE, P.M., 2006. Endothelium-derived hyperpolarizing factor: where are we now? *Arteriosclerosis, Thrombosis, and Vascular Biology,* **26**(6), pp. 1215-1225.

FIASCHI-TAESCH, N., TAKANE, K.K., MASTERS, S., LOPEZ-TALAVERA, J.C. and STEWART, A.F., 2004. Parathyroid-hormone-related protein as a regulator of pRb and the cell cycle in arterial smooth muscle. *Circulation,* **110**(2), pp. 177-185.

FLEMING, J.M., GINSBURG, E., OLIVER, S.D., GOLDSMITH, P. and VONDERHAAR, B.K., 2012. Hornerin, an S100 family protein, is functional in breast cells and aberrantly expressed in breast cancer. *BMC cancer,* **12**, pp. 266-2407-12-266.

FRANCESCHI, C. and CAMPISI, J., 2014. Chronic inflammation (inflammaging) and its potential contribution to age-associated diseases. *The journals of gerontology.Series A, Biological sciences and medical sciences,* **69 Suppl 1**, pp. S4-9.

FRANCKHAUSER, S., ELIAS, I., ROTTER SOPASAKIS, V., FERRE, T., NAGAEV, I., ANDERSSON, C.X., AGUDO, J., RUBERTE, J., BOSCH, F. and SMITH, U., 2008. Overexpression of Il6 leads to hyperinsulinaemia, liver inflammation and reduced body weight in mice. *Diabetologia,* **51**(7), pp. 1306-1316.

FREEMAN, W.M., WALKER, S.J. and VRANA, K.E., 1999. Quantitative RT-PCR: pitfalls and potential. *BioTechniques,* **26**(1), pp. 112-22, 124-5.

FREUND, A., ORJALO, A.V., DESPREZ, P.Y. and CAMPISI, J., 2010. Inflammatory networks during cellular senescence: causes and consequences. *Trends in molecular medicine,* **16**(5), pp. 238-246.

FRITZSCHE, S. and SPRINGER, S., 2014. Pulse-chase analysis for studying protein synthesis and maturation. *Current protocols in protein science,* **78**, pp. 30.3.1-23.

GALLEY, H.F. and WEBSTER, N.R., 2004. Physiology of the endothelium. *British journal of anaesthesia,* **93**(1), pp. 105-113.

GARNACHO, C., SHUVAEV, V., THOMAS, A., MCKENNA, L., SUN, J., KOVAL, M., ALBELDA, S., MUZYKANTOV, V. and MURO, S., 2008. RhoA activation and actin reorganization involved in endothelial CAM-mediated endocytosis of anti-PECAM carriers: critical role for tyrosine 686 in the cytoplasmic tail of PECAM-1. *Blood,* **111**(6), pp. 3024-3033.

GHOSH, S., MAY, M.J. and KOPP, E.B., 1998. NF-kappa B and Rel proteins: evolutionarily conserved mediators of immune responses. *Annual Review of Immunology,* **16**, pp. 225-260.

GOLIGORSKY, M.S., 2005. Endothelial cell dysfunction: can't live with it, how to live without it. *American journal of physiology.Renal physiology,* **288**(5), pp. F871-80.

GONZALEZ, L.C., GHADAOUIA, S., MARTINEZ, A. and RODIER, F., 2016. Premature aging/senescence in cancer cells facing therapy: good or bad? *Biogerontology,* **17**(1), pp. 71-87.

GOODMAN, C.A. and HORNBERGER, T.A., 2013a. Measuring protein synthesis with SUnSET: a valid alternative to traditional techniques? *Exercise and sport sciences reviews,* **41**(2), pp. 107-115.

GOODMAN, C.A. and HORNBERGER, T.A., 2013b. Measuring protein synthesis with SUnSET: a valid alternative to traditional techniques? *Exercise and sport sciences reviews,* **41**(2), pp. 107-115.

GORDON, R.R. and NELSON, P.S., 2012. Cellular senescence and cancer chemotherapy resistance. *Drug resistance updates : reviews and commentaries in antimicrobial and anticancer chemotherapy,* **15**(1-2), pp. 123-131.

GREEN, D.R., GALLUZZI, L. and KROEMER, G., 2011. Mitochondria and the autophagy-inflammation-cell death axis in organismal aging. *Science (New York, N.Y.),* **333**(6046), pp. 1109-1112.

GREENBERG, M.E. and ZIFF, E.B., 1984. Stimulation of 3T3 cells induces transcription of the c-fos proto-oncogene. *Nature,* **311**(5985), pp. 433-438.

GREENWOOD, J., WANG, Y. and CALDER, V.L., 1995. Lymphocyte adhesion and transendothelial migration in the central nervous system: the role of LFA-1, ICAM-1, VLA-4 and VCAM-1. off. *Immunology,* **86**(3), pp. 408-415.

GRIFFIOEN, A.W., DAMEN, C.A., BLIJHAM, G.H. and GROENEWEGEN, G., 1996. Tumor angiogenesis is accompanied by a decreased inflammatory response of tumor-associated endothelium. *Blood,* **88**(2), pp. 667-673.

HA, M.K., SOO CHO, J., BAIK, O.R., LEE, K.H., KOO, H.S. and CHUNG, K.Y., 2006. Caenorhabditis elegans as a screening tool for the endothelial cell-derived putative aging-related proteins detected by proteomic analysis. *Proteomics,* **6**(11), pp. 3339-3351.

HALLIWELL, B., 2006. Reactive species and antioxidants. Redox biology is a fundamental theme of aerobic life. *Plant Physiology,* **141**(2), pp. 312-322.

HAMPEL, B., FORTSCHEGGER, K., RESSLER, S., CHANG, M.W., UNTERLUGGAUER, H., BREITWIESER, A., SOMMERGRUBER, W., FITZKY, B., LEPPERDINGER, G., JANSEN-DURR, P., VOGLAUER, R. and GRILLARI, J., 2006a. Increased expression of extracellular proteins as a hallmark of human endothelial cell in vitro senescence. *Experimental gerontology,* **41**(5), pp. 474-481.

HAMPEL, B., FORTSCHEGGER, K., RESSLER, S., CHANG, M.W., UNTERLUGGAUER, H., BREITWIESER, A., SOMMERGRUBER, W., FITZKY, B., LEPPERDINGER, G., JANSEN-DURR, P., VOGLAUER, R. and GRILLARI, J., 2006b. Increased expression of extracellular proteins as a hallmark of human endothelial cell in vitro senescence. *Experimental gerontology,* **41**(5), pp. 474-481.

HAMPEL, B., FORTSCHEGGER, K., RESSLER, S., CHANG, M.W., UNTERLUGGAUER, H., BREITWIESER, A., SOMMERGRUBER, W., FITZKY, B., LEPPERDINGER, G., JANSEN-DURR, P., VOGLAUER, R. and GRILLARI, J., 2006c. Increased expression of extracellular proteins as a hallmark of human endothelial cell in vitro senescence. *Experimental gerontology,* **41**(5), pp. 474-481.

HAMPTON, M.B. and ORRENIUS, S., 1997. Dual regulation of caspase activity by hydrogen peroxide: implications for apoptosis. *FEBS letters,* **414**(3), pp. 552-556.

HARALDSEN, G., KVALE, D., LIEN, B., FARSTAD, I.N. and BRANDTZAEG, P., 1996. Cytokine-regulated expression of E-selectin, intercellular adhesion molecule-1 (ICAM-1), and vascular cell adhesion molecule-1 (VCAM-1) in human microvascular endothelial cells. *Journal of immunology (Baltimore, Md.: 1950),* **156**(7), pp. 2558-2565.

HARE, I., EVANS, R., FORTNEY, J., MOSES, B., PIKTEL, D., SLONE, W. and GIBSON, L.F., 2016. Chemotherapy-induced Dkk-1 expression by primary human mesenchymal stem cells is p53 dependent. *Medical oncology (Northwood, London, England),* **33**(10), pp. 113-016-0826-9. Epub 2016 Sep 1.

HAYFLICK, L. and MOORHEAD, P.S., 1961. The serial cultivation of human diploid cell strains. *Experimental cell research,* **25**, pp. 585-621.

HEO, J.S., KIM, H.O., SONG, S.Y., LEW, D.H., CHOI, Y. and KIM, S., 2016. Poly-L-lysine Prevents Senescence and Augments Growth in Culturing Mesenchymal Stem Cells Ex Vivo. *BioMed research international,* **2016**, pp. 8196078.

HISAMATSU, D. and NAKA-KANEDA, H., 2016. Reversing multiple age-related pathologies by controlling the senescence-associated secretory phenotype of stem cells. *Neural regeneration research,* **11**(11), pp. 1746-1747.

HODGE, K., HAVE, S.T., HUTTON, L. and LAMOND, A.I., 2013. Cleaning up the masses: Exclusion lists to reduce contamination with HPLC-MS/MSâ˜†. *Journal of Proteomics,* **88**, pp. 92-103.

HONDA, K., TAKAOKA, A. and TANIGUCHI, T., 2006. Type I interferon [corrected] gene induction by the interferon regulatory factor family of transcription factors. *Immunity,* **25**(3), pp. 349-360.

HUO, Y., HAFEZI-MOGHADAM, A. and LEY, K., 2000. Role of vascular cell adhesion molecule-1 and fibronectin connecting segment-1 in monocyte rolling and adhesion on early atherosclerotic lesions. *Circulation research,* **87**(2), pp. 153-159.

ICHIM, G., LOPEZ, J., AHMED, S.U., MUTHALAGU, N., GIAMPAZOLIAS, E., DELGADO, M.E., HALLER, M., RILEY, J.S., MASON, S.M., ATHINEOS, D., PARSONS, M.J., VAN DE KOOIJ, B., BOUCHIER-HAYES, L., CHALMERS, A.J., ROOSWINKEL, R.W., OBERST, A., BLYTH, K., REHM, M., MURPHY, D.J. and TAIT, S.W., 2015. Limited mitochondrial permeabilization causes DNA damage and genomic instability in the absence of cell death. *Molecular cell,* **57**(5), pp. 860-872.

IIYAMA, K., HAJRA, L., IIYAMA, M., LI, H., DICHIARA, M., MEDOFF, B.D. and CYBULSKY, M.I., 1999. Patterns of vascular cell adhesion molecule-1 and intercellular adhesion molecule-1 expression in rabbit and mouse atherosclerotic lesions and at sites predisposed to lesion formation. *Circulation research,* **85**(2), pp. 199-207.

JAFFE, E.A., NACHMAN, R.L., BECKER, C.G. and MINICK, C.R., 1973. Culture of human endothelial cells derived from umbilical veins. Identification by morphologic and immunologic criteria. *The Journal of clinical investigation,* **52**(11), pp. 2745-2756.

JEE, H.J., KIM, H.J., KIM, A.J., BAE, Y.S., BAE, S.S. and YUN, J., 2009. UV light induces premature senescence in Akt1-null mouse embryonic fibroblasts by increasing intracellular levels of ROS. *Biochemical and biophysical research communications,* **383**(3), pp. 358-362.

JEON, H.Y., KIM, J.K., HAM, S.W., OH, S.Y., KIM, J., PARK, J.B., LEE, J.Y., KIM, S.C. and KIM, H., 2016. Irradiation induces glioblastoma cell senescence and senescence-associated secretory phenotype. *Tumour biology : the journal of the International Society for Oncodevelopmental Biology and Medicine,* **37**(5), pp. 5857-5867.

JEYAPALAN, J.C., FERREIRA, M., SEDIVY, J.M. and HERBIG, U., 2007a. Accumulation of senescent cells in mitotic tissue of aging primates. *Mechanisms of ageing and development,* **128**(1), pp. 36-44.

JEYAPALAN, J.C., FERREIRA, M., SEDIVY, J.M. and HERBIG, U., 2007b. Accumulation of senescent cells in mitotic tissue of aging primates. *Mechanisms of ageing and development,* **128**(1), pp. 36-44.

JIANG, J., LIU, H.L., LIU, Z.H., TAN, S.W. and WU, B., 2015. Identification of cystatin SN as a novel biomarker for pancreatic cancer. *Tumour biology : the journal of the International Society for Oncodevelopmental Biology and Medicine,* **36**(5), pp. 3903-3910.

JONES, R.G., PLAS, D.R., KUBEK, S., BUZZAI, M., MU, J., XU, Y., BIRNBAUM, M.J. and THOMPSON, C.B., 2005. AMP-activated protein kinase induces a p53-dependent metabolic checkpoint. *Molecular cell,* **18**(3), pp. 283-293.

JONSSON-RYLANDER, A.C., NILSSON, T., FRITSCHE-DANIELSON, R., HAMMARSTROM, A., BEHRENDT, M., ANDERSSON, J.O., LINDGREN, K., ANDERSSON, A.K., WALLBRANDT, P., ROSENGREN, B., BRODIN, P., THELIN, A., WESTIN, A., HURT-CAMEJO, E. and LEE-SOGAARD, C.H., 2005. Role of ADAMTS-1 in atherosclerosis: remodeling of carotid artery, immunohistochemistry, and proteolysis of versican. *Arteriosclerosis, Thrombosis, and Vascular Biology,* **25**(1), pp. 180-185.

JUN, J.I. and LAU, L.F., 2010. Cellular senescence controls fibrosis in wound healing. *Aging,* **2**(9), pp. 627-631.

KATLINSKAYA, Y.V., KATLINSKI, K.V., YU, Q., ORTIZ, A., BEITING, D.P., BRICE, A., DAVAR, D., SANDERS, C., KIRKWOOD, J.M., RUI, H., XU, X., KOUMENIS, C., DIEHL, J.A. and FUCHS, S.Y., 2016. Suppression of type I interferon signaling overcomes oncogene-induced senescence and mediates melanoma development and progression. *Cell reports,* **15**(1), pp. 171-180.

KEPPLER, D., ZHANG, J., BIHANI, T. and LIN, A.W., 2011a. Novel expression of CST1 as candidate senescence marker. *The journals of gerontology.Series A, Biological sciences and medical sciences,* **66**(7), pp. 723-731.

KEPPLER, D., ZHANG, J., BIHANI, T. and LIN, A.W., 2011b. Novel expression of CST1 as candidate senescence marker. *The journals of gerontology.Series A, Biological sciences and medical sciences,* **66**(7), pp. 723-731.

KHAN, S.Y., AWAD, E.M., OSZWALD, A., MAYR, M., YIN, X., WALTENBERGER, B., STUPPNER, H., LIPOVAC, M., UHRIN, P. and BREUSS, J.M., 2017. Premature senescence of endothelial cells upon chronic exposure to TNFalpha can be prevented by N-acetyl cysteine and plumericin. *Scientific reports,* **7**, pp. 39501.

KIM, Y.K., KO, S.H., WOO, J.S., LEE, S.H. and JUNG, J.S., 1998. Difference in H2O2 toxicity between intact renal tubules and cultured proximal tubular cells. *Biochemical pharmacology,* **56**(4), pp. 489-495.

KRISHNAMURTHY, J., RAMSEY, M.R., LIGON, K.L., TORRICE, C., KOH, A., BONNER-WEIR, S. and SHARPLESS, N.E., 2006. p16INK4a induces an age-dependent decline in islet regenerative potential. *Nature,* **443**(7110), pp. 453-457.

KRISHNAMURTHY, J., TORRICE, C., RAMSEY, M.R., KOVALEV, G.I., AL-REGAIEY, K., SU, L. and SHARPLESS, N.E., 2004. Ink4a/Arf expression is a biomarker of aging. *The Journal of clinical investigation,* **114**(9), pp. 1299-1307.

KRIZHANOVSKY, V., YON, M., DICKINS, R.A., HEARN, S., SIMON, J., MIETHING, C., YEE, H., ZENDER, L. and LOWE, S.W., 2008. Senescence of activated stellate cells limits liver fibrosis. *Cell,* **134**(4), pp. 657-667.

KROUWER, V.J., HEKKING, L.H., LANGELAAR-MAKKINJE, M., REGAN-KLAPISZ, E. and POST, J.A., 2012. Endothelial cell senescence is associated with disrupted cell-cell junctions and increased monolayer permeability. *Vascular cell,* **4**(1), pp. 12-824X-4-12.

KRTOLICA, A., PARRINELLO, S., LOCKETT, S., DESPREZ, P.Y. and CAMPISI, J., 2001a. Senescent fibroblasts promote epithelial cell growth and tumorigenesis: a link between cancer and aging. *Proceedings of the National Academy of Sciences of the United States of America,* **98**(21), pp. 12072-12077.

KRTOLICA, A., PARRINELLO, S., LOCKETT, S., DESPREZ, P.Y. and CAMPISI, J., 2001b. Senescent fibroblasts promote epithelial cell growth and tumorigenesis: a link between cancer and aging. *Proceedings of the National Academy of Sciences of the United States of America,* **98**(21), pp. 12072-12077.

KUILMAN, T., MICHALOGLOU, C., MOOI, W.J. and PEEPER, D.S., 2010. The essence of senescence. *Genes & development,* **24**(22), pp. 2463-2479.

KUMAR, S., MILLIS, A.J. and BAGLIONI, C., 1992. Expression of interleukin 1-inducible genes and production of interleukin 1 by aging human fibroblasts. *Proceedings of the National Academy of Sciences of the United States of America,* **89**(10), pp. 4683-4687.

KUNKEL, E.J., DUNNE, J.L. and LEY, K., 2000a. Leukocyte arrest during cytokine-dependent inflammation in vivo. *Journal of immunology (Baltimore, Md.: 1950),* **164**(6), pp. 3301-3308.

KUNKEL, E.J., DUNNE, J.L. and LEY, K., 2000b. Leukocyte arrest during cytokine-dependent inflammation in vivo. *Journal of immunology (Baltimore, Md.: 1950),* **164**(6), pp. 3301-3308.

LANDMESSER, U. and DREXLER, H., 2005. The clinical significance of endothelial dysfunction. *Current opinion in cardiology,* **20**(6), pp. 547-551.

LARA, J., COOPER, R., NISSAN, J., GINTY, A.T., KHAW, K.T., DEARY, I.J., LORD, J.M., KUH, D. and MATHERS, J.C., 2015. A proposed panel of biomarkers of healthy ageing. *BMC medicine,* **13**, pp. 222-015-0470-9.

LAVIN, M.F., 2008. Ataxia-telangiectasia: from a rare disorder to a paradigm for cell signalling and cancer. *Nature reviews.Molecular cell biology,* **9**(10), pp. 759-769.

LAWSON, C. and WOLF, S., 2009. ICAM-1 signaling in endothelial cells. *Pharmacological reports : PR,* **61**(1), pp. 22-32.

LAZZERINI DENCHI, E., ATTWOOLL, C., PASINI, D. and HELIN, K., 2005. Deregulated E2F activity induces hyperplasia and senescence-like features in the mouse pituitary gland. *Molecular and cellular biology,* **25**(7), pp. 2660-2672.

LEES, H., WALTERS, H. and COX, L.S., 2016. Animal and human models to understand ageing. *Maturitas,* **93**, pp. 18-27.

LEEUWENBERG, J.F., SMEETS, E.F., NEEFJES, J.J., SHAFFER, M.A., CINEK, T., JEUNHOMME, T.M., AHERN, T.J. and BUURMAN, W.A., 1992. E-selectin and intercellular adhesion molecule-1 are released by activated human endothelial cells in vitro. *Immunology,* **77**(4), pp. 543-549.

LIAO, E.C., HSU, Y.T., CHUAH, Q.Y., LEE, Y.J., HU, J.Y., HUANG, T.C., YANG, P.M. and CHIU, S.J., 2014. Radiation induces senescence and a bystander effect through metabolic alterations. *Cell death & disease,* **5**, pp. e1255.

LIU, D. and HORNSBY, P.J., 2007a. Senescent human fibroblasts increase the early growth of xenograft tumors via matrix metalloproteinase secretion. *Cancer research,* **67**(7), pp. 3117-3126.

LIU, D. and HORNSBY, P.J., 2007b. Senescent human fibroblasts increase the early growth of xenograft tumors via matrix metalloproteinase secretion. *Cancer research,* **67**(7), pp. 3117-3126.

LOWE, D. and RAJ, K., 2014a. Premature aging induced by radiation exhibits pro-atherosclerotic effects mediated by epigenetic activation of CD44 expression. *Aging cell,* **13**(5), pp. 900-910.

LOWE, D. and RAJ, K., 2014b. Premature aging induced by radiation exhibits pro-atherosclerotic effects mediated by epigenetic activation of CD44 expression. *Aging cell,* **13**(5), pp. 900-910.

LOWE, D. and RAJ, K., 2014c. Premature aging induced by radiation exhibits pro-atherosclerotic effects mediated by epigenetic activation of CD44 expression. *Aging cell,* **13**(5), pp. 900-910.

MARCUM, J.A., MCKENNEY, J.B. and ROSENBERG, R.D., 1984. Acceleration of thrombin-antithrombin complex formation in rat hindquarters via heparinlike molecules bound to the endothelium. *The Journal of clinical investigation,* **74**(2), pp. 341-350.

MARCUM, J.A. and ROSENBERG, R.D., 1985. Heparinlike molecules with anticoagulant activity are synthesized by cultured endothelial cells. *Biochemical and biophysical research communications,* **126**(1), pp. 365-372.

MARTHANDAN, S., BAUMGART, M., PRIEBE, S., GROTH, M., SCHAER, J., KAETHER, C., GUTHKE, R., CELLERINO, A., PLATZER, M., DIEKMANN, S. and HEMMERICH, P., 2016. Conserved Senescence Associated Genes and Pathways in Primary Human Fibroblasts Detected by RNA-Seq. *PloS one,* **11**(5), pp. e0154531.

MARTINON, F., BURNS, K. and TSCHOPP, J., 2002. The inflammasome: a molecular platform triggering activation of inflammatory caspases and processing of proIL-beta. *Molecular cell,* **10**(2), pp. 417-426.

MASON, R.G., SHARP, D., CHUANG, H.Y. and MOHAMMAD, S.F., 1977. The endothelium: roles in thrombosis and hemostasis. *Archives of Pathology & Laboratory Medicine,* **101**(2), pp. 61-64.

MATSUSHITA, H., CHANG, E., GLASSFORD, A.J., COOKE, J.P., CHIU, C.P. and TSAO, P.S., 2001. eNOS activity is reduced in senescent human endothelial cells: Preservation by hTERT immortalization. *Circulation research,* **89**(9), pp. 793-798.

MCKEEHAN, W. and HARDESTY, B., 1969. *The mechanism of cycloheximide inhibition of protein synthesis in rabbit reticulocytes.*

MCKIERNAN, E., MCDERMOTT, E.W., EVOY, D., CROWN, J. and DUFFY, M.J., 2011. The role of S100 genes in breast cancer progression. *Tumour biology : the journal of the International Society for Oncodevelopmental Biology and Medicine,* **32**(3), pp. 441-450.

MEDZHITOV, R., 2010. Inflammation 2010: new adventures of an old flame. *Cell,* **140**(6), pp. 771-776.

MENGHINI, R., CASAGRANDE, V., CARDELLINI, M., MARTELLI, E., TERRINONI, A., AMATI, F., VASA-NICOTERA, M., IPPOLITI, A., NOVELLI, G., MELINO, G., LAURO, R. and FEDERICI, M., 2009. MicroRNA 217 modulates endothelial cell senescence via silent information regulator 1. *Circulation,* **120**(15), pp. 1524-1532.

METCALF, D.J., NIGHTINGALE, T.D., ZENNER, H.L., LUI-ROBERTS, W.W. and CUTLER, D.F., 2008. Formation and function of Weibel-Palade bodies. *Journal of cell science,* **121**(Pt 1), pp. 19-27.

MICHALOGLOU, C., VREDEVELD, L.C., SOENGAS, M.S., DENOYELLE, C., KUILMAN, T., VAN DER HORST, C.M., MAJOOR, D.M., SHAY, J.W., MOOI, W.J. and PEEPER, D.S., 2005a. BRAFE600-associated senescence-like cell cycle arrest of human naevi. *Nature,* **436**(7051), pp. 720-724.

MICHALOGLOU, C., VREDEVELD, L.C., SOENGAS, M.S., DENOYELLE, C., KUILMAN, T., VAN DER HORST, C.M., MAJOOR, D.M., SHAY, J.W., MOOI, W.J. and PEEPER, D.S., 2005b. BRAFE600-associated senescence-like cell cycle arrest of human naevi. *Nature,* **436**(7051), pp. 720-724.

MICHALOGLOU, C., VREDEVELD, L.C., SOENGAS, M.S., DENOYELLE, C., KUILMAN, T., VAN DER HORST, C.M., MAJOOR, D.M., SHAY, J.W., MOOI, W.J. and PEEPER, D.S., 2005c. BRAFE600-associated senescence-like cell cycle arrest of human naevi. *Nature,* **436**(7051), pp. 720-724.

MINAMINO, T. and KOMURO, I., 2002. Role of telomere in endothelial dysfunction in atherosclerosis. *Current opinion in lipidology,* **13**(5), pp. 537-543.

MINAMINO, T., MIYAUCHI, H., YOSHIDA, T., ISHIDA, Y., YOSHIDA, H. and KOMURO, I., 2002a. Endothelial cell senescence in human atherosclerosis: role of telomere in endothelial dysfunction. *Circulation,* **105**(13), pp. 1541-1544.

MINAMINO, T., MIYAUCHI, H., YOSHIDA, T., ISHIDA, Y., YOSHIDA, H. and KOMURO, I., 2002b. Endothelial cell senescence in human atherosclerosis: role of telomere in endothelial dysfunction. *Circulation,* **105**(13), pp. 1541-1544.

MONTMINY, M.R. and BILEZIKJIAN, L.M., 1987. Binding of a nuclear protein to the cyclic-AMP response element of the somatostatin gene. *Nature,* **328**(6126), pp. 175-178.

MOREY, J.S., RYAN, J.C. and VAN DOLAH, F.M., 2006. Microarray validation: factors influencing correlation between oligonucleotide microarrays and real-time PCR. *Biological Procedures Online,* **8**, pp. 175-193.

MOTAMED, K. and SAGE, E.H., 1998. SPARC inhibits endothelial cell adhesion but not proliferation through a tyrosine phosphorylation-dependent pathway. *Journal of cellular biochemistry,* **70**(4), pp. 543-552.

MULLER, W.A., 2002. Leukocyte-endothelial cell interactions in the inflammatory response. *Laboratory investigation; a journal of technical methods and pathology,* **82**(5), pp. 521-533.

MUN, G.I. and BOO, Y.C., 2010. Identification of CD44 as a senescence-induced cell adhesion gene responsible for the enhanced monocyte recruitment to senescent endothelial cells. *American journal of physiology.Heart and circulatory physiology,* **298**(6), pp. H2102-11.

MURPHY, J.F., LENNON, F., STEELE, C., KELLEHER, D., FITZGERALD, D. and LONG, A.C., 2005a. Engagement of CD44 modulates cyclooxygenase induction, VEGF generation, and proliferation in human vascular endothelial cells. *FASEB journal : official publication of the Federation of American Societies for Experimental Biology,* **19**(3), pp. 446-448.

MURPHY, J.F., LENNON, F., STEELE, C., KELLEHER, D., FITZGERALD, D. and LONG, A.C., 2005b. Engagement of CD44 modulates cyclooxygenase induction, VEGF generation, and proliferation in human vascular endothelial cells. *FASEB journal : official publication of the Federation of American Societies for Experimental Biology,* **19**(3), pp. 446-448.

NAGARAJU, G.P., DONTULA, R., EL-RAYES, B.F. and LAKKA, S.S., 2014. Molecular mechanisms underlying the divergent roles of SPARC in human carcinogenesis. *Carcinogenesis,* **35**(5), pp. 967-973.

NAKAE, J., KITAMURA, T., KITAMURA, Y., BIGGS, W.H.,3rd, ARDEN, K.C. and ACCILI, D., 2003. The forkhead transcription factor Foxo1 regulates adipocyte differentiation. *Developmental cell,* **4**(1), pp. 119-129.

NAKAJIMA, M., HASHIMOTO, M., WANG, F., YAMANAGA, K., NAKAMURA, N., UCHIDA, T. and YAMANOUCHI, K., 1997. Aging decreases the production of PGI2 in rat aortic endothelial cells. *Experimental gerontology,* **32**(6), pp. 685-693.

NARITA, M., NUNEZ, S., HEARD, E., NARITA, M., LIN, A.W., HEARN, S.A., SPECTOR, D.L., HANNON, G.J. and LOWE, S.W., 2003. Rb-mediated heterochromatin formation and silencing of E2F target genes during cellular senescence. *Cell,* **113**(6), pp. 703-716.

NARUSE, K., SHIMIZU, K., MURAMATSU, M., TOKI, Y., MIYAZAKI, Y., OKUMURA, K., HASHIMOTO, H. and ITO, T., 1994. Long-term inhibition of NO synthesis promotes atherosclerosis in the hypercholesterolemic rabbit thoracic aorta. PGH2 does not contribute to impaired endothelium-dependent relaxation. *Arteriosclerosis and Thrombosis : A Journal of Vascular Biology / American Heart Association,* **14**(5), pp. 746-752.

NATHAN, C., 2002. Points of control in inflammation. *Nature,* **420**(6917), pp. 846-852.

NEGRUTSKII, B.S. and EL'SKAYA, A.V., 1998. Eukaryotic translation elongation factor 1 alpha: structure, expression, functions, and possible role in aminoacyl-tRNA channeling. *Progress in nucleic acid research and molecular biology,* **60**, pp. 47-78.

NICHOLLS, C., PINTO, A.R., LI, H., LI, L., WANG, L., SIMPSON, R. and LIU, J.P., 2012. Glyceraldehyde-3-phosphate dehydrogenase (GAPDH) induces cancer cell senescence by interacting with telomerase RNA component. *Proceedings of the National Academy of Sciences of the United States of America,* **109**(33), pp. 13308-13313.

O'BRIEN, K.D., MCDONALD, T.O., CHAIT, A., ALLEN, M.D. and ALPERS, C.E., 1996. Neovascular expression of E-selectin, intercellular adhesion molecule-1, and vascular cell adhesion molecule-1 in human atherosclerosis and their relation to intimal leukocyte content. *Circulation,* **93**(4), pp. 672-682.

OHUCHIDA, K., MIZUMOTO, K., MURAKAMI, M., QIAN, L.W., SATO, N., NAGAI, E., MATSUMOTO, K., NAKAMURA, T. and TANAKA, M., 2004. Radiation to stromal fibroblasts increases invasiveness of pancreatic cancer cells through tumor-stromal interactions. *Cancer research,* **64**(9), pp. 3215-3222.

OLIVE, M., HARTEN, I., MITCHELL, R., BEERS, J.K., DJABALI, K., CAO, K., ERDOS, M.R., BLAIR, C., FUNKE, B., SMOOT, L., GERHARD-HERMAN, M., MACHAN, J.T., KUTYS, R., VIRMANI, R., COLLINS, F.S., WIGHT, T.N., NABEL, E.G. and GORDON, L.B., 2010. Cardiovascular pathology in Hutchinson-Gilford progeria: correlation with the vascular pathology of aging. *Arteriosclerosis, Thrombosis, and Vascular Biology,* **30**(11), pp. 2301-2309.

OLTERSDORF, T., ELMORE, S.W., SHOEMAKER, A.R., ARMSTRONG, R.C., AUGERI, D.J., BELLI, B.A., BRUNCKO, M., DECKWERTH, T.L., DINGES, J., HAJDUK, P.J., JOSEPH, M.K., KITADA, S., KORSMEYER, S.J., KUNZER, A.R., LETAI, A., LI, C., MITTEN, M.J., NETTESHEIM, D.G., NG, S., NIMMER, P.M., O'CONNOR, J.M., OLEKSIJEW, A., PETROS, A.M., REED, J.C., SHEN, W., TAHIR, S.K., THOMPSON, C.B., TOMASELLI, K.J., WANG, B., WENDT, M.D., ZHANG, H., FESIK, S.W. and ROSENBERG, S.H., 2005. An inhibitor of Bcl-2 family proteins induces regression of solid tumours. *Nature,* **435**(7042), pp. 677-681.

ONAT, D., BRILLON, D., COLOMBO, P.C. and SCHMIDT, A.M., 2011. Human vascular endothelial cells: a model system for studying vascular inflammation in diabetes and atherosclerosis. *Current diabetes reports,* **11**(3), pp. 193-202.

OSTERUD, B., BAJAJ, M.S. and BAJAJ, S.P., 1995. Sites of tissue factor pathway inhibitor (TFPI) and tissue factor expression under physiologic and pathologic conditions. On behalf of the

Subcommittee on Tissue factor Pathway Inhibitor (TFPI) of the Scientific and Standardization Committee of the ISTH. *Thrombosis and haemostasis,* **73**(5), pp. 873-875.

OVADYA, Y. and KRIZHANOVSKY, V., 2014. Senescent cells: SASPected drivers of age-related pathologies. *Biogerontology,* **15**(6), pp. 627-642.

OZCAN, S., ALESSIO, N., ACAR, M.B., MERT, E., OMERLI, F., PELUSO, G. and GALDERISI, U., 2016. Unbiased analysis of senescence associated secretory phenotype (SASP) to identify common components following different genotoxic stresses. *Aging,* **8**(7), pp. 1316-1329.

OZKOR, M.A. and QUYYUMI, A.A., 2011. Endothelium-derived hyperpolarizing factor and vascular function. *Cardiology research and practice,* **2011**, pp. 156146.

PANT, S., DESHMUKH, A., GURUMURTHY, G.S., POTHINENI, N.V., WATTS, T.E., ROMEO, F. and MEHTA, J.L., 2014. Inflammation and atherosclerosis--revisited. *Journal of cardiovascular pharmacology and therapeutics,* **19**(2), pp. 170-178.

PARK, J.G., RYU, S.Y., JUNG, I.H., LEE, Y.H., KANG, K.J., LEE, M.R., LEE, M.N., SONN, S.K., LEE, J.H., LEE, H., OH, G.T., MOON, K. and SHIM, H., 2013. Evaluation of VCAM-1 antibodies as therapeutic agent for atherosclerosis in apolipoprotein E-deficient mice. *Atherosclerosis,* **226**(2), pp. 356-363.

PARRINELLO, S., COPPE, J.P., KRTOLICA, A. and CAMPISI, J., 2005. Stromal-epithelial interactions in aging and cancer: senescent fibroblasts alter epithelial cell differentiation. *Journal of cell science,* **118**(Pt 3), pp. 485-496.

PASSOS, J.F., NELSON, G., WANG, C., RICHTER, T., SIMILLION, C., PROCTOR, C.J., MIWA, S., OLIJSLAGERS, S., HALLINAN, J., WIPAT, A., SARETZKI, G., RUDOLPH, K.L., KIRKWOOD, T.B. and VON ZGLINICKI, T., 2010. Feedback between p21 and reactive oxygen production is necessary for cell senescence. *Molecular systems biology,* **6**, pp. 347.

PASSOS, J.F., SARETZKI, G., AHMED, S., NELSON, G., RICHTER, T., PETERS, H., WAPPLER, I., BIRKET, M.J., HAROLD, G., SCHAEUBLE, K., BIRCH-MACHIN, M.A., KIRKWOOD, T.B. and VON ZGLINICKI, T., 2007. Mitochondrial dysfunction accounts for the stochastic heterogeneity in telomere-dependent senescence. *PLoS biology,* **5**(5), pp. e110.

PELLEGRINI, M., CELESTE, A., DIFILIPPANTONIO, S., GUO, R., WANG, W., FEIGENBAUM, L. and NUSSENZWEIG, A., 2006. Autophosphorylation at serine 1987 is dispensable for murine Atm activation in vivo. *Nature,* **443**(7108), pp. 222-225.

PILARSKI, L.M., YACYSHYN, B.R., JENSEN, G.S., PRUSKI, E. and PABST, H.F., 1991. Beta 1 integrin (CD29) expression on human postnatal T cell subsets defined by selective CD45 isoform expression. *Journal of immunology (Baltimore, Md.: 1950),* **147**(3), pp. 830-837.

POBER, J.S. and COTRAN, R.S., 1990. Cytokines and endothelial cell biology. *Physiological Reviews,* **70**(2), pp. 427-451.

POLAKIS, P., 2012. Wnt signaling in cancer. *Cold Spring Harbor perspectives in biology,* **4**(5), pp. 10.1101/cshperspect.a008052.

POURRAJAB, F., VAKILI ZARCH, A., HEKMATIMOGHADDAM, S. and ZARE-KHORMIZI, M.R., 2015. The master switchers in the aging of cardiovascular system, reverse senescence by microRNA signatures; as highly conserved molecules. *Progress in biophysics and molecular biology,* **119**(2), pp. 111-128.

PRATTICHIZZO, F., GIULIANI, A., RECCHIONI, R., BONAFE, M., MARCHESELLI, F., DE CAROLIS, S., CAMPANATI, A., GIULIODORI, K., RIPPO, M.R., BRUGE, F., TIANO, L., MICUCCI, C., CERIELLO, A., OFFIDANI, A., PROCOPIO, A.D. and OLIVIERI, F., 2016a. Anti-TNF-alpha treatment modulates SASP and SASP-related microRNAs in endothelial cells and in circulating angiogenic cells. *Oncotarget,* **7**(11), pp. 11945-11958.

PRATTICHIZZO, F., GIULIANI, A., RECCHIONI, R., BONAFE, M., MARCHESELLI, F., DE CAROLIS, S., CAMPANATI, A., GIULIODORI, K., RIPPO, M.R., BRUGE, F., TIANO, L., MICUCCI, C., CERIELLO, A., OFFIDANI, A., PROCOPIO, A.D. and OLIVIERI, F., 2016b. Anti-TNF-alpha treatment modulates SASP and SASP-related microRNAs in endothelial cells and in circulating angiogenic cells. *Oncotarget,* **7**(11), pp. 11945-11958.

PUNCHARD, N.A., WHELAN, C.J. and ADCOCK, I., 2004. The Journal of Inflammation. *Journal of inflammation (London, England),* **1**(1), pp. 1.

RAHMAN, A., KEFER, J., BANDO, M., NILES, W.D. and MALIK, A.B., 1998a. E-selectin expression in human endothelial cells by TNF-alpha-induced oxidant generation and NF-kappaB activation. *The American Journal of Physiology,* **275**(3 Pt 1), pp. L533-44.

RAHMAN, A., KEFER, J., BANDO, M., NILES, W.D. and MALIK, A.B., 1998b. E-selectin expression in human endothelial cells by TNF-alpha-induced oxidant generation and NF-kappaB activation. *The American Journal of Physiology,* **275**(3 Pt 1), pp. L533-44.

RAO, R.M., YANG, L., GARCIA-CARDENA, G. and LUSCINSKAS, F.W., 2007. Endothelial-dependent mechanisms of leukocyte recruitment to the vascular wall. *Circulation research,* **101**(3), pp. 234-247.

REISS, Y. and ENGELHARDT, B., 1999. T cell interaction with ICAM-1-deficient endothelium in vitro: transendothelial migration of different T cell populations is mediated by endothelial ICAM-1 and ICAM-2. *International immunology,* **11**(9), pp. 1527-1539.

RENNIE, M.J., SMITH, K. and WATT, P.W., 1994. Measurement of human tissue protein synthesis: an optimal approach. *The American Journal of Physiology,* **266**(3 Pt 1), pp. E298-307.

REVECHON, G., VICECONTE, N., MCKENNA, T., CARVAJAL, A.S., VRTACNIK, P., STENVINKEL, P., LUNDGREN, T., HULTENBY, K., FRANCO, I. and ERIKSSON, M., 2017. Rare progerin-expressing preadipocytes and adipocytes contribute to tissue depletion over time. *Scientific reports,* **7**(1), pp. 4405-017-04492-0.

RICHARDSON, M.R., LAI, X., WITZMANN, F.A. and YODER, M.C., 2010. Venous and arterial endothelial proteomics: mining for markers and mechanisms of endothelial diversity. *Expert review of proteomics,* **7**(6), pp. 823-831.

RITSCHKA, B., STORER, M., MAS, A., HEINZMANN, F., ORTELLS, M.C., MORTON, J.P., SANSOM, O.J., ZENDER, L. and KEYES, W.M., 2017. The senescence-associated secretory phenotype induces cellular plasticity and tissue regeneration. *Genes & development,* **31**(2), pp. 172-183.

ROBERTSON, J., LANG, S., LAMBERT, P.A. and MARTIN, P.E., 2010. Peptidoglycan derived from Staphylococcus epidermidis induces Connexin43 hemichannel activity with consequences on the innate immune response in endothelial cells. *The Biochemical journal,* **432**(1), pp. 133-143.

RODIER, F. and CAMPISI, J., 2011. Four faces of cellular senescence. *The Journal of cell biology,* **192**(4), pp. 547-556.

RODIER, F., COPPE, J.P., PATIL, C.K., HOEIJMAKERS, W.A., MUNOZ, D.P., RAZA, S.R., FREUND, A., CAMPEAU, E., DAVALOS, A.R. and CAMPISI, J., 2009. Persistent DNA damage signalling triggers senescence-associated inflammatory cytokine secretion. *Nature cell biology,* **11**(8), pp. 973-979.

RODRIGUEZ, G., MAGO, N. and ROSA, F., 2009. Role of inflammation in atherogenesis. *Investigacion clinica,* **50**(1), pp. 109-129.

SAGRIPANTI, A. and CARPI, A., 2000. Antithrombotic and prothrombotic activities of the vascular endothelium. *Biomedicine & pharmacotherapy = Biomedecine & pharmacotherapie,* **54**(2), pp. 107-111.

SCHACHINGER, V., BRITTEN, M.B. and ZEIHER, A.M., 2000. Prognostic impact of coronary vasodilator dysfunction on adverse long-term outcome of coronary heart disease. *Circulation,* **101**(16), pp. 1899-1906.

SCHMIDT, E.K., CLAVARINO, G., CEPPI, M. and PIERRE, P., 2009. SUnSET, a nonradioactive method to monitor protein synthesis. *Nature methods,* **6**(4), pp. 275-277.

SCHNEIDER-POETSCH, T., JU, J., EYLER, D.E., DANG, Y., BHAT, S., MERRICK, W.C., GREEN, R., SHEN, B. and LIU, J.O., 2010. Inhibition of eukaryotic translation elongation by cycloheximide and lactimidomycin. *Nature chemical biology,* **6**(3), pp. 209-217.

SCHNELLMANN, R.G., 1988. Mechanisms of t-butyl hydroperoxide-induced toxicity to rabbit renal proximal tubules. *The American Journal of Physiology,* **255**(1 Pt 1), pp. C28-33.

SHAO, L., FENG, W., LI, H., GARDNER, D., LUO, Y., WANG, Y., LIU, L., MENG, A., SHARPLESS, N.E. and ZHOU, D., 2014. Total body irradiation causes long-term mouse BM injury via induction of HSC premature senescence in an Ink4a- and Arf-independent manner. *Blood,* **123**(20), pp. 3105-3115.

SHAY, J.W., WRIGHT, W.E. and WERBIN, H., 1991. Defining the molecular mechanisms of human cell immortalization. *Biochimica et biophysica acta,* **1072**(1), pp. 1-7.

SHELTON, D.N., CHANG, E., WHITTIER, P.S., CHOI, D. and FUNK, W.D., 1999. Microarray analysis of replicative senescence. *Current biology : CB,* **9**(17), pp. 939-945.

SHIMIZU, Y., IRANI, A.M., BROWN, E.J., ASHMAN, L.K. and SCHWARTZ, L.B., 1995. Human mast cells derived from fetal liver cells cultured with stem cell factor express a functional CD51/CD61 (alpha v beta 3) integrin. *Blood,* **86**(3), pp. 930-939.

SILVA, G.C., ABBAS, M., KHEMAIS-BENKHIAT, S., BURBAN, M., RIBEIRO, T.P., TOTI, F., IDRIS-KHODJA, N., CORTES, S.F. and SCHINI-KERTH, V.B., 2017. Replicative senescence promotes

prothrombotic responses in endothelial cells: Role of NADPH oxidase- and cyclooxygenase-derived oxidative stress. *Experimental gerontology,* **93**, pp. 7-15.

SMITH, J.R. and LINCOLN, D.W.,2nd, 1984. Aging of cells in culture. *International review of cytology,* **89**, pp. 151-177.

SPENCER, J.P., JENNER, A., ARUOMA, O.I., CROSS, C.E., WU, R. and HALLIWELL, B., 1996. Oxidative DNA damage in human respiratory tract epithelial cells. Time course in relation to DNA strand breakage. *Biochemical and biophysical research communications,* **224**(1), pp. 17-22.

TAHARA, H., SATO, E., NODA, A. and IDE, T., 1995. Increase in expression level of p21sdi1/cip1/waf1 with increasing division age in both normal and SV40-transformed human fibroblasts. *Oncogene,* **10**(5), pp. 835-840.

TAKAISHI, M., MAKINO, T., MOROHASHI, M. and HUH, N.H., 2005. Identification of human hornerin and its expression in regenerating and psoriatic skin. *The Journal of biological chemistry,* **280**(6), pp. 4696-4703.

TALAPATRA, S., WAGNER, J.D. and THOMPSON, C.B., 2002. Elongation factor-1 alpha is a selective regulator of growth factor withdrawal and ER stress-induced apoptosis. *Cell death and differentiation,* **9**(8), pp. 856-861.

THOMAS, S.L., ALAM, R., LEMKE, N., SCHULTZ, L.R., GUTIERREZ, J.A. and REMPEL, S.A., 2010. PTEN augments SPARC suppression of proliferation and inhibits SPARC-induced migration by suppressing SHC-RAF-ERK and AKT signaling. *Neuro-oncology,* **12**(9), pp. 941-955.

TOBA, H., DE CASTRO BRAS, L.E., BAICU, C.F., ZILE, M.R., LINDSEY, M.L. and BRADSHAW, A.D., 2016. Increased ADAMTS1 mediates SPARC-dependent collagen deposition in the aging myocardium. *American journal of physiology.Endocrinology and metabolism,* **310**(11), pp. E1027-35.

TOUSSAINT, O., MEDRANO, E.E. and VON ZGLINICKI, T., 2000. Cellular and molecular mechanisms of stress-induced premature senescence (SIPS) of human diploid fibroblasts and melanocytes. *Experimental gerontology,* **35**(8), pp. 927-945.

TREISMAN, R., 1986. Identification of a protein-binding site that mediates transcriptional response of the c-fos gene to serum factors. *Cell,* **46**(4), pp. 567-574.

TRIGUEROS-MOTOS, L., GONZALEZ, J.M., RIVERA, J. and ANDRES, V., 2011. Hutchinson-Gilford progeria syndrome, cardiovascular disease and oxidative stress. *Frontiers in bioscience (Scholar edition),* **3**, pp. 1285-1297.

TURK, V., STOKA, V., VASILJEVA, O., RENKO, M., SUN, T., TURK, B. and TURK, D., 2012. Cysteine cathepsins: from structure, function and regulation to new frontiers. *Biochimica et biophysica acta,* **1824**(1), pp. 68-88.

UETSUKI, T., NAITO, A., NAGATA, S. and KAZIRO, Y., 1989. Isolation and characterization of the human chromosomal gene for polypeptide chain elongation factor-1 alpha. *The Journal of biological chemistry,* **264**(10), pp. 5791-5798.

UNTERLUGGAUER, H., HAMPEL, B., ZWERSCHKE, W. and JANSEN-DURR, P., 2003. Senescence-associated cell death of human endothelial cells: the role of oxidative stress. *Experimental gerontology,* **38**(10), pp. 1149-1160.

UROSEVIC, J., GARCIA-ALBENIZ, X., PLANET, E., REAL, S., CESPEDES, M.V., GUIU, M., FERNANDEZ, E., BELLMUNT, A., GAWRZAK, S., PAVLOVIC, M., MANGUES, R., DOLADO, I., BARRIGA, F.M., NADAL, C., KEMENY, N., BATLLE, E., NEBREDA, A.R. and GOMIS, R.R., 2014. Colon cancer cells colonize the lung from established liver metastases through p38 MAPK signalling and PTHLH. *Nature cell biology,* **16**(7), pp. 685-694.

VAKKILA, J. and LOTZE, M.T., 2004. Inflammation and necrosis promote tumour growth. *Nature reviews.Immunology,* **4**(8), pp. 641-648.

VALLABHAPURAPU, S. and KARIN, M., 2009. Regulation and function of NF-kappaB transcription factors in the immune system. *Annual Review of Immunology,* **27**, pp. 693-733.

VAN DE STOLPE, A. and VAN DER SAAG, P.T., 1996. Intercellular adhesion molecule-1. *Journal of Molecular Medicine (Berlin, Germany),* **74**(1), pp. 13-33.

VAN HINSBERGH, V.W., 2012. Endothelium--role in regulation of coagulation and inflammation. *Seminars in immunopathology,* **34**(1), pp. 93-106.

VAN HOEWYK, D., 2016. Use of the non-radioactive SUnSET method to detect decreased protein synthesis in proteasome inhibited Arabidopsis roots. *Plant methods,* **12**, pp. 20-016-0120-z. eCollection 2016.

VASILE, E., TOMITA, Y., BROWN, L.F., KOCHER, O. and DVORAK, H.F., 2001. Differential expression of thymosin beta-10 by early passage and senescent vascular endothelium is modulated by VPF/VEGF: evidence for senescent endothelial cells in vivo at sites of atherosclerosis. *FASEB journal : official publication of the Federation of American Societies for Experimental Biology,* **15**(2), pp. 458-466.

VATHIPADIEKAL, V., WANG, V., WEI, W., WALDRON, L., DRAPKIN, R., GILLETTE, M., SKATES, S. and BIRRER, M., 2015. Creation of a Human Secretome: A Novel Composite Library of Human Secreted Proteins: Validation Using Ovarian Cancer Gene Expression Data and a Virtual Secretome Array. *Clinical cancer research : an official journal of the American Association for Cancer Research,* **21**(21), pp. 4960-4969.

WANG, F., MARSHALL, C.B., YAMAMOTO, K., LI, G.Y., PLEVIN, M.J., YOU, H., MAK, T.W. and IKURA, M., 2008. Biochemical and structural characterization of an intramolecular interaction in FOXO3a and its binding with p53. *Journal of Molecular Biology,* **384**(3), pp. 590-603.

WANG, J., SHOU, J. and CHEN, X., 2000. Dickkopf-1, an inhibitor of the Wnt signaling pathway, is induced by p53. *Oncogene,* **19**(14), pp. 1843-1848.

WANG, J.C. and BENNETT, M., 2012. Aging and atherosclerosis: mechanisms, functional consequences, and potential therapeutics for cellular senescence. *Circulation research,* **111**(2), pp. 245-259.

WANG, S., MOERMAN, E.J., JONES, R.A., THWEATT, R. and GOLDSTEIN, S., 1996. Characterization of IGFBP-3, PAI-1 and SPARC mRNA expression in senescent fibroblasts. *Mechanisms of ageing and development,* **92**(2-3), pp. 121-132.

WANG, X., MARTINDALE, J.L., LIU, Y. and HOLBROOK, N.J., 1998. The cellular response to oxidative stress: influences of mitogen-activated protein kinase signalling pathways on cell survival. *The Biochemical journal,* **333 (Pt 2)**(Pt 2), pp. 291-300.

WON, C.H., KWON, O.S., KANG, Y.J., YOO, H.G., LEE, D.H., CHUNG, J.H., KIM, K.H., PARK, W.S., PARK, N.H., CHO, K., KWON, S.O., CHOI, J.S. and EUN, H.C., 2012. Comparative secretome analysis of human follicular dermal papilla cells and fibroblasts using shotgun proteomics. *BMB reports,* **45**(4), pp. 253-258.

WU, Z., MEYER-HOFFERT, U., REITHMAYER, K., PAUS, R., HANSMANN, B., HE, Y., BARTELS, J., GLASER, R., HARDER, J. and SCHRODER, J.M., 2009. Highly complex peptide aggregates of the S100 fused-type protein hornerin are present in human skin. *The Journal of investigative dermatology,* **129**(6), pp. 1446-1458.

XU, M., TCHKONIA, T., DING, H., OGRODNIK, M., LUBBERS, E.R., PIRTSKHALAVA, T., WHITE, T.A., JOHNSON, K.O., STOUT, M.B., MEZERA, V., GIORGADZE, N., JENSEN, M.D., LEBRASSEUR, N.K. and KIRKLAND, J.L., 2015. JAK inhibition alleviates the cellular senescence-associated secretory phenotype and frailty in old age. *Proceedings of the National Academy of Sciences of the United States of America,* **112**(46), pp. E6301-10.

YAN, Q. and SAGE, E.H., 1999. SPARC, a matricellular glycoprotein with important biological functions. *The journal of histochemistry and cytochemistry : official journal of the Histochemistry Society,* **47**(12), pp. 1495-1506.

YANAKA, M., HONMA, T., SATO, K., SHINOHARA, N., ITO, J., TANAKA, Y., TSUDUKI, T. and IKEDA, I., 2011a. Increased monocytic adhesion by senescence in human umbilical vein endothelial cells. *Bioscience, biotechnology, and biochemistry,* **75**(6), pp. 1098-1103.

YANAKA, M., HONMA, T., SATO, K., SHINOHARA, N., ITO, J., TANAKA, Y., TSUDUKI, T. and IKEDA, I., 2011b. Increased monocytic adhesion by senescence in human umbilical vein endothelial cells. *Bioscience, biotechnology, and biochemistry,* **75**(6), pp. 1098-1103.

YANG, Y.H., DUDOIT, S., LUU, P., LIN, D.M., PENG, V., NGAI, J. and SPEED, T.P., 2002. Normalization for cDNA microarray data: a robust composite method addressing single and multiple slide systematic variation. *Nucleic acids research,* **30**(4), pp. e15.

YENTRAPALLI, R., AZIMZADEH, O., BARJAKTAROVIC, Z., SARIOGLU, H., WOJCIK, A., HARMS-RINGDAHL, M., ATKINSON, M.J., HAGHDOOST, S. and TAPIO, S., 2013. Quantitative proteomic analysis reveals induction of premature senescence in human umbilical vein endothelial cells exposed to chronic low-dose rate gamma radiation. *Proteomics,* **13**(7), pp. 1096-1107.

YENTRAPALLI, R., AZIMZADEH, O., KRAEMER, A., MALINOWSKY, K., SARIOGLU, H., BECKER, K.F., ATKINSON, M.J., MOERTL, S. and TAPIO, S., 2015. Quantitative and integrated proteome and microRNA analysis of endothelial replicative senescence. *Journal of proteomics,* **126**, pp. 12-23.

YIN, X., BERN, M., XING, Q., HO, J., VINER, R. and MAYR, M., 2013. Glycoproteomic analysis of the secretome of human endothelial cells. *Molecular & cellular proteomics : MCP,* **12**(4), pp. 956-978.

YIN, Y., ZHOU, Z., LIU, W., CHANG, Q., SUN, G. and DAI, Y., 2017. *Vascular endothelial cells senescence is associated with NOD-like receptor family pyrin domain-containing 3 (NLRP3) inflammasome activation via reactive oxygen species (ROS)/thioredoxin-interacting protein (TXNIP) pathway.*

YOUM, Y.H., GRANT, R.W., MCCABE, L.R., ALBARADO, D.C., NGUYEN, K.Y., RAVUSSIN, A., PISTELL, P., NEWMAN, S., CARTER, R., LAQUE, A., MUNZBERG, H., ROSEN, C.J., INGRAM, D.K., SALBAUM, J.M. and DIXIT, V.D., 2013. Canonical Nlrp3 inflammasome links systemic low-grade inflammation to functional decline in aging. *Cell metabolism,* **18**(4), pp. 519-532.

YOUM, Y.H., KANNEGANTI, T.D., VANDANMAGSAR, B., ZHU, X., RAVUSSIN, A., ADIJIANG, A., OWEN, J.S., THOMAS, M.J., FRANCIS, J., PARKS, J.S. and DIXIT, V.D., 2012. The Nlrp3 inflammasome promotes age-related thymic demise and immunosenescence. *Cell reports,* **1**(1), pp. 56-68.

YOUNG, M.R., 2012. Endothelial cells in the eyes of an immunologist. *Cancer immunology, immunotherapy : CII,* **61**(10), pp. 1609-1616.

ZAINUDDIN, A., CHUA, K.H., ABDUL RAHIM, N. and MAKPOL, S., 2010. Effect of experimental treatment on GAPDH mRNA expression as a housekeeping gene in human diploid fibroblasts. *BMC molecular biology,* **11**, pp. 59-2199-11-59.

ZHAN, H., SUZUKI, T., AIZAWA, K., MIYAGAWA, K. and NAGAI, R., 2010. Ataxia telangiectasia mutated (ATM)-mediated DNA damage response in oxidative stress-induced vascular endothelial cell senescence. *The Journal of biological chemistry,* **285**(38), pp. 29662-29670.

ZHOU, M., DIWU, Z., PANCHUK-VOLOSHINA, N. and HAUGLAND, R.P., 1997. A stable nonfluorescent derivative of resorufin for the fluorometric determination of trace hydrogen peroxide: applications in detecting the activity of phagocyte NADPH oxidase and other oxidases. *Analytical Biochemistry,* **253**(2), pp. 162-168.

ZHU, C., YU, Y., MONTANI, J.P., MING, X.F. and YANG, Z., 2017. Arginase-I enhances vascular endothelial inflammation and senescence through eNOS-uncoupling. *BMC research notes,* **10**(1), pp. 82-017-2399-x.

9 Appendix

9.1 Appendix I

Abstracts and publications:

1. Sadaf Afreen, Dr Karl E Herbert. How Can I Make My Heart Young? poster presentation PGR festival, University of Leicester, June 2015. http://www2.le.ac.uk/institution/fpgr-archive/2015/meet/2015/sadaf-afreen

2. Sadaf Afreen, Farai Mutongwizo, Dr Gary Willars & Dr Nina Storey. Cardioprotective effects of GLP-1 7-36 and its major circulating metabolite, GLP-1 9-36 amide. Abstract, 4th Focused Cell Signalling, Leicester, UK, 23-24April.

3. Sadaf Afreen, Dr Karl E Herbert. CST1 discriminates between senescence due to replicative and stress-induced endothelial cell aging. Abstract, ATVB Scientific Session 2017, Minneapolis, 6-9 May 2017.

4. Sadaf Afreen, Dr Karl E Herbert. Adherence of monocytes to endothelial cells involves CD44 in replicative senescence but not in stress-induced senescence. Abstract, ICSA conference 2017, Paris, 16-19May, 2017.

5. Hypoxia downregulates protein S expression. VS Pilli, A Datta, S Afreen, D Catalano, G Szabo, R Majumder, Blood 132 (4), 452-455

9.2 Appendix II

9.3 Appendix II

Liquid Chromatography Tandem Mass Spectrometry Protein List:

List of all proteins identified during LC-MS/MS for secretome of senescent endothelial cells (for reference see chapter 5)

10 kDa heat shock protein, mitochondrial
14-3-3 protein beta/alpha
14-3-3 protein epsilon
14-3-3 protein gamma
14-3-3 protein zeta/delta
60 kDa heat shock protein, mitochondrial
6-phosphogluconolactonase
Actin, alpha cardiac muscle 1
Actin, cytoplasmic 1
Acyl carrier protein, mitochondrial
Adenylate kinase 2, mitochondrial
A-kinase anchor protein 12
Alcohol dehydrogenase [NADP(+)]
Alcohol dehydrogenase 1 OS=Saccharomyces cerevisiae
Aldose reductase
Alpha-actinin-4
Alpha-enolase
Alpha-N-acetylglucosaminidase
Aminopeptidase N
Amyloid beta A4 protein
Annexin A1
Annexin A3
Annexin A5
Annexin A6
Apolipoprotein A-I
Arylsulfatase A
Aspartate aminotransferase, cytoplasmic
Aspartate aminotransferase, mitochondrial
Astrocytic phosphoprotein PEA-15
ATP synthase subunit beta, mitochondrial
ATP-citrate synthase
Attractin
Band 4.1-like protein 3
Basal cell adhesion molecule
Basement membrane-specific heparan sulfate proteoglycan core protein
Beta-2-microglobulin
Biotinidase
Bleomycin hydrolase
Brain acid soluble protein 1
Branched-chain-amino-acid aminotransferase, mitochondrial
BTB/POZ domain-containing protein KCTD12
Cadherin-2
Calmodulin
Calmodulin-like protein 3
Calmodulin-like protein 5
Calreticulin
Caspase-14
Caspase-3
Catalase
Catenin delta-1
Cathepsin B
Cathepsin D

Cathepsin Z
Cation-independent mannose-6-phosphate receptor
C-C motif chemokine 14
CD109 antigen
CD166 antigen
CD44 antigen
CD59 glycoprotein
Cell surface glycoprotein MUC18
Cellular nucleic acid-binding protein
Chloride intracellular channel protein 1
Citrate synthase, mitochondrial
Coactosin-like protein
Collagen alpha-1(I) chain
Collagen alpha-1(III) chain
Collagen alpha-1(V) chain
Collagen alpha-1(VI) chain
Collagen alpha-1(XVIII) chain
Complement component C1q receptor
Connective tissue growth factor
Corneodesmosin
C-type lectin domain family 14 member A
Cystatin-A
Cystatin-B
Cystatin-C
Cysteine-rich motor neuron 1 protein
Cytochrome c
Cytosol aminopeptidase
D-dopachrome decarboxylase
Deoxyribonuclease-2-alpha
Desmocollin-1
Desmoglein-1
Desmoplakin
Dihydrolipoyl dehydrogenase, mitochondrial
Dihydropteridine reductase
Dihydropyrimidinase-related protein 2
Di-N-acetylchitobiase
Dipeptidyl peptidase 3
Dystroglycan
EGF-containing fibulin-like extracellular matrix protein 1
Elongation factor 1-alpha 2
Endoglin
Endoplasmic reticulum aminopeptidase 2
Endoplasmic reticulum resident protein 29
Endothelial cell-specific molecule 1
Endothelial protein C receptor
Enoyl-CoA delta isomerase 1, mitochondrial
Ephrin type-B receptor 2
Ephrin-B1
Epididymal secretory protein E1
Epididymis-specific alpha-mannosidase
ERO1-like protein alpha
Eukaryotic translation initiation factor 4B
Ezrin
Farnesyl pyrophosphate synthase
Fatty acid-binding protein, epidermal
Fibrinogen alpha chain
Fibronectin
Fibulin-1
Filaggrin-2
Filamin-C
Follistatin-related protein 1
Fumarate hydratase, mitochondrial
Galectin-1
Galectin-7
Gamma-enolase
Gamma-glutamylcyclotransferase

GDH/6PGL endoplasmic bifunctional protein
GDP-fucose protein O-fucosyltransferase 1
GDP-L-fucose synthase
Gelsolin
Glucosamine-6-phosphate isomerase 1
Glucosamine-6-phosphate isomerase 2
Glutamate dehydrogenase 1, mitochondrial
Glutathione reductase, mitochondrial
Glutathione S-transferase omega-1
Glutathione S-transferase P
Glutathione synthetase
Glyceraldehyde-3-phosphate dehydrogenase
Glycogenin-1
Glyoxalase domain-containing protein 4
Golgi membrane protein 1
Granulins
Group XV phospholipase A2
GrpE protein homolog 1, mitochondrial
Heat shock 70 kDa protein 1A/1B
Heat shock 70 kDa protein 4
Hematological and neurological expressed 1-like protein
Heme-binding protein 2
Heterogeneous nuclear ribonucleoprotein A1
Heterogeneous nuclear ribonucleoprotein D0
Heterogeneous nuclear ribonucleoproteins A2/B1
High mobility group protein HMGI-C
Histidine ammonia-lyase
Hornerin
Hypoxanthine-guanine phosphoribosyltransferase
Ig gamma-1 chain C region
Ig gamma-2 chain C region
Insulin-like growth factor-binding protein 7
Integrin alpha-5
Inter-alpha-trypsin inhibitor heavy chain H2
Intercellular adhesion molecule 2
Isoform 1 of Ubiquitin-conjugating enzyme E2 variant 1
Isoform 2 of Annexin A2
Isoform 2 of Arginase-1
Isoform 2 of Clusterin
Isoform 2 of Delta-aminolevulinic acid dehydratase
Isoform 2 of Dermcidin
Isoform 2 of Endoplasmic reticulum aminopeptidase 1
Isoform 2 of Eukaryotic initiation factor 4A-II
Isoform 2 of Eukaryotic translation initiation factor 5A-1
Isoform 2 of Fructose-bisphosphate aldolase A
Isoform 2 of Glucose-6-phosphate isomerase
Isoform 2 of Glyoxalase domain-containing protein 4
Isoform 2 of Hematological and neurological expressed 1 protein
Isoform 2 of Histone H2B type 2-F
Isoform 2 of Nucleoside diphosphate kinase A
Isoform 2 of Peptidyl-prolyl cis-trans isomerase NIMA-interacting 4
Isoform 2 of Receptor-type tyrosine-protein phosphatase mu
Isoform 2 of Small EDRK-rich factor 2
Isoform 2 of Spliceosome RNA helicase DDX39B
Isoform 2 of Transketolase
Isoform 2 of Tyrosine-protein phosphatase non-receptor type substrate 1
Isoform 3 of Acylpyruvase FAHD1, mitochondrial
Isoform 3 of Alpha-actinin-1
Isoform 3 of Calumenin
Isoform 3 of Drebrin
Isoform 3 of Hepatoma-derived growth factor
Isoform 3 of Integrin beta-1
Isoform 3 of L-lactate dehydrogenase A chain
Isoform 3 of Malate dehydrogenase, cytoplasmic
Isoform 3 of Nucleoside diphosphate kinase B
Isoform 3 of Receptor-type tyrosine-protein phosphatase kappa

Isoform 3 of Sulfatase-modifying factor 2
Isoform 4 of Alpha-actinin-1
Isoform 4 of Cadherin-13
Isoform 4 of Caldesmon
Isoform 4 of Calumenin
Isoform 4 of Protein tweety homolog 3
Isoform 5 of Acyl-CoA-binding protein
Isoform 5 of AP-3 complex subunit delta-1
Isoform 5 of Branched-chain-amino-acid aminotransferase, cytosolic
Isoform 5 of Cysteine-rich with EGF-like domain protein 2
Isoform 5 of Neuronal cell adhesion molecule
Isoform 5 of Radixin
Isoform 6 of Calpastatin
Isoform 6 of Inactive tyrosine-protein kinase 7
Isoform 7 of Tumor protein D54
Isoform 8 of Filamin-B
Isoform B of Membrane cofactor protein
Isoform Beta of Apoptosis regulator BAX
Isoform HMG-R of High mobility group protein HMG-I/HMG-Y
Isoform LAMP-2C of Lysosome-associated membrane glycoprotein 2
Isoform MBP-1 of Alpha-enolase
Isoform Sap-mu-9 of Prosaposin
Junction plakoglobin
Keratin, type I cytoskeletal 10
Keratin, type I cytoskeletal 13
Keratin, type I cytoskeletal 14
Keratin, type I cytoskeletal 16
Keratin, type I cytoskeletal 17
Keratin, type I cytoskeletal 9
Keratin, type II cytoskeletal 1
Keratin, type II cytoskeletal 1b
Keratin, type II cytoskeletal 2 epidermal
Keratin, type II cytoskeletal 4
Keratin, type II cytoskeletal 5
Keratin, type II cytoskeletal 6A
Keratin, type II cytoskeletal 6B
Keratin, type II cytoskeletal 78
Keratinocyte proline-rich protein
Lactoylglutathione lyase
Laminin subunit alpha-4
Laminin subunit beta-1
Laminin subunit gamma-1
Latexin
Leucine-rich repeat transmembrane protein FLRT2
Leukocyte elastase inhibitor
Leukotriene A-4 hydrolase
LIM SH3 domain protein 1
L-lactate dehydrogenase B chain and
Low-density lipoprotein receptor
Lymphatic vessel endothelial hyaluronic acid receptor 1
Lysosomal protective protein
Lysosome membrane protein 2
Lysosome-associated membrane glycoprotein 1
Malate dehydrogenase, mitochondrial
Mesencephalic astrocyte-derived neurotrophic factor
Metallothionein-2
Microtubule-associated protein 1B
Microtubule-associated protein 4
Moesin
Multimerin-1
Multiple coagulation factor deficiency protein 2
Myristoylated alanine-rich C-kinase substrate
N(G),N(G)-dimethylarginine dimethylaminohydrolase 1
N(G),N(G)-dimethylarginine dimethylaminohydrolase 2
N-acetylgalactosamine-6-sulfatase
NAD(P)H-hydrate epimerase

NAD-dependent malic enzyme, mitochondrial
Nestin
Neudesin
Neuroblast differentiation-associated protein AHNAK
Neuropilin-1
Neuropilin-2
Niemann-Pick C1 protein
NKG2D ligand 2
Non-histone chromosomal protein HMG-14
N-sulphoglucosamine sulphohydrolase
Nuclear transport factor 2
Nucleobindin-1
Omega-amidase NIT2
PDZ and LIM domain protein 5
Pentraxin-related protein PTX3
Peptidyl-prolyl cis-trans isomerase A
Peptidyl-prolyl cis-trans isomerase B
Peptidyl-prolyl cis-trans isomerase FKBP10
Peptidyl-prolyl cis-trans isomerase FKBP2
Peptidyl-prolyl cis-trans isomerase-like 1
Peroxiredoxin-1
Peroxiredoxin-2
Peroxiredoxin-4
Peroxiredoxin-6
PEST proteolytic signal-containing nuclear protein
Phosphatidylethanolamine-binding protein 1
Phosphoglucomutase-1
Phosphoglucomutase-2
Phosphoglycerate kinase 1
Phosphoglycerate mutase 1
Phospholipase D3
Phosphoserine aminotransferase
Pituitary tumor-transforming gene 1 protein-interacting protein
Plasminogen activator inhibitor 1
Plastin-3
Platelet basic protein
Platelet endothelial cell adhesion molecule
Platelet factor 4 variant
Prelamin-A/C
Procollagen-lysine,2-oxoglutarate 5-dioxygenase 1
Procollagen-lysine,2-oxoglutarate 5-dioxygenase 3
Protein canopy homolog 2
Protein CDV3 homolog
Protein CYR61
Protein disulfide-isomerase A3
Protein FAM3C
Protein jagged-1
Protein LYRIC
Protein NipSnap homolog 3A
Protein S100-A11
Protein S100-A13
Protein S100-A6
Protein S100-A7
Protein S100-A8
Protein S100-A9
Protein-glutamine gamma-glutamyltransferase E
Pterin-4-alpha-carbinolamine dehydratase
Purine nucleoside phosphorylase
Putative GTP cyclohydrolase 1 type 2 NIF3L1
Putative hydroxypyruvate isomerase
Putative phospholipase B-like 2
Putative trypsin-6
Pyridoxal kinase
Quinone oxidoreductase
Quinone oxidoreductase PIG3
Rab GDP dissociation inhibitor beta

Ras-related protein Rab-7a
Receptor-type tyrosine-protein phosphatase F
Receptor-type tyrosine-protein phosphatase gamma
Reticulocalbin-1
Reticulocalbin-3
Reticulon-4
Rho GDP-dissociation inhibitor 1
Rho GDP-dissociation inhibitor 2
Ribonuclease pancreatic
Ribonuclease T2
Roundabout homolog 4
S-adenosylmethionine synthase isoform type-2
Scavenger receptor class F member 1
Semaphorin-6B
Serine/threonine-protein phosphatase CPPED1
Serpin B12
Serpin B6
Serpin B9
Serpin H1
Serum albumin
Serum deprivation-response protein
SH3 domain-binding glutamic acid-rich-like protein
SH3 domain-binding glutamic acid-rich-like protein 3
Sialate O-acetylesterase
SPARC
Src substrate cortactin
Sulfhydryl oxidase 1
Superoxide dismutase [Cu-Zn]
Thioredoxin
Thioredoxin domain-containing protein 12
Thioredoxin domain-containing protein 5
Thioredoxin reductase 1, cytoplasmic
Thioredoxin reductase 2, mitochondrial
Thioredoxin-dependent peroxide reductase, mitochondrial
Thrombospondin-1
Thymosin beta-4
Transaldolase
Transferrin receptor protein 1
Transgelin-2
Trans-Golgi network integral membrane protein 2
Translation machinery-associated protein 7
Translationally-controlled tumor protein
Triosephosphate isomerase
Tripeptidyl-peptidase 1
Tropomyosin alpha-3 chain
Trypsin-1
Trypsin-2
Tubulin alpha-1B chain
Tubulin-specific chaperone A
Tumor necrosis factor receptor superfamily member 1A
Tyrosine-protein kinase receptor Tie-1
Tyrosine-protein kinase receptor UFO
Ubiquitin thioesterase OTUB1
Ubiquitin-40S ribosomal protein S27a
UMP-CMP kinase
UPF0556 protein C19orf10
Urokinase plasminogen activator surface receptor
UV excision repair protein RAD23 homolog B
Vacuolar protein sorting-associated protein 26A
Very low-density lipoprotein receptor
Vesicular integral-membrane protein VIP36
Vimentin
Vinculin
von Willebrand factor
Xaa-Pro dipeptidase
Zinc-alpha-2-glycoprotein

Table 9-1:List of identified protein in LC-MS/MS.

Complete list of proteins identified in replicative senescent (REPS) stress induced premature senescent (SIPS) and young HUVECs secretome treated with phorbol myristate acetate (PMA) in LC-MS/MS. Data were obtained from a pool of three biological replicates. List of differentially expressed proteins and details concerning protein identification in REPS, SIPS and control are respectively shown in Supplementary Tables in the CD attached.

9.4 Appendix III

Microarray data normalisation using R.

Following table, plots and dendrogram represent microarray data (chapter 4) normalisation using R

Figure 3 and 4 represent expression distribution normalisation

Figure 5 represents MDS plot

Figure 6 and 7 represents MA plots

Figure 8 represents cluster dendrogram

Hyb_Name	Sample_Name
5634871010_B	C1
5634871010_J	C2
5634871010_E	C3
5634871010_A	C4
5634871010_H	C5
5634871010_C	C6
5634871010_K	REPS 1
5634871010_D	REPS 2
5634871010_G	REPS 3
5634871010_L	REPS 4
5634871010_F	REPS 5
5634871010_I	REPS 6
5634871022_C	SC 1
5634871022_G	SC2
5634871022_I	SC3
5634871022_H	SC4
5634871022_B	SC5
5634871022_K	SC6
5634871022_D	SIPS 1

5634871022_E	**SIPS 2**
5634871022_L	**SIPS 3**
5634871022_A	**SIPS 4**
5634871022_J	**SIPS 5**
5634871022_F	**SIPS 6**

Table 9-2: Determination of HUVECs samples REPS, SIPS, S-control and control with microarray probe id.

1)

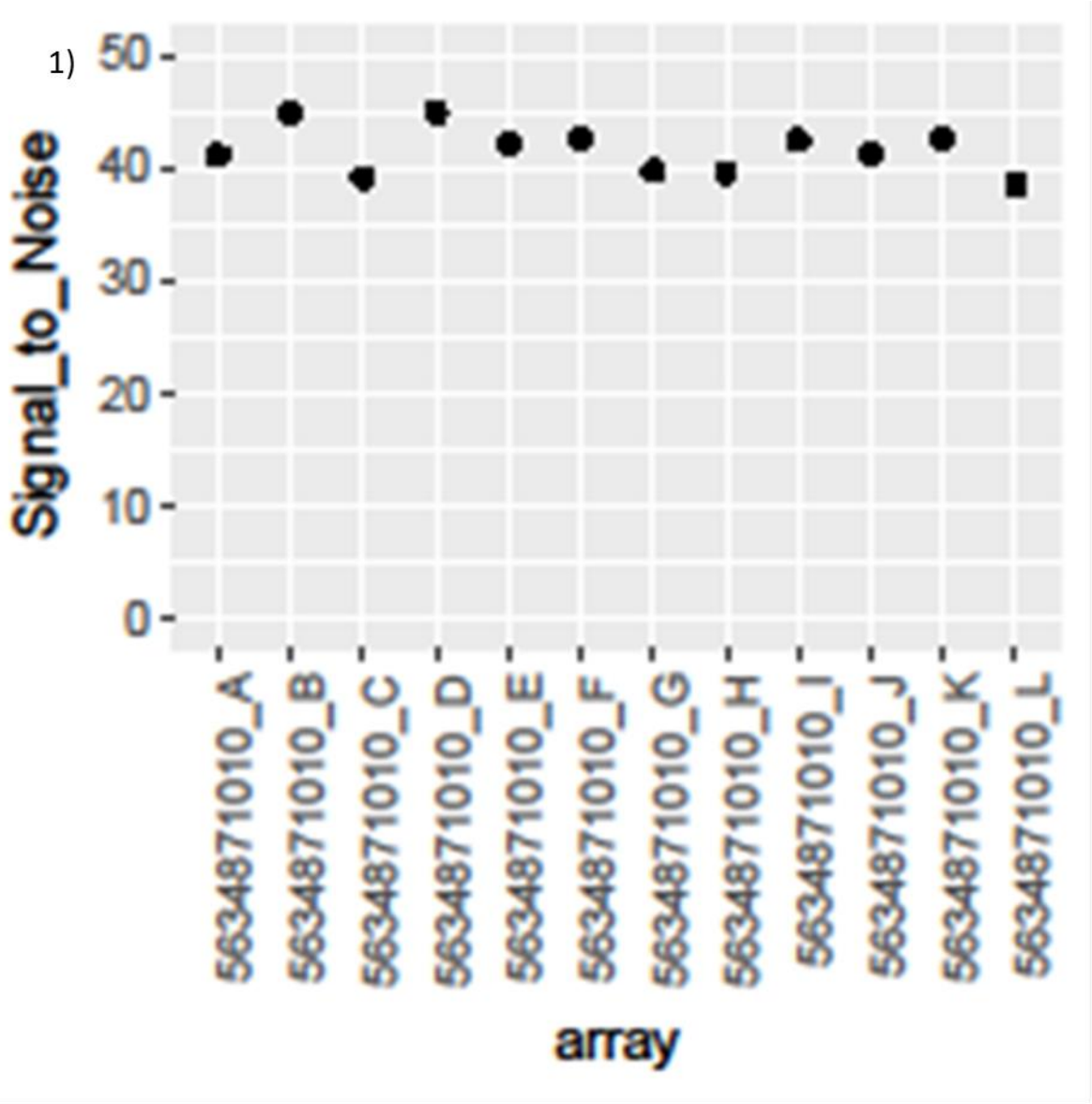

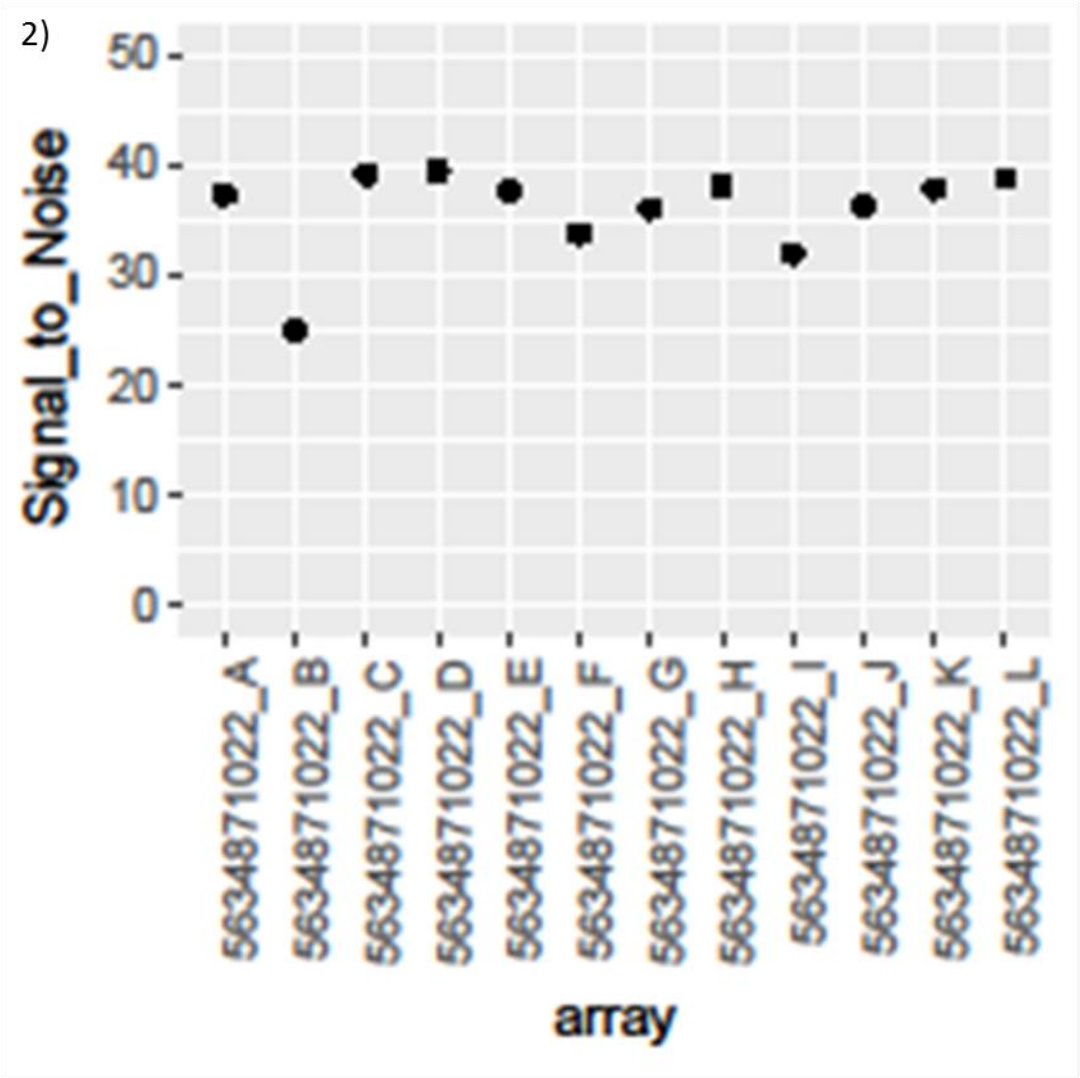

Figure 9-1: Determination of noise to signal ratio for 1) control and REPS 2) SIPS and SIPS control.

3)

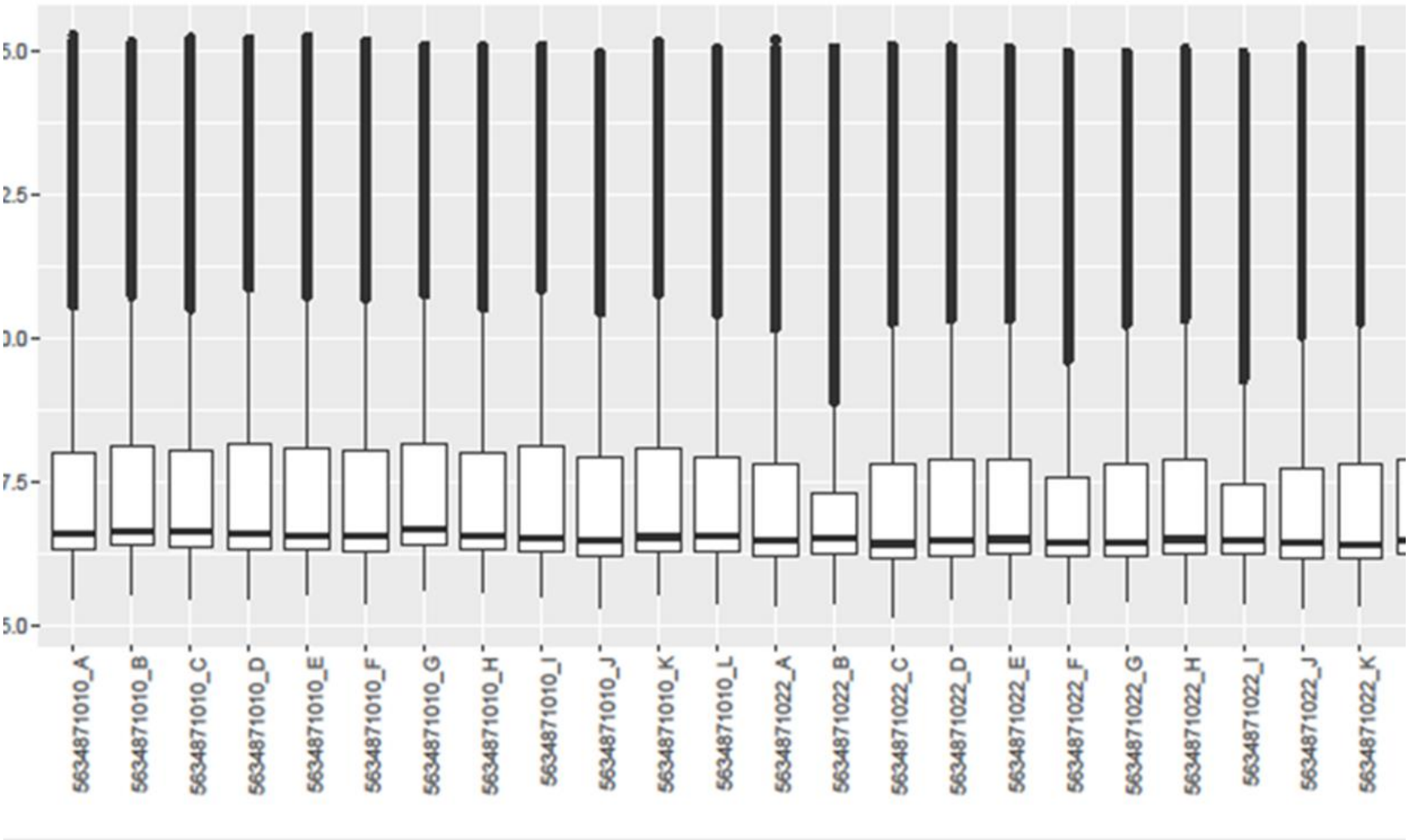
5.0
2.5
0.0
7.5
5.0
5634871010_A
5634871010_B
5634871010_C
5634871010_D
5634871010_E
5634871010_F
5634871010_G
5634871010_H
5634871010_I
5634871010_J
5634871010_K
5634871010_L
5634871022_A
5634871022_B
5634871022_C
5634871022_D
5634871022_E
5634871022_F
5634871022_G
5634871022_H
5634871022_I
5634871022_J
5634871022_K

4)

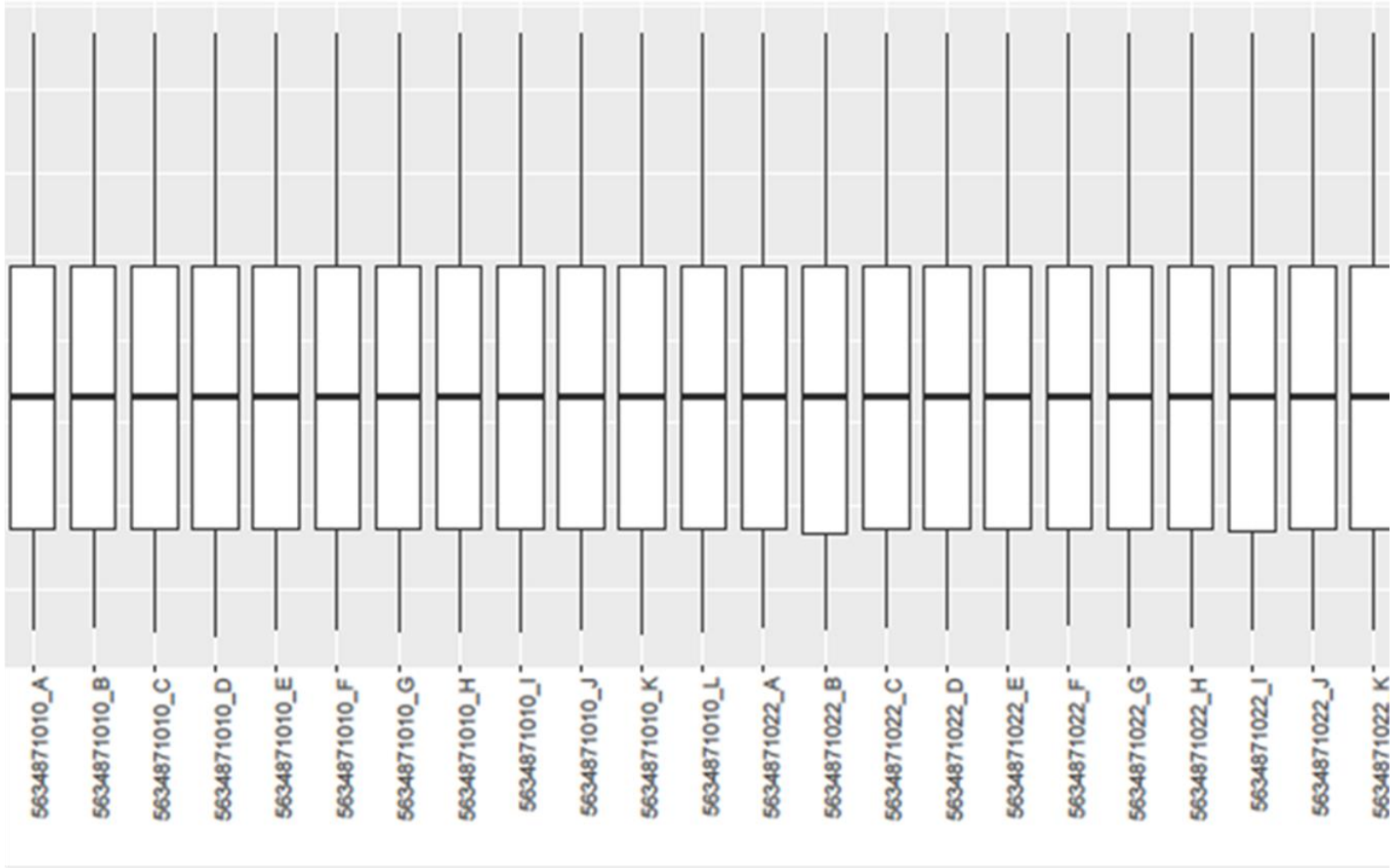

Figure 9-2: Represents samples distribution

expression 3) before normalisation and 4) after normalisation.

5)

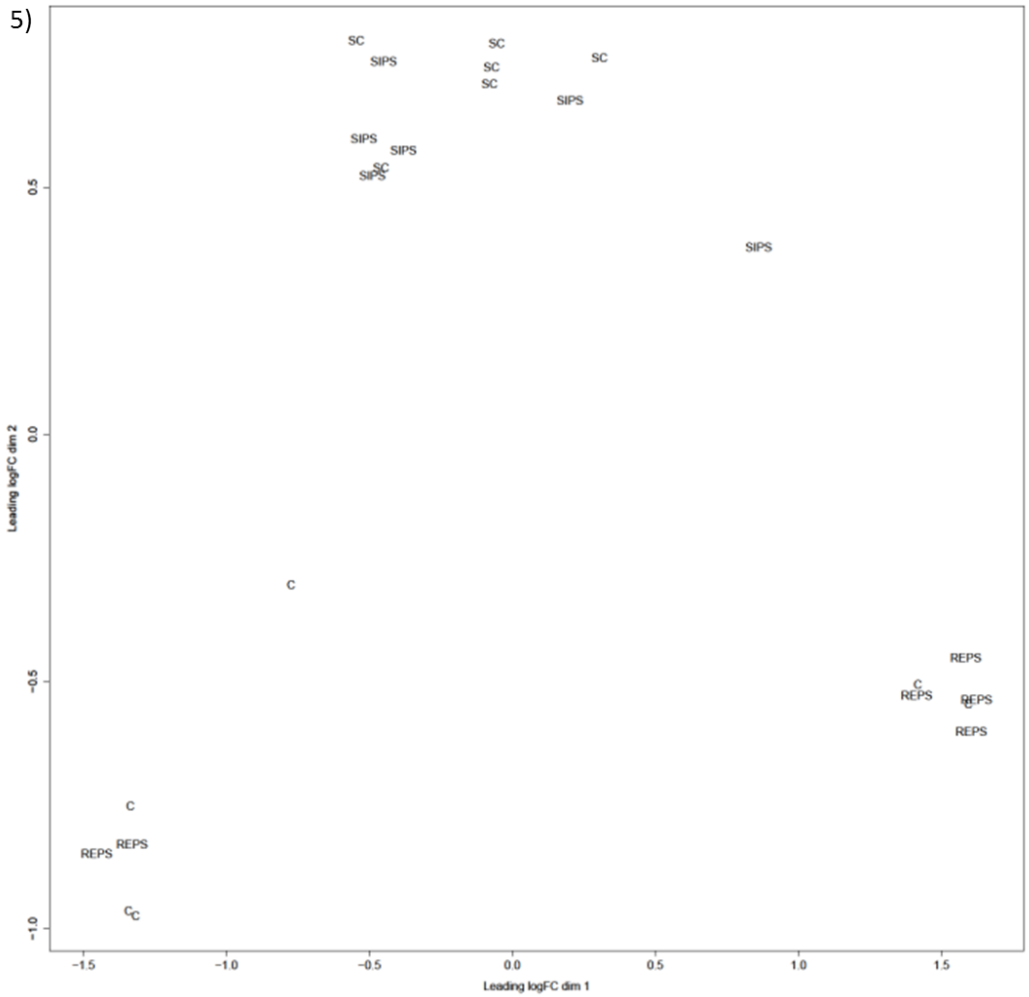

Figure 9-3: Represents MDS plot.

6)

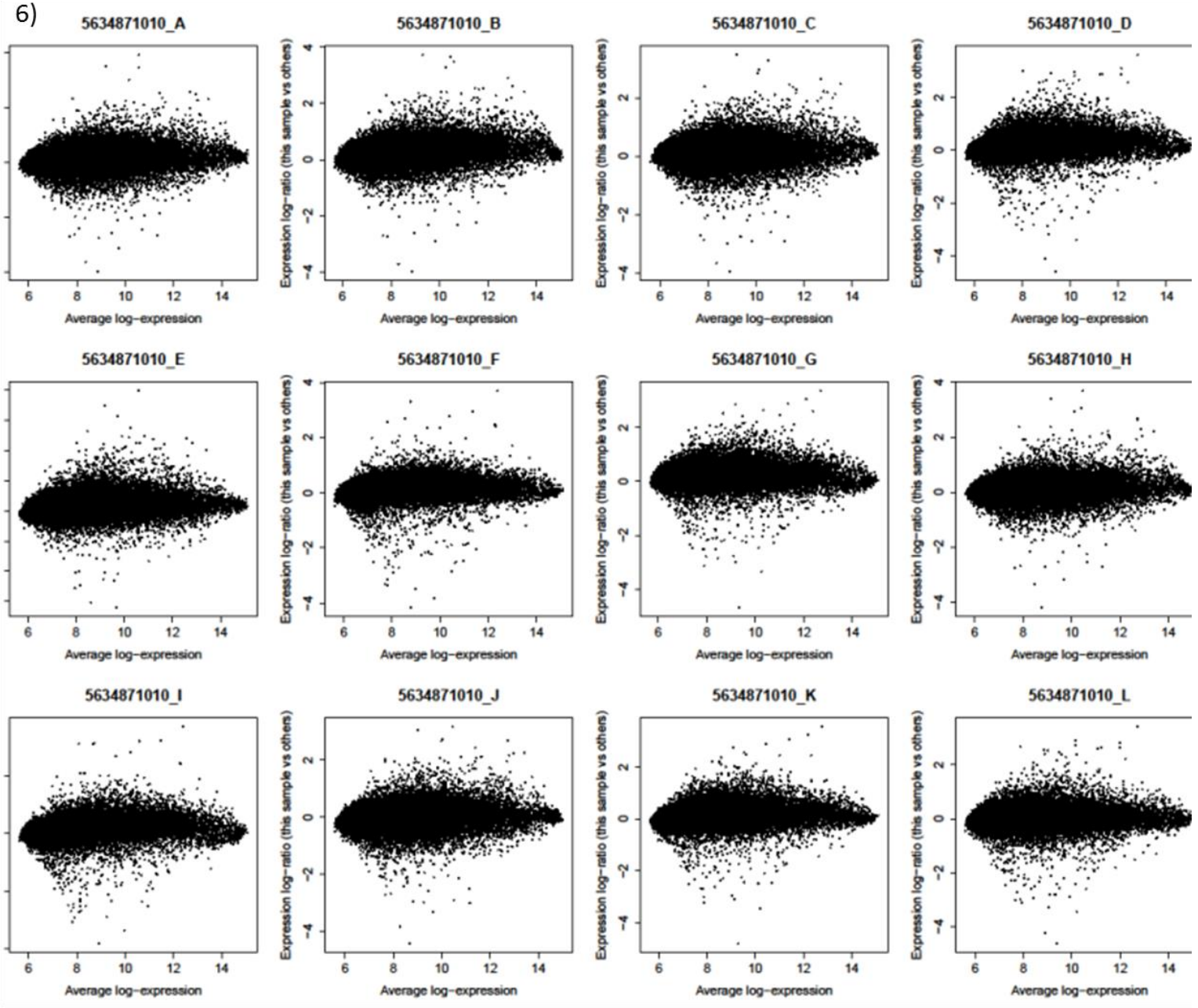
5634871010_A
5634871010_B
5634871010_C
5634871010_D
5634871010_E
5634871010_F
5634871010_G
5634871010_H
5634871010_I
5634871010_J
5634871010_K
5634871010_L
Expression log−ratio (this sample vs others)
Average log−expression

7)

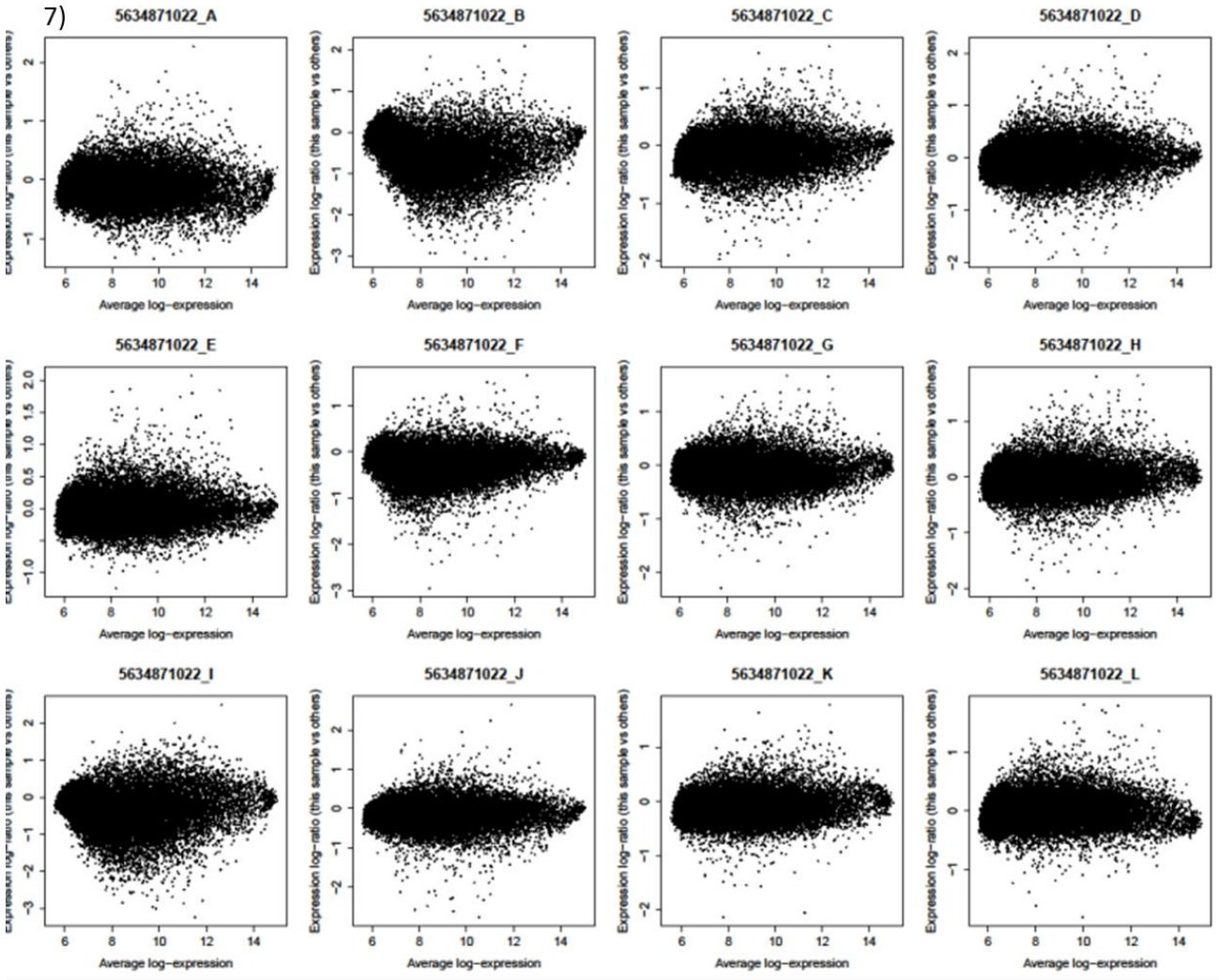

Figure 9-4: MA plots representing all 24 samples.

8)

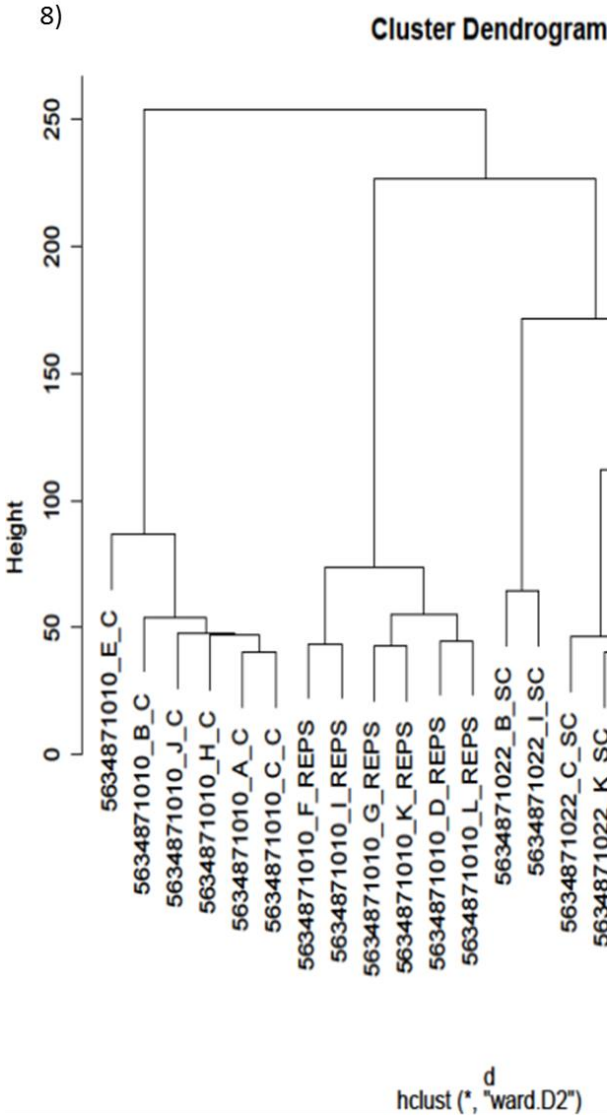

Figure 9-5: Cluster dendrogram representing relationship between all samples.

9.5 Appendix IV

3 separate database literature searches showing Senescent endothelial cells Proteomics

OVID
1.
Proteome analysis of irradiated endothelial cells reveals persistent alteration in protein degradation and the RhoGDI and NO signalling pathways.
Azimzadeh O; Subramanian V; Stander S; Merl-Pham J; Lowe D; Barjaktarovic Z; Moertl S; Raj K; Atkinson MJ; Tapio S.
International Journal of Radiation Biology. 1-9, 2017 Jul 11.
[Journal Article]
UI: 28697312
Authors Full Name
Azimzadeh, Omid; Subramanian, Vikram; Stander, Susanne; Merl-Pham, Juliane; Lowe, Donna; Barjaktarovic, Zarko; Moertl, Simone; Raj, Ken; Atkinson, Michael J; Tapio, Soile.
Link to the Ovid Full Text or citation:
Click here for full text options
Link to the External Link Resolver:
elink
8.
Altered vimentin protein expression in human dermal microvascular endothelial cells after ultraviolet or intense pulsed light treatment.
Shin JU; Lee WJ; Oh SH; Kim DY; Kim DS; Jung I; Lee JH.
Lasers in Surgery & Medicine. 46(5):431-8, 2014 Jul.
[Evaluation Studies. Journal Article. Research Support, Non-U.S. Gov't]
UI: 24737666
Authors Full Name
Shin, Jung U; Lee, Won Jai; Oh, Sang Ho; Kim, Do Young; Kim, Dae Suk; Jung, Inhee; Lee, Ju Hee.
Link to the Ovid Full Text or citation:
Click here for full text options
Link to the External Link Resolver:
elink
17.
Searching for genes involved in arteriosclerosis: proteomic analysis of cultured
human umbilical vein endothelial cells undergoing replicative senescence.
Kamino H; Hiratsuka M; Toda T; Nishigaki R; Osaki M; Ito H; Inoue T; Oshimura M.
Cell Structure & Function. 28(6):495-503, 2003 Dec.
[Journal Article. Research Support, Non-U.S. Gov't]
UI: 15004419
Authors Full Name
Kamino, Hiroki; Hiratsuka, Masaharu; Toda, Tosifusa; Nishigaki, Ryuichi; Osaki, Mitsuhiko; Ito, Hisao; Inoue, Toshiaki; Oshimura, Mitsuo.
Link to the Ovid Full Text or citation:
Click here for full text options
Link to the External Link Resolver:
Elink

Paneni, F., Costantino, S., Kränkel, N., Cosentino, F., Lüscher, T.F.
Reprogramming ageing and longevity genes restores paracrine angiogenic properties of early outgrowth cells
(2016) European Heart Journal, 37 (22), pp. 1733-1737. Cited 5 times.
DOI: 10.1093/eurheartj/ehw073
Document Type: Article
Source: Scopus

2) Prattichizzo, F., Giuliani, A., Recchioni, R., Bonafè, M., Marcheselli, F., De Carolis, S., Campanati, A., Giuliodori, K., Rippo, M.R., Brugè, F., Tiano, L., Micucci, C., Ceriello, A., Offidani, A., Procopio, A.D., Olivieri, F.
Anti-TNF-α treatment modulates SASP and SASP-related microRNAs in endothelial cells and in circulating angiogenic cells
(2016) Oncotarget, 7 (11), pp. 11945-11958. Cited 7 times.
DOI: 10.18632/oncotarget.7858
Document Type: Article
Source: Scopus

3) Prattichizzo, F., Bonafè, M., Ceka, A., Giuliani, A., Rippo, M.R., Re, M., Antonicelli, R., Procopio, A.D., Olivieri, F.
Endothelial cell senescence and inflammaging: MicroRNAs as biomarkers and innovative therapeutic
tools
(2016) Current Drug Targets, 17 (4), pp. 388-397. Cited 4 times.
Document Type: Article
Source: Scopus

4) Dauwe, D., Pelacho, B., Wibowo, A., Walravens, A.-S., Verdonck, K., Gillijns, H., Caluwe, E., Pokreisz, P., van Gastel, N., Carmeliet, G., Depypere, M., Maes, F., Van den Driessche, N., Droogne, W., van Cleemput, J., Vanhaecke, J., Prosper, F., Verfaillie, C., Luttun, A., Janssens, S.
Neovascularization potential of blood outgrowth endothelial cells from patients with stable ischemic
heart failure is preserved
(2016) Journal of the American Heart Association, 5 (4), art. no. e002288, .
DOI: 10.1161/JAHA.115.002288

Document Type: Article
Source: Scopus

5) Yentrapalli, R., Azimzadeh, O., Kraemer, A., Malinowsky, K., Sarioglu, H., Becker, K.-F., Atkinson, M.J., Moertl, S., Tapio, S.
Quantitative and integrated proteome and microRNA analysis of endothelial replicative senescence
(2015) Journal of Proteomics, 126, pp. 12-23. Cited 1 time.
DOI: 10.1016/j.jprot.2015.05.023
Document Type: Article
Source: Scopus

6) Azimzadeh, O., Sievert, W., Sarioglu, H., Merl-Pham, J., Yentrapalli, R., Bakshi, M.V., Janik, D., Ueffing, M., Atkinson, M.J., Multhoff, G., Tapio, S.
Integrative proteomics and targeted transcriptomics analyses in cardiac endothelial cells unravel
mechanisms of long-term radiation-induced vascular dysfunction
(2015) Journal of Proteome Research, 14 (2), pp. 1203-1219. Cited 16 times.
DOI: 10.1021/pr501141b
Document Type: Article
Source: Scopus

7) Zolla, V., Nizamutdinova, I.T., Scharf, B., Clement, C.C., Maejima, D., Akl, T., Nagai, T., Luciani, P., Leroux, J.-C., Halin, C., Stukes, S., Tiwari, S., Casadevall, A., Jacobs, W.R., Entenberg, D., Zawieja, D.C., Condeelis, J., Fooksman, D.R., Gashev, A.A., Santambrogio, L.
Aging-related anatomical and biochemical changes in lymphatic collectors impair lymph transport, fluid homeostasis, and pathogen clearance
(2015) Aging Cell, . Article in Press. Cited 7 times.
DOI: 10.1111/acel.12330
Document Type: Article in Press
Source: Scopus

8) Shin, J.U., Lee, W.J., Oh, S.H., Kim, D.Y., Kim, D.S., Jung, I., Lee, J.H.
Altered vimentin protein expression in human dermal microvascular endothelial cells after ultraviolet
or intense pulsed light treatment
(2014) Lasers in Surgery and Medicine, 46 (5), pp. 431-438. Cited 3 times.
DOI: 10.1002/lsm.22253
Document Type: Article

Source: Scopus

9) Csiszar, A., Gautam, T., Sosnowska, D., Tarantini, S., Banki, E., Tucsek, Z., Toth, P., Losonczy, G., Koller, A., Reglodi, D., Giles, C.B., Wren, J.D., Sonntag, W.E., Ungvari, Z.
Caloric restriction confers persistent anti-oxidative, pro-angiogenic, and anti-inflammatory effects and promotes anti-aging miRNA expression profile in cerebromicrovascular endothelial cells of aged rats
(2014) American Journal of Physiology - Heart and Circulatory Physiology, 307 (3), pp. H292-H306. Cited 31 times.
DOI: 10.1152/ajpheart.00307.2014
Document Type: Article
Source: Scopus

10) Yentrapalli, R., Azimzadeh, O., Barjaktarovic, Z., Sarioglu, H., Wojcik, A., Harms-Ringdahl, M., Atkinson, M.J., Haghdoost, S., Tapio, S.
Quantitative proteomic analysis reveals induction of premature senescence in human umbilical vein

endothelial cells exposed to chronic low-dose rate gamma radiation
(2013) Proteomics, 13 (7), pp. 1096-1107. Cited 38 times.
DOI: 10.1002/pmic.201200463
Document Type: Article
Source: Scopus

11) Buján, J., Pascual, G., Bellón, J.M.
Interaction between ageing, inflammation process, and the occurence of varicose veins
(2008) Phlebolymphology, 15 (4), pp. 123-130. Cited 2 times.
Document Type: Article
Source: Scopus

12) Ha, M.K., Cho, J.S., Baik, O.-R., Hoon, L.K., Koo, H.-S., Chung, K.Y.
Caenorhabditis elegans as a screening tool for the endothelial cell-derived putative aging-related proteins detected by proteomic analysis
(2006) Proteomics, 6 (11), pp. 3339-3351. Cited 10 times.
DOI: 10.1002/pmic.200500395
Document Type: Article
Source: Scopus

13) Hampel, B., Fortschegger, K., Ressler, S., Chang, M.W., Unterluggauer, H., Breitwieser, A.,

Sommergruber, W., Fitzky, B., Lepperdinger, G., Jansen-Dürr, P., Voglauer, R., Grillari, J.
Increased expression of extracellular proteins as a hallmark of human endothelial cell in vitro senescence
(2006) Experimental Gerontology, 41 (5), pp. 474-481. Cited 41 times.
DOI: 10.1016/j.exger.2006.03.001
Document Type: Article
Source: Scopus

14) Eman, M.R., Regan-Klapisz, E., Pinkse, M.W.H., Koop, I.M., Haverkamp, J., Heck, A.J.R., Verkleij, A.J., Post, J.A.
Protein expression dynamics during replicative senescence of endothelial cells studied by 2-D differences in-gel electrophoresis
(2006) Electrophoresis, 27 (8), pp. 1669-1682. Cited 18 times.
DOI: 10.1002/elps.200500746
Document Type: Article
Source: Scopus

15) Lee, J.H., Chung, K.Y., Bang, D., Lee, K.H.
Searching for aging-related proteins in human dermal microvascular endothelial cells treated with
anti-aging agents
(2006) Proteomics, 6 (4), pp. 1351-1361. Cited 29 times.
DOI: 10.1002/pmic.200500287
Document Type: Article
Source: Scopus

16) Chang, M.W.-F., Grillari, J., Mayrhofer, C., Fortschegger, K., Allmaier, G., Marzban, G., Katinger, H., Voglauer, R.
Comparison of early passage, senescent and hTERT immortalized endothelial cells
(2005) Experimental Cell Research, 309 (1), pp. 121-136. Cited 66 times.
DOI: 10.1016/j.yexcr.2005.05.002
Document Type: Article
Source: Scopus

17) Ha, M.K., Chung, K.Y., Bang, D., Park, Y.K., Lee, K.H.
Proteomic analysis of the proteins expressed by hydrogen peroxide treated cultured human dermal microvascular endothelial cells

(2005) Proteomics, 5 (6), pp. 1507-1519. Cited 13 times.
DOI: 10.1002/pmic.200401043
Document Type: Article
Source: Scopus

18) Ha, M.K., Chung, K.Y., Lee, J.H., Bang, D., Park, Y.K., Lee, K.H.
Expression of psoriasis-associated fatty acid-binding protein in senescent human dermal microvascular endothelial cells
(2004) Experimental Dermatology, 13 (9), pp. 543-550. Cited 6 times.
DOI: 10.1111/j.0906-6705.2004.00196.x
Document Type: Article
Source: Scopus

19) Kamino, H., Hiratsuka, M., Toda, T., Nishigaki, R., Osaki, M., Ito, H., Inoue, T., Oshimura, M.
Searching for genes involved in arteriosclerosis: Proteomic analysis of cultured human umbilical vein
endothelial cells undergoing replicative senescence
(2003) Cell Structure and Function, 28 (6), pp. 495-503. Cited 27 times.
DOI: 10.1247/csf.28.495
Document Type: Article
Source: Scopus